MYOCARDIAL REMODELING DURING PATHOPHYSIOLOGY: RELEVANCE FOR CARDIAC DYSFUNCTION

Elise Laura Kessler

ISBN: 978-90-393-6898-5
Cover Design: Anna Schröder and Elise Kessler
Heart made by: Laura Cameron, www.lostinthewood.co.uk
Layout: Anna Schröder, annamachtdas.de
Printed by: PrintSupport4U

MYOCARDIAL REMODELING DURING PATHOPHYSIOLOGY:
RELEVANCE FOR CARDIAC DYSFUNCTION

MYOCARDIALE REMODELLERING TIJDENS PATHOFYSIOLOGIE:
RELEVANTIE VOOR CARDIALE DYSFUNCTIE
(met een samenvatting in het Nederlands)

MYOKARDIALE REMODELLIERUNG IN DER PATHOFYSIOLOGIE:
RELEVANZ FÜR KARDIALE DYSFUNKTION
(mit einer Zusammenfassung in deutscher Sprache)

PROEFSCHRIFT

ter verkrijging van de graad van doctor aan de Universiteit Utrecht op gezag van de rector magnificus, prof.dr. G.J. van der Zwaan, ingevolge het besluit van het college voor promoties in het openbaar te verdedigen op donderdag 25 januari 2018 des middags te 2.30 uur

door

Elise Laura Kessler

geboren op 6 september 1988
te Karlsruhe, Duitsland

Promotor: Prof.dr. M.A. Vos
Copromotor: Dr. A.A.B. van Veen

The research described in this thesis was supported by CVON2012-10 PREDICT.
Financial support by the Dutch Heart Foundation for the publication of this thesis is gratefully acknowledged.
Financial support by ChipSoft N.V. for the publication of this thesis is gratefully acknowledged.

Voor
Opa & Näne

Ik mis jullie!

Content

Part 2

Appendix

“

If you want to change the world,
pick up your pen and write.

Martin Luther

Chapter

1

Preface and thesis outline

Preface

MYOCARDIAL REMODELING

Upon various forms of cardiac damage or disease, such as myocardial infarction, pressure overload or genetic cardiomyopathies, the heart attempts to adapt to its altered circumstances by myocardial remodeling, consisting of electrical, structural and contractile remodeling. Even though myocardial tissue remodeling is a natural rescue process that is initiated to maintain sufficient blood supply to the organs throughout the body, when remodeling is massive and heterogeneous, it aggravates the damage, eventually leading to heart failure (HF).[1]

Electrical remodeling impedes the excitability of cardiomyocytes and impulse propagation within the heart, thereby also triggering development of cardiac arrhythmias.[2] Structural remodeling includes inflammation, apoptosis, hypertrophy (to reduce wall stress) and fibrosis formation, initially increasing cardiac strength by stiffening of the cardiac muscle, but ultimately impairing cardiac pump function.[3,4] Fibrosis even further facilitates the onset of life-threatening cardiac arrhythmias, specifically when it develops in a heterogeneous manner.[5] To our opinion, contractile remodeling crosses the bridge between the electrical and structural remodeling, as it includes alterations in calcium handling (also having an electrical component) and remodeling of the myofilaments, which in turn includes a structural aspect.

Myocardial remodeling therefore compromises the fine-tuning of cardiac function, posing it as a potential adjustable target. This can for instance be studied in consisting pathophysiologies in humans, or aspects of cardiac remodeling can be modified and investigated in experimental animal models. In this thesis, we focused on myocardial remodeling of mainly the intercalated disc (ID) and tissue architecture during various cardiomyopathies (Dilated Cardiomyopathy (DCM), Hypertrophic Cardiomyopathy (HCM), Ischemic Cardiomyopathy (ICM), and Arrhythmogenic Cardiomyopathy (ACM)); and upon pressure overload in mice, where we studied the effect of fibrosis and inflammation.

THE INTERCALATED DISC

An important entity in myocardial remodeling is the ID. This is the region between the longitudinal ends of two adjacent cardiomyocytes, where junctions for mechanical and electrical coupling of the cells are embedded. The main junctions in the ID for mechanical attachment are the adherens junctions and the desmosomes, whereas electrical coupling is ensured by gap junctions.[6]

Adherens junctions mainly consist of N-cadherin (Ncad), Plakoglobin and β-catenin, connecting the actin filaments of two adjacent cardiomyocytes. Desmosomes are composed of Desmoglein-2 (DSG-2), Desmocollin-2 (DSC-2), Plakophilin-2 (PKP-2), Desmoplakin-2 (DSP-2) and also Plakoglobin.[7] These desmosomal junctions link to the intermediate filaments. Electrical coupling is guaranteed by gap junctions, which connect the cytoplasm of two adjacent

cardiomyocytes, and are also able to facilitate the transfer of small molecules. One gap junction consists of two connexons (hemichannels), composed of hexagonally arranged connexin proteins. In the ventricles, gap junctions mainly consist of Connexin-43 (Cx43).[6,8,9] Furthermore, various other components are found at the ID, such as the sodium channel $Na_v1.5$ that is responsible for the excitability of cardiomyocytes.[10]

PATHOPHYSIOLOGY OF THE ID

Multiple different mutations in proteins of the ID have shown a plethora of pathophysiological consequences. Mutations in desmosomal proteins for instance have been associated with, among others, DCM and ACM. Desmoplakin (DSP) and DSG-2 mutations are associated with human DCM and cardiac knockout of Plakoglobin leads to DCM in mice.[12,13] Furthermore, PKP2 mutations can lead to either DCM or ACM phenotypes.[14,15] Because of the particular arrhythmogenic character of ACM, this indicates that mutations in proteins that facilitate the structural orchestration of cardiac muscle, can lead to electrical remodeling, often preceding the signs of structural remodeling in these patients.[16,17] In DCM, proteins such as Plakoglobin, but also the electrical junction-protein Cx43 have been reported to be affected. Also in ACM, mutations in e.g. PKP2 cause heterogeneous downregulation of Cx43, $Na_V1.5$ and Plakoglobin.[18-22] This in turn leads to heterogeneous electrical activation, again often seen primary to heterogeneous contraction.[23,24] Comparably, in heart failure patients, reduced levels of Cx43 and $Na_V1.5$ are commonly reported.[19,25] In combination with the presence of fibrosis, such reductions were found to be highly arrhythmogenic in murine models.[26,27]

It is important to realize that components of the ID can interact with various intra- and extra-cellular proteins, but the different junctions, and even individual proteins of these junctions, also seem to be able to interact with each other to form macro-molecular complexes.[7] Therefore, mutations or alterations in one protein or sub-complex will probably result in destabilization of the whole ID-equilibrium.

Furthermore, although the composition of the ID has been studied extensively, still many proteins are located at the ID, with no known function until this day. Besides that, it is not unlikely that the amount of proteins known to reside in the ID is still incomplete. To enable proper mapping of the ID geography, function of all proteins of the ID should be investigated. One of the less-known proteins in regard to cardiac function that we previously confirmed to be part of the ID, is Flotillin-2.[11]

AIM AND RESEARCH QUESTION

In this thesis, we focused on the role of myocardial remodeling upon human cardiomyopathies, or artificially induced pressure overload in mice.

Our central questions were:

- Part 1: Myocardial remodeling of the ID
  - Which molecular alterations can be identified in the ID during e.g. ACM and DCM?
  - What is the role of yet unknown members of the ID?
- Part 2: Myocardial remodeling in experimental models of chronic heart failure
  - What is the role of fibrosis and inflammation in myocardial remodeling?
  - Can target-driven intervention ameliorate or even prevent fibrosis and heart failure?

To answer these questions, we mainly studied human cardiac material and genetically modified mice by performing electrophysiological, biomolecular and histological experiments.

THESIS OUTLINE

This thesis commences with **chapter 2**, a review on heterogeneity in myocardial remodeling. This chapter poses an overview of the different remodeling processes observed during various cardiomyopathies (DCM, HCM, ICM and ACM), and introduces the aspect of heterogeneity as an important risk factor for cardiac failure. The subsequent chapters are divided into two parts: 1) Myocardial remodeling of the ID, including chapter 3, 4 and 5; and 2) Myocardial remodeling of tissue architecture upon pressure overload, including chapter 6 and 7. In detail, in **chapter 3**, the role of heterogeneous tissue remodeling in ACM is presented. ACM is characterized by heterogeneous downregulation of proteins of the ID, subsequently leading to heterogeneous electrical activation. In this chapter, we studied the composition of the IDs of right-ventricular septum biopsies and post-mortem specimens from ACM patients, focusing on PKP2, Plakoglobin, Cx43 and the sodium channel $Na_v1.5$. In **chapter 4**, we investigated the molecular alterations in the ID of 7 post-mortem ventricular specimens of pediatric patients with DCM compared to age-matched controls. Here, we describe the disturbed localization of DSG-2 and high amounts of heterogeneously distributed fibrosis in pediatric patients with DCM. In **chapter 5**, we investigated the role of a newly identified protein in the ID: Flotillin-2 and its family member Flotillin-1 in the heart. In this study, we used ventricular cardiac samples from patients with DCM, ACM and control specimens to assess the amount of these proteins in health and disease. Next, we made use of a murine knockout model and neonatal rat cardiomyocytes with reduced amounts of Flotillins in an attempt to unravel the role of these proteins in cardiac physiology.

In part 2 of this thesis, we used different strains of genetically modified mice that were subjected to chronic pressure overload to study cardiac tissue remodeling in a time-lined fashion. **Chapter 6** describes the effect of a connective tissue growth factor (CTGF) knockout in mice subjected to chronic pressure overload using the transverse aortic constriction (TAC) model. Increased levels of CTGF are reported in several forms of cardiac disease and this is commonly regarded as one of the causative factors associated with formation of fibrosis. In the experimen-

tal model, we hypothesized that CTGF knockout would impede fibrosis formation and therefore could preserve cardiac function. In **chapter 7 and its addendum**, in two different studies we focused on the effect of suppressed inflammation on myocardial remodeling in mice subjected to chronic pressure overload. For this purpose we used a Toll-like receptor-2 (TLR2) knockout and hypothesized that the KO mice would show reduced levels of cardiac fibrosis together with more preserved cardiac function compared to WT TAC mice. Furthermore, in the addendum, we investigated, whether this postulated beneficial effect of modified cardiac inflammation could be related to the absence of TLR2 in inflammatory cells, or in cardiomyocytes.
In **chapter 8**, all results are put into perspective and generally discussed.

References

1. Ponikowski P, Voors AA, Anker SD, et al. 2016 ESC Guidelines for the diagnosis and treatment of acute and chronic heart failure: The Task Force for the diagnosis and treatment of acute and chronic heart failure of the European Society of Cardiology (ESC) Developed with the special contribution of the Heart Failure Association (HFA) of the ESC. Eur Heart J.2016;37(27):2129-2200.

2. Kleber AG, Rudy Y. Basic mechanisms of cardiac impulse propagation and associated arrhythmias. Physiol Rev.2004;84(2):431-488.

3. Grossman W, Jones D, McLaurin LP. Wall stress and patterns of hypertrophy in the human left ventricle. J Clin Invest.1975;56(1):56-64.

4. Swynghedauw B. Molecular mechanisms of myocardial remodeling. Physiol Rev.1999;79(1):215-262.

5. de Jong S, van Veen TA, van Rijen HV, de Bakker JM. Fibrosis and cardiac arrhythmias. J Cardiovasc Pharmacol.2011;57(6):630-638.

6. Noorman M, van der Heyden MA, van Veen TA, et al. Cardiac cell-cell junctions in health and disease: Electrical versus mechanical coupling. J Mol Cell Cardiol.2009;47(1):23-31.

7. Vermij SH, Abriel H, van Veen TA. Refining the molecular organization of the cardiac intercalated disc. Cardiovasc Res.2017;10.1093/cvr/cvw259.

8. Elfgang C, Eckert R, Lichtenberg-Frate H, et al. Specific permeability and selective formation of gap junction channels in connexin-transfected HeLa cells. J Cell Biol.1995;129(3):805-817.

9. Smith JH, Green CR, Peters NS, Rothery S, Severs NJ. Altered patterns of gap junction distribution in ischemic heart disease. An immunohistochemical study of human myocardium using laser scanning confocal microscopy. Am J Pathol.1991;139(4):801-821.

10. Balser JR. Structure and function of the cardiac sodium channels. Cardiovasc Res.1999;42(2):327-338.

11. Soni S, Raaijmakers AJ, Raaijmakers LM, et al. A Proteomics Approach to Identify New Putative Cardiac Intercalated Disk Proteins. PLoS One.2016;11(5):e0152231.

12. Norgett EE, Hatsell SJ, Carvajal-Huerta L, et al. Recessive mutation in desmoplakin disrupts desmoplakin-intermediate filament interactions and causes dilated cardiomyopathy, woolly hair and keratoderma. Hum Mol Genet.2000;9(18):2761-2766.

13. Posch MG, Posch MJ, Geier C, et al. A missense variant in desmoglein-2 predisposes to dilated cardiomyopathy. Mol Genet Metab.2008;95(1-2):74-80.

14. Ramond F, Janin A, Di Filippo S, et al. Homozygous PKP2 deletion associated with neonatal left ventricle noncompaction. Clin Genet.2017;91(1):126-130.

15. Cerrone M, Noorman M, Lin X, et al. Sodium current deficit and arrhythmogenesis in a murine model of plakophilin-2 haploinsufficiency. Cardiovasc Res.2012;95(4):460-468.

16. Akdis D, Brunckhorst C, Duru F, Saguner AM. Arrhythmogenic Cardiomyopathy: Electrical and Structural Phenotypes. Arrhythm Electrophysiol Rev.2016;5(2):90-101.

17. Corrado D, Link MS, Calkins H. Arrhythmogenic Right Ventricular Cardiomyopathy. N Engl J Med.2017;376(15):1489-1490.

18. Pluess M, Daeubler G, Dos Remedios CG, Ehler E. Adaptations of cytoarchitecture in human dilated cardiomyopathy. Biophys Rev.2015;7:25-32.

19. Kostin S, Rieger M, Dammer S, et al. Gap junction remodeling and altered connexin43 expression in the failing human heart. Mol Cell Biochem.2003;242(1-2):135-144.

20. Kitamura H, Yoshida A, Ohnishi Y, et al. Correlation of connexin43 expression and late ventricular potentials in nonischemic dilated cardiomyopathy. Circ J.2003;67(12):1017-1021.

21. Asimaki A, Tandri H, Huang H, et al. A new diagnostic test for arrhythmogenic right ventricular cardiomyopathy. N Engl J Med.2009;360(11):1075-1084.

22. Sato PY, Musa H, Coombs W, et al. Loss of plakophilin-2 expression leads to decreased sodium current and slower conduction velocity in cultured cardiac myocytes. Circ Res.2009;105(6):523-526.

23. Teske AJ, Cox MG, Te Riele AS, et al. Early detection of regional functional abnormalities in asymptomatic ARVD/C gene carriers. J Am Soc Echocardiogr.2012;25(9):997-1006.

24. Sarvari SI, Haugaa KH, Anfinsen OG, et al. Right ventricular mechanical dispersion is related to malignant arrhythmias: a study of patients with arrhythmogenic right ventricular cardiomyopathy and subclinical right ventricular dysfunction. Eur Heart J.2011;32(9):1089-1096.

25. Peters NS. New insights into myocardial arrhythmogenesis: distribution of gap-junctional coupling in normal, ischaemic and hypertrophied human hearts. Clin Sci (Lond).1996;90(6):447-452.

26. Stein M, Noorman M, van Veen TA, et al. Dominant arrhythmia vulnerability of the right ventricle in senescent mice. Heart Rhythm.2008;5(3):438-448.

27. Jansen JA, van Veen TA, de Jong S, et al. Reduced Cx43 expression triggers increased fibrosis due to enhanced fibroblast activity. Circ Arrhythm Electrophysiol.2012;5(2):380-390.

“

Nothing in life is to be feared,
it is only to be understood.
Now is the time to understand more,
so that we may fear less.

Marie Curie

Chapter

2

Passive ventricular remodeling in cardiac disease: Focus on heterogeneity

Elise L. Kessler[a], Mohamed Boulaksil[a,b], Harold V. M. van Rijen[a], Marc A. Vos[a] and Toon A. B. van Veen[a]

[a] *Division of Heart and Lungs, Department of Medical Physiology, University Medical Center Utrecht, Utrecht, Netherlands*
[b] *Department of Cardiology, Radboud University Medical Center, Nijmegen, Netherlands*

Frontiers in Physiology 2014; 5: 482

Abstract

Passive ventricular remodeling is defined by the process of molecular ventricular adaptation to different forms of cardiac pathophysiology. It includes changes in tissue architecture, such as hypertrophy, fiber disarray, alterations in cell size and fibrosis. Besides that, it also includes molecular remodeling of gap junctions, especially those composed by Connexin-43 proteins (Cx43) in the ventricles that affect cell-to-cell propagation of the electrical impulse, and changes in the sodium channels that modify excitability. All those alterations appear mainly in a heterogeneous manner, creating irregular and inhomogeneous electrical and mechanical coupling throughout the heart. This can predispose to reentry arrhythmias and adds to a further deterioration into heart failure. In this review, passive ventricular remodeling is described in Hypertrophic Cardiomyopathy (HCM), Dilated Cardiomyopathy (DCM), Ischemic Cardiomyopathy (ICM), and Arrhythmogenic Cardiomyopathy (ACM), with a main focus on the heterogeneity of those alterations mentioned above.

Introduction

The lifelong purpose of the heart is maintenance of cardiac output and supply of all organs with an appropriate amount of oxygen and nutrients. At the same time it steers the controlled homeostasis of the blood via clearance of waste products, drugs and imbalanced levels of ions and proteins in the lungs, liver, and kidneys. To be able to fulfill this task, the heart has to adapt its workload to the needs of the body.[1] Many different diseases like coronary artery disease, myocardial infarction, hypertension, dysfunction of valves, congenital heart disease, lung diseases, diabetes, anemia, hyperthyroidism, and or arrhythmia/dysrhythmia can alter the performance of the heart.[2-4] In order to preserve cardiac output under these conditions, the heart will start several compensatory mechanisms, like the Frank Starling mechanism, neuro-humoral activation, and inflammatory responses.[5,6] Moreover, the heart starts to modify the gene program that shapes the individual cells that compose the organ. This in an attempt to adapt chronically to the new requirements of its environment. These adaptations together will result in myocardial remodeling that most often has heterogeneous characteristics.[7]

By nature, the heart itself is a rather heterogeneous organ: morphologically, the right and left side as well as atria and ventricles show various differences in cell constellations, hemodynamics and their respective electrical characteristics.[8] The different resistances in peripheral and pulmonary circulation for instance are causative for the differences between left and right ventricle anatomy (right ventricular wall is much thinner than the left wall). Also with respect to molecular make-up and microarchitecture of the cardiac muscle significant differences exist. The way the fibers are orientated within the left and right ventricle is not comparable. Electrical impulse propagation faces differences in conduction velocity between left and right ventricles but also with the specialized conduction system. Part of that relies on differences in expression level and pattern of gap junction channels and the ion channels that underlie action potential generation.

The sodium channel protein $Na_V1.5$, for instance, is heterogeneously distributed throughout the ventricles and the cardiac conduction system in healthy hearts.[9] Besides that, two pools of $Na_V1.5$ channels can be found in cardiomyocytes: a lateral pool and a pool in the intercalated disc that co- exist and interact with different proteins.[10] Also Cx43 is found in different densities within the healthy heart e.g., regarding the posterior and anterior wall of the ventricles.[11]

Beyond the natural heterogeneity that is found under the normal physiological functioning of the heart, this review will focus on the heterogenic aspect that is involved in passive remodeling of the ventricles under pathophysiological conditions. Passive remodeling is defined as the chronic molecular and structural adaptations in ventricular cardiomyocytes and alterations in gene expression as induced by different forms of heart disease. Active remodeling, in contrast, is defined as phosphorylation processes that e.g., result from sympathic and parasympathic imbalance. This is exampled by the increase in heart rate that is facilitated through alterations in phosphorylation of ion channels (e.g., L–type calcium channels) in the sinus node.

One of the most crucial and maladaptive factors of passive remodeling in the ventricles is heterogeneity in electrical and structural remodeling. In that perspective we will discuss factors associated with conduction and propagation of excitation, but not with respect to repolarization (e.g., potassium currents, heterogeneity in action potential duration), and contraction (e.g., calcium-handling and sarcomeric proteins). During remodeling, heterogeneous alterations in three factors contribute to increase the propensity to arrhythmias and to develop heart failure: (1) tissue architecture such as hypertrophy, fibrosis, fiber disarray, and cell size, (2) electrical coupling by means of gap junctions and especially those composed of Cx43, and (3) electrical excitability due to changes in sodium channels that are mainly composed of $Na_v1.5$.[12-14]

We will address remodeling of these factors during Dilated Cardiomyopathy (DCM), Hypertrophic Cardiomyopathy (HCM), Ischemic Cardiomyopathy (ICM) and Arrhythmogenic Cardiomyopathy (ACM), previously known as Arrhythmogenic Right Ventricular Cardiomyopathy/Dysplasia (ARVC/D). In general, DCM can be identified by cardiac chamber dilatation and reduced systolic function often leading to congestive heart failure. It is the most commonly occurring cardiomyopathy in adults and children and is associated with muscle dysfunction and/or volume overload. On the other hand, in children DCM is mostly caused by myocarditis and neuro-humoral diseases.[15] DCM is defined as the presence of left ventricular fractional shortening (< 25%) and/or LVEF< 45% and left ventricular end-diastolic dimensions (LVED,d) of >117% of the predicted value by the Henry formula.[16] It can also be caused by a variety of genetic mutations that are uncovered upon analysis of family history and molecular genetic testing. These forms, however, are referred to as familial dilated cardiomyopathy (FDC).[17] HCM has been defined by the World Health Organization as the presence of left or biventricular hypertrophy, in absence of any cardiac or systemic cause.[18] When this definition is used, the general prevalence is about 1:500.[19] However, HCM can also be caused by mutations in genes encoding for cardiac sarcomeric and myofilament proteins; for the latter already more than 1400 mutations have been identified increasing the prevalence even more.[20,21]

ICM results from myocardial ischemia and is characterized by remodeling due to myocardial infarction, which eventually triggers loss of contractility, still being the leading cause of ventricular dysfunction worldwide (reviewed in[22]).

Finally, ACM is a non-ischemic progressive and predominantly heritable heart disease associated with cardiac arrhythmias and sudden cardiac death.[23] ACM is characterized through replacement of cardiomyocytes by fibro-fatty tissue.[24,25] About 60% of the cases have a hereditary basis and mutations causing ACM have been found in several desmosomal genes like Desmoplakin,[26] Plakoglobin,[27] Plakophilin-2,[28,29] Desmocollin-2,[30,31] and Desmoglein.[32] Moreover, genes not related to the desmosome can be affected such as the transmembrane protein 43 (TMEM-43), phospholamban (PLN), desmin and transforming growth factor beta-3 (TGF-β3).[33-36]

In addition, a variety of mutations in several ion channels that add to action potential generation have been described to trigger pro-arrhythmic remodeling of the heart. This subset of arrhythmogenic cardiac diseases is, however, beyond the scope of this review.

Tissue Architecture

Several extrinsic and intrinsic factors can lead to alterations in cardiac workload. Those changes can trigger growth of individual myocytes leading to cardiac hypertrophy. An increased amount of hypertrophy is associated with a decreased conduction velocity of the electrical impulse.[37-39] Moreover, metaplasia of fibroblasts into myofibroblasts, a more contractile and collagen producing cell type can increase the deposition of the extracellular matrix (ECM) leading to fibrosis.[40] This is further supported by an increased rate of cell death - necrosis and apoptosis - and inflammatory processes such as the secretion of TNF-α or IL-6.[41,42] Besides that, also alterations in myocardial fiber orientation can importantly affect characteristics of cardiac impulse propagation.[43]

HYPERTROPHY AND CELL SIZE

The key feature of hypertrophy in general is an increased cell size that electrically can be measured as an increase in cell capacitance. Hypertrophy and increased cell size counteract the increased wall tension as caused by changes in cardiac workload (Laplace's law). Therefore, hypertrophy is seen as a compensatory mechanism. However, cardiac impulse propagation as well as conduction velocity gradually decrease with increasing severity of hypertrophy[37-39] leading to an elevated risk for heart failure and sudden cardiac death.[44]

In DCM mainly the cell length is increased and this is associated by dilation and systolic disturbances of predominantly the left ventricle. Also both ventricles can be impaired, but generally with normal left ventricular wall thickness.[18,45] The effect of eccentric hypertrophy on electrical signaling has been addressed in several animal models. An increase in conduction velocity was shown in a rabbit model, where a combined pressure- and volume overload increased heart weight by about 100%, and both cell length and width were increased by about 30%. Delayed activation was indicated by an increase in QRS duration from 50 ms in control to 58 ms in rabbits with DCM. Parallel and transverse to fiber orientation, however, epicardial conduction velocity appeared increased by 18 and 16%, respectively while transmural conduction velocity was unchanged. The authors of this study concluded that the increased cell size was responsible for the increase in longitudinal and transverse conduction velocity. Moreover, they concluded that the increased conduction velocity could not sufficiently compensate for the increased heart size, which was causative for the prolonged QRS durations.[46] In a dog model of rapid pacing, it has been shown that QRS duration and cell length were increased, while cell width was reduced. Besides, transmural conduction velocity was reduced in both RV and LV, while Cx43 expression was reduced only in LV. As such, reduced cell width seems to play a dominant role in the reduced conduction velocity.[47] In mouse models, where DCM was induced by transverse aortic constriction (TAC), cell size, and the amount of hypertrophy was significantly increased after 6 weeks of TAC. This was leading to prolongations of PQ, QT, and QRS intervals, and slowing of right ventricular conduction velocity parallel to the fiber orientation.[48]

Data of a recent study with DCM patients showed elevated levels of myosin light-chain kinase and CRP that could possibly serve as diagnostic biomarkers for hypertrophy.[49]

In HCM, primarily cell width is increased[49] leading to hypertrophy without dilation of the ventricles.[19] This affects conduction of the electrical impulse as has been shown using computer modeling, where conduction velocity increased with cell size, and cell size was determined to be the dominant factor affecting conduction velocity.[50] Also for HCM, several animal models have been described. In a rat model, where RV-HCM was induced by injections with monocrotaline (leading to pulmonary hypertension), increased cell width and lateralized Cx43 expression were found, while cell length was unaffected. Conduction velocity parallel to the fiber orientation was decreased, although perpendicular to the fiber orientation the conduction velocity was unchanged.[51] Similar results were obtained in another study that used the same rat model with monocrotaline induced pressure overload. In this study, RV cell width was increased, but again cell length remained unaffected. In the left ventricle, cell width and length were both decreased. Moreover, longer action potentials (at 90% repolarization), prolongation of the effective refractory period, and slowing of the longitudinal conduction velocity occurred.[52] Besides the rat model, LV epicardial mapping was also performed in patients after chronic thromboembolic pulmonary hypertension. Comparable to the experimental model, these patients also showed prolongation of the effective refractory period and conduction slowing.[52] In ICM, cardiac hypertrophy can be found in the majority of patients.[53,54] In MRL (Murphy Roths Large) mice exhibiting an ICM phenotype, increased cell size and hypertrophy lead to a faster progression toward heart failure than in controls.[55] Moreover, electrocardiographic left ventricular hypertrophy embedded a predictive value for arrhythmias and mortality in ICM patients, making it an important factor to consider during diagnosis.[56] In ACM no gross cardiac hypertrophy has been reported and the individual cell size is not increased either. Therefore, hypertrophy is not included as a parameter into the revised Task Force Criteria that are used to diagnose ACM.[57]

FIBROSIS AND MYOCARDIAL FIBER DISARRAY

In the healthy heart, cardiac myocytes are embedded in the ECM, a network of multiple molecules, proteins and thin intertwining strands of collagen fibers, synthesized by cardiac fibroblasts.[58] This network ensures tissue strength and allows cell-cell contact between neighboring cells.[59] Cardiac fibrosis is the inappropriately high amount of collagen deposition in the heart during pathophysiological remodeling, which hampers electrical conduction and enables the development of arrhythmias.[60] In addition, also cardiomyocyte fiber orientation plays an important role in the propagation of the electrical signal and fiber disarray can further facilitate the generation of ventricular arrhythmias.[61,62] This was recently shown in a study that combined data from neonatal rat cardiomyocytes and computer models.[63]

Fibrosis can be divided into replacement fibrosis (compact and patchy) and reactive fibrosis (interstitial and diffuse).[7] Typical examples of these four different forms we published before and are expressed in figure 1 of a review article by the de Jong *et al.* (2011).[64] Replacement fi-

brosis occurs after clearance of dead myocytes, where cardiac cells will be replaced by collagen fibers facilitating the preservation of the structure of the myocardium as well as the clearance of debris.[64] This normally includes compact or patchy fibrosis that is generated after an infarct or in due to chronic pressure overload. These processes have been described both in patients and in experimental animal models.[65] Compact fibrosis is created, when a whole area is replaced by fibrosis and no viable myocytes are left. Although this seems to be dramatic for the cardiac contractile performance, this form is the least arrhythmogenic.[66] Patchy fibrosis describes areas, where fibrosis and myocardial cells are confounded. In this case, collagen fibers are long strands disturbing the electrical signal propagation.[67] Reactive fibrosis describes the process when more collagen is produced than degraded without a loss of viable cardiomyocytes. This includes interstitial and diffuse fibrosis and can be caused by mutations and changes in gene expression, a phenotypical switch from fibroblasts into myofibroblasts, as well as due to aging.[68] Interstitial fibrosis is localized in between the individual cells. High interstitial collagen content causes reduced compliance and electrical impairment[69] possibly leading to arrhythmias and heart failure.[70] Diffuse fibrosis is comparable to patchy fibrosis, however, the collagen strands are short and this form is less arrhythmogenic.[71]

In murine animal models that can be followed and analyzed at different time points after the experimental intervention has been made, chronic pressure overload initially leads to reactive fibrosis and in later stages this may change into a heterogeneous deposition of replacement fibrosis. The switch is likely caused by the fact that at a certain time point proper nutrient supply to the cells fails to maintain a minimal level.[72]

Myocardial fiber disarray is the result of altered fiber orientation after e.g., an infarct. Adjacent cardiomyocytes are then mostly aligned in a perpendicular way or obliquely to each other in or around the collagen.[73] Nowadays, predominantly computer models are used to simulate possible alterations and effects on electrical propagation caused by fiber disarray. Computer models are by definition artificial and similarly to genetic engineered animal models, care should be taken by extrapolating these results to the human heart. However, these mathematical models may provide valuable additive insight, since they allow studying the effects induced by individual alterations but also the summation of more than one altered factor can be studied systemically. With such models, risk of cardiac death can be predicted in e.g. long QT patients and various factors can be implemented at the same time like cell size, wall thickness, action potential duration and fibrosis.[74]

In DCM predominantly patchy areas of interstitial and replacement fibrosis can be found, but also perivascular patterns have been described.[7,75] In HCM patients, interstitial fibrosis predominates.[7] In mice with chronic pressure overload, next to hypertrophy, increased levels of interstitial fibrosis have been reported in many cases.[48,65,76] Moreover, myocardial disarray is one of the hallmarks of HCM.[73] Although it is also present in other cardiac diseases and even in physiologically aged hearts, through the presence in high quantities it is specific for HCM making it a highly sensitive and useful marker.[77]

In ICM, infarcted myocytes are replaced predominantly by heterogeneously distributed replacement- and interstitial fibrosis creating islands of cardiomyocytes surrounded by scar tissue.

This so-called 'labyrinth' of viable strands of cardiomyocytes surrounded by insulating areas of fibrosis creates disconnection of myocytes that leads to excitation blocks and arrhythmias.[78,79] In murine infarct models, fiber disarray has been reported in the infarct border zone, although to a much lesser extent than in HCM.[80]

ACM is characterized by degeneration of cardiomyocytes and fibro-fatty replacement.[24] One theory is that altered cell-cell adhesion due to mutations in genes encoding for structures of the intercalated disc, e.g., the desmosomes, causes injuries to myocytes. This promotes cell death and leads to replacement by fibro-fatty tissue.[25] Histologically, analysis of fibrosis and fiber orientation can help to diagnose any of the diseases above described. Moreover, in all diseases, fibrosis leads to conduction blocks, which increase the propensity to develop reentry arrhythmias, or promotes the manifestation of ectopic impulse generation in relatively uncoupled clusters of cardiomyocytes due to disease-induced remodeling of the expressed ion channels.

ELECTRICAL COUPLING - GAP JUNCTIONS

Gap junctions in the heart are agglomerates of channels that connect the cytoplasm of two adjoining cells allowing electrical coupling between the cardiomyocytes as well as the exchange of certain small molecules, metabolites and ions up to a size of approximately 1 kDa.[81,82] One gap junction channel consists of two hemi-channels (connexons), each delivered by one of the two adjoining cells (Figure 1). The two connexons dock in the intercellular space to form a functional channel. The connexons are composed of connexin proteins. In cardiomyocytes the three main isoforms that are expressed are Connexin-40 (Cx40), Connexin-45 (Cx45), and Connexin-43 (Cx43) with Cx43 being predominant in ventricular cardiomyocytes.

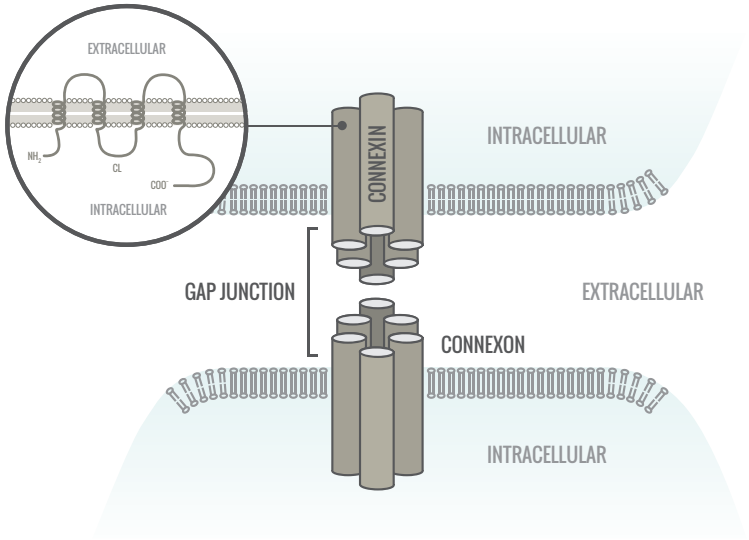

Figure 1. The cardiac gap junction. Gap junctions are located in the intercalated disc. They consist of two hemichannels (connexons) connecting across the intercellular space. Each hemichannel is provided by one cell and connexons are composed of six hexagonally arranged connexin proteins.

Together with adherens junctions and desmosomes, gap junctions are localized in the intercalated disc (ID), a step-like specialized membrane structure at the longitudinal cell edges between two cells (Figure 2). In those ID's, gap junctions are normally present in the regions parallel (interplicate) to the longitudinal axis of the cardiomyocytes.[80]

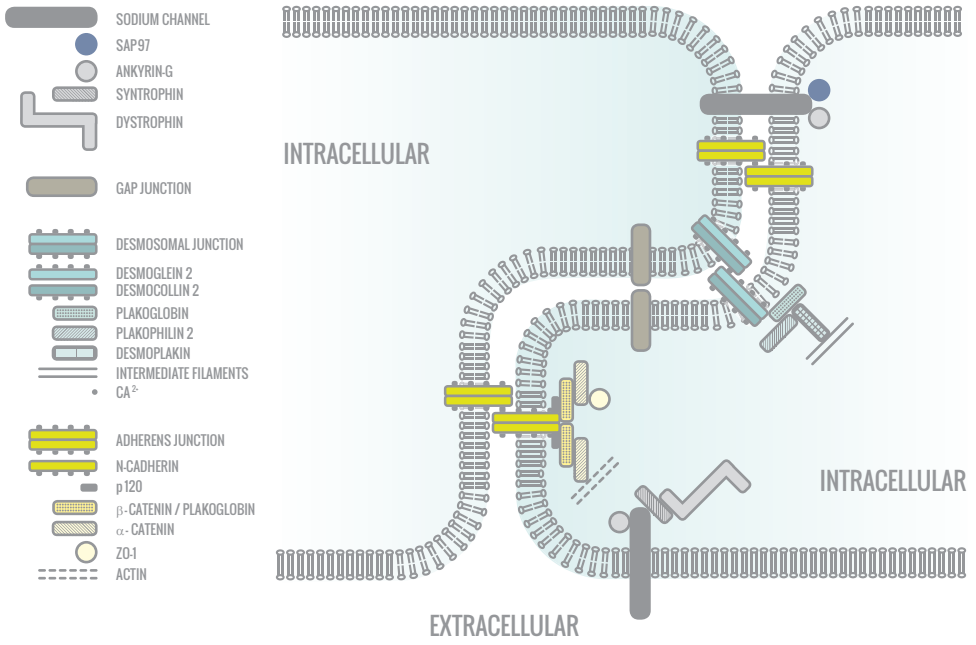

Figure 2. The intercalated disc (ID). The intercalated disc is the region between two cardiomyocytes, where different junctions are located: Gap junctions, adherens junctions, and desmosomal junctions as well as ion channels. They all form macromolecular protein complexes with different functions.

In patients of all four types of cardiac disease, a reduction in ventricular Cx43 localized at the ID has been found.[45,83,84] Using genetically engineered animal models, a plethora of data have been collected regarding to role of Cx43, using Cx43 knock out (KO) animal models. In 1995, the first Cx43 KO model revealed that these mice died perinatally due to major heart problems (malformation of the outflow tract) and cardiac failure.[85] Since then, conditional Cx43 KO mice and haploinsufficient animals have been generated. Nevertheless, results obtained from studies with heterozygous KO animals are contradicting. Mice showed reduced expression of Cx43 up to 50%, and in some studies this reduction resulted in reduced conduction velocity,[86-88] while other studies in which a similar reduction in Cx43 was achieved, no alterations in conduction velocity were reported.[13,89-91] These contradicting results triggered to invent a different approach to reduce Cx43 expression, and also to circumvent the problem of perinatal death in homozygous KO mice. This was achieved through generation of two conditional KO mouse models.[92] In the first model, one coding region of the Cx43 gene was replaced by the fusion construct Cre-

ER(t) and the other Cx43 allele was flanked by loxP [93] resulting in a 50% reduced expression of Cx43 under basic conditions ($Cx43^{CreER(t)/fl}$). Exposure to an agent activating the Cre recombinase (e.g., Tamoxifen) resulted in a further reduction of Cx43 expression up to maximally 95%.[13] In the second model, the Cre gene was placed behind an alpha-myosin heavy-chain (αMHC) promoter resulting in the deletion of the floxed Cx43 gene ($\alpha MHC\text{-}Cre/Cx43^{fl/fl}$), once the promoter got activated.[94] In this way, the Cx43 gene was knocked out around birth allowing those animals to develop normally during gestational stages. In both models, mice died due to arrhythmias. In the case of the $\alpha MHC\text{-}Cre/Cx43^{fl/fl}$ mice death occurs around 1 or 2 months after birth[94] and in the case of the $Cx43^{CreER(t)/fl}$ mice died within 1 month after induction of the deletion.[95]

In cell cultures of neonatal mouse cardiomyocytes with genetically reduced levels of Cx43, no differences in action potential amplitude or minimum diastolic potential could be found compared to wild type cells. However, dV/dtmax and action potential duration was increased.[96] Also intercellular conductance was reduced and propagation was slower and highly discontinuous.[97] In tissue strands composed of these cells and wild type cells, propagation velocity decreased significantly, when the amount of wild type cells was less than 50%. Again, excitation between wild the two types of cells was highly discontinuous.[98]

In humans, DCM is linked to a reduced expression of Cx43, especially seen together with lateralization.[99-102] In animal models this observation was confirmed repeatedly. In mice with forced retinoic acid signaling,[103] Cx43 expression was reduced and lateralized, with in one study some upregulation of Cx40 in the ventricles.[104] This led to an increase in QRS duration, a reduction in conduction velocity and an increased spatial dispersion of conduction velocity.[103,104] Cx43 downregulation was also confirmed in mice with a knockout of muscle LIM protein (an acronym of the three gene products Lin-11, Isl-1 and Mec-3),[105] and in a guinea pig model of chronic pressure overload.[106] However, in another mouse model with longstanding pressure overload, no reductions in total Cx43 could be observed, but 44% of the animals displayed arrhythmias.[76] In a rabbit DCM model of a combined volume and pressure overload, reduced mid-myocardial Cx43 was reported, QRS duration was prolonged and arrhythmias were inducible.[46] Besides this animal model, another DCM rabbit model induced by volume overload showed a reduction in Cx43 expression in different groups.[107,108] In a dog model of DCM (induced by RV pacing), lateralized Cx43 expression was described and immunofluorescent signals were decreased in the left ventricle, but not in the right. Moreover, arrhythmias could be induced and QRS duration was prolonged. This was associated with a reduced longitudinal and transversal conduction velocity in both LV and RV.[109] It was also reported that downregulation of Cx43 triggered fibrosis formation after pressure overload thereby connecting the different passive changes in the heart.[110] The latter study showed that the severity of fibrosis could directly be related to the amount of Cx43 downregulation.

In HCM patients, in an early stage of the disease, an initial increase in Cx43 expression was described together with extensive lateral staining. In later stages, Cx43 was reduced and heterogeneously distributed.[101] Other groups showed a reduction in Cx43 without lateralization, or even lateralization without changes in Cx43 expression levels.[83,111] Animal models confirm

some of the observed changes in humans. As already described in the hypertrophy section, in a rat model where HCM was induced using monocrotaline, a decrease in Cx43 expression at the ID with lateralization was shown[51] resulting in reduced longitudinal conduction velocity. The transverse conduction velocity and also cell width were unaltered. The reduced longitudinal conduction velocity was probably not caused by the overall diminishing of Cx43, because normally mild changes in coupling do not affect conduction velocity. Moreover, increased lateral expression of Cx43 and hypertrophy did not sufficiently lower resistance perpendicular to the fiber orientation to alter transversal conduction velocity.[13,112,113] More likely the altered source/sink ratios due to the changed axial/perpendicular resistance ratio might have influenced the conduction velocity. In another rat model, where chronically elevated pulmonary pressure triggered development of HCM, the overall amount of Cx43 remained the same, but it was heterogeneously distributed.[114] In two different rabbit models of HCM (one with a mutation in troponin-1 and one with the beta-MyHC-Q403 mutation), a significant increase in total mid-myocardial expression of Cx43 has been described, including phosphorylated Cx43.[115,116] In an UM-X7.1 cardiomyopathic hamster model of HCM (leading to loss of cytoskeletal delta-sarcoglycan protein and therefore to cardiac remodeling, failure, and mortality) hypertrophy, a decrease in Cx43 mRNA, increased amounts of fibrosis and arrhythmias were seen after 20 weeks.[117,118] Cardiac hypertrophy and heart failure can also be induced by overexpression of constitutively active form of cardiac Calcineurin-A (CnA) in the mouse heart. Next to hypertrophy these mice develop rapidly after birth extensive amounts of fibrosis and show a high incidence of arrhythmias.[119] In this model reduced Cx43 signals in the IDs and decreased conduction velocity can be observed.[120] In mice undergoing TAC, heterogeneous and partly reduced signals of Cx43 have been reported leading to dispersed impulse conduction.[48,76]

In ICM, ischemia reduces gap junction permeability and induces lateralization of Cx43.[83,121,122] The infarct border zone (the region bordering healthy and infarcted tissue) will, in that respect, be most at risk of remodeling. Already in 1991, Smith *et al.* reported gap junction remodeling in this zone, including reduced and lateralized Cx43 signals.[80] This was also confirmed in dogs[123-125] and patients.[45] In patients, alterations were even detected at areas distant from the border zone.[101] Moreover, an upregulation in Cx45 could be observed in the border zone, resulting in reduced gap junctional communication due to the intrinsic different properties of the Cx45 gap junction channels.[126] The observation of reduced and heterogeneously distributed Cx43 could also be confirmed in rabbit models.[127] However, in transgenic mice with 50% of the normal Cx43 expression level, the post-infarction area was smaller than in controls.[128] This would suggest that preservation of Cx43 is not per se beneficial for maintenance of function of the infarcted heart. Zhang *et al.* (2010) even proposed to be careful with increasing Cx43 expression in heart diseases until the meaning of alterations in expression of Cx43 upon myocardial infarction is fully understood.[129] We have to keep in mind, however, that Cx43 gap junction channels not only are responsible for propagation of the electrical impulse in the heart, but also for metabolic coupling of the cardiomyocytes. In that respect, a smaller infarct size might rely on a reduced spreading of pro-apoptotic death signals due to a reduced level of intercellular coupling.

In ACM, reduced Cx43 expression has been reported in several studies. Theories are that Cx43 remodeling is triggered by abnormal mechanical coupling to mutations in proteins composing junctions that support the structure of the cardiomyocytes.[84] The different junctions in the ID assemble and form clusters. Therefore, dysfunction of one junction/protein influences the functioning of others.[130] In human studies, heterogeneous disturbances in Cx43 signals, decreased presence in the intercalated disc, and lateralization of the signal has been reported in all different forms of ACM.[84,131] Although previously thought that this would predominantly be in the right ventricle, these changes are not exclusive and can also be found in the left ventricle and the septum.[132] In general, this leads to scattered impulse conduction, which increases the susceptibility to arrhythmias.[133] In the first attempts to investigate ACM in animal models, Plakophilin-2 (PKP-2) mutations (the most abundant mutated desmosomal protein in humans) were used. In mice, homozygous null mutations in PKP-2 are lethal whereas heterozygous mutations do not show any or only little phenotype.[134,135] Therefore, it is suggested that the abundant phenotypical presentation of ACM in patients is, on top of the genetic mutation, dependent on additional factors (e.g., inflammation, exercise). To study the familial cases, initially, two different familial forms of ACM have been studied with mutations in desmosomal genes different from PKP-2: Naxos disease [mutation in Plakoglobin (PKG)];[136-138] and Carvajal- syndrome [Desmoplakin (DPK)].[139,140] In patients, in both diseases, Cx43 is reduced in both ventricles in the early phase of the disease and an increase in non-phosphorylated Cx43 was detected that might be associated with accelerated down-regulation of the protein.[84,141] An *in vitro* model for Naxos disease using neonatal rat cardiomyocytes transfected with an adenovirus encoding the PKG 2057del2 mutation recapitulated all abnormalities seen in patients: reduced Plakoglobin and Cx43 signal at the IDs, increased apoptosis and secretion of inflammatory mediators.[142] Moreover, a zebrafish model with the same mutation was used to screen for potential drugs to intervene with the development and progression of ACM.[142] This latter study revealed promising results for future therapy since disease-causing targets could be identified and in vitro studies showed prevention and even regression of the disease when the intervention was applied in the early phases of cardiac remodeling (as discussed in the addendum to chapter 8).

Excitability

Proper contraction of the heart also results from a finely tuned impulse generation, which feeds propagation. In ventricular cardiomyocytes, action potential generation is initiated by the fast and robust depolarization as caused by the opening of the voltage-dependent Na^+ channels.[143] Already in 1921, Daly and Clark showed in frogs that rate, propagation velocity and force of the cardiac contraction were reduced in solutions containing a reduced (extracellular) sodium concentration.[144]

The human sodium channel consists of one alpha and four beta subunits. The alpha subunit consists of four homologous domains connected by cytoplasmic linkers (Figure 3). Each of those domains consists in turn of six transmembrane sequences.[145]

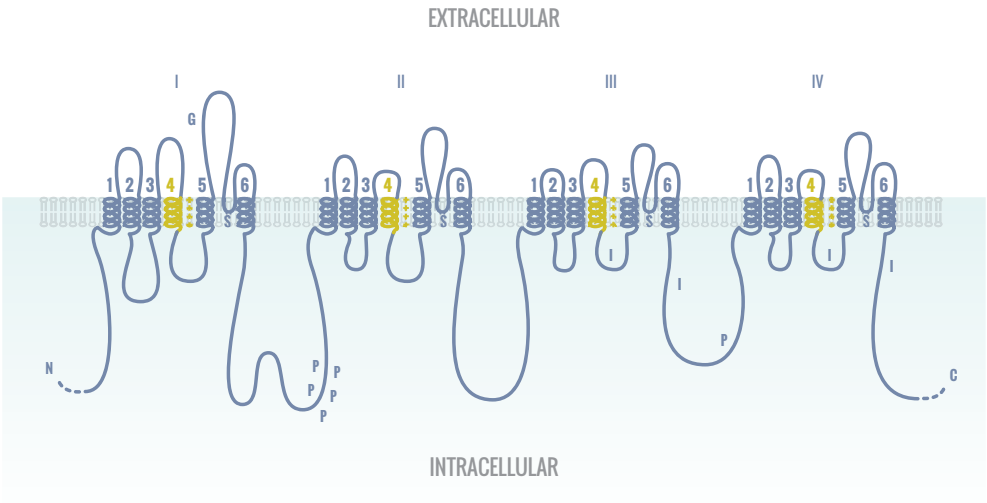

Figure 3. The alpha subunit of the human sodium channel. The alpha subunit of the human sodium channel consists of four homologous domains connected by cytoplasmic linkers. Each domain is composed of six trans-membrane sequences. G, glycosylation; P, phosphorylation; S, ion selectivity; I, inactivation sites. Positive (+) charges in S4 are crucial for transmembrane voltage sensing.

In cardiomyocytes two different pools of $Na_V1.5$ channels co-exist, namely at the lateral membranes where the channel interacts with the dystrophin-syntrophin complex and in the ID where it binds SAP97 (Figure 2).[10] Both pools are thought to interact with different proteins. At the ID, it is envisioned that $Na_V1.5$ can influence e.g., Cx43 in the gap junctions and *vice versa*.[146] Initially, much work on excitability has been performed in vitro using neonatal rat cardiomyocytes. Lateron, *in vivo* experiments on reduced excitability have been performed in genetically engineered mice models. SCN5a haploinsufficient mice showed about a 50% reduction of so-

dium current, while having a normal survival rate.[147] ECG analysis showed a prolonged RR interval, P-wave duration, PR interval, QRS duration, and QT interval together with an age related aggravation of the phenotype.[148] In those SCN5a haploinsuffient mice, QRS prolongation and conduction slowing was observed. However, in young mice, epicardial conduction velocity was not reduced in the left ventricle and only mildly reduced in the right. The reduction in conduction velocity became more dominant in both ventricles in older mice (12–17 months) where it was associated with increased fibrosis and altered Cx43 expression.[149]

In patients with the 1795InsD mutation in the *SCN5a* gene, bradycardia, conduction delay, QT prolongation, and right precordial ST-elevation can be detected. To investigate the cause of sodium channel related diseases, and in particular the above mentioned one, Remme *et al.* created a 1798InsD mouse model, which is the mouse analog of 1795InsD in human, where indeed a single mutation leads to a phenotype of bradycardia, right ventricular conduction slowing, and QT prolongation.[150] Given the enormous amount of sodium channel mutations leading to a pro-arrhythmic phenotype in patients, generation of such mouse models significantly has contributed to a better understanding of the underlying etiology. In a DCM dog model, in which disease was induced through RV pacing, neither sodium current density, nor upstroke velocity of the action potential in left ventricular endo- or epicardial myocytes differed from control individuals.[47,151] Similarly, in a DCM rabbit model, sodium current density did not differ from controls in left ventricular myocytes.[46] Recent data from a Torsade de Pointes sensitive canine heart model after chronic AV block (CAVB) confirm that no changes in I_{Na} appear, although increased cell size was reported.[133]

HCM patients showed increased CaMKII phosphorylation of $Na_v1.5$ channels, which is in general associated with a delayed inactivation of the current.[152,153] Increased late sodium current leads to prolonged repolarization (and therefore an increased action potential duration) and arrhythmias as has been shown in patients and several animal models.[153-157] Increased late sodium current also causes changes in calcium metabolism and homeostasis, influencing cell metabolism and contractile functioning of the cells. This in turn may lead to hypertrophy.[153] In mice with Calcineurin-induced cardiac hypertrophy, reduced $Na_V1.5$ protein and RNA amounts could be found in the IDs.[120]

ICM is also associated with increased late I_{Na}.[158,159] Various causes can lead to an increase of intracellular sodium concentration in ischemic cardiomyocytes. First, ischemia seems to increase the amplitude of the late I_{Na} significantly.[160] Anaerobic glycolysis, due to lack of sufficient oxygen supply to the cells, leads to a decrease of ATP and leaking of protons via the cardiac Na/H exchanger (NHE1). Because of that, more sodium enters the cell.[161] Moreover, a reduction of Na^+/K^+ ATPase pump activity will cause an additional decrease of sodium extrusion.[162] Increased sodium levels will activate the Na/Ca exchanger. This, in turn, leads to an increased concentration of calcium in the cell and a reduction in intracellular pH. The altered ion concentrations will lead to drastic changes in cellular metabolism, signal transduction, electrophysiological characteristics and contractile properties, probably leading to cell damage and cell death.[163-165]

In the early stages of hypoxia, an increase in intracellular sodium concentration was observed in rat hearts that returned back to pre-infarction levels, when ischemia was of short duration.[161] When sodium is persistently elevated, the subsequent increased calcium levels may be prevented by late sodium current inhibition through ranolazine.[166] Moreover, a NHE1 inhibitor has been reported to show cardio-protective effects after infarction in a rat model.[167] Although controversial results have been published later on about NHE1, it is still under investigation and thought to be one of the most effective post-infarct treatments.[168] Next to adherens-, gap- and desmosomal junctions, also ion channels are located in the ID and it becomes more and more clear that in ACM alterations in subcellular localization of sodium channels is importantly involved in the consequences of cardiac remodeling.[169] In patients, a reduced localization of $Na_V1.5$ in the ID has been reported.[131] In cultured cardiomyocytes, the reduced expression of PKP-2, caused a subsequent reduction in the sodium current and a slower conduction velocity.[170] Besides that, loss of expression of Ankyrin-G, an important protein that anchors the voltage-gated sodium channel, leads to disturbances in PKP-2 and Cx43 expression. The other way around, loss of PKP-2 causes a reduction in expression of Ankyrin-G as well as of $Na_V1.5$, thereby confirming the role of sodium channels in this disease.[171] Besides that, in zebrafish and neonatal rat cardiomyocytes containing the mentioned 2057del2 Plakoglobin (related to Naxos disease), a marked reduction in I_{Na} current density was observed.[142] In these neonatal rat cardiomyocytes, the immunofluorescent $Na_V1.5$ signal at the membrane was reduced, but total cell content appeared unchanged.[142] This reduction in I_{Na} and consequently a reduced conduction velocity has also previously been shown in transgenic mice with a Desmoglein-2 mutation.[172] Moreover, reduced heterogeneous expression of Cx43 in conditional knockout mice caused decreased expression of $Na_V1.5$, reduced sodium current and an increased vulnerability of those mice for arrhythmias.[110] Similarly, PKP-2 haploinsufficiency in mice resulted in a sodium current deficit and arrhythmogenesis when triggered with flecainide.[173] The importance of these finding was reflected in a study of Cerrone *et al.* which showed that in patients with a mutation in PKP-2, provocation with flecainide triggered arrhythmias suggesting that also in these patients a concomitant sodium current deficit existed.[174]

Heterogeneity

The natural mode of functional heterogeneity within the normal cardiac performance is also of importance during heart disease. Due to, e.g., pulmonary disease or aortic stenosis, different parts of the heart are affected prior to the other, leading to heterogenic alterations that conflict with the natural organization. In ACM, where disease-dependent changes often start in the right ventricle, the left ventricle can remain relatively unaffected in the early stages of disease.

In an opposite fashion aortic stenosis will first remodel the left ventricle before right ventricular involvement manifests. Differently, right ventricular remodeling due to pulmonary hypertension might simultaneously trigger LV remodeling (atrophy) due to a reduced filling.[52]
These different types of remodeling are part of various diseases and are by definition heterogeneous, since all of those diseases have different causes and therefore treatment options.[175]
Cardiac remodeling deteriorating into heart failure most likely depends on a combination of the mechanisms as described in this article, and it is characterized by heterogeneous remodeling of excitation-contraction coupling.[176,177] Pathophysiological heterogeneity in cardiac tissue sustains ventricular tachycardia, stabilizes reentry arrhythmias and provides substrate for sustained tachycardia.[177,178]
Passive heterogeneous ventricular remodeling in the heart is one of the most destructive features of cardiac remodeling and every remodeling mechanism itself shows the worst outcome, when occurring heterogeneously. In this article, several mechanisms of passive remodeling have been described during DCM, HCM, ICM and ACM. Passive remodeling of tissue architecture was investigated focusing on fibrosis, alterations in cell size, hypertrophy and fiber disarray. Disturbances in electrical coupling were discussed by describing changes in the distribution of the gap junction protein Cx43. Remodeling of electrical excitability was studied using the sodium channel protein $Na_V1.5$.
To summarize, different types of fibrosis occur in all of the four discussed heart diseases and act as modulators of impulse propagation ranging from conduction slowing, increased dispersion of conduction and even conduction block. Moreover, it can alter the structure of the heart, e.g., alterations in cellular dimensions, which is caused by modifications in molecular pathways that control normal cellular physiology. As a consequence this may lead to reductions in excitability and cell-to-cell conduction.[71,78] Heterogeneously distributed fibrosis can even create a "labyrinth" in the heart facilitating reentry arrhythmias.[179] Therefore, this is considered to be worse than only local interstitial fibrosis since it would be more difficult for electrical signals to propagate though a labyrinth of fibrotic patches than only being obstructed by single fibers.[71,180] This idea was strengthened by a study where reduction of heterogeneous patchy fibrosis was one-on-one correlated to a reduction of arrhythmias.[181]
Hypertrophy can be detected in HCM and ICM. Changes in cell size are the key features of HCM and DCM, whereby HCM is characterized by an increase in cell width and DCM by an increase in cell length. Myocardial fiber disarray mainly occurs in HCM, where it is even used as a biomarker. It can also be observed in ICM, but to a much lesser extend. Heterogeneously distributed hypertrophy, myocardial fiber disarray and changes in cell size can lead to alterations in impulse propagation and conduction velocity causing disturbed signaling, deregulated contractions, and eventually heart failure.[37-39,44] Pathophysiological heterogeneity in the sense of right *vs.* left ventricles or atria can also worsen disease phenotype as is classically illustrated by the fact that progressive LV dysfunction eventually results in RV failure too with consequently, pulmonary remodeling and edema.[182]
Heterogeneous distribution, de-phosphorylation and a reduction of Cx43 signals in the ID are characteristics found in all four different heart diseases. They are one of the key features of

ACM,[131] but also occur in DCM, ICM, and late stages of HCM. This can lead to a reduction in longitudinal and an increase in transverse conduction (reducing the normal anisotropic mode of conduction) causing heterogeneous propagation (increased dispersion of conduction) and arrhythmogenesis. At these places signaling (mechanical or electrical) will be more difficult leading to deregulated intercellular coupling.[76] The heterogeneous distribution of the different proteins and structures can be sub-divided into macro and micro heterogeneity. Macro heterogeneity compares the different regions in the heart, whereas micro heterogeneity is a measure for local heterogeneity.[110]

Changes in expression and distribution of the sodium channel protein $Na_V1.5$ can also be seen in HCM, DCM, and ACM. Homogeneous distribution of $Na_V1.5$ throughout different parts of the heart is crucial for normal conduction, although functional expression levels differ between epicard, endocard, and conduction system.[9,143] Heterogeneous distribution, caused by a local increase or decrease of sodium channels possibly facilitates arrhythmogenesis and therefore heart failure, since the sodium current will be hampered or fastened locally.[183,184] Although these heterogeneous maladaptations can have effects when occurring alone, they are often found to trigger arrhythmias and eventually heart failure due to a combination of simultaneous alterations in different factors. Therefore, great care should be taken when investigating one single mechanism of remodeling, since a heterogeneous adaptation of one mechanism can also cause others to develop or are even linked to each other. This concept is illustrated by several studies, which report a simulataneous downregulation and de-phosphorylation of Cx43, and $Na_V1.5$,[90,131,185] and even link this combination to an increased deposition of fibrotic materials.[149] These studies example the complexity of cardiac remodeling during pathophysiology in relation to the increase in propensity to develop arrhythmias.

Regarding the future perspective of cardiac research, one should focus on these connections between heterogeneous changes in single factors within the heart that lead to the total picture of heterogeneous remodeling. This might unravel currently unknown relationships between the various forms of maladaptation and help to improve the search for treatment options. In a study that was mentioned before, long term administration of the antihypertensive drugs eplerenone or losartan in a mouse model of extreme aging not only reduced the amount of interstitial and patchy fibrosis, but also preserved a homogeneous pattern of gap junctional coupling. This preservation of the normal substrate for conduction resulted in a significantly reduced amount of arrhythmias.[181] Beyond pharmacological interventions, pacing strategies (like cardiac resynchronization therapy) that aim to correct the abnormal sequence of activation, e.g., due to bundle branch block or electrical remodeling, will provide further future perspectives to improve performance of the remodeled heart.

References

1. Kemp CD, Conte JV. The pathophysiology of heart failure. Cardiovasc Pathol.2012;21(5):365-371.

2. Lloyd-Jones DM, Larson MG, Leip EP, et al. Lifetime risk for developing congestive heart failure: the Framingham Heart Study. Circulation.2002;106(24):3068-3072.

3. van Rijen HV, van Veen TA, Gros D, Wilders R, de Bakker JM. Connexins and cardiac arrhythmias. Adv Cardiol.2006;42:150-160.

4. Roger VL, Go AS, Lloyd-Jones DM, et al. Heart disease and stroke statistics--2011 update: a report from the American Heart Association. Circulation.2011;123(4):e18-e209.

5. Westerhof N, O'Rourke MF. Haemodynamic basis for the development of left ventricular failure in systolic hypertension and for its logical therapy. J Hypertens.1995;13(9):943-952.

6. Lee CS, Tkacs NC. Current concepts of neurohormonal activation in heart failure: mediators and mechanisms. AACN Adv Crit Care.2008;19(4):364-385; quiz 386-367.

7. Swynghedauw B. Molecular mechanisms of myocardial remodeling. Physiol Rev.1999;79(1):215-262.

8. Zimmer HG. Some aspects of cardiac heterogeneity. Basic Res Cardiol.1994;89(2):101-117.

9. Remme CA, Verkerk AO, Hoogaars WM, et al. The cardiac sodium channel displays differential distribution in the conduction system and transmural heterogeneity in the murine ventricular myocardium. Basic Res Cardiol.2009;104(5):511-522.

10. Petitprez S, Zmoos AF, Ogrodnik J, et al. SAP97 and dystrophin macromolecular complexes determine two pools of cardiac sodium channels Nav1.5 in cardiomyocytes. Circ Res.2011;108(3):294-304.

11. Strom M, Wan X, Poelzing S, Ficker E, Rosenbaum DS. Gap junction heterogeneity as mechanism for electrophysiologically distinct properties across the ventricular wall. Am J Physiol Heart Circ Physiol.2010;298(3):H787-794.

12. Kleber AG, Rudy Y. Basic mechanisms of cardiac impulse propagation and associated arrhythmias. Physiol Rev.2004;84(2):431-488.

13. van Rijen HV, Eckardt D, Degen J, et al. Slow conduction and enhanced anisotropy increase the propensity for ventricular tachyarrhythmias in adult mice with induced deletion of connexin43. Circulation.2004;109(8):1048-1055.

14. Bowers SL, Borg TK, Baudino TA. The dynamics of fibroblast-myocyte-capillary interactions in the heart. Ann N Y Acad Sci.2010;1188:143-152.

15. Towbin JA, Lowe AM, Colan SD, et al. Incidence, causes, and outcomes of dilated cardiomyopathy in children. JAMA.2006;296(15):1867-1876.

16. Mestroni L, Rocco C, Gregori D, et al. Familial dilated cardiomyopathy: evidence for genetic and phenotypic heterogeneity. Heart Muscle Disease Study Group. J Am Coll Cardiol.1999;34(1):181-190.

17. Hershberger RE, Hedges DJ, Morales A. Dilated cardiomyopathy: the complexity of a diverse genetic architecture. Nat Rev Cardiol.2013;10(9):531-547.

18. Richardson P, McKenna W, Bristow M, et al. Report of the 1995 World Health Organization/International Society and Federation of Cardiology Task Force on the Definition and Classification of cardiomyopathies. Circulation.1996;93(5):841-842.

19. Maron BJ. Hypertrophic cardiomyopathy: a systematic review. JAMA.2002;287(10):1308-1320.

20. Maron BJ, Maron MS, Semsarian C. Genetics of hypertrophic cardiomyopathy after 20 years: clinical perspectives. J Am Coll Cardiol.2012;60(8):705-715.

21. Efthimiadis GK, Pagourelias ED, Gossios T, Zegkos T. Hypertrophic cardiomyopathy in 2013: Current speculations and future perspectives. World J Cardiol.2014;6(2):26-37.

22. Wu AH. Management of patients with non-ischaemic cardiomyopathy. Heart.2007;93(3):403-408.

23. Corrado D, Basso C, Thiene G. Arrhythmogenic right ventricular cardiomyopathy: diagnosis, prognosis, and treatment. Heart.2000;83(5):588-595.

24. Thiene G, Nava A, Corrado D, Rossi L, Pennelli N. Right ventricular cardiomyopathy and sudden death in young people. N Engl J Med.1988;318(3):129-133.

25. Saffitz JE, Asimaki A, Huang H. Arrhythmogenic right ventricular cardiomyopathy: new insights into disease mechanisms and diagnosis. J Investig Med.2009;57(8):861-864.

26. Rampazzo A, Nava A, Malacrida S, et al. Mutation in human desmoplakin domain binding to plakoglobin causes a dominant form of arrhythmogenic right ventricular cardiomyopathy. Am J Hum Genet.2002;71(5):1200-1206.

27. Asimaki A, Syrris P, Wichter T, Matthias P, Saffitz JE, McKenna WJ. A novel dominant mutation in plakoglobin causes arrhythmogenic right ventricular cardiomyopathy. Am J Hum Genet.2007;81(5):964-973.

28. Gerull B, Heuser A, Wichter T, et al. Mutations in the desmosomal protein plakophilin-2 are common in arrhythmogenic right ventricular cardiomyopathy. Nat Genet.2004;36(11):1162-1164.

29. van Tintelen JP, Entius MM, Bhuiyan ZA, et al. Plakophilin-2 mutations are the major determinant of familial arrhythmogenic right ventricular dysplasia/cardiomyopathy. Circulation.2006;113(13):1650-1658.

30. Heuser A, Plovie ER, Ellinor PT, et al. Mutant desmocollin-2 causes arrhythmogenic right ventricular cardiomyopathy. Am J Hum Genet.2006;79(6):1081-1088.

31. Syrris P, Ward D, Evans A, et al. Arrhythmogenic right ventricular dysplasia/cardiomyopathy associated with mutations in the desmosomal gene desmocollin-2. Am J Hum Genet.2006;79(5):978-984.

32. Pilichou K, Nava A, Basso C, et al. Mutations in desmoglein-2 gene are associated with arrhythmogenic right ventricular cardiomyopathy. Circulation.2006;113(9):1171-1179.

33. Beffagna G, Occhi G, Nava A, et al. Regulatory mutations in transforming growth factor-beta3 gene cause arrhythmogenic right ventricular cardiomyopathy type 1. Cardiovasc Res.2005;65(2):366-373.

34. Merner ND, Hodgkinson KA, Haywood AF, et al. Arrhythmogenic right ventricular cardiomyopathy type 5 is a fully penetrant, lethal arrhythmic disorder caused by a missense mutation in the TMEM43 gene. Am J Hum Genet.2008;82(4):809-821.

35. Otten E, Asimaki A, Maass A, et al. Desmin mutations as a cause of right ventricular heart failure affect the intercalated disks. Heart Rhythm.2010;7(8):1058-1064.

36. van der Zwaag PA, van Rijsingen IA, Asimaki A, et al. Phospholamban R14del mutation in patients diagnosed with dilated cardiomyopathy or arrhythmogenic right ventricular cardiomyopathy: evidence supporting the concept of arrhythmogenic cardiomyopathy. Eur J Heart Fail.2012;14(11):1199-1207.

37. Winterton SJ, Turner MA, O'Gorman DJ, Flores NA, Sheridan DJ. Hypertrophy causes delayed conduction in human and guinea pig myocardium: accentuation during ischaemic perfusion. Cardiovasc Res.1994;28(1):47-54.

38. Cooklin M, Wallis WR, Sheridan DJ, Fry CH. Changes in cell-to-cell electrical coupling associated with left ventricular hypertrophy. Circ Res.1997;80(6):765-771.

39. McIntyre H, Fry CH. Abnormal action potential conduction in isolated human hypertrophied left ventricular myocardium. J Cardiovasc Electrophysiol.1997;8(8):887-894.

40. Davis J, Molkentin JD. Myofibroblasts: trust your heart and let fate decide. J Mol Cell Cardiol.2014;70:9-18.

41. Gill C, Mestril R, Samali A. Losing heart: the role of apoptosis in heart disease--a novel therapeutic target? FASEB J.2002;16(2):135-146.

42. Nian M, Lee P, Khaper N, Liu P. Inflammatory cytokines and postmyocardial infarction remodeling. Circ Res.2004;94(12):1543-1553.

43. Vetter FJ, Simons SB, Mironov S, Hyatt CJ, Pertsov AM. Epicardial fiber organization in swine right ventricle and its impact on propagation. Circ Res.2005;96(2):244-251.

44. Myerburg RJ, Kessler KM, Castellanos A. Sudden cardiac death. Structure, function, and time-dependence of risk. Circulation.1992;85(1 Suppl):I2-10.

45. Dupont E, Matsushita T, Kaba RA, et al. Altered connexin expression in human congestive heart failure. J Mol Cell Cardiol.2001;33(2):359-371.

46. Wiegerinck RF, Verkerk AO, Belterman CN, et al. Larger cell size in rabbits with heart failure increases myocardial conduction velocity and QRS duration. Circulation.2006;113(6):806-813.

47. Akar FG, Spragg DD, Tunin RS, Kass DA, Tomaselli GF. Mechanisms underlying conduction slowing and arrhythmogenesis in nonischemic dilated cardiomyopathy. Circ Res.2004;95(7):717-725.

48. Boulaksil M, Noorman M, Engelen MA, et al. Longitudinal arrhythmogenic remodelling in a mouse model of longstanding pressure overload. Neth Heart J.2010;18(10):509-515.

49. Branishte T, Minciuna V, Braniste A. Aspects of molecular mechanisms in myocardial hypertrophy, particular morphological changes and cell bioenergetic characteristics in patients with dilated cardiomyopathy. Rev Med Chir Soc Med Nat Iasi.2013;117(4):851-856.

50. Spach MS, Heidlage JF, Dolber PC, Barr RC. Electrophysiological effects of remodeling cardiac gap junctions and cell size: experimental and model studies of normal cardiac growth. Circ Res.2000;86(3):302-311.

51. Uzzaman M, Honjo H, Takagishi Y, et al. Remodeling of gap junctional coupling in hypertrophied right ventricles of rats with monocrotaline-induced pulmonary hypertension. Circ Res.2000;86(8):871-878.

52. Hardziyenka M, Campian ME, Verkerk AO, et al. Electrophysiologic remodeling of the left ventricle in pressure overload-induced right ventricular failure. J Am Coll Cardiol.2012;59(24):2193-2202.

53. Kannel WB, Dawber TR, Kagan A, Revotskie N, Stokes J, 3rd. Factors of risk in the development of coronary heart disease--six year follow-up experience. The Framingham Study. Ann Intern Med.1961;55:33-50.

54. Zaino EC, Tabor SH. Cardiac Hypertrophy in Acute Myocardial Infarction. A Study Based on 100 Autopsied Cases. Circulation.1963;28:1081-1083.

55. Smiley D, Smith MA, Carreira V, et al. Increased fibrosis and progression to heart failure in MRL mice following ischemia/reperfusion injury. Cardiovasc Pathol.2014;23(6):327-334.

56. Bender SR, Friedman DJ, Markowitz SM, Lerman BB, Okin PM. Electrocardiographic left ventricular hypertrophy predicts arrhythmia and mortality in patients with ischemic cardiomyopathy. J Interv Card Electrophysiol.2012;34(3):237-245.

57. Marcus FI, McKenna WJ, Sherrill D, et al. Diagnosis of arrhythmogenic right ventricular cardiomyopathy/dysplasia: proposed modification of the Task Force Criteria. Eur Heart J.2010;31(7):806-814.

58. Manabe I, Shindo T, Nagai R. Gene expression in fibroblasts and fibrosis: involvement in cardiac hypertrophy. Circ Res.2002;91(12):1103-1113.

59. Weber KT, Sun Y, Tyagi SC, Cleutjens JP. Collagen network of the myocardium: function, structural remodeling and regulatory mechanisms. J Mol Cell Cardiol.1994;26(3):279-292.

60. Krenning G, Zeisberg EM, Kalluri R. The origin of fibroblasts and mechanism of cardiac fibrosis. J Cell Physiol.2010;225(3):631-637.

61. Brugada J, Boersma L, Kirchhof CJ, Heynen VV, Allessie MA. Reentrant excitation around a fixed obstacle in uniform anisotropic ventricular myocardium. Circulation.1991;84(3):1296-1306.

62. Punske BB, Taccardi B, Steadman B, et al. Effect of fiber orientation on propagation: electrical mapping of genetically altered mouse hearts. J Electrocardiol.2005;38(4 Suppl):40-44.

63. Kudryashova NN, Teplenin AS, Orlova YV, Selina LV, Agladze K. Arrhythmogenic role of the border between two areas of cardiac cell alignment. J Mol Cell Cardiol.2014;76:227-234.

64. de Jong S, Zwanenburg JJ, Visser F, et al. Direct detection of myocardial fibrosis by MRI. J Mol Cell Cardiol.2011;51(6):974-979.

65. Xia Y, Lee K, Li N, Corbett D, Mendoza L, Frangogiannis NG. Characterization of the inflammatory and fibrotic response in a mouse model of cardiac pressure overload. Histochem Cell Biol.2009;131(4):471-481.

66. de Bakker JM, van Capelle FJ, Janse MJ, et al. Reentry as a cause of ventricular tachycardia in patients with chronic ischemic heart disease: electrophysiologic and anatomic correlation. Circulation.1988;77(3):589-606.

67. de Bakker JM, van Capelle FJ, Janse MJ, et al. Slow conduction in the infarcted human heart. ‚Zigzag' course of activation. Circulation.1993;88(3):915-926.

68. Biernacka A, Frangogiannis NG. Aging and Cardiac Fibrosis. Aging Dis.2011;2(2):158-173.

69. Rohr S. Myofibroblasts in diseased hearts: new players in cardiac arrhythmias? Heart Rhythm.2009;6(6):848-856.

70. Janicki JS, Brower GL. The role of myocardial fibrillar collagen in ventricular remodeling and function. J Card Fail.2002;8(6 Suppl):S319-325.

71. Kawara T, Derksen R, de Groot JR, et al. Activation delay after premature stimulation in chronically diseased human myocardium relates to the architecture of interstitial fibrosis. Circulation.2001;104(25):3069-3075.

72. Isoyama S, Nitta-Komatsubara Y. Acute and chronic adaptation to hemodynamic overload and ischemia in the aged heart. Heart Fail Rev.2002;7(1):63-69.

73. Hughes SE. The pathology of hypertrophic cardiomyopathy. Histopathology.2004;44(5):412-427.

74. Hoefen R, Reumann M, Goldenberg I, et al. In silico cardiac risk assessment in patients with long QT syndrome: type 1: clinical predictability of cardiac models. J Am Coll Cardiol.2012;60(21):2182-2191.

75. Nakayama Y, Shimizu G, Hirota Y, et al. Functional and histopathologic correlation in patients with dilated cardiomyopathy: an integrated evaluation by multivariate analysis. J Am Coll Cardiol.1987;10(1):186-192.

76. Boulaksil M, Winckels SK, Engelen MA, et al. Heterogeneous Connexin43 distribution in heart failure is associated with dispersed conduction and enhanced susceptibility to ventricular arrhythmias. Eur J Heart Fail.2010;12(9):913-921.

77. Hughes SE, McKenna WJ. New insights into the pathology of inherited cardiomyopathy. Heart.2005;91(2):257-264.

78. Fenoglio JJ, Jr., Ursell PC, Kellogg CF, Drusin RE, Weiss MB. Diagnosis and classification of myocarditis by endomyocardial biopsy. N Engl J Med.1983;308(1):12-18.

79. Weber KT, Sun Y, Diez J. Fibrosis: a living tissue and the infarcted heart. J Am Coll Cardiol.2008;52(24):2029-2031.

80. Smith JH, Green CR, Peters NS, Rothery S, Severs NJ. Altered patterns of gap junction distribution in ischemic heart disease. An immunohistochemical study of human myocardium using laser scanning confocal microscopy. Am J Pathol.1991;139(4):801-821.

81. Elfgang C, Eckert R, Lichtenberg-Frate H, et al. Specific permeability and selective formation of gap junction channels in connexin-transfected HeLa cells. J Cell Biol.1995;129(3):805-817.

82. Noorman M, van der Heyden MA, van Veen TA, et al. Cardiac cell-cell junctions in health and disease: Electrical versus mechanical coupling. J Mol Cell Cardiol.2009;47(1):23-31.

83. Peters NS, Green CR, Poole-Wilson PA, Severs NJ. Reduced content of connexin43 gap junctions in ventricular myocardium from hypertrophied and ischemic human hearts. Circulation.1993;88(3):864-875.

84. Kaplan SR, Gard JJ, Protonotarios N, et al. Remodeling of myocyte gap junctions in arrhythmogenic right ventricular cardiomyopathy due to a deletion in plakoglobin (Naxos disease). Heart Rhythm.2004;1(1):3-11.

85. Reaume AG, de Sousa PA, Kulkarni S, et al. Cardiac malformation in neonatal mice lacking connexin43. Science.1995;267(5205):1831-1834.

86. Guerrero PA, Schuessler RB, Davis LM, et al. Slow ventricular conduction in mice heterozygous for a connexin43 null mutation. J Clin Invest.1997;99(8):1991-1998.

87. Thomas SA, Schuessler RB, Berul CI, et al. Disparate effects of deficient expression of connexin43 on atrial and ventricular conduction: evidence for chamber-specific molecular determinants of conduction. Circulation.1998;97(7):686-691.

88. Eloff BC, Lerner DL, Yamada KA, Schuessler RB, Saffitz JE, Rosenbaum DS. High resolution optical mapping reveals conduction slowing in connexin43 deficient mice. Cardiovasc Res.2001;51(4):681-690.

89. Morley GE, Vaidya D, Samie FH, Lo C, Delmar M, Jalife J. Characterization of conduction in the ventricles of normal and heterozygous Cx43 knockout mice using optical mapping. J Cardiovasc Electrophysiol.1999;10(10):1361-1375.

90. Stein M, van Veen TA, Remme CA, et al. Combined reduction of intercellular coupling and membrane excitability differentially affects transverse and longitudinal cardiac conduction. Cardiovasc Res.2009;83(1):52-60.

91. Stein M, van Veen TA, Hauer RN, de Bakker JM, van Rijen HV. A 50% reduction of excitability but not of intercellular coupling affects conduction velocity restitution and activation delay in the mouse heart. PLoS One.2011;6(6):e20310.

92. Orban PC, Chui D, Marth JD. Tissue- and site-specific DNA recombination in transgenic mice. Proc Natl Acad Sci U S A.1992;89(15):6861-6865.

93. Feil R, Brocard J, Mascrez B, LeMeur M, Metzger D, Chambon P. Ligand-activated site-specific recombination in mice. Proc Natl Acad Sci U S A.1996;93(20):10887-10890.

94. Gutstein DE, Liu FY, Meyers MB, Choo A, Fishman GI. The organization of adherens junctions and desmosomes at the cardiac intercalated disc is independent of gap junctions. J Cell Sci.2003;116(Pt 5):875-885.

95. Eckardt D, Theis M, Degen J, et al. Functional role of connexin43 gap junction channels in adult mouse heart assessed by inducible gene deletion. J Mol Cell Cardiol.2004;36(1):101-110.
96. Thomas SP, Kucera JP, Bircher-Lehmann L, Rudy Y, Saffitz JE, Kleber AG. Impulse propagation in synthetic strands of neonatal cardiac myocytes with genetically reduced levels of connexin43. Circ Res.2003;92(11):1209-1216.
97. Beauchamp P, Choby C, Desplantez T, et al. Electrical propagation in synthetic ventricular myocyte strands from germline connexin43 knockout mice. Circ Res.2004;95(2):170-178.
98. Beauchamp P, Desplantez T, McCain ML, et al. Electrical coupling and propagation in engineered ventricular myocardium with heterogeneous expression of connexin43. Circ Res.2012;110(11):1445-1453.
99. Kitamura H, Ohnishi Y, Yoshida A, et al. Heterogeneous loss of connexin43 protein in nonischemic dilated cardiomyopathy with ventricular tachycardia. J Cardiovasc Electrophysiol.2002;13(9):865-870.
100. Kitamura H, Yoshida A, Ohnishi Y, et al. Correlation of connexin43 expression and late ventricular potentials in nonischemic dilated cardiomyopathy. Circ J.2003;67(12):1017-1021.
101. Kostin S, Rieger M, Dammer S, et al. Gap junction remodeling and altered connexin43 expression in the failing human heart. Mol Cell Biochem.2003;242(1-2):135-144.
102. Salameh A, Krautblatter S, Karl S, et al. The signal transduction cascade regulating the expression of the gap junction protein connexin43 by beta-adrenoceptors. Br J Pharmacol.2009;158(1):198-208.
103. Hall DG, Morley GE, Vaidya D, et al. Early onset heart failure in transgenic mice with dilated cardiomyopathy. Pediatr Res.2000;48(1):36-42.
104. van Veen TA, van Rijen HV, Wiegerinck RF, et al. Remodeling of gap junctions in mouse hearts hypertrophied by forced retinoic acid signaling. J Mol Cell Cardiol.2002;34(10):1411-1423.
105. Ehler E, Horowits R, Zuppinger C, et al. Alterations at the intercalated disk associated with the absence of muscle LIM protein. J Cell Biol.2001;153(4):763-772.
106. Wang X, Li F, Campbell SE, Gerdes AM. Chronic pressure overload cardiac hypertrophy and failure in guinea pigs: II. Cytoskeletal remodeling. J Mol Cell Cardiol.1999;31(2):319-331.
107. Goldfine SM, Walcott B, Brink PR, Magid NM, Borer JS. Myocardial connexin43 expression in left ventricular hypertrophy resulting from aortic regurgitation. Cardiovasc Pathol.1999;8(1):1-6.
108. Haugan K, Miyamoto T, Takeishi Y, et al. Rotigaptide (ZP123) improves atrial conduction slowing in chronic volume overload-induced dilated atria. Basic Clin Pharmacol Toxicol.2006;99(1):71-79.

109. Akar FG, Nass RD, Hahn S, et al. Dynamic changes in conduction velocity and gap junction properties during development of pacing-induced heart failure. Am J Physiol Heart Circ Physiol.2007;293(2):H1223-1230.

110. Jansen JA, van Veen TA, de Jong S, et al. Reduced Cx43 expression triggers increased fibrosis due to enhanced fibroblast activity. Circ Arrhythm Electrophysiol.2012;5(2):380-390.

111. Sepp R, Severs NJ, Gourdie RG. Altered patterns of cardiac intercellular junction distribution in hypertrophic cardiomyopathy. Heart.1996;76(5):412-417.

112. Palka P, Lange A, Fleming AD, et al. Differences in myocardial velocity gradient measured throughout the cardiac cycle in patients with hypertrophic cardiomyopathy, athletes and patients with left ventricular hypertrophy due to hypertension. J Am Coll Cardiol.1997;30(3):760-768.

113. Jongsma HJ, Wilders R. Gap junctions in cardiovascular disease. Circ Res.2000;86(12):1193-1197.

114. Sasano C, Honjo H, Takagishi Y, et al. Internalization and dephosphorylation of connexin43 in hypertrophied right ventricles of rats with pulmonary hypertension. Circ J.2007;71(3):382-389.

115. Sanbe A, James J, Tuzcu V, et al. Transgenic rabbit model for human troponin I-based hypertrophic cardiomyopathy. Circulation.2005;111(18):2330-2338.

116. Ripplinger CM, Li W, Hadley J, et al. Enhanced transmural fiber rotation and connexin 43 heterogeneity are associated with an increased upper limit of vulnerability in a transgenic rabbit model of human hypertrophic cardiomyopathy. Circ Res.2007;101(10):1049-1057.

117. Ambra R, Di Nardo P, Fantini C, et al. Selective changes in DNA binding activity of transcription factors in UM-X7.1 cardiomyopathic hamsters. Life Sci.2002;71(20):2369-2381.

118. Sato T, Ohkusa T, Honjo H, et al. Altered expression of connexin43 contributes to the arrhythmogenic substrate during the development of heart failure in cardiomyopathic hamster. Am J Physiol Heart Circ Physiol.2008;294(3):H1164-1173.

119. Molkentin JD, Lu JR, Antos CL, et al. A calcineurin-dependent transcriptional pathway for cardiac hypertrophy. Cell.1998;93(2):215-228.

120. Bierhuizen MF, Boulaksil M, van Stuijvenberg L, et al. In calcineurin-induced cardiac hypertrophy expression of Nav1.5, Cx40 and Cx43 is reduced by different mechanisms. J Mol Cell Cardiol.2008;45(3):373-384.

121. Dhein S. Cardiac ischemia and uncoupling: gap junctions in ischemia and infarction. Adv Cardiol.2006;42:198-212.

122. Beardslee MA, Lerner DL, Tadros PN, et al. Dephosphorylation and intracellular redistribution of ventricular connexin43 during electrical uncoupling induced by ischemia. Circ Res.2000;87(8):656-662.

123. Peters NS, Coromilas J, Severs NJ, Wit AL. Disturbed connexin43 gap junction distribution correlates with the location of reentrant circuits in the epicardial border zone of healing canine infarcts that cause ventricular tachycardia. Circulation.1997;95(4):988-996.
124. Huang XD, Sandusky GE, Zipes DP. Heterogeneous loss of connexin43 protein in ischemic dog hearts. J Cardiovasc Electrophysiol.1999;10(1):79-91.
125. Cabo C, Yao J, Boyden PA, et al. Heterogeneous gap junction remodeling in reentrant circuits in the epicardial border zone of the healing canine infarct. Cardiovasc Res.2006;72(2):241-249.
126. Yamada KA, Rogers JG, Sundset R, Steinberg TH, Saffitz J. Up-regulation of connexin45 in heart failure. J Cardiovasc Electrophysiol.2003;14(11):1205-1212.
127. Tansey EE, Kwaku KF, Hammer PE, et al. Reduction and redistribution of gap and adherens junction proteins after ischemia and reperfusion. Ann Thorac Surg.2006;82(4):1472-1479.
128. Kanno S, Kovacs A, Yamada KA, Saffitz JE. Connexin43 as a determinant of myocardial infarct size following coronary occlusion in mice. J Am Coll Cardiol.2003;41(4):681-686.
129. Zhang Y, Wang H, Kovacs A, Kanter EM, Yamada KA. Reduced expression of Cx43 attenuates ventricular remodeling after myocardial infarction via impaired TGF-beta signaling. Am J Physiol Heart Circ Physiol.2010;298(2):H477-487.
130. Agullo-Pascual E, Cerrone M, Delmar M. Arrhythmogenic cardiomyopathy and Brugada syndrome: diseases of the connexome. FEBS Lett.2014;588(8):1322-1330.
131. Noorman M, Hakim S, Kessler E, et al. Remodeling of the cardiac sodium channel, connexin43, and plakoglobin at the intercalated disk in patients with arrhythmogenic cardiomyopathy. Heart Rhythm.2013;10(3):412-419.
132. Noorman M, Groeneweg JA, Asimaki A, et al. End stage of arrhythmogenic cardiomyopathy with severe involvement of the interventricular septum. Heart Rhythm.2013;10(2):283-289.
133. Boulaksil M, Jungschleger JG, Antoons G, et al. Drug-induced torsade de pointes arrhythmias in the chronic AV block dog are perpetuated by focal activity. Circ Arrhythm Electrophysiol.2011;4(4):566-576.
134. Ruiz P, Brinkmann V, Ledermann B, et al. Targeted mutation of plakoglobin in mice reveals essential functions of desmosomes in the embryonic heart. J Cell Biol.1996;135(1):215-225.
135. Grossmann KS, Grund C, Huelsken J, et al. Requirement of plakophilin 2 for heart morphogenesis and cardiac junction formation. J Cell Biol.2004;167(1):149-160.
136. Protonotarios N, Tsatsopoulou A, Patsourakos P, et al. Cardiac abnormalities in familial palmoplantar keratosis. Br Heart J.1986;56(4):321-326.
137. McKoy G, Protonotarios N, Crosby A, et al. Identification of a deletion in plakoglobin in arrhythmogenic right ventricular cardiomyopathy with palmoplantar keratoderma and woolly hair (Naxos disease). Lancet.2000;355(9221):2119-2124.
138. Protonotarios N, Tsatsopoulou A. Naxos disease and Carvajal syndrome: cardiocutaneous disorders that highlight the pathogenesis and broaden the spectrum of arrhythmogenic right ventricular cardiomyopathy. Cardiovasc Pathol.2004;13(4):185-194.

139. Carvajal-Huerta L. Epidermolytic palmoplantar keratoderma with woolly hair and dilated cardiomyopathy. J Am Acad Dermatol.1998;39(3):418-421.
140. Norgett EE, Hatsell SJ, Carvajal-Huerta L, et al. Recessive mutation in desmoplakin disrupts desmoplakin-intermediate filament interactions and causes dilated cardiomyopathy, woolly hair and keratoderma. Hum Mol Genet.2000;9(18):2761-2766.
141. Kaplan SR, Gard JJ, Carvajal-Huerta L, Ruiz-Cabezas JC, Thiene G, Saffitz JE. Structural and molecular pathology of the heart in Carvajal syndrome. Cardiovasc Pathol.2004;13(1):26-32.
142. Asimaki A, Kapoor S, Plovie E, et al. Identification of a new modulator of the intercalated disc in a zebrafish model of arrhythmogenic cardiomyopathy. Sci Transl Med.2014;6(240):240ra274.
143. Clancy CE, Kass RS. Defective cardiac ion channels: from mutations to clinical syndromes. J Clin Invest.2002;110(8):1075-1077.
144. Daly Ide B, Clark AJ. The action of ions upon the frog's heart. J Physiol.1921;54(5-6):367-383.
145. Balser JR. Structure and function of the cardiac sodium channels. Cardiovasc Res.1999;42(2):327-338.
146. Delmar M. Connexin43 regulates sodium current; ankyrin-G modulates gap junctions: the intercalated disc exchanger. Cardiovasc Res.2012;93(2):220-222.
147. Papadatos GA, Wallerstein PM, Head CE, et al. Slowed conduction and ventricular tachycardia after targeted disruption of the cardiac sodium channel gene Scn5a. Proc Natl Acad Sci U S A.2002;99(9):6210-6215.
148. Royer A, van Veen TA, Le Bouter S, et al. Mouse model of SCN5A-linked hereditary Lenegre's disease: age-related conduction slowing and myocardial fibrosis. Circulation.2005;111(14):1738-1746.
149. van Veen TA, Stein M, Royer A, et al. Impaired impulse propagation in Scn5a-knockout mice: combined contribution of excitability, connexin expression, and tissue architecture in relation to aging. Circulation.2005;112(13):1927-1935.
150. Remme CA, Verkerk AO, Nuyens D, et al. Overlap syndrome of cardiac sodium channel disease in mice carrying the equivalent mutation of human SCN5A-1795insD. Circulation.2006;114(24):2584-2594.
151. Kaab S, Nuss HB, Chiamvimonvat N, et al. Ionic mechanism of action potential prolongation in ventricular myocytes from dogs with pacing-induced heart failure. Circ Res.1996;78(2):262-273.
152. Wagner S, Dybkova N, Rasenack EC, et al. Ca2+/calmodulin-dependent protein kinase II regulates cardiac Na+ channels. J Clin Invest.2006;116(12):3127-3138.
153. Coppini R, Ferrantini C, Yao L, et al. Late sodium current inhibition reverses electromechanical dysfunction in human hypertrophic cardiomyopathy. Circulation.2013;127(5):575-584.
154. Jelicks LA, Siri FM. Effects of hypertrophy and heart failure on [Na+]i in pressure-overloaded guinea pig heart. Am J Hypertens.1995;8(9):934-943.

155. Undrovinas AI, Maltsev VA, Sabbah HN. Repolarization abnormalities in cardiomyocytes of dogs with chronic heart failure: role of sustained inward current. Cell Mol Life Sci.1999;55(3):494-505.
156. Gray RP, McIntyre H, Sheridan DS, Fry CH. Intracellular sodium and contractile function in hypertrophied human and guinea-pig myocardium. Pflugers Arch.2001;442(1):117-123.
157. Meszaros J, Khananshvili D, Hart G. Mechanisms underlying delayed afterdepolarizations in hypertrophied left ventricular myocytes of rats. Am J Physiol Heart Circ Physiol.2001;281(2):H903-914.
158. Ju YK, Saint DA, Gage PW. Hypoxia increases persistent sodium current in rat ventricular myocytes. J Physiol.1996;497 (Pt 2):337-347.
159. Huang B, El-Sherif T, Gidh-Jain M, Qin D, El-Sherif N. Alterations of sodium channel kinetics and gene expression in the postinfarction remodeled myocardium. J Cardiovasc Electrophysiol.2001;12(2):218-225.
160. Hammarstrom AK, Gage PW. Hypoxia and persistent sodium current. Eur Biophys J.2002;31(5):323-330.
161. Tani M, Neely JR. Role of intracellular Na+ in Ca2+ overload and depressed recovery of ventricular function of reperfused ischemic rat hearts. Possible involvement of H+-Na+ and Na+-Ca2+ exchange. Circ Res.1989;65(4):1045-1056.
162. Xiao XH, Allen DG. Role of Na(+)/H(+) exchanger during ischemia and preconditioning in the isolated rat heart. Circ Res.1999;85(8):723-730.
163. Silverman HS, Stern MD. Ionic basis of ischaemic cardiac injury: insights from cellular studies. Cardiovasc Res.1994;28(5):581-597.
164. Imahashi K, Kusuoka H, Hashimoto K, Yoshioka J, Yamaguchi H, Nishimura T. Intracellular sodium accumulation during ischemia as the substrate for reperfusion injury. Circ Res.1999;84(12):1401-1406.
165. Allen DG, Xiao XH. Role of the cardiac Na+/H+ exchanger during ischemia and reperfusion. Cardiovasc Res.2003;57(4):934-941.
166. Soliman D, Wang L, Hamming KS, et al. Late sodium current inhibition alone with ranolazine is sufficient to reduce ischemia- and cardiac glycoside-induced calcium overload and contractile dysfunction mediated by reverse-mode sodium/calcium exchange. J Pharmacol Exp Ther.2012;343(2):325-332.
167. Huber JD, Bentzien J, Boyer SJ, et al. Identification of a potent sodium hydrogen exchanger isoform 1 (NHE1) inhibitor with a suitable profile for chronic dosing and demonstrated cardioprotective effects in a preclinical model of myocardial infarction in the rat. J Med Chem.2012;55(16):7114-7140.
168. Karmazyn M. NHE-1: still a viable therapeutic target. J Mol Cell Cardiol.2013;61:77-82.
169. Balse E, Steele DF, Abriel H, Coulombe A, Fedida D, Hatem SN. Dynamic of ion channel expression at the plasma membrane of cardiomyocytes. Physiol Rev.2012;92(3):1317-1358.
170. Sato PY, Musa H, Coombs W, et al. Loss of plakophilin-2 expression leads to decreased sodium current and slower conduction velocity in cultured cardiac myocytes. Circ Res.2009;105(6):523-526.

171. Sato PY, Coombs W, Lin X, et al. Interactions between ankyrin-G, Plakophilin-2, and Connexin43 at the cardiac intercalated disc. Circ Res.2011;109(2):193-201.
172. Rizzo S, Lodder EM, Verkerk AO, et al. Intercalated disc abnormalities, reduced Na(+) current density, and conduction slowing in desmoglein-2 mutant mice prior to cardiomyopathic changes. Cardiovasc Res.2012;95(4):409-418.
173. Cerrone M, Noorman M, Lin X, et al. Sodium current deficit and arrhythmogenesis in a murine model of plakophilin-2 haploinsufficiency. Cardiovasc Res.2012;95(4):460-468.
174. Cerrone M, Lin X, Zhang M, et al. Missense mutations in plakophilin-2 cause sodium current deficit and associate with a Brugada syndrome phenotype. Circulation.2014;129(10):1092-1103.
175. Coronel R, Wilders R, Verkerk AO, Wiegerinck RF, Benoist D, Bernus O. Electrophysiological changes in heart failure and their implications for arrhythmogenesis. Biochim Biophys Acta.2013;1832(12):2432-2441.
176. Coronel R, de Groot JR, van Lieshout JJ. Defining heart failure. Cardiovasc Res.2001;50(3):419-422.
177. Ripplinger CM, Krinsky VI, Nikolski VP, Efimov IR. Mechanisms of unpinning and termination of ventricular tachycardia. Am J Physiol Heart Circ Physiol.2006;291(1):H184-192.
178. Pazo D, Kramer L, Pumir A, Kanani S, Efimov I, Krinsky V. Pinning force in active media. Phys Rev Lett.2004;93(16):168303.
179. Engelman ZJ, Trew ML, Smaill BH. Structural heterogeneity alone is a sufficient substrate for dynamic instability and altered restitution. Circ Arrhythm Electrophysiol.2010;3(2):195-203.
180. Tanaka K, Zlochiver S, Vikstrom KL, et al. Spatial distribution of fibrosis governs fibrillation wave dynamics in the posterior left atrium during heart failure. Circ Res.2007;101(8):839-847.
181. Stein M, Boulaksil M, Jansen JA, et al. Reduction of fibrosis-related arrhythmias by chronic renin-angiotensin-aldosterone system inhibitors in an aged mouse model. Am J Physiol Heart Circ Physiol.2010;299(2):H310-321.
182. Chen Y, Guo H, Xu D, et al. Left ventricular failure produces profound lung remodeling and pulmonary hypertension in mice: heart failure causes severe lung disease. Hypertension.2012;59(6):1170-1178.
183. Wagner S, Ruff HM, Weber SL, et al. Reactive oxygen species-activated Ca/calmodulin kinase IIdelta is required for late I(Na) augmentation leading to cellular Na and Ca overload. Circ Res.2011;108(5):555-565.
184. Shryock JC, Song Y, Rajamani S, Antzelevitch C, Belardinelli L. The arrhythmogenic consequences of increasing late INa in the cardiomyocyte. Cardiovasc Res.2013;99(4):600-611.
185. Jansen JA, Noorman M, Musa H, et al. Reduced heterogeneous expression of Cx43 results in decreased Nav1.5 expression and reduced sodium current that accounts for arrhythmia vulnerability in conditional Cx43 knockout mice. Heart Rhythm.2012;9(4):600-607.

PART 1

MYOCARDIAL REMODELING OF THE INTERCALATED DISC

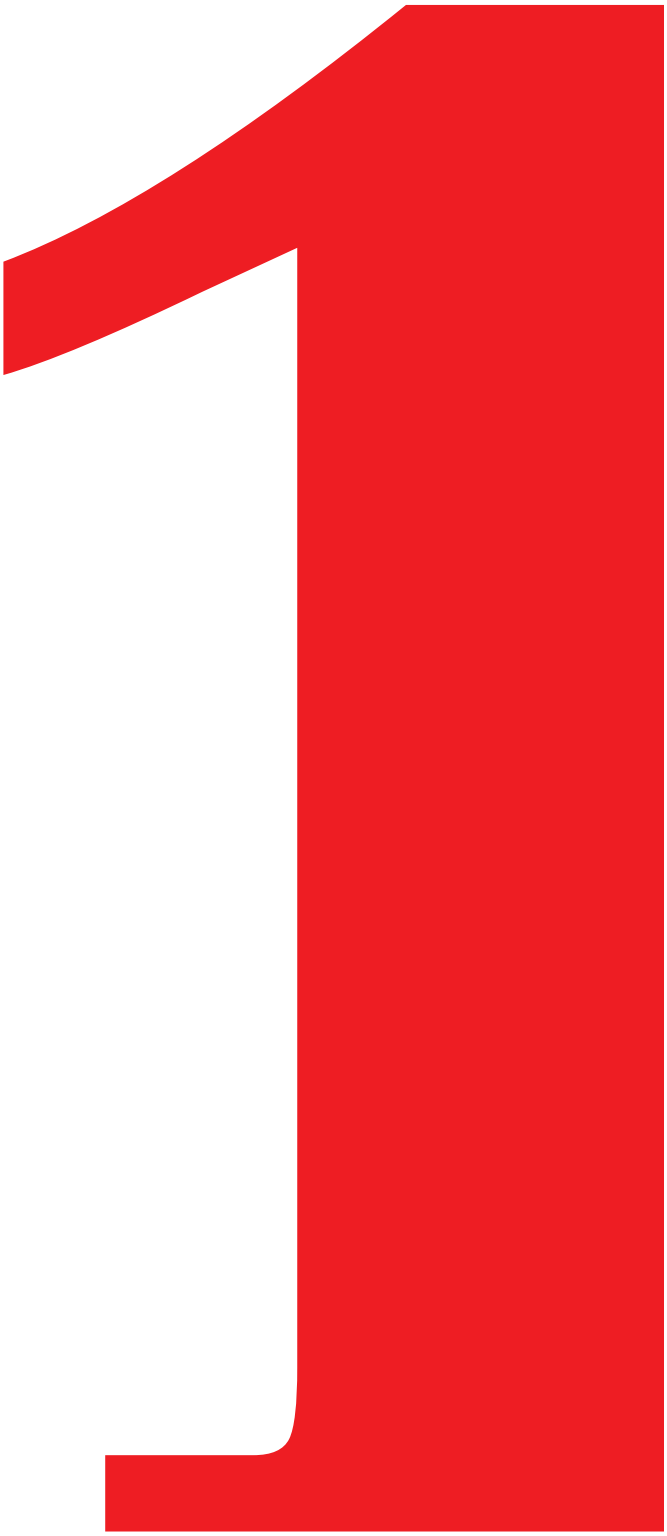

“

Never put off till tomorrow,
what you can do
the day after tomorrow just as well.

Mark Twain

Chapter

3

Remodeling of the cardiac sodium channel, Connexin-43 and Plakoglobin at the intercalated disc in patients with Arrhythmogenic Cardiomyopathy

Maartje Noorman[a,*], Sara Hakim[a,*], **Elise L. Kessler**[a,*], Judith Groeneweg[b,c], Moniek G.P.J. Cox[b,c], Angeliki Asimaki[d], Harold V.M. van Rijen[a], Leonie van Stuijvenberg[a], Halina Chkourko[e], Marcel A.G. van der Heyden[a], Marc A. Vos[a], Nicolaas de Jonge[c], Jasper J. van der Smagt[f], Dennis Dooijes[f], Aryan Vink[g], Roel A. de Weger[g], Andras Varro[h], Jacques M.T. de Bakker[b], Jeffrey E. Saffitz[d], Thomas J. Hund[i], Peter J. Mohler[j], Mario Delmar[e], Richard N.W. Hauer[b,c], Toon A.B. van Veen[a]

*These authors contributed equally to this study.

[a] *Department of Medical Physiology, University Medical Center Utrecht, Utrecht, The Netherlands*
[b] *Interuniversity Cardiology Institute of the Netherlands, Utrecht, The Netherlands*
[c] *Department of Cardiology, University Medical Center Utrecht, Utrecht, The Netherlands*
[d] *Department of Pathology, Beth Israel Deaconess Medical Center and Harvard Medical School, Boston, USA*
[e] *The Leon H Charney Division of Cardiology, New York University School of Medicine, New York, USA*
[f] *Department of Genetics, University Medical Center Utrecht, Utrecht, The Netherlands*
[g] *Department of Pathology, University Medical Center Utrecht, Utrecht, The Netherlands*
[h] *Department of Pharmacology and Pharmacotherapy, Faculty of Medicine, University of Szeged, Hungary*
[i] *The Dorothy M. Davis Heart and Lung Research Institute, The Ohio State University College of Engineering, Department of Biomedical Engineering, The Ohio State University, Columbus, USA*
[j] *The Dorothy M. Davis Heart and Lung Research Institute, Department of Internal Medicine, Division of Cardiovascular Medicine and Department of Physiology and Cell Biology, The Ohio State University Medical Center, Columbus, USA*

Heart Rhythm 2013; 10(3): 412-419

Abstract

Background: Arrhythmogenic Cardiomyopathy (ACM) is closely associated with desmosomal mutations in a majority of patients. Arrhythmogenesis in patients with ACM is likely related to remodeling of cardiac gap junctions and increased levels of fibrosis. Recently, using experimental models, we also identified sodium channel dysfunction secondary to desmosomal dysfunction. The aim of the present study was to assess the immunoreactive signal levels of the sodium channel protein $Na_V1.5$, as well as Connexin-43 and Plakoglobin, in myocardial specimens obtained from ACM patients.

Methods: Left and right ventricular free wall postmortem material was obtained from 5 patients with ACM and 5 controls matched for age and sex. Right ventricular septal biopsies were taken from another 15 patients with ACM. All patients fulfilled the 2010 revised Task Force Criteria for the diagnosis of ACM. Immunohistochemical analyses were performed using antibodies against Cx43, Plakoglobin, $Na_V1.5$, Plakophilin-2, and N-cadherin.

Results: N-Cadherin and Desmoplakin immunoreactive signals and distribution were normal in ACM patients compared to control. Plakophilin-2 signals were unaffected, unless a PKP2 mutation predicting haploinsufficiency was present. Distribution was unchanged compared to control. Immunoreactive signal levels of Plakoglobin, Cx43 and $Na_V1.5$ were disturbed in 74%, 70% and 65% of the patients, respectively.

Conclusions: A reduced immunoreactive signal of Plakoglobin, Cx43 and $Na_V1.5$ at the intercalated discs can be observed in a large majority of the patients. Decreased levels of $Na_V1.5$ might contribute to arrhythmia vulnerability and provides a new clinically relevant tool for future risk assessment strategies.

Introduction

Arrhythmogenic Cardiomyopathy (ACM), previously known as Arrhythmogenic Right Ventricular Cardiomyopathy/Dysplasia (ARVC/D), is a heart muscle disease characterized by replacement of predominantly the right ventricle (RV) with fibro-fatty scar tissue. In later stages of the disease, also the left ventricle (LV) and the interventricular septum (IVS) can be affected. Recently, also patients with a predominant LV involvement have been described.[1] Patients generally present with syncope, palpitations and sudden cardiac death.[2] Mutations in genes encoding for desmosomal proteins, which are important for intercellular mechanical coupling, are associated with this disease in about 60% of the patients.[3-9]

The arrhythmogenic phenotype of ACM suggests that, although the mutated genes do not code for channel proteins, these gene products associate with molecules that are relevant for electrical function. In particular, several studies have identified a disturbed immunolocalization of Connexin-43 (Cx43), the major ventricular gap junction protein, in ACM myocardium.[10-12] In several other forms of cardiomyopathy, a heterogeneous downregulation and de-phosphorylation of Cx43 are strongly associated with an increased propensity for development of life threatening ventricular arrhythmias.[13-16]

ACM is clinically diagnosed according to the revised Task Force Criteria (TFC),[17] based on global or regional dysfunction and structural alterations, tissue characterization of the ventricular wall, re- and depolarization or conduction abnormalities, arrhythmias, genetics and family history. Still, many cases remain un- or misdiagnosed, because of the multiple facets of the clinical manifestation of the disease.

It has been described that immunoreactivity of Plakoglobin was reduced in a high percentage of ACM patients compared either to controls, or to patients with other underlying cardiac disease such as Dilated or Hypertrophic Cardiomyopathy.[12] This early reduction in immunoreactivity for Plakoglobin appeared not only present in the RV, but also in the macroscopically unaffected LV and IVS. Based on this finding it was suggested that immunoreactivity of Plakoglobin could be a tool to discriminate ACM patients from healthy subjects and patients with other forms of heart disease. However, more recent studies have shown that Plakoglobin signals are also reduced in sarcoidosis and giant cell myocarditis.[18,19]

Recently we reported that a reduction in Cx43 protein can lead to reduced sodium channel ($Na_V1.5$) expression and function in a mouse model of severely reduced Cx43 and in isolated neonatal rat ventricular cardiomyocytes.[20] Furthermore, *in vitro* silencing of Plakophilin-2 (PKP2), one of the desmosomal proteins that is often mutated in ACM patients, also leads to a decreased sodium current.[21] In addition, PKP2-haploinsufficient mice showed a significant sodium current deficit.[22] Whether desmosomal deficiency and the ACM phenotype correlate with changes in the distribution of proteins relevant to the sodium channel complex in the human heart, remains to be defined. This knowledge could also be relevant to the indication or contraindication of sodium channel blockers in these patients.

In this study we used immunohistochemistry to identify the immunoreactive signal levels and distribution of Cx43, Plakoglobin and $Na_V1.5$ in ACM patients as compared to controls. Our data show that these levels and distribution of Cx43, Plakoglobin and $Na_V1.5$ are affected in the large majority of ACM patients.

Material & methods

PATIENT SAMPLES AND TISSUE PROCESSING

Left and right ventricular free wall (LVFW and RVFW) myocardium (on average 2-4 cm^3) was obtained from 5 ACM patients (AC1-5, post-mortem) and from 5 age and sex matched controls with no underlying heart disease (C1-5). Right ventricular septal biopsies (RVSB, 2-4 mm^3) were obtained from another 15 ACM patients (AC6-20). All patients consented to clinical evaluation according to the TFC. All material used in this study was flash frozen in liquid nitrogen. Frozen samples were cryo-sectioned at a thickness of 10 µm.

PATIENT SCREENING

From 18/20 ACM patients, DNA was available to screen for mutations in the PKP2, DSP, DSG2, DSC2, Plakoglobin, TMEM43 and PLN genes by direct sequencing. In addition, using multiple ligation-dependent probe amplification, the PKP2 gene was screened for large exon deletions. Genetic screening was performed upon the patients' written consent.

IMMUNOHISTOCHEMISTRY

Frozen material was serially sectioned generating sections of 10 µm thickness that were collected on aminopropyltriethoxysilane (AAS) coated glass slides. Immunohistochemistry was performed as described previously.[23] Once the labeling was completed, analysis of the results was perform using a Nikon eclipse 80i microscope equipped for epifluorescence. Independent analysis of the different patients was performed blinded by 3 observers/experiment. First, for each and every patient an overall conclusion was drawn upon which pictures supportive to the overall conclusion were captured using a Nikon digital sight DS-BMWe camera and NIS Elements BR3.0 software (using equal exposure times). Primary antibodies against N-Cadherin (mouse, Sigma, 1:800), PKP2 (mouse, Progen, undiluted-1:1000), Plakoglobin (mouse, Sigma, 1:100,000), $Na_V1.5$ (rabbit, custom-made,[23] 1:100), and Cx43 (mouse, Transduction Labs, 1:200 and rabbit, Zymed, 1:250) were used. Secondary labeling was performed with appropriate Texas Red (1:100) and FITC (1:250) conjugated whole IgG antibodies (Jackson Laboratories). Blinded cross-evaluation for $Na_V1.5$ labeling of material from 9 patients was performed in Utrecht and in New York.

Results

PATIENT CHARACTERISTICS

Characteristics of the 5 controls and the 20 ACM patients are shown in table 1. Molecular genetic analysis of 18 out of 20 ACM patients revealed 5 different *PKP2* mutations in 11 patients. In addition to a pathogenic *PKP2* mutation, one of those patients also carried unclassified variants in *TMEM43* (p.Arg240Cys) and *DSG2* (p.Ala358Thr). One patient had unclassified variants in *DSC2* and *DSG2*,[2] showed a mutation in *PLN* (p.Arg14del) and 4 did not present any mutations in the analyzed genes.

In supplementary table 1 additional clinical characteristics of the ACM patients are provided, including age at which first symptoms occurred, and separate Task Force criteria for ACM diagnosis.

IMMUNOREACTIVE SIGNALS AND DISTRIBUTION OF DESMOSOMAL PROTEINS

As depicted in figure 1, double-labeling with antibodies against N-Cadherin (NCad) and PKP2 revealed that the immunoreactive proteins co-localized at the intercalated discs (IDs) of ACM patients (exampled by AC8, -9 and -10), identical to the pattern seen in controls (see C1 as an example). Ncad, an adherens junction protein in which no mutations in humans have been documented, was used as a marker for the ID. Reduced immunoreactive signals of Ncad have never been documented in ACM patients, and as such, also serves as a control to verify tissue quality/preservation. Indeed, in all controls and patients we studied the distribution of immunoreactive Ncad was similar.

Next, we studied the signals and distribution of PKP2 in tissue from ACM patients with deletion of exons 1-4 of PKP2, which likely causes PKP2 haplo-insufficiency (AC6, -7, and -8). Results were compared to those obtained from controls, ACM patients with no identified mutation (AC10), or ACM patients having a missense mutation that thus far has not been associated with trafficking defects (AC9). In controls, as well as in tissue from ACM patients without identified *PKP2* mutation (AC10) or a p.Cys796Arg mutation (AC9), PKP2 immunoreactive signal levels and distribution were highly comparable. However, in the two ACM patients with a deletion of *PKP2* exons 1-4 (AC7 and -8) and one with a deletion of exons 1-14 (AC6), the intensity of the PKP2 immunoreactive signal was clearly reduced (see Figure 1 by AC 8). In contrast to this decreased signal intensity, distribution of PKP2 was not affected, since it still showed a complete overlap with Ncad at the ID.

Table 1. Clinical characteristics of controls and ACM patients. RVFW and LVFW post-mortem material was used from control 1-5 and AC 1-5. Right ventricular septal biopsies were examined from AC 6-20. All ACM patients had a TFC score ≥4 or were diagnosed after autopsy or heart transplantation. Abbreviations: NA: not applicable, ND: not determined, HTX: heart transplantation. TFC: Task Force Criteria (TFC value indicates number of criteria; major criterion counts for 2 points, minor criterion for 1 point). UV: unclassified variant.

Patient	Age	Age 1st symptoms	Sex	TFC	Mutation
Control 1	36	NA	M	NA	NA
Control 2	38	NA	M	NA	NA
Control 3	40	NA	M	NA	NA
Control 4	35	NA	F	NA	NA
Control 5	44	NA	F	NA	NA
AC 1	27	16	M	autopsy	None
AC 2	43	24	M	8	None
AC 3	63	55	F	autopsy	None
AC 4	63	59	M	HTX	ND
AC 5	25	25	M	autopsy	ND
AC 6	16	16	M	9	*PKP2* deletion exons 1-14, *DSG2* uv, *TMEM43* p.Arg240Cys uv
AC 7	39	34	M	10	*PKP2* deletion exons 1-4
AC 8	72	69	M	8	*PKP2* deletion exons 1-4
AC 9	74	65	M	9	*PKP2* p.Cys796Arg
AC 10	77	76	M	7	None
AC 11	47	43	F	5	PLN c.40_42delAGA p.Arg14del
AC 12	38	37	M	7	UV in DSC2 and UV in DSG2 (not pathogenic)
AC 13	30	22	F	5	PKP2 c.235C>T p.Arg79X
AC 14	65	59	F	8	PKP2 c.235C>T p.Arg79X
AC 15	39	17	F	6	PKP2 c.2146-1G>C p.IVS10-1G>C
AC 16	49	48	F	6	PKP2 c.1211-1212insT p.Leu404fs
AC 17	58	34	M	10	PKP2: c.1211-1212insT p. Leu404fs
AC 18	48	41	M	4	PLN c.40_42delAGA p.Arg14del
AC 19	41	29	F	9	PKP2 c.2146-1G>C p.IVS10-1G>C
AC 20	23	17	F	7	PKP2: c.1211-1212insT p. Leu404fs

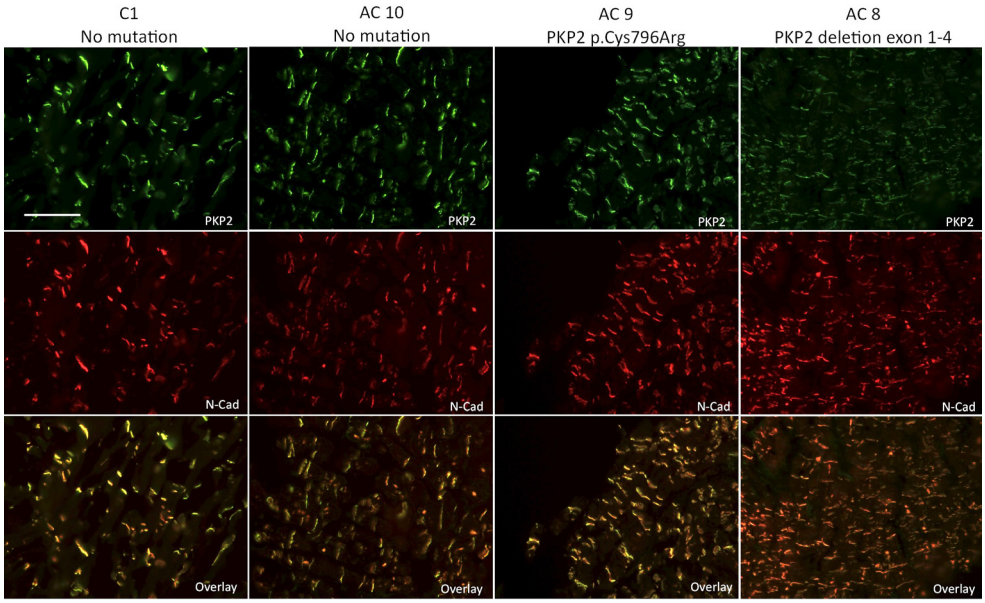

Figure 1. Undisturbed Plakophilin2 distribution in ACM regardless of mutations. PKP2 is normally present in the intercalated disc in ACM patients, regardless of whether a mutation is present in the PKP2 gene. Haploinsuffiency of PKP2 (in AC8) also showed undisturbed PKP2 distribution. However, reduced signal intensity of PKP2 was identified. Ncad is used as a marker for the intercalated disc. Scale bar equals 100 µm.

DISTRIBUTION AND IMMUNOREACTIVE SIGNAL LEVELS OF PLAKOGLOBIN, CX43 AND $NA_v1.5$

Previous studies have shown that alterations in Plakoglobin expression and distribution can serve as biomarkers, to facilitate diagnosis of ACM.[12] Complementary studies also revealed that tissue preservation and dilution of the anti-Plakoglobin antibody critically determined the appropriateness of evaluation.[24] Serial antibody dilutions were therefore used to determine the best conditions under which the presence or absence of a Plakoglobin signal at the intercalated disc, segregated with the clinical diagnosis of ACM. At a dilution of 1:100,000 Plakoglobin signals were clearly present in the 5 control patients where they co-localized with Ncad at the ID (Figure 2A, right panels). In 5/19 ACM patients, Plakoglobin labeling was comparable to controls but in 14/19 (74%) patients, Plakoglobin signals were clearly reduced and sometimes even completely absent whereas double labeling with antibodies raised against Ncad always revealed a normal pattern of Ncad at the ID (Figure 2B, right panel).

Analysis of cryo-material from the RVFW (AC1-5) and RVSB (AC6-20) revealed that Cx43 immunoreactive signal was disturbed (ranging from mild to severe) in 14/20 (70%) patients when compared to the pattern found in the 5 control Individuals. Figure 2A shows that in control material (left panels), Cx43 and Ncad closely overlap, while this overlay is partially disrupted

in a large percentage of AC patients (Figure 2B, left panels). In ACM patients, labeling of Cx43 was not only reduced but also clearly heterogeneously distributed. In controls, Cx43 was found almost exclusively at the ID. However, in ACM patients, Cx43 signal was not only reduced at the ID, but also sparely present at the lateral sides of the myocytes.

Similarly, double labeling of $Na_V1.5$ and Ncad revealed a reduced immunoreactive signal of $Na_V1.5$ in 12/17 (65%) patients with labeling in all 5 controls being normal (Figure 2A, mid panels). Again, the alterations ranged from reduced signal intensity of $Na_V1.5$ (with normal Ncad counterstaining) to complete absence of $Na_V1.5$ (Figure 2B, mid panels). A blinded cross-evaluation on material of 9 ACM patients, performed by the group in NYU (New York) confirmed the assessment made in a separate center in 8/9 cases. Three patients classified as unaffected were recognized as such, and only in 1/6 affected patients the evaluation of $Na_V1.5$ downregulation was not independently confirmed (patient AC18).

We also performed a double labeling of $Na_V1.5$ and Cx43 (Figure 3). In areas where Cx43 was normally present in the intercalated disc (upper panels) both in controls and in patients, $Na_V1.5$ was also present at the ID. We expected, based on previous results in mice[20] that in areas with a disturbed Cx43 signal, $Na_V1.5$ would also show a similarly disturbed pattern. In figure 3 (middle panels) an area of disturbed Cx43 expression is shown (arrows) and in this place also $Na_V1.5$ signal is reduced. However, we were unable to confirm that in every patient with a disturbed pattern of Cx43, $Na_V1.5$ was concomitantly reduced. We also identified patients that presented a disturbance in Cx43 pattern, without a reduced $Na_V1.5$, and the other way around: patients with reduced $Na_V1.5$ and unchanged Cx43. This is exampled by the lower panels in figure 3 where in one area both phenomena are presented. The asterisk illustrates an ID where Cx43 signal is disturbed while $Na_V1.5$ is normal and the arrow-head illustrates the opposite: normal Cx43 signal with disturbed $Na_V1.5$.

Supplementary table 2 displays an overview of the results for each and every patient studied (AC1-AC20) regarding the evaluation of immunoreactive signals for $Na_V1.5$, Plakoglobin and Cx43. Interestingly, of the 12 patients that showed disturbed signals for $Na_V1.5$, 9 patients also showed disturbed signals for Plakoglobin and of those 9 double-affected patients, 6 patients showed in addition disturbed immunoreactive signals for Cx43, too. Another interesting observation is that in all patients in which Plakoglobin was disturbed (14/19), the disturbance in Plakoglobin was always accompanied with a disturbance in signals for $Na_V1.5$, Cx43, or both (AC18 excluded being judged inconclusive for $Na_V1.5$). Supplementary figure 1 summarizes these results as displayed in a Venn-diagram. When we combined these data with the individual TFC scores as listed in table 1, the data might suggest that those patients that based on immunohistochemical analysis were the most affected (meaning disturbed immunoreactive signals for all three proteins tested: $Na_V1.5$, Cx43 and Plakoglobin) tended to have slightly higher TFC scores than those that were only affected for 1 or 2 proteins. The average TFC score of those patients was 8.0±0.9, (SEM, n=5 since AC5 did not have a TFC score) while the TFC score in the remaining other 11 with one or two factors affected was 7.1±0.5. Statistical analysis, however, did not result in a statistical significant correlation (r=0.37). In addition, no statistical significant correlation could be detected when we tested the individual TFC scores against the amount of disturbed parameters (being 1, 2 or 3) thereby not selecting the nature of the distur-

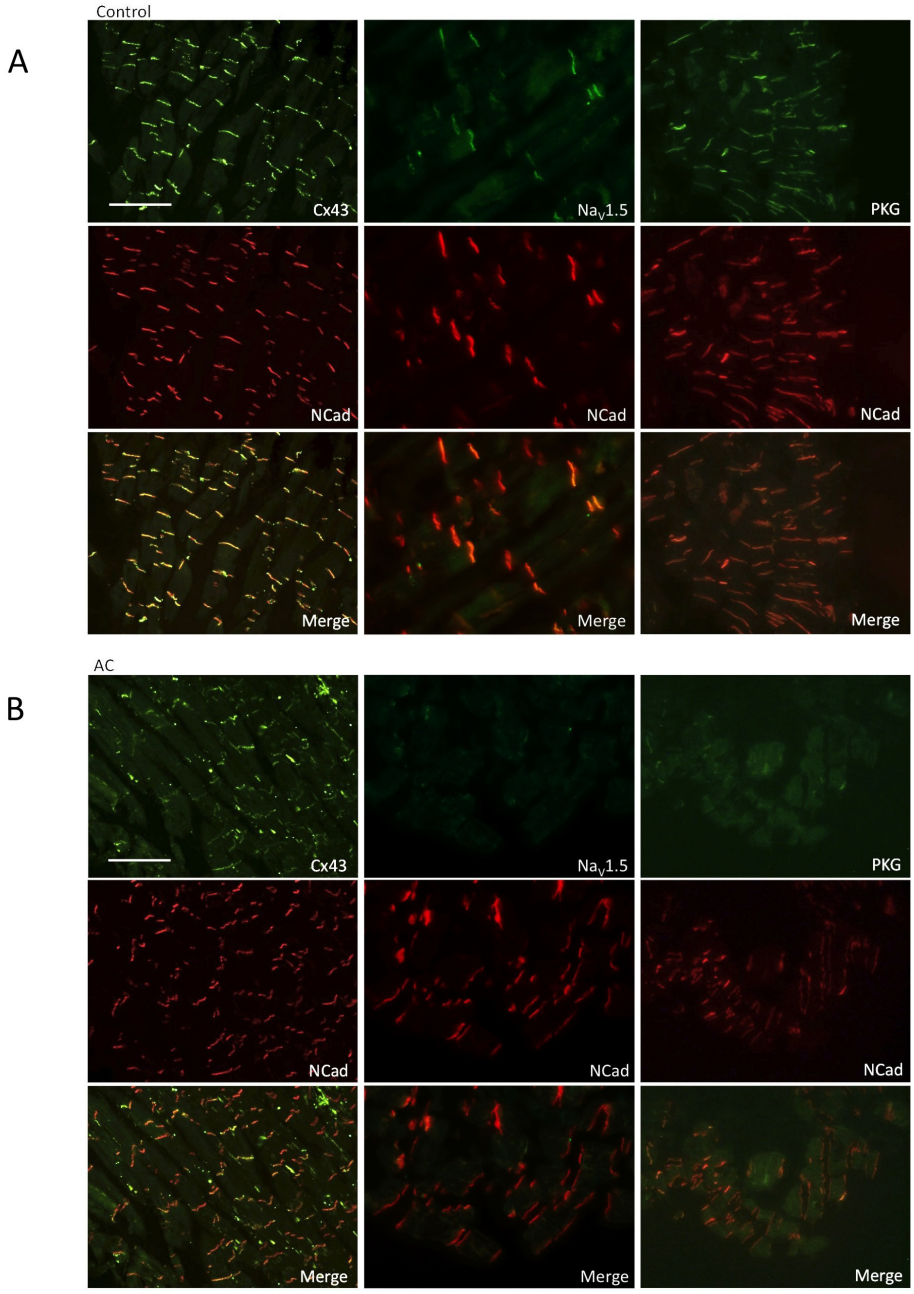

Figure 2. Expression patterns for Cx43, $Na_V1.5$ and PKG. Double labelings with N-Cadherin. A large subset of the patients **(B)** showed reduced immunoreactive signal levels for Cx43, $Na_V1.5$ and/or PKG compared to control **(A)**.

bed parameter. Finally, there was no significant relation between being affected for Plakoglobin and the amount of additional affected other parameters (p=0.41). Obviously, this statistical testing is highly limited by the amount of included patients and the even smaller amount of patients that were present in the different subgroups as illustrated in supplementary figure 1.

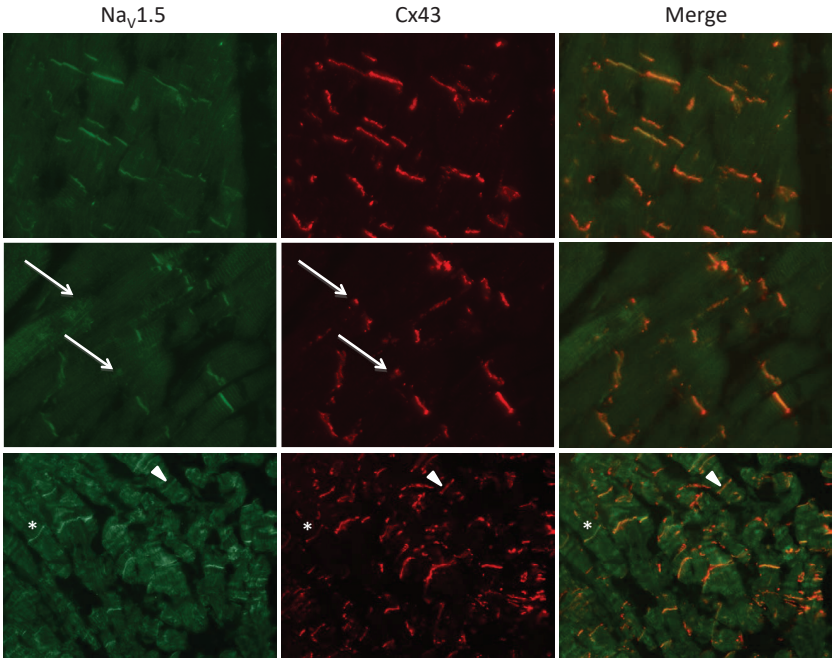

Figure 3. Double labeling of Cx43 and Na$_V$1.5. Upper panels show a region with unaffected Cx43 and Na$_V$1.5 resulting in a strong overlay. Middle panels show a region of disturbed Cx43 signal, where also immunoreactive signal intensity of Na$_V$1.5 is reduced (respective IDs marked with arrows). The lower panels display examples of IDs where either Na$_V$1.5 is normal with a reduced signal of Cx43 (asterisk) or disturbed Na$_V$1.5 with normal Cx43 (arrowheads).

Discussion

We have used an immunohistochemical approach to assess the signal intensity and distribution of immunoreactive proteins in samples of human tissue obtained from patients with clinical diagnosis of ACM. Our results showed that in a large majority of tissue specimens, immunoreactive signals for Cx43, Plakoglobin, and/or $Na_V1.5$ were substantially disturbed and heterogeneously distributed. The observations were apparent, regardless of whether mutations in desmosomal genes were found. In contrast, immunoreactive signals for Ncad and PKP2 were normal, except in the case of tissue from patients with a genotype that likely would probably lead to PKP2 haploinsufficiency through deletion of the first 4, or all of the exons.

Several studies have shown a connection between disturbances in mechanical coupling, electrical coupling and excitability of cardiomyocytes.[20,21,25] These observations were merely derived from artificial systems, where an extreme reduction of one of the components was induced. In the present study, we have used human ACM patient material where immunoreactive signals of the mechanical components appeared generally unaffected, despite the fact that mutations in the mechanical components were present in a large proportion of cases. Since the protein immunoreactivity is highly subjected to tissue preservation and experimental conditions, we assessed detection of a given protein with various antibody dilutions. The observed reduction of PKP2 signal-intensity in patients predicted to be haplo-insufficient suggests that the PKP2 antibody dilution was adequate to detect variations in signal intensity (see Figure 1). In addition, control experiments in which the antibody used against PKP2 was further diluted up to 1000 times more than the regular concentration used, still revealed equal but lower intensities of PKP2 in control and patients without a mutation in PKP2 (data not shown).

Mutations in desmosomal proteins are associated with the ACM phenotype. A common occurrence is a heterogeneous distribution of cardiac Cx43 at the intercalated discs.[10-12] In the present study, we show for the first time that also junctional immunoreactive signal of $Na_V1.5$ expression is decreased in a large subset of our patients. In general, safe and normal conduction depends on appropriate excitability (facilitated through the $Na_V1.5$ channels), cell-to-cell conduction through Cx43 gap junctions, and tissue geometry (preferred absence of massive insulating fibrosis). Pro-arrhythmic alterations in the latter two factors have been recognized in ACM patients before. The common disturbance of Cx43 signals, but not of the desmosomal proteins that we described is consistent with the results of Fidler *et al.*,[26] which showed that RVSB of four patients with a *PKP2* mutation all displayed a disturbed Cx43 pattern, with no changes in PKP2 distribution in 3 of the four cases. Of note, the *PKP2* mutations included in our study and those described in the study of Fidler *et al.* are different. In the latter case, the mutations were not expected to impair the trafficking of PKP2 to the ID.

Though multiple components involved in the molecular basis of ACM have been identified, the sequence of events that lead to disruption of the macromolecular complex that is situated at the ID still remains fairly unresolved. Whether the molecules of the desmosome, the gap junc-

tions and the sodium channel complex interact directly, or through unknown molecular partners, remains to be defined. *In vitro* studies in which PKP2 was deleted by interference strategies revealed a concomitant decrease in intercellular communication, excitability and impulse propagation.[21,27] On the other hand, reduced presence of Plakoglobin (also known as γ-catenin) at the ID may lead to replacement with β-catenin, which in turn reduces intra-nuclear levels of β-catenin and as such transcriptional reduction of Cx43.[28,29] Notably, in all patients within this study, in which Plakoglobin signals appeared disturbed, this was always accompanied with a disturbance in immunoreactive signal either of Cx43, or $Na_V1.5$, or both.

Animal studies in genetically engineered mice have shown that a combination of genetically reduced $Na_V1.5$ and Cx43 levels did induce conduction slowing without, however, exhausting conduction reserve and a resulting increased propensity to arrhythmias.[30] Genetically reduced Cx43 levels on its own appeared also able to induce a reduction of $Na_V1.5$ dependent sodium current.[20,31] When these conditions were exacerbated in a model of aged mice with reduced levels of Cx43 and $Na_V1.5$, as well as increased amounts of fibrosis, conduction reserve exhausted and a significant incidence of arrhythmias could be recorded.[32] The latter situation fits very well with the progressive deterioration as seen in the ACM disease model where increasing amounts of fibrosis are found in the later phase of the disease. Additional insight into the inter-relation of Cx43 and the preservation of cardiac structure was provided in a follow up study in which we showed enhanced fibrosis in mice with reduced Cx43 expression; the latter seemed consequent to enhanced fibroblast activity rather than increased proliferation of these cells.[33]

Though the present study concentrated on a few molecules thought to be relevant to the electrical phenotype, the spectrum of molecular remodeling in ACM hearts is likely to be much broader. Within our limitations, our data do suggest that a reduced abundance of $Na_V1.5$ immunoreactive protein at the ID may be a component of the molecular profile in some ACM cases. The latter may, in turn, be a component of the electrophysiological substrate present in ACM patients. As in the case of patients suspected of Brugada syndrome, a sodium channel blocker challenge might help for identification and/or stratification of patients at risk of ACM, particularly those in the concealed phase of the disease. As a proof of principle, we recently showed that flecainide administration to young heterozygous PKP2 mice with structurally normal hearts (no fibrosis or adiposis detected) led to a high incidence of ventricular arrhythmias and sudden death, whereas the same flecainide challenge did not cause either arrhythmias or death in control littermates.[22]

Study limitations

The immunohistochemical data presented in this study merely show qualitative differences between controls and patients. Immunoreactive signals of several ID-associated proteins have been studied in autopsy material from controls and patients and these data have been compared to data obtained with RVSB. These septal biopsies were taken from ACM patients that were still under clinical evaluation and were both limited in amount and size, which excludes introduction of additional quantification methodology via Western blotting or by patch clamp. We also did not include a detailed analysis of the degree of fibro-fatty replacement. Though fibrosis was apparent in al biopsies studied, the septal tissue is regarded to be less representative in this aspect.

One of the important limitations of our study is the narrow range of contrast that we have been able to obtain in our microscopic images. It is important to note, though, that working with human material poses particular technical challenges. We have gone to great lengths to protect the quality of the tissue, despite the limitations inherent to its collection. Yet, across the board, issues like background fluorescence, autofluorescence of fibrotic material, or protein immunoreactivity, prevent the signal obtained in human tissue samples from being as sharp and crisp as those that can be obtained from animal tissue, or from cell preparations. Within those limitations, we have placed emphasis on collecting and processing the samples in the most homogeneous, consistent way. This has allowed us to compare the immunoreactive signals obtained from different patients, and this method of analysis is consistent with a number of previous publications on this subject and the best alternative to the realities of studies involving human subjects.

Conclusion

Immunohistochemical analysis in ACM reveals reduced signals for Cx43, Plakoglobin and/or $Na_V1.5$ in a majority of patients. The newly identified reduction of $Na_V1.5$ sodium channels might importantly contribute to arrhythmia vulnerability in ACM patients and could, in the future, be added as an element of evaluation for risk stratification. Our data further support the notion that deficiency in the abundance and/or function of the sodium channel complex may be one of the multiple arrhythmogenic substrates present in the hearts of patients afflicted with mutations in desmosomal proteins and as such, at risk of ventricular fibrillation and sudden cardiac death.

References

1. Sen-Chowdhry S, Syrris P, Prasad SK, et al. Left-dominant arrhythmogenic cardiomyopathy: an under-recognized clinical entity. J Am Coll Cardiol.2008;52(25):2175-2187.

2. Saffitz JE. The pathobiology of arrhythmogenic cardiomyopathy. Annu Rev Pathol.2011;6:299-321.

3. Asimaki A, Syrris P, Wichter T, Matthias P, Saffitz JE, McKenna WJ. A novel dominant mutation in plakoglobin causes arrhythmogenic right ventricular cardiomyopathy. Am J Hum Genet.2007;81(5):964-973.

4. Heuser A, Plovie ER, Ellinor PT, et al. Mutant desmocollin-2 causes arrhythmogenic right ventricular cardiomyopathy. Am J Hum Genet.2006;79(6):1081-1088.

5. Syrris P, Ward D, Evans A, et al. Arrhythmogenic right ventricular dysplasia/cardiomyopathy associated with mutations in the desmosomal gene desmocollin-2. Am J Hum Genet.2006;79(5):978-984.

6. Pilichou K, Nava A, Basso C, et al. Mutations in desmoglein-2 gene are associated with arrhythmogenic right ventricular cardiomyopathy. Circulation.2006;113(9):1171-1179.

7. Rampazzo A, Nava A, Malacrida S, et al. Mutation in human desmoplakin domain binding to plakoglobin causes a dominant form of arrhythmogenic right ventricular cardiomyopathy. Am J Hum Genet.2002;71(5):1200-1206.

8. Gerull B, Heuser A, Wichter T, et al. Mutations in the desmosomal protein plakophilin-2 are common in arrhythmogenic right ventricular cardiomyopathy. Nat Genet.2004;36(11):1162-1164.

9. Cox MG, van der Zwaag PA, van der Werf C, et al. Arrhythmogenic right ventricular dysplasia/cardiomyopathy: pathogenic desmosome mutations in index-patients predict outcome of family screening: Dutch arrhythmogenic right ventricular dysplasia/cardiomyopathy genotype-phenotype follow-up study. Circulation.2011;123(23):2690-2700.

10. Kaplan SR, Gard JJ, Carvajal-Huerta L, Ruiz-Cabezas JC, Thiene G, Saffitz JE. Structural and molecular pathology of the heart in Carvajal syndrome. Cardiovasc Pathol.2004;13(1):26-32.

11. Kaplan SR, Gard JJ, Protonotarios N, et al. Remodeling of myocyte gap junctions in arrhythmogenic right ventricular cardiomyopathy due to a deletion in plakoglobin (Naxos disease). Heart Rhythm.2004;1(1):3-11.

12. Asimaki A, Tandri H, Huang H, et al. A new diagnostic test for arrhythmogenic right ventricular cardiomyopathy. N Engl J Med.2009;360(11):1075-1084.

13. van Rijen HV, Eckardt D, Degen J, et al. Slow conduction and enhanced anisotropy increase the propensity for ventricular tachyarrhythmias in adult mice with induced deletion of connexin43. Circulation.2004;109(8):1048-1055.

14. Gutstein DE, Morley GE, Vaidya D, et al. Heterogeneous expression of Gap junction channels in the heart leads to conduction defects and ventricular dysfunction. Circulation.2001;104(10):1194-1199.

15. Wiegerinck RF, van Veen TA, Belterman CN, et al. Transmural dispersion of refractoriness and conduction velocity is associated with heterogeneously reduced connexin43 in a rabbit model of heart failure. Heart Rhythm.2008;5(8):1178-1185.

16. Boulaksil M, Winckels SK, Engelen MA, et al. Heterogeneous Connexin43 distribution in heart failure is associated with dispersed conduction and enhanced susceptibility to ventricular arrhythmias. Eur J Heart Fail.2010;12(9):913-921.

17. Marcus FI, McKenna WJ, Sherrill D, et al. Diagnosis of arrhythmogenic right ventricular cardiomyopathy/dysplasia: proposed modification of the task force criteria. Circulation.2010;121(13):1533-1541.

18. Winterfield JR, Lee J, Asimaki A, et al. Plakoglobin abnormalities and arrhythmogenesis in idiopathic cardiomyopathies. Heart Rhythm.2010;7(5S):S113.

19. Asimaki A, Tandri H, Duffy ER, et al. Altered desmosomal proteins in granulomatous myocarditis and potential pathogenic links to arrhythmogenic right ventricular cardiomyopathy. Circ Arrhythm Electrophysiol.2011;4(5):743-752.

20. Jansen JA, Noorman M, Musa H, et al. Reduced heterogeneous expression of Cx43 results in decreased Nav1.5 expression and reduced sodium current that accounts for arrhythmia vulnerability in conditional Cx43 knockout mice. Heart Rhythm.2012;9(4):600-607.

21. Sato PY, Musa H, Coombs W, et al. Loss of plakophilin-2 expression leads to decreased sodium current and slower conduction velocity in cultured cardiac myocytes. Circ Res.2009;105(6):523-526.

22. Cerrone M, Noorman M, Lin X, et al. Sodium Current Deficit and Arrhythmogenesis in a Murine Model of Plakophilin-2 Haploinsufficiency. Cardiovasc Res.2012;cvs218 [pii] 10.1093/cvr/cvs218.

23. Hund TJ, Koval OM, Li J, et al. A beta(IV)-spectrin/CaMKII signaling complex is essential for membrane excitability in mice. J Clin Invest.2010;120(10):3508-3519.

24. Munkholm J, Christensen AH, Svendsen JH, Andersen CB. Usefulness of immunostaining for plakoglobin as a diagnostic marker of arrhythmogenic right ventricular cardiomyopathy. Am J Cardiol.2012;109(2):272-275.

25. Oxford EM, Musa H, Maass K, Coombs W, Taffet SM, Delmar M. Connexin43 remodeling caused by inhibition of plakophilin-2 expression in cardiac cells. Circ Res.2007;101(7):703-711.

26. Fidler LM, Wilson GJ, Liu F, et al. Abnormal connexin43 in arrhythmogenic right ventricular cardiomyopathy caused by plakophilin-2 mutations. J Cell Mol Med.2009;13(10):4219-4228.

27. Sato PY, Coombs W, Lin X, et al. Interactions between ankyrin-G, Plakophilin-2, and Connexin43 at the cardiac intercalated disc. Circ Res.2011;109(2):193-201.

28. van der Heyden MA, Rook MB, Hermans MM, et al. Identification of connexin43 as a functional target for Wnt signalling. J Cell Sci.1998;111 (Pt 12):1741-1749.

29. Garcia-Gras E, Lombardi R, Giocondo MJ, et al. Suppression of canonical Wnt/beta-catenin signaling by nuclear plakoglobin recapitulates phenotype of arrhythmogenic right ventricular cardiomyopathy. J Clin Invest.2006;116(7):2012-2021.

30. Stein M, van Veen TA, Remme CA, et al. Combined reduction of intercellular coupling and membrane excitability differentially affects transverse and longitudinal cardiac conduction. Cardiovasc Res.2009;83(1):52-60.

31. Desplantez T, McCain ML, Beauchamp P, et al. Connexin43 ablation in foetal atrial myocytes decreases electrical coupling, partner connexins, and sodium current. Cardiovasc Res.2012;94(1):58-65.

32. Stein M, Boulaksil M, Jansen JA, et al. Reduction of fibrosis-related arrhythmias by chronic renin-angiotensin-aldosterone system inhibitors in an aged mouse model. Am J Physiol Heart Circ Physiol.2010;299(2):H310-321.

33. Jansen JA, van Veen TA, de Jong S, et al. Reduced Cx43 Expression Triggers Increased Fibrosis Due to Enhanced Fibroblast Activity. Circ Arrhythm Electrophysiol.2012;-CIRCEP.111.966580 [pii] 10.1161/CIRCEP.111.966580.

Supplementary material

Supplementary Table 1. Patient characteristics. Major and minor criteria according to the Task Force Criteria and age of first symptoms are shown. Abbreviations: VF: ventricular fibrillation, LBBB: left bundle branch block, VT: ventricular tachycardia, TAD: terminal activation duration, PVC: premature ventricular complex.

Patient	Age	Sex	1st Symptoms + age (yrs)	Diagnostic Task Force Criteria	
				Major	Minor
AC 1	27	M	VF (16)	Autopsy	
AC 2	43	M	LBBB VT (24)	Epsilon waves, structural abnormalities	Negative T waves in V4-6, prolonged TAD, LBBB VT
AC 3	63	F	Decompensation (55)	Autopsy	
AC 4	63	M	Decompensation (59)	Heart Transplant	
AC 5	25	M	VF (25)	Autopsy	
AC 6	16	M	LBBB VT (16)	LBBB VT with superior axis, negative T waves V1-4, akinesia + dilatation RV	Late potentials
AC 7	39	M	LBBB VT (34)	LBBB VT with superior axis, negative T waves V1-3, akinesia in dilated RV	
AC 8	72	M	Syncope (69)	akinetic areas in dilated RV, son with AC	Late potentials, >500PVCs/24h, negative T waves V1-2,
AC 9	74	M	LBBB VT (65)	Epsilon waves, negative T waves V1-3, akinesia in dilated RV.	LBBB VT, late potentials
AC 10	77	M	LBBB VT (76)	LBBB VT with superior axis, dyskinesia in dilated RV	Late potentials
AC 11	47	F	NSVT (43)	LBBB VT with superior axis, negative T waves V1-3, structural major abnormalities	Minor abnormalities on biopsy
AC 12	38	M	RBBB VT (37)	LBBB VT with superior axis, negative T waves V1-3, structural major abnormalities	Prolonged TAD, late potentials
AC 13	30	F	Family screening (22)	Father with AC, structural major abnormalities	LBBB VT with inferior axis, minor abnormalities on biopsy
AC 14	65	F	Family screening (59)	Negative T waves V1-3, epsilon waves V1-3, brother with AC, structural major abnormalities	LBBB VT with inferior axis
AC 15	39	F	Family screening (17)	Father with AC, structural major abnormalities	Prolonged TAD, late potentials, LBBB VT with inferior axis
AC 16	49	F	Family screening (48)	Negative T waves in V1-3, LBBB VT with superior axis, brother with AC	Minor abnormalities on biopsy
AC 17	58	M	LBBB VT (34)	Epsilon waves V1-3, LBBB VT with superior axis, structural major abnormalities	Negative V1-2
AC 18	48	M	LBBB VT (41)	Structural major abnormalities	Prolonged TAD, LBBB VT with inferior axis
AC 19	41	F	LBBB VT (29)	Negative T waves V1-3, LBBB VT with superior axis, father with AC, structural major abnormalities	Prolonged TAD, minor abnormalities on biopsy
AC 20	23	F	Family screening (17)	Negative T waves V1-3, father with AC, structural major abnormalities	Prolonged TAD, >500 PVCs/24h

Supplementary Table 2. Summary of results. Table summarizing all immunolabeling results of the 20 included ACM patients, their age, gender, Task Force Criteria (TFC) score and the results upon labeling $Na_v1.5$, PKG and Cx43. 0: unaffected immunoreactive signals; X: disturbed immunoreactive signals; 0/X*: discrepancy in interpretation between Utrecht analysis and NY analysis; N.D. : analysis not performed due to lack of more material.

Patient	Age	Sex	TFC	$Na_v1.5$	PKG	Cx43
AC 1	27	M	autopsy	0	0	X
AC 2	43	M	8	0	X	X
AC 3	63	F	autopsy	X	0	X
AC 4	63	M	HTX	N.D.	N.D.	X
AC 5	25	M	autopsy	X	X	X
AC 6	16	M	9	N.D.	X	X
AC 7	39	M	10	X	X	0
AC 8	72	M	8	X	0	0
AC 9	74	M	9	X	X	X
AC 10	77	M	7	X	X	X
AC 11	47	F	5	X	X	X
AC 12	38	M	7	X	X	0
AC 13	30	F	5	X	0	0
AC 14	65	F	8	0	0	X
AC 15	39	F	6	X	X	0
AC 16	49	F	6	0	X	X
AC 17	58	M	10	X	X	X
AC 18	48	M	4	0/X*	X	0
AC 19	41	F	9	X	X	X
AC 20	23	F	7	0	X	X

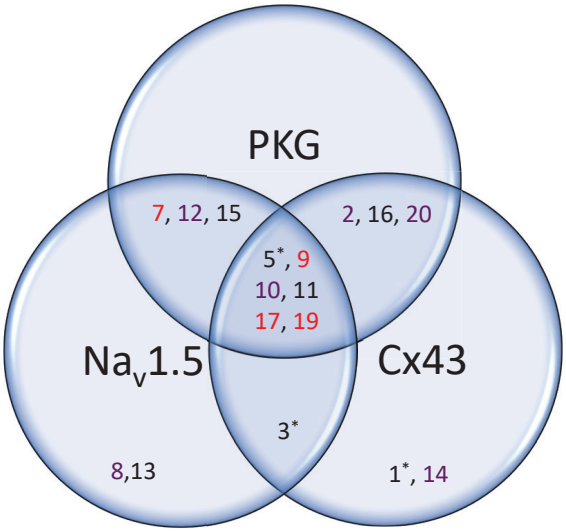

4*: only Cx43 x tested
6: Cx43 x, PKG x, Na$_v$1.5 N.D
18: Cx43 0, PKG x, Na$_v$1.5 inconclusive

Black*: no TFC score
Black: TFC 4-6
Purple: TFC 7-8
Red: TFC 9-10

Supplementary Figure 1. Venn-diagram of the data included in Supplementary Table 2 in combination with the patient-specific TFC scores. The three components Na$_v$1.5, Cx43 and PKG represent disturbed immunoreactive signals for that particular protein. The numbers indicate the individual ACM patients. The three different colours black, purple and red indicate TFC scores of, 4-6, 7-8 and 9-10 respectively. * : no TFC score available, x: disturbed signal, 0: undisturbed signal.

“

Science is simply
the word we use to describe
a method of organizing
our curiosity.

Tim Minchin

Chapter

4

Disturbed Desmoglein-2 in the intercalated disc of pediatric patients with Dilated Cardiomyopathy

Elise L. Kessler[a], Peter G.J. Nikkels[b], Toon A.B. van Veen[a]

[a] *Department of Medical Physiology, University Medical Center Utrecht, Utrecht, The Netherlands*
[b] *Department of Pathology, University Medical Center Utrecht, Utrecht, The Netherlands*

Human Pathology 2017; 67:101-108

Abstract

Background: Dilated Cardiomyopathy (DCM) leads to disturbed contraction and force transduction, and is associated with substantial mortality in all age groups. Involvement of a disrupted composition of the intercalated disc (ID) has been reported. However, in children, little is established about such subcellular changes during disease, because of the pathological mix-up with the ongoing cardiac maturation. This leaves maladaptive remodeling often undetected. We aimed at illustrating subcellular alterations in children diagnosed with DCM compared to age-matched controls, focusing on ID proteins known to be crucially stable under healthy conditions and destabilized during cardiac injury in adults.

Methods: Left ventricular or septal pediatric specimens were collected from 7 individuals diagnosed with DCM (age: 23 weeks *in utero* - 8 weeks postnatal) and age-matched controls that died of non-cardiovascular cause. We determined the amount of fibrosis and localization of ID proteins by immunohistochemistry.

Results: In pediatric DCM, most ID proteins follow similar spatio-temporal changes in localization as in controls. However, although no mutations were found, the signal of the desmosomal protein Desmoglein-2 was reduced in all pediatric DCM specimens, but not in controls or adult DCM patients. Endocardial and transmural fibrosis was increased in all pediatric DCM patients compared to age-matched controls.

Conclusion: Composition of the ID in pediatric DCM patients is similar to controls, except for the localization of Desmoglein-2 and presence of severe fibrosis. This suggests that the architecture of desmosomes is already disturbed in the early stages of DCM. These findings contribute to the understanding of pediatric DCM.

Introduction

Dilated Cardiomyopathy (DCM) is associated with substantial mortality in all age groups.[1,2] It is characterized by left ventricular (LV) dilatation and systolic dysfunction. Moreover, it is often accessorized by arrhythmias and eventually culminates into heart failure (HF).[1] DCM in adults is either acquired (e.g. upon ischemic and structural heart disease) or congenital.[3] In congenital forms of DCM, common mutations are found in genes encoding for proteins of the cytoskeleton or the sarcomeres (e.g. actin or β-myosin heavy chain (β-MYH)).[4] An important substructure of the cellular cytoskeleton, responsible for electrochemical and mechanical connection between two adjacent cardiomyocytes, is the intercalated disc (ID). The ID contains three major types of junctions: adherens junctions, desmosomes and gap junctions: Adherens junctions are responsible for cell-to-cell anchorage and force transduction consisting of the transmembrane protein N-cadherin (Ncad) coupled to the intercellular proteins β-catenin and Plakoglobin. Desmosomes link cells to intermediate filaments and consist of the transmembrane proteins Desmocollin-2 (DSC-2) and Desmoglein-2 (DSG-2), connected to the intercellular proteins Desmoplakin-1 (DSP-1), Plakophilin-2 (PKP-2) and also Plakoglobin. Gap junctions are composed of connexins and enable electrical impulse propagation by exchange of small molecules. In the ventricles, the main expressed isoform is Connexin-43 (Cx43).[5] This classification, however, is an oversimplification and many proteins of the individual junctions actually interact with each other and also with other parts of the ID, like ion channels (e.g. $Na_V1.5$).[6]

Genetic modifications of one or more of these ID proteins can lead to maladaptive cardiac remodeling: Ncad, DSP-1 and DSG-2 knockout, and homozygous Plakoglobin or β-catenin mutations cause disintegration of the myocardium and embryonic death in mice; the same holds true for Cx43 deficiency due to malformation or absence of a cardiac outflow tract.[7-11] Also in DCM, ID proteins are involved: DSP-1 and DSG-2 mutations cause DCM in adults, and inducible cardiac restricted knockout of Plakoglobin leads to DCM in mice.[12,13] Expression of a non-degradable isoform of β-catenin causes DCM and premature death in young mice.[14] As was recently communicated, a homozygous PKP-2 mutation was associated with non-compaction DCM and resulted in premature death of the unborn child.[15]

Regional differences in left ventricular (LV) function of pediatric DCM patients point at heterogeneous expression of contractile proteins related to the contractile performance of the heart.[16] This might be substantiated by alterations in the contractile proteins itself, but also in (calcium sensitive) proteins involved in force-generation, or in proteins involved in force transduction like the proteins that constitute the ID.[5] Increased levels of Ncad, Plakoglobin and β-catenin for instance have been reported in adult DCM, although less prominent in early postnatal tissue.[17] Alterations in the levels and localization of Cx43 seem less obvious since they have been reported to be decreased, unaltered or even upregulated when compared to controls.[17-19]

This suggests that the ID plays an important role in the progression of DCM. The molecular organization of the ID in adult controls and DCM patients is known (recapitulated in supplementary figure 1). However, children have been reported to differ from adults in clinical presentation, symptoms and causes and less is known about potential molecular modifications of the ID.
The embryonic human heart is not yet completely developed until after birth and still many important changes occur in the heart of an infant. Several ID proteins are located in the cytoplasm until late embryonic stages or even until after birth as we previously described.[20] Cell-polarization leads to translocation of these proteins, first to the lateral side of the cell, and subsequently towards the ID.[20] It is still unknown, how the heart is able to maintain its function during embryonic and early postnatal development without a fully developed ID. To complicate an appropriate interpretation, in children molecular changes due to maladaptive remodeling can be hidden by the still ongoing alterations that take place due to progressive cardiac development during the early postnatal period of life.

In this study, we obtained specimens of 7 deceased children diagnosed with DCM to investigate subcellular alterations in these pediatric patients compared to age-matched controls. Despite relatively low prevalence in children (1 in 100,000 under the age of 18; 8 in 100,000 under the age of 1[3,21,22]), DCM is the leading cause of HF and heart transplantations (HTx) in pediatric patients.[23] Therefore, studying the ID in pediatric DCM might provide new insights into cardiac development and remodeling processes.

Material & methods

Little is known about molecular alterations in pediatric patients with DCM. With this study, we aimed at identifying subcellular spatio-temporal differences between 7 pediatric DCM and age-matched control specimens.[20] Furthermore, we validated our findings in adult DCM and control specimens. We performed fluorescent immunohistochemistry on proteins of the ID. The amount of collagen was determined by a Picrosirius Red staining.

CARDIAC SPECIMENS

All cardiac specimens were obtained from the biobank of the Department of Pathology, University Medical Center Utrecht, the Netherlands. Tissue was made available for research purposes after informed written consent in accordance with the institutional guidelines. Pediatric samples were postmortem left ventricular or septal myocardium obtained from 7 pediatric patients diagnosed with DCM and 7 age-matched controls, who died without any pathological evidence of cardiac involvement. Adult specimens were explanted hearts of DCM patients or postmortem myocardium of controls with a non-cardiovascular cause of death. Age, gender,

genetic background and anatomical features of all pediatric individuals are listed in table 1. Two pediatric individuals (DCM-23 and DCM6) carried a Myosin heavy chain-7 (*MYH-7*) mutation. Four specimens (DCM-30, DCM-32, DCM2 and DCM8) were genetically screened and no mutation with a documented causal relationship to DCM was found. One specimen was not available for genetic screening (DCM4).

IMMUNOFLUORESCENT HISTOCHEMISTRY AND MICROSCOPY

Cardiac samples were snap-frozen or fixated in formalin and embedded in paraffin. 10µm cryo-sections were generated. To visualize cardiac fibrosis, 3µm paraffin sections were generated and stained with 0.1% Picrosirius Red solution as described previously.[24] To assess the organization of ID-related proteins of interest, immunolabeling was performed on cryosections as described previously.[25] Mouse monoclonal primary antibodies were used for adherens junction associated protein β-catenin (Sigma Aldrich, 1:500), and the desmosomal proteins PKP-2 (Progen, undiluted), Plakoglobin (Sigma Aldrich, 1:1000), DSP-1 (Progen, 1:10), DSG-2 (Progen, 1:10) and DSC-2 (Millipore, 1:100). Rabbit polyclonal primary antibodies were used for adherens junction protein Ncad (Sigma, 1:800), sodium channel $Na_V1.5$ (custom-made[26], 1:250) and gap junction protein Cx43 (Thermo Scientific, 1:200). Secondary labeling was performed with fluorescein isothiocyanate conjugated whole IgG antibody (Jackson Laboratories, 1:250). After immunolabeling, sections were analyzed with a Nikon Eclipse 80i epifluorescence microscope and images were taken using a Nikon digital sight DS-2MBWc camera and NIS Elements BR 3.0 software. During all experiments, DCM and control specimens were labeled for the same protein at the same time and representative pictures were taken at the same day in a blinded fashion.

Results

In a previous study we extensively analyzed the subcellular localization of several ID-associated proteins, and the spatio-temporal alterations that these proteins are subjected to during pre- and post-natal maturation of the healthy left ventricular or septal myocardium.[20] In the current study we were able to reproduce these data in control tissue age-matched to the pediatric specimens as listed in table 1.

Figure 1 summarizes those spatio-temporal changes in distribution as found in control tissue, the four squares refer to individual cardiomyocytes at the indicated time points (23 weeks *in utero*, 4 weeks, 22 weeks and 7 years). The proteins of the adherens junctions and the desmosomes (blue squares) initially (23 weeks *i.u.*) reside at multiple positions in the cardiomyocytes. At 4 weeks, and more pronounced at 22 weeks postnatal, they translocated to the ID with only some residual labeling left at the lateral membranes. The sodium channels ($Na_V1.5$, green circles) show a predominantly diffuse cytoplasmic labeling during the prenatal stage with a

progressive translocation to the lateral membrane around week 4 and to the ID around week 22, though in a less extensive mode when compared to the junctional proteins. At this latter time-point, localization of Cx43 (orange triangles) still fails to reach the ID and is found in a combination of diffuse labeling with some signals at the lateral cell sides. The age of 7 years has been included in the scheme for a comparison of the situation seen in adults because from this age on, localization of the tested proteins of the ID remains stable.[20]

Table1. Pediatric patient characteristics. DCM-23 to DCM8 are pediatric patients diagnosed with DCM. CTR-23 to CTR7y are pediatric controls that died of a non-cardiac cause. * indicates sisters. Abbreviations: i.u. = in utero; f = female and m = male; MYH7 = Myosin Heavy Chain-7; NA = not applicable.

Name	Age	Gender	Genetics	Heart weight (g)	Body weight (g)	Cardiac anatomy	Saliences
DCM-23	23 weeks i.u.	f	MYH7 mutation	4.8	750	normal	non-compaction CM
DCM-30	30 weeks i.u.	m	genetically screened	16.7	1600	normal	
DCM-32	32 weeks i.u.	f	genetically screened	22.7	3260	normal	Pulmonary hypoplasia
DCM2	2 weeks	f	genetically screened *	40.0	3820	normal	Tachycardia
DCM4	4 weeks	m	not screened	42.0	4060	normal	Pulmonary hypertension
DCM6	6 weeks	m	MYH7 mutation	35.6	5600	normal	Suspected arrhythmias
DCM8	8 weeks	f	genetically screened *	43.7	4140	atrial-septal defect	
CTR-23	23 weeks i.u.	f	NA	3.8	473	normal	
CTR-30	30 weeks i.u.	f	NA	13.2	1895	normal	
CTR-31	31 weeks i.u.	f	NA	11.9	2360	normal	
CTR0	0 weeks	m	NA	20.4	3240	normal	
CTR4	4 weeks	f	NA	25.3	4400	normal	
CTR6	6 weeks	m	NA	25.7	4100	normal	
CTR22	22 weeks	m	NA	31.7	7500	normal	
CTR7y	7 years	f	NA	204.0	-	normal	

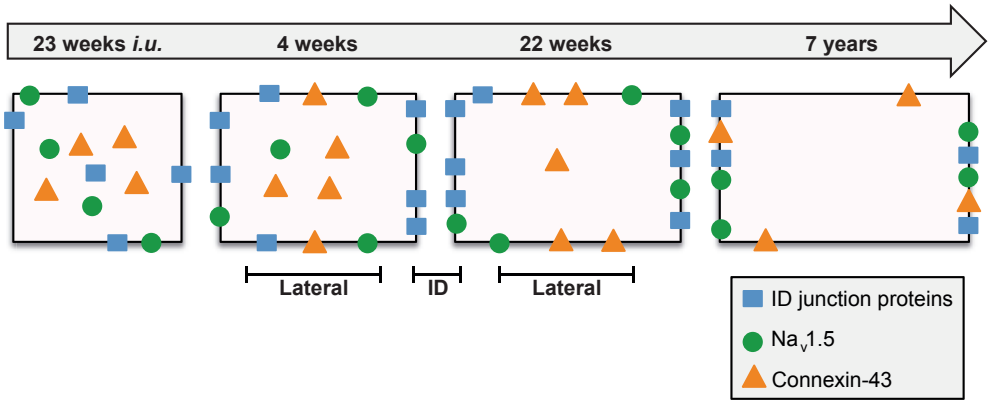

Figure 1. Translocation of ID related proteins during normal pediatric development. The four squares refer to individual cardiomyocytes at the indicated time points (23 weeks in utero, 4 weeks, 22 weeks and 7 years). Proteins of adherens junctions and desmosomes (blue squares), $Na_v1.5$ (green circles) and Connexin-43 (orange triangles) translocate from the cytoplasm laterally and to the ID at different time-points.

ADHERENS JUNCTIONS, GAP JUNCTIONS AND SODIUM CHANNELS

Proteins of the adherens junction Ncad, Plakoglobin and β-catenin followed the same spatio-temporal alterations in localization in pediatric DCM patients as compared to age-matched controls. All proteins were present at the ID at about 4 weeks of age (figure 2). However, DCM8 showed slightly increased lateral staining compared to controls.

In pediatric DCM specimen, gap junction protein Cx43 like in age-matched controls was visualized as signals in the cytoplasm and at the lateral side of the cardiomyocytes. Sodium channel $Na_v1.5$ signals were also normally distributed in pediatric DCM samples compared to age-matched controls. Representative pictures of all those proteins are shown in figure 2.

DESMOSOMAL JUNCTIONS

Desmosomal proteins are reported to translocate to the ID around birth. DSP-1, DSC-2 and PKP-2 followed the same spatio-temporal alterations in localization in pediatric DCM patients as in age-matched controls (Figure 3).

DSG-2 was present in IDs of all adult and pediatric control samples, and similarly also in adult DCM samples. Strikingly, in pediatric DCM samples, signals were reduced and heterogeneously distributed throughout the myocardium. Examples are shown in figure 4. It has to be noted that in order to even visualize these DSG-2 signals in pediatric DCM specimens, a much higher exposure time had to be handled when compared to that used for the controls and the adult samples.

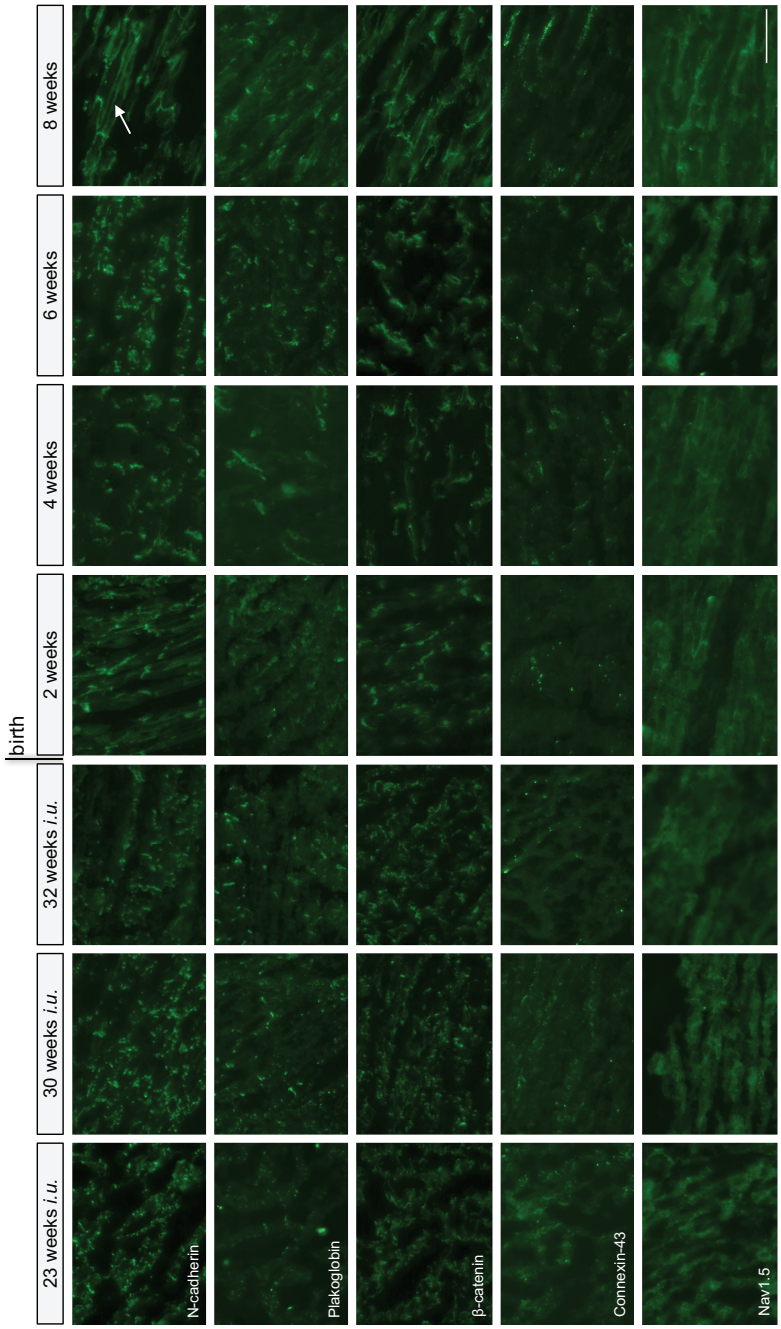

Figure 2. Spatio-temporal organization of proteins related to the ID in 7 pediatric patients with DCM. Immunofluorescence of tissue at different stages of cardiac development for adherens junction proteins N-cadherin, Plakoglobin and β-catenin, gap junction protein Connexin-43 and sodium channel $Na_v1.5$. Localization is comparable to signals seen in age-matched controls. Scale bar indicates 50µm. Arrow indicates N-cadherin lateralization.

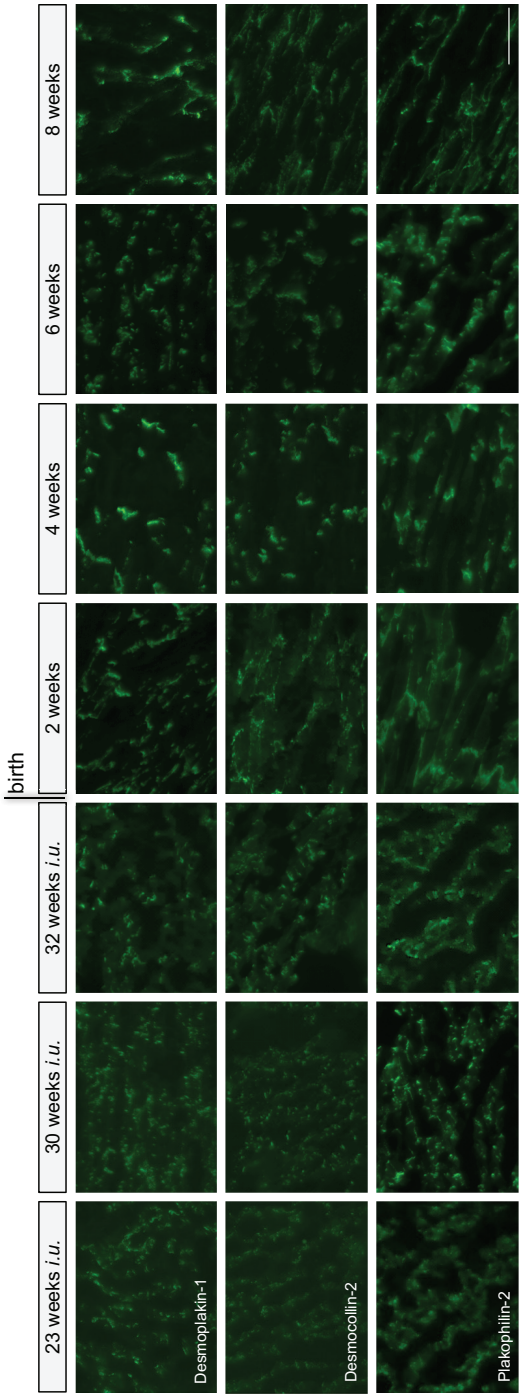

Figure 3. Spatio-temporal organization of desmosomal proteins in 7 pediatric patients with DCM. Immunofluorescence shows subcellular movement of desmosomal proteins during development comparable to that in age-matched controls. Desmoplakin-1, Desmocollin-2 and Plakophilin-2 are all located in the ID at about 2 weeks after birth. Scale bar indicates 50µm.

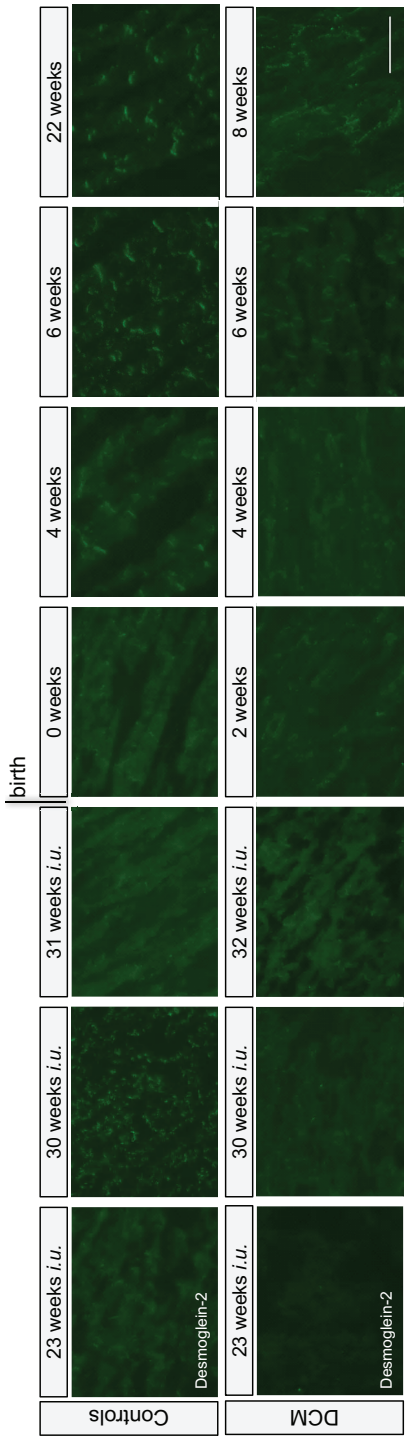

Figure 4. Spatio-temporal organization of Desmoglein-2 in pediatric patients with DCM and age-matched controls. Lower panel: Immunofluorescence in 7 pediatric DCM specimens (age: 23 weeks in utero - 8 weeks) shows low signal intensity and delayed movement of Desmoglein-2 towards the ID compared to age-matched controls (upper panel). Scale bar indicates 50µm.

FIBROSIS

Picrosirius Red was used to stain for collagen in the heart. In the pediatric control tissue hardly any fibrosis could be detected. However, in specimens of all pediatric DCM patients the amount of endocardial and transmural fibrosis was robustly increased. Representative pictures are shown in figure 5.

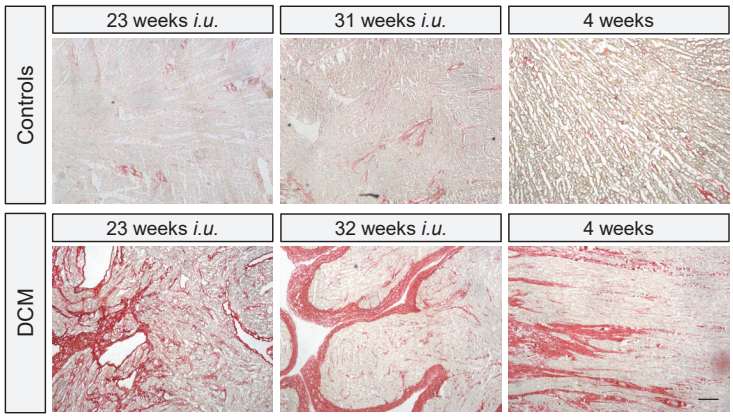

Figure 5. Fibrosis in pediatric controls and DCM patients. Representative pictures of amount of fibrosis assessed by Picrosirius Red staining. Pediatric DCM patients show substantially more endocardial and transmural (interstitial and patchy) fibrosis compared to controls. Scale bar indicates 200µm.

Discussion

Adult DCM has been extensively investigated. Pediatric DCM research, on the other hand has mainly focused on genetics, diagnosis and treatment, and less is known about the involvement of subcellular alterations, especially about the potential contribution of spatio-temporal rearrangement of the ID during disease. This is partially because of the sparse knowledge on this aspect during normal cardiac development and ethical difficulties of obtaining pediatric specimens. In this study, we were able to study 7 specimens of pediatric DCM and age-matched controls. We aimed at detecting differences and congruities in ID proteins between pediatric DCM and age-matched controls.

Our data show that almost all of the investigated proteins follow the same spatio-temporal course in pediatric DCM patients and controls: proteins of the adherens junction Ncad, Plakoglobin and β-catenin were present at the ID after about 4 weeks and signals were comparable to age-matched controls with the only exception of DCM8, which showed lateral labeling of Ncad (arrow in figure 2). Although all three proteins have been reported to be upregulated in adult DCM, this was not visible in our pediatric samples. However, increased signal localization at the ID in adults could have resulted from re-activation of embryonic gene patterning during HF.[27] In embryonic and early postnatal tissue, these gene expression profiles are ongoing and as such no increase might be expected or visible during pathological conditions.

$Na_V1.5$ and the desmosomal proteins DSP-1, DSC-2 and PKP-2 also showed comparable signals in patients and controls, and do not seem to be altered in the adult patients that were studied. Moreover, we also checked for Desmoplakin-2 signals, since a switch from isoform DSP-1 to DSP-2 has been reported in Naxos disease.[28] Both isoforms originate from alternative splicing of the same transcript and are expressed in the skin, but only DSP-1 is reported to be present in the heart.[29] However, no increase in DSP-2 was seen in pediatric DCM compared to controls (data not shown).

Cx43 was not yet visible in the ID, but only in the cytosol and at the lateral site of the cells. Therefore, disturbances in Cx43 might not be detectable and because of the subcellular position of the Cx43 proteins, their function in pediatric cardiac tissue might differ substantially from that in adult tissue. Since reports in adults are conflicting, later time-points could be interesting to add when available.

The only exception of spatio-temporal alterations in pediatric DCM patients is the desmosomal protein DSG-2. In pediatric controls, DSG-2 translocates to the ID after about 4 to 6 weeks postnatal, while in DCM patients it was heterogeneously distributed, signal intensities were reduced and still found lateral after 8 weeks. This suggests that translocation of DSG-2 is delayed or disturbed in DCM patients. In adult DCM and control individuals DSG-2 signals were normal and comparable to control tissues. Although mutations in DSG-2 have been associated with DCM,[13,30] to our knowledge, in absence of such mutations, a reduction in, or redistribution of DSG-2 has never been reported in literature. Although 6 out of 7 of our pediatric patients were

genetically screened, no DSG-2 mutations could be found. This suggests that reduced DSG-2 signals are a result of the disease process rather than a cause. In this regard, however, we can not exclude that thus far undetected genetic aberrancies might have been present in these children that could have a secondary effect on DSG-2. DSG-2 and DSC-2 mediate cardiomyocyte adhesion by calcium dependent dimerization.[31] Reduction and heterogeneous distribution of DSG-2 could weaken the myocardium and cause an imbalanced force transduction and disturbed calcium handling. In turn, disturbed calcium handling could also worsen the course of the disease by impeding adhesion through weakening of DSG-2 and DSC-2 dimerization. This loss of mechanical strength might even facilitate fibrosis formation. Experimental studies in mice demonstrate that DSG-2 is crucial for cardiomyocyte anchorage and overexpression of a mutated form DSG-2 caused ID disruption, slowed conduction and arrhythmias.[32,33] Knockout during embryogenesis appeared lethal, but mice with a cardiomyocyte specific ablation were born healthy and developed Arrhythmogenic Cardiomyopathy (ACM) later in life.[11,34]

The amount of myocardial and endocardial fibrosis was higher in pediatric patients compared to age-matched controls. Fibrosis causes cardiac stiffness and probably mechanistically adds to the occurrence of cardiac arrhythmias and premature death. In general, increased amounts of fibrosis, especially when distributed heterogeneously, are a main contributor to arrhythmias and HF.[5]

DCM-23 and DCM6 had a mutation in the MYH-7 gene that encodes for β-myosin heavy chain. A variety of site-specific mutations in MYH-7 lead to a broad spectrum of cardiomyopathies, including different forms of DCM and HCM.[35] Mouse models with a mutated form of the gene reveal less energetically efficient sarcomeres and show a weakening of the actin-binding site.[36] This mutation has also been described in patients with non-compaction DCM.[37] Whether this mutation also results in alterations in the composition of the ID is currently still unknown.

Conclusion

In the majority of pediatric patients with DCM that we studied, spatio-temporal distribution of several ID proteins was comparable to age-matched controls, except for DSG-2 signals. Moreover, the amount of fibrosis was highly increased in these patients. All together, these observations suggest that development of desmosomal junctions is disturbed in these DCM patients, even in very early stages of cardiac development. This might have contributed to the lethal cardiomyopathy in these children. These findings add further knowledge to the understanding of molecular cardiac development during health and disease and the progression of DCM in children.

References

1. Maron BJ, Towbin JA, Thiene G, et al. Contemporary definitions and classification of the cardiomyopathies: an American Heart Association Scientific Statement from the Council on Clinical Cardiology, Heart Failure and Transplantation Committee; Quality of Care and Outcomes Research and Functional Genomics and Translational Biology Interdisciplinary Working Groups; and Council on Epidemiology and Prevention. Circulation.2006;113(14):1807-1816.

2. Alvarez JA, Orav EJ, Wilkinson JD, et al. Competing risks for death and cardiac transplantation in children with dilated cardiomyopathy: results from the pediatric cardiomyopathy registry. Circulation.2011;124(7):814-823.

3. Hershberger RE, Hedges DJ, Morales A. Dilated cardiomyopathy: the complexity of a diverse genetic architecture. Nat Rev Cardiol.2013;10(9):531-547.

4. Towbin JA, Bowles NE. Dilated cardiomyopathy: a tale of cytoskeletal proteins and beyond. J Cardiovasc Electrophysiol.2006;17(8):919-926.

5. Kessler EL, Boulaksil M, van Rijen HV, Vos MA, van Veen TA. Passive ventricular remodeling in cardiac disease: focus on heterogeneity. Front Physiol.2014;5:482.

6. Vermij SH, Abriel H, van Veen TA. Refining the molecular organization of the cardiac intercalated disc. Cardiovasc Res.2017;10.1093/cvr/cvw259.

7. Gallicano GI, Bauer C, Fuchs E. Rescuing desmoplakin function in extra-embryonic ectoderm reveals the importance of this protein in embryonic heart, neuroepithelium, skin and vasculature. Development.2001;128(6):929-941.

8. Bierkamp C, McLaughlin KJ, Schwarz H, Huber O, Kemler R. Embryonic heart and skin defects in mice lacking plakoglobin. Dev Biol.1996;180(2):780-785.

9. Chen ZQ, Lefebvre D, Bai XH, Reaume A, Rossant J, Lye SJ. Identification of two regulatory elements within the promoter region of the mouse connexin 43 gene. J Biol Chem.1995;270(8):3863-3868.

10. Haegel H, Larue L, Ohsugi M, Fedorov L, Herrenknecht K, Kemler R. Lack of beta-catenin affects mouse development at gastrulation. Development.1995;121(11):3529-3537.

11. Eshkind L, Tian Q, Schmidt A, Franke WW, Windoffer R, Leube RE. Loss of desmoglein 2 suggests essential functions for early embryonic development and proliferation of embryonal stem cells. Eur J Cell Biol.2002;81(11):592-598.

12. Norgett EE, Hatsell SJ, Carvajal-Huerta L, et al. Recessive mutation in desmoplakin disrupts desmoplakin-intermediate filament interactions and causes dilated cardiomyopathy, woolly hair and keratoderma. Hum Mol Genet.2000;9(18):2761-2766.

13. Posch MG, Posch MJ, Geier C, et al. A missense variant in desmoglein-2 predisposes to dilated cardiomyopathy. Mol Genet Metab.2008;95(1-2):74-80.

14. Hirschy A, Croquelois A, Perriard E, et al. Stabilised beta-catenin in postnatal ventricular myocardium leads to dilated cardiomyopathy and premature death. Basic Res Cardiol.2010;105(5):597-608.

15. Ramond F, Janin A, Di Filippo S, et al. Homozygous PKP2 deletion associated with neonatal left ventricle noncompaction. Clin Genet.2017;91(1):126-130.

16. Tariq M, Ware SM. Importance of genetic evaluation and testing in pediatric cardiomyopathy. World J Cardiol.2014;6(11):1156-1165.

17. Pluess M, Daeubler G, Dos Remedios CG, Ehler E. Adaptations of cytoarchitecture in human dilated cardiomyopathy. Biophys Rev.2015;7:25-32.

18. Kostin S, Dammer S, Hein S, Klovekorn WP, Bauer EP, Schaper J. Connexin 43 expression and distribution in compensated and decompensated cardiac hypertrophy in patients with aortic stenosis. Cardiovasc Res.2004;62(2):426-436.

19. Kitamura H, Yoshida A, Ohnishi Y, et al. Correlation of connexin43 expression and late ventricular potentials in nonischemic dilated cardiomyopathy. Circ J.2003;67(12):1017-1021.

20. Vreeker A, van Stuijvenberg L, Hund TJ, Mohler PJ, Nikkels PG, van Veen TA. Assembly of the cardiac intercalated disk during pre- and postnatal development of the human heart. PLoS One.2014;9(4):e94722.

21. Wilkinson JD, Landy DC, Colan SD, et al. The pediatric cardiomyopathy registry and heart failure: key results from the first 15 years. Heart Fail Clin.2010;6(4):401-413, vii.

22. Puggia I, Merlo M, Barbati G, et al. Natural History of Dilated Cardiomyopathy in Children. J Am Heart Assoc.2016;5(7).

23. Kirk R, Dipchand AI, Rosenthal DN, et al. The International Society for Heart and Lung Transplantation Guidelines for the management of pediatric heart failure: Executive summary. [Corrected]. J Heart Lung Transplant.2014;33(9):888-909.

24. Fontes MS, Kessler EL, van Stuijvenberg L, et al. CTGF knockout does not affect cardiac hypertrophy and fibrosis formation upon chronic pressure overload. J Mol Cell Cardiol.2015;88:82-90.

25. van Veen TA, van Rijen HV, Wiegerinck RF, et al. Remodeling of gap junctions in mouse hearts hypertrophied by forced retinoic acid signaling. J Mol Cell Cardiol.2002;34(10):1411-1423.

26. Hund TJ, Koval OM, Li J, et al. A beta(IV)-spectrin/CaMKII signaling complex is essential for membrane excitability in mice. J Clin Invest.2010;120(10):3508-3519.

27. Dirkx E, da Costa Martins PA, De Windt LJ. Regulation of fetal gene expression in heart failure. Biochim Biophys Acta.2013;1832(12):2414-2424.

28. Uzumcu A, Norgett EE, Dindar A, et al. Loss of desmoplakin isoform I causes early onset cardiomyopathy and heart failure in a Naxos-like syndrome. J Med Genet.2006;43(2):e5.

29. Cowin P, Kapprell HP, Franke WW. The complement of desmosomal plaque proteins in different cell types. J Cell Biol.1985;101(4):1442-1454.

30. Garcia-Pavia P, Syrris P, Salas C, et al. Desmosomal protein gene mutations in patients with idiopathic dilated cardiomyopathy undergoing cardiac transplantation: a clinico-pathological study. Heart.2011;97(21):1744-1752.
31. Chitaev NA, Troyanovsky SM. Direct Ca2+-dependent heterophilic interaction between desmosomal cadherins, desmoglein and desmocollin, contributes to cell-cell adhesion. J Cell Biol.1997;138(1):193-201.
32. Rizzo S, Lodder EM, Verkerk AO, et al. Intercalated disc abnormalities, reduced Na(+) current density, and conduction slowing in desmoglein-2 mutant mice prior to cardiomyopathic changes. Cardiovasc Res.2012;95(4):409-418.
33. Schlipp A, Schinner C, Spindler V, et al. Desmoglein-2 interaction is crucial for cardiomyocyte cohesion and function. Cardiovasc Res.2014;104(2):245-257.
34. Kant S, Holthofer B, Magin TM, Krusche CA, Leube RE. Desmoglein 2-Dependent Arrhythmogenic Cardiomyopathy Is Caused by a Loss of Adhesive Function. Circ Cardiovasc Genet.2015;8(4):553-563.
35. McNally EM, Golbus JR, Puckelwartz MJ. Genetic mutations and mechanisms in dilated cardiomyopathy. J Clin Invest.2013;123(1):19-26.
36. Schmitt JP, Debold EP, Ahmad F, et al. Cardiac myosin missense mutations cause dilated cardiomyopathy in mouse models and depress molecular motor function. Proc Natl Acad Sci U S A.2006;103(39):14525-14530.
37. Klaassen S, Probst S, Oechslin E, et al. Mutations in sarcomere protein genes in left ventricular noncompaction. Circulation.2008;117(22):2893-2901.

Supplementary material

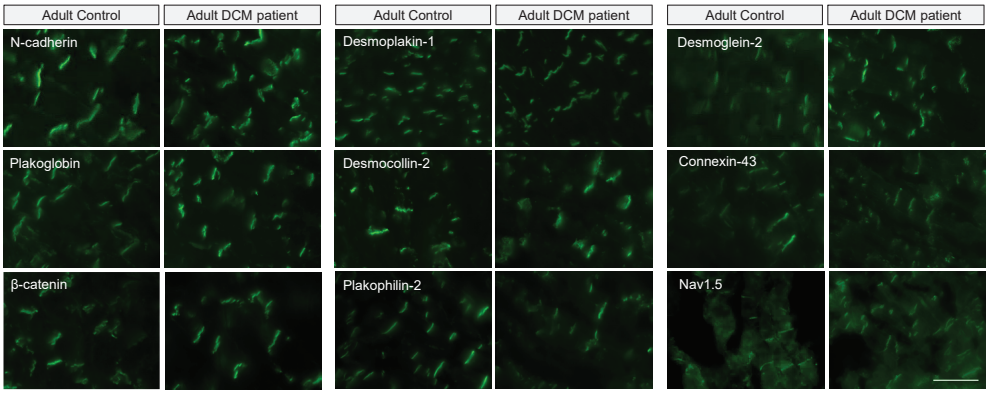

Supplementary Figure 1. Localization of ID proteins in adult controls and DCM patients. Representative pictures of immunofluorescence for N-cadherin, Plakoglobin, β-catenin, Desmoplakin-1, Desmocollin-2, Plakophilin-2, Desmoglein-2, Connexin-43 and $Na_v1.5$. All proteins are located in the ID in controls and DCM patients without substantial differences in signal intensities. Scale bar indicates 50μm.

“

I have not failed.
I’ve successfully discovered
10.000 things that won’t work.

Thomas Edison

Chapter

5

A quest for the biological function of Flotillins within the cardiac intercalated disc

Elise L. Kessler[a], Leonie van Stuijvenberg[a], Joëlle van Bennekom[a], Joanne van Bavel[a], Mathilde R. Rivaud[a], Anne Zwartsen[b,c], Teun P. de Boer[a], Antje Banning[d], Ritva Tikkanen[d], Carol A. Remme[e], Marc A. Vos[a], Toon A.B. van Veen[a]

[a] *Department of Medical Physiology, Division of Heart & Lungs, University Medical Center Utrecht, Utrecht University, Utrecht, The Netherlands*
[b] *Dutch Poisons Information Center (DPIC), University Medical Center Utrecht, Utrecht University, Utrecht, The Netherlands*
[c] *Neurotoxicology Research Group, Division Toxicology, Institute for Risk Assessment Sciences (IRAS), Faculty of Veterinary Medicine, Utrecht University, Utrecht, The Netherlands*
[d] *Institute of Biochemistry, Medical Faculty, University of Giessen, Germany*
[e] *Department of Clinical and Experimental Cardiology, Academic Medical Center, University of Amsterdam, The Netherlands*

A study in progress

Abstract

Background: The contribution of the intercalated disc (ID) during cardiac remodeling has become an important subject in nowadays research efforts. However, still not all molecules residing in the ID have been described and their role is often unknown. This is e.g. the case for the Flotillins, which are known to be present in the cardiac ID and contribute to stabilization of cadherins and desmosomes. They are involved in tumorigenesis and metastasis, but their role in the heart and/or during adverse myocardial remodeling is so far unknown. In this study, we aimed at identifying the role of Flotillin-1 and Flotillin-2 upon cardiac remodeling.

Methods: Presence of Flotillin-1 was determined in human and murine ventricular control samples by fluorescent immunolabeling. Besides, effect of Flotillin knockout (KO) on proteins of the ID and in electrical excitation and conduction were investigated in cardiac samples of wild-type (WT), Flotillin-1 KO, Flotilin-2 KO or double KO mice. This was achieved by Western Blotting, real-time qPCR, histochemistry and fluorescent immunolabeling. Consequences of Flotillin knockdown (KD) on cardiac function were studied in neonatal rat cardiomyocytes (NRCMs) transfected with siRNAs against Flotillin-1, Flotillin-2 or both Flotillins using Western Blotting, electrophysiological measurements and multi-electrode array (MEA) recordings.

Results: Flotillin KO did not cause fibrosis or hypertrophy or changes in the expression of most of the ID proteins. However, protein amount of the cardiac sodium channel $Na_V1.5$ was significantly decreased in Flotillin-1 and Flotillin-1/2 KO mice compared to WT mice. Furthermore, spike amplitude and slope of the electrical signal were significantly decreased in Flotillin-1 and Flotillin-2 KD NRCMs. In addition, spike slope was significantly decreased in Flotillin-2 KD NRCMs compared to control cells. Sodium current density showed a tendency towards a decrease in double KD NRCMs compared to the scrambled cells.

Conclusions: In this study, we demonstrated that Flotillin-1 is also present in the cardiac ID and it influences the amount of $Na_V1.5$ at the ID. This seems to affect excitability.

Introduction

Maladaptive cardiac remodeling, compromised propagation of the electrical impulse and heart disease are often associated with alterations in the intercalated disc (ID), which is the mechanical and electrical contact-region between adjacent cardiomyocytes.[1] The major structures in the ID are gap junctions, adherens junctions, desmosomes and ion channels.[2] Gap junctions enable the electrical coupling between cardiomyocytes and allow small molecules to pass from one cytosol to the other. The main gap-junction protein in the ventricles is Connexin-43 (Cx43).[3] Adherens junctions and desmosomes are responsible for the mechanical coupling: adherens junctions mainly consist of N-cadherin (Ncad), Plakoglobin and β-catenin, connecting actin filaments of two cardiomyocytes; desmosomes are composed of Desmoglein-2 (DSG-2), Desmocollin-2 (DSC-2), Plakophilin-2 (PKP2), Desmoplakin-2 (DSP-2) and also Plakoglobin.[4] These desmosomal junctions link to the intermediate filaments. Ion channels, such as the sodium channel $Na_V1.5$, enable excitation of the cardiomyocytes.[4]
Despite the accumulating knowledge about the ID, its exact content and composition is not yet fully comprehended. Recently, as derived from a proteomics study in which enriched cardiac membrane fractions were analyzed and the obtained data were subjected to system biology approaches, various proteins were suggested to be present in the cardiac ID of humans, mice, rats and dogs.[5] For many of those proteins precise location and function in the heart were thus far unknown. One of these proteins was Flotillin-2, for which the localization at the ID was confirmed by immunohistochemical labeling. Moreover, its levels at the ID were shown to be changed in patients with Arrhythmogenic Cardiomyopathy (ACM) and Dilated Cardiomyopathy (DCM) when compared to control specimens, thereby suggesting a role in cardiac remodeling.[5]

THE FLOTILLIN FAMILY

The Flotillin family, also known as the Reggie family, consists of Flotillin-1/Reggie-2 and Flotillin-2/Reggie-1. These differently named proteins were simultaneously discovered in neurons during axon regeneration (hence the name Reggies) and floating in lipid rafts (hence the name Flotillins).[6,7] Flotillins are highly conserved among species and expressed in almost all vertebrate cell types.[8-10] Both Flotillin isoforms are homologous proteins with an amino acid sequence identity of about 50%. The proteins consist of two parts: the N-terminus that mainly regulates their membrane interaction and the C-terminus that is responsible for oligomerization.[11]
In general, Flotillin-2 is predominantly seen at the cell membranes, although it does not contain a transmembrane domain and therefore does not traverse the membrane.[9,12,13] Due to sequence differences in the palmitoylation sites, Flotillin-1 is a more soluble protein and next to the plasma membrane also present in intracellular organelles like the nucleus, the Golgi complex and late endosomes.[12,14-16] At the plasma membrane, Flotillins co-assemble and form stable clusters, distributed over the cell-to-cell contacts of most cells.[9,17] After hetero-oligomerization, Flotillins can translocate to intercellular compartments, where Flotillin-2 has been

reported to stabilize Flotillin-1.[18-20] Short hairpin RNA mediated decrease and knockout (KO) of Flotillin-2 therefore results in a reduction of Flotillin-1, but Flotillin-1 KO also seems to induce a partial degradation of Flotillin-2, suggesting redundancy or dependency between the family members.[11,21]

FLOTILLIN FUNCTION

Although Flotillins are known to play a role in various cellular processes (e.g. cargo trafficking,[22] endocytosis,[23] phagocytosis,[24] cell-cell and cell-matrix adhesion through actin association,[16,25] cell growth,[22] cell motility and migration,[25] membrane trafficking,[26] signal transduction such as insulin signaling,[15] T cell activation[27] and cadherin recruitment and recycling[28,29]), their behavior upon cardiac remodeling has not yet been thoroughly studied. Furthermore, despite the evidence for the importance of Flotillins in many cellular processes, Flotillin-1, Flotillin-2 or Flotillin-1/2 KO mice are viable, and global KO in all cell types does not show a major phenotype.[30]

In pathophysiology, Flotillins are primarily known for their role in cancer, where both Flotillins promote tumorigenesis and metastasis.[31-33] Up-regulation of Flotillin-2 for instance, supports the invasive potential of melanoma cells, and overexpression of Flotillin-1 leads to bladder carcinomas.[34,35] Flotillin-2 deficiency in turn causes a reduction in tumorigenicity and e.g. lung metastases,[21] and leads to less cell spreading in HeLa cells.[19]

Interestingly, expression of Flotillins seems to be important for the formation, organization and stabilization of adherens junctions and desmosomes.[28,29] Flotillins are able to co-immunoprecipitate with Ncad, α-catenin, β-catenin, E-cadherin, Plakoglobin and DSG.[28,36-38] Flotillin knockdown (KD) in carcinoma epidermoid cells seems to regulate E-cadherin recycling, and results in weakening of the desmosomal adhesion.[28,36,37] However, none of these interactions have been validated in cardiac tissue and their influence on other components of the ID or cardiac excitation and conduction have not yet been described.

With this study, we aimed at identifying the role of Flotillin-2 and its homologous protein Flotillin-1 in the heart. We therefore studied its expression upon cardiac remodeling in human cardiac specimen and investigated its relationship to the ID. Special focus was the potential relationship of Flotillins with functionality of desmosomal and adherens junction proteins, but also with gap junction protein Cx43 and the sodium channel $Na_V1.5$. Furthermore, we used a knockout (KO) mouse model and cultured neonatal rat cardiomyocytes (NRCMs) treated with siRNAs to explore the consequences of gene silencing for cardiac excitation and conduction.

Material & methods

To investigate the role of Flotillin-1 and Flotillin-2 in the heart, different models were used. 1) Sections of ventricular cardiac tissue from human and murine control hearts; 2) Hearts from wildtype (WT) mice, Flotillin-1 KO, Flotillin-2 KO and Flotillin-1/2 KO mice; and 3) ventricular NRCMs, which were either untreated (control) or transfected with a scrambled siRNA (scrambled), siRNA against Flotillin-1 (Flotillin-1 KD), siRNA against Flotillin-2 (Flotillin-2 KD) or both siRNAs (Flotillin-1/2 KD).

ORIGIN OF MATERIAL AND ETHICAL STATEMENTS

The human cardiac specimen was obtained from the Biobank of the Department of Pathology, University Medical Center Utrecht, The Netherlands. Tissue was made available for research purposes after informed written consent in accordance with the appropriate institutional guidelines.

All murine cardiac specimens of WT, Flotillin-1, Flotillin-2 and Flotillin-1/2 C57BL/6J KO mice were generously provided by the group of Ritva Tikkanen, Institute of Biochemistry, Medical Faculty, University of Giessen, Germany. Genetically engineered Flotillin-1 and Flotillin-2 mice were generated as described previously,[31,39] and Flotillin-1/2 mice were crossed in Giessen. Shortly, exon one was deleted using a Cre-Lox-system and KO was confirmed by Southern Blot. After sacrifice by cervical dislocation, hearts were shock frozen in liquid nitrogen and stored at -80 °C. Male and female mice from the following groups were used for experiments and analyses: wildtype mice (WT, age 5.1±0.1 months), Flotillin-1 KO mice (Flot1 KO, age 5.4±0.1 months), Flotillin-2 KO mice (Flot2 KO, age 4.9±0.6 months) and Flotillin-1 and 2 KO mice (Flot-1/2 KO, 4.8±0.1 months).

For the isolation of NRCMs, pregnant Wistar RCC rats were purchased from Envigo, The Netherlands. Experiments on neonatal rats were conducted with consent of the Experimental Animal Ethics Committee of the University Utrecht, The Netherlands. Cells were isolated and transfected as described below.

ISOLATION OF VENTRICULAR NEONATAL RAT CARDIOMYOCYTES

NRCM were isolated from hearts of 1- to 2-day old rats. Neonatal rats were sacrificed by decapitation, hearts were excised aseptically, and vessels and atria removed. Ventricles were washed in Solution A (Hanks' Buffered Salt Solution-based medium) and minced into small pieces of ±2 mm^3. Tissue pieces were then transferred into a sterile glass bottle containing 14 mL SolutionA supplemented with 2.5% Trypsin (Gibco by Life Technologies, Breda, The Netherlands) and 10 µg/mL DNAse (Gibco) and shaken in a water bath set to 37 °C for 15 minutes. Next, the solution was mixed by pipetting up-and-down and the supernatant was transferred into a sterile 50 mL tube. Fresh enzyme solution was added to the sediment and shaken again for 15 minutes. The tube containing supernatant was centrifuged 3 minutes at 1100 rpm without brake, superna-

tant was discarded, and pellet was dissolved in Ham's F10 medium (Thermo Fisher Scientific, Breda, The Netherlands) without calcium and magnesium. This was repeated 4-5 times until all tissue pieces were dissolved and all supernatants were collected.
To remove cell debris, cells were filtered and pre-plated in uncoated culture dishes for 2 hours to enrich the myocytes population and to remove fibroblasts and other non-cardiomyocytes. Afterwards, cells were collected by centrifugation for 3 minutes at 1100 rpm with brake, and 10 mL fresh Hams' F10 supplemented with 5 % fetal calf serum (Lonza, Verviers, Belgium), penicillin/streptomycin (Lonza) and L-Glutamine (Lonza) was added. Then, cells were counted and cultured on laminin-coated (Roche, Mannheim, Germany) cell culture dishes at a density of 250,000 cells/cm^2 for Western Blotting, on transparent Multi Electrode Array (MEA) plates (Axion Biosystems Inc., Atlanta, USA) at a density of 1.15 x 106 cells/cm^2 to create a monolayer, or at a density of 12,500 cells/cm^2 for electrophysiological measurements. Twenty-four hours after plating, medium was changed.

FLUORESCENT IMMUNOLABELING

Immunolabeling of 10 µm thick human and murine four-chamber-view cryo sections was performed as described previously,[40] using mouse monoclonal antibodies against pan-cadherin (1:800, Sigma-Aldrich) and rabbit polyclonal antibodies against Flotillin-1 (1:100, Sigma-Aldrich). Secondary labeling was achieved by appropriate fluorescein isothiocyanate (FITC, 1:250) or Alexa Fluor 594 (1:100) conjugated anti-mouse or anti-rabbit whole IgG antibodies (Jackson ImmunoResearch Europe, Newmarket, United Kingdom).

IMMUNOBLOTTING

Immunoblotting was performed as described previously.[40] Total cardiac cellular protein from mice (WT, Flotillin-1 KO mice, Flotillin-2 KO mice and Flotillin-1/2 KO mice) were blotted. For Immunoblotting of siRNA experiments, ventricular NRCMs were plated on 24 wells plates and scraped 24 hours after transfection. Cells were lysed in a stringent lysis buffer supplemented with protease inhibitors.
All protein samples were separated on a 10 % (or 7 % for $Na_V1.5$) SDS-PAGE gel, electro-transferred on nitrocellulose membranes and blocked with 5 % milk powder. Equality of protein transfer was assessed by a Ponceau-S staining. Membranes were incubated with mouse monoclonal antibodies against pan-cadherin (1:10,000, Sigma-Aldrich), DSG-2 (1:1000, Progen, Heidelberg, Germany), PKP2 (1:250, Progen), Plakoglobin (1:4000, Sigma-Aldrich), DSC-2 (1:500, Millipore, Temecula, CA, USA), Cx43 (1:250, BD Transduction Laboratories, Breda, The Netherlands) or Cx43 (1:250, Invitrogen, Camarillo, USA), and $Na_V1.5$ (1:250, Sigma-Aldrich), and rabbit polyclonal antibodies against Flotillin-1 (1:250, Sigma-Aldrich) and Flotillin-2 (1:250, Thermo Scientific). Secondary labeling was performed with an HRP-conjugated anti-mouse whole IgG antibody (1:7000, Jackson ImmunoResearch Laboratories Inc., Newmarket, United Kingdom) or a HRP-conjugated anti-rabbit whole IgG antibody (1:7000, BioRad Laboratories, Hercules, USA). Detection was performed using standard ECL procedure (Santa Cruz Biotechnology Inc., Heidelberg, Germany) with ChemiDoc XRS system (BioRad Laboratories). Quantification analy-

sis was performed using ImageJ 1.48v software (National Institutes of Health, USA), where the protein of interest was corrected for the corresponding area taken from the Ponceau-S staining.

REAL-TIME QUANTITATIVE PCR

RT-qPCR on cardiac murine tissue was performed using TaqMan Gene Expression Assays (Applied Biosystems by Life Technologies Corp., Carlsbad, CA, USA) as described earlier.[41] Relative mRNA expression levels were determined for Flotillin-2, Flotillin-1, Collagen 1α1, Collagen 1α2, Collagen 3α1, brain natriuretic peptide (BNP), Ncad, Plakoglobin, DSP, DSG-2, Cx43, $Na_V1.5$ and L-type Ca-channel (all from Applied Biosystems by Life Technologies Corp., Carlsbad, USA). Geometric mean of GAPDH, Beta-2 microglobulin (B2m) and TATA-binding protein (Tbp) (Applied Biosystems) were used as internal controls, since the levels did not differ between group samples (for assay-IDs see Supplementary Table 1).

IMMUNOHISTOCHEMISTRY

To detect cardiac fibrosis in murine hearts, 10 µm thick four-chamber-view cryo sections that were fixated in paraformaldehyde were stained with 0.1% Picrosirius Red solution, as described previously.[42] After staining, sections were digitally scanned using Aperio ScanScope XT (Leica Microsystems BV, Son, The Netherlands) and pictures were taken using NDPview2 (Hamamatsu Photonics KK, Shizuoka, Japan). The amount of fibrosis was determined using ImageJ 1.48v software (National Institutes of Health, USA), where the percentage of fibrosis was calculated as the fibrosis positive signal in the ventricles relative to the total ventricular surface area.

CO-IMMUNOPRECIPITATION OF FLOTILLINS

To investigate possible binding partners of Flotillins, Co-Immunoprecipitations (Co-IPs) were performed. Frozen murine hearts were pulverized and incubated in IP-buffer (20mM HEPES, 125mM NaCl, 10 % glycerol, 1mM EDTA, 1mM EGTA, 1mM dithiothreitol, 1 % Triton X-100 pH 7.6, fresh added 50mM NaF, 1mM Na_3VO_4, 1mM PMSF and 1µg/ml aprotinin from bovine lungs (Sigma-Aldrich, St. Louis, USA)) for 30 minutes. All steps were performed on ice or at 4 °C. Lysate was centrifuged at 14.000 rpm for 10 minutes and protein concentration was measured in the supernatant. CoIP-samples of 1mg protein were first incubated (pre-cleared) with protein A- and G-agarose beads (Sigma-Aldrich) for one hour and centrifuged at 1000rpm for 1 minute. The pellet was used to generate Pre-Cleared samples in order to check, whether proteins would be able to bind to the beads without presence of any antibodies. The supernatant was distributed over two tubes and one part was incubated with 1 µg antibody (mouse monoclonal antibodies against pan-cadherin (Sigma-Aldrich), DSG-2 (Progen), Plakoglobin (Sigma-Aldrich), Cx43 (BD Transduction Laboratories), and rabbit polyclonal antibodies against pan-cadherin (Invitrogen), Flotillin-1 (Sigma-Aldrich) and Flotillin-2 (Cell Signaling Technology and (Thermos Scientific) for 2 hours. The other part was incubated without primary antibodies in order to check, whether the secondary antibody could be able to a-specifically bind to the protein. Afterwards, again protein A- and G-agarose beads were added and incubated overnight. The next day, after centrifugation, the pellet was washed with 0.3 % Triton in IP-buffer and the supernatant was used for Immunoblotting.

FLOTILLIN KD IN NRCM BY SIRNA TRANSFECTION

Seventy-two hours after NRCM isolation, cells were transfected using Lipofectamine RNAiMAX (Thermo Fisher Scientific), with either 50 nM siRNA against Flotillin-1 (Flot1 (ID 64665) Trilencer-27 Rat siRNA (SR514199), Origene Technologies, Inc.), 20 nM siRNA against Flotillin-2 (Flot2 (ID 83764) Trilencer-27 Rat siRNA (SR 500907), Origene Technologies, Inc.) or both. Transfection with 10 nM scrambled siRNA (Trilencer-27 Universal Scrambled Negative Control siRNA duplex (SR 30004)) and non-transfected cells were used as controls.

ELECTROPHYSIOLOGICAL MEASUREMENTS

NRCMs were plated on laminin-coated (Roche) cell culture dishes and transfected with siRNAs (scrambled or Flotillin1/2 KD). Peak inward sodium current (I_{Na}) measurements were performed 24 hours of transfection as previously described using a HEKA EPC-10 Double Plus amplifier (HEKA, Lambrecht, Germany) controlled by PatchMaster 2.43.[43]

MULTI-ELECTRODE ASSAY (MEA) RECORDINGS

Field potential of the NRCM monolayers 96 hours after plating was measured using laminin-coated 48-well MEA plates. Each well contains 16 nano-textured gold microelectrodes (~40–50 µm in diameter; 350 µm center-to-center spacing) with 4 integrated ground-electrodes, resulting in an array of 768 micro¬electrodes (Axion Biosystems Inc.). Signals were recorded using a Maestro 768-channel amplifier with integrated heating system and temperature controller (constant temperature of 37 °C). The data acquisition interface, Axion's Integrated Studio (AxIS Maestro v2.1, (Axion Biosystems Inc.) was used to manage data acquisition.

Raw data files on the spontaneously beating cardiomyocytes were recorded with Maestro acquisition settings with a sampling frequency of 12.5kHz/channel using cardiac low amplitude settings (1200x gain, 0.1-200 Hz band-pass filter).

Raw data files were re-recorded and spikes were detected using the AxIS spike detector (adaptive threshold) with a minimum/maximum beat period of 250 ms/5s. Further analyses were performed on 30 consecutive stable beats per well of the re-recorded files. Data from four experiments were combined in a factor correction as described in Ruijter *et al.* 2015.[44]

STATISTICS

Data are expressed as mean ± standard error of the mean (SEM). Statistical analyses were performed using appropriate parametric or non-parametric tests (students t-test or one-way ANOVA followed by Tukey's multiple comparisons test or Kruskal-Wallis followed by Dunn's multiple comparison test). All analyses were performed with GraphPad Prism 6.0 (GraphPad Software Inc., La Jolla, USA) or SPSS 20.0 (IBM SPSS Statistics for Windows, Armonk, USA). A value of $p<0.05$ was considered statistically significant.

Results

FLOTILLINS IN THE HEART AND THE CARDIAC INTERCALATED DISC

Previously, Flotillin-2 was confirmed to be present in the ID of human and animal cardiac tissue and to be changed in patients with DCM and ACM.[5] Beyond our interest regarding the interaction of Flotillins with proteins residing in the cardiac desmosomes and adherens junctions, in order to substantiate our focus on the potential relationship between the Flotillin proteins and proteins involved in excitation and conduction, we reanalyzed unpublished data from a different ongoing study. In that study, we used the expression levels of various proteins in SCN5A-1798 InsD mice and performed an eQTL analysis against the ECG parameters QRS and QT. This revealed a significant and negative correlation for the expression level of in particular Flotillin -1, and to a lower extent Flotillin-2 against QRS, suggesting that these proteins were related to excitation and conduction (data not shown). In figure 1, we show that next to Flotillin-2, also Flotillin-1 is present in human and murine IDs.

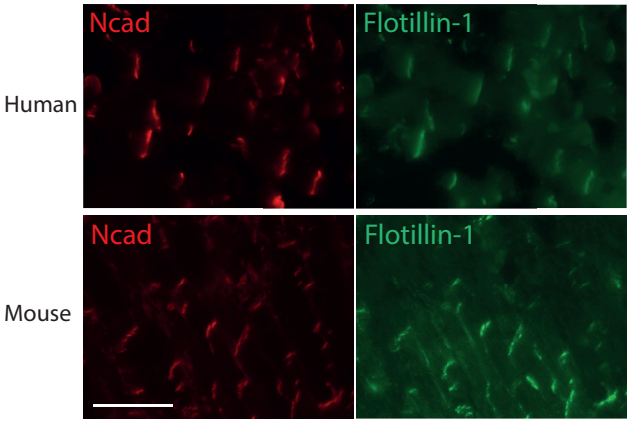

Figure 1. Flotillins in the ID and in cardiac tissue before and after cardiac remodeling. Representative images of Flotillin-1 expression (green) and N-cadherin expression (red) in human and murine ventricular tissue. N-cadherin was used as marker for intercalated discs. Scale bar represents 50 µm.

FLOTILLIN KO: ID AND STRUCTURAL REMODELING

Total KO of Flotillin-1, Flotillin-2 or both Flotillins in genetically engineered mice was confirmed by Western Blot and real-time qPCR (Figure 2A, and 2B, respectively). Interestingly, KO of Flotillin-1 caused a decrease in Flotillin-2 protein levels in those mice, whereas the inverse was also true in the Flotillin-2 KO mice (Figure 2A). A similar trend, though less pronounced, could be appreciated from the qPCR data.

No overt structural changes were seen in hearts of both Flotillin KO mice and no increased fibrosis was detected by Sirius Red staining (Supplementary Figure 1A and B). In line with that, mRNA levels of collagens were unchanged, except for Collagen-1α1 (Col-1α1), which was significantly increased in Flotillin-1/2 KO mice compared to Flotillin-1 KO mice (Supplementary Figure 1C). Furthermore, mRNA levels of the hypertrophic marker brain natriuretic peptide (BNP) were similar between all groups (Supplementary Figure 1C).
Since Flotillins have previously been reported to interact with each other, but also with Ncad, Plakoglobin and DSG-2 in epithelial cells, myoblasts or keratinocytes, we investigated this in the heart and studied the consequences of Flotillin KO on their mRNA and protein levels.
First of all, we confirmed that in cardiac tissue, both Flotillins bind to each other (Supplementary Figure 2A, left panel) and Flotillin-1 indeed binds to Ncad (Supplementary Figure 2A, middle panel). However, Flotillin-1 and Flotillin-2 did not bind to Plakoglobin (Supplementary Figure 2A, middle and right panel), and Flotillin-2 did not bind to Ncad (Supplementary Figure 2A, right panel). Unfortunately, most of the other ID proteins were found to bind unspecifically to the precipitation beads and therefore specific binding to the 'fishing' antibodies could not be determined (examples shown in Supplementary Figure 2B). Furthermore, no significant changes in protein levels were seen in Ncad or Plakoglobin or their respective mRNA levels (Figure 2C and 2D, respectively), with exception of a significant increase of DSG-2 mRNA in Flotillin-1/2 KO mice compared to WT mice (Figure 2D). Other ID proteins, such as PKP2 and DSC-2 were unchanged (data not shown).
In addition, protein levels of $Na_V1.5$ and Cx43, and mRNA levels of $Na_V1.5$, Cx43 and L-type Calcium channel were evaluated. Protein levels of $Na_V1.5$ were significantly reduced in Flotillin-1 and Flotillin-1/2 KO mice compared to WT animals (Figure 3A). Cx43 protein and its non-phosphorylated version (Cx43NP) were not altered upon Flotillin KO (Figure 3B), whereas mRNA levels of Cx43, L-type Ca-channel and $Na_V1.5$ were also not changed (Figure 3C).

CARDIAC FUNCTION AFTER FLOTILLIN KD

To test the effect of Flotillin KD on cardiac function, including cardiac conduction and excitability, NRCMs were transfected with siRNAs against Flotillin-1 or Flotillin-2 and functional measurements were performed.
From every experiment, a few wells were used to validate efficiency of transfection by Western Blot. Treatment of NRCMs with siRNAs against Flotillin-1 or Flotillin-2, but not with scrambled siRNAs, resulted in a partial KD of both proteins (Figure 4A). If an siRNA against Flotillin-1 was transfected, amounts of Flotillin-1, but also Flotillin-2 were decreased and *vice versa*, comparable to what was detected in KO mice.
Electrophysiological measurements were performed on scrambled and double KD cells. Peak sodium current showed a tendency towards a decrease upon double KD of Flotillins in NRCMs (Figure 4B).
In order to measure cardiac function and electrical cardiac signaling, MEA experiments were performed on NRCMs. Supplementary Figure 3 shows examples of the trace generated by the electrical signal obtained from 16 electrodes (left) and one electrode (right). Measurements that could be extracted are the spike amplitude (mV) of the signal, the spike slope (V/s, interpreted as the dV/dt) and the beat period (s, comparable to the RR interval of an ECG).

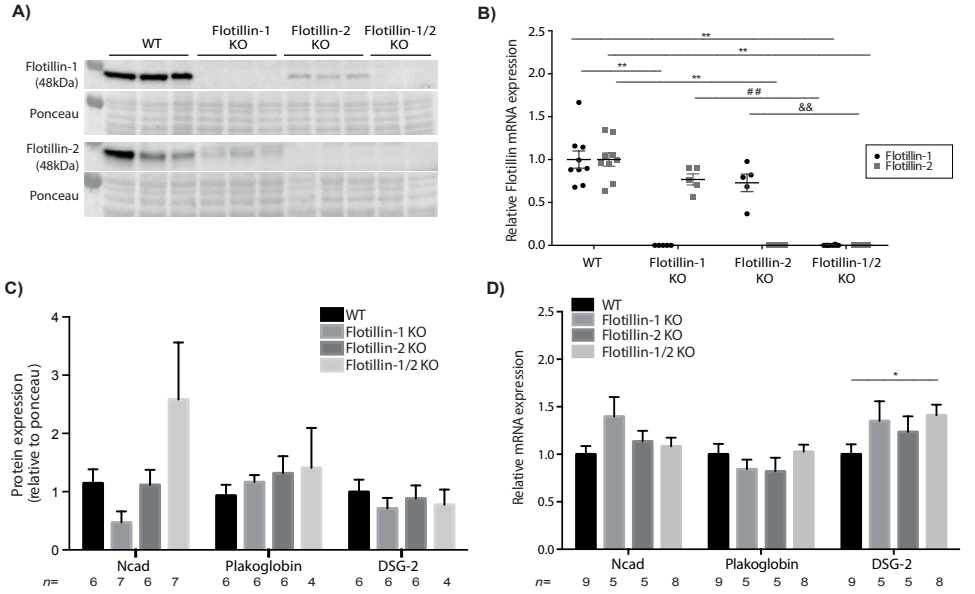

Figure 2. Molecular ID changes upon Flotillin knockout in mice. **A)** Representative Western Blot of Flotillin-1 and Flotillin-2 with respective Ponceau staining in wildtype (WT), Flotillin-1 knockout (KO), Flotillin-2 KO and Flotillin-1/2 KO mice. **B)** Relative mRNA expression of Flotillin-1 and Flotillin-2 assessed by RT-qPCR in WT, Flotillin-1 KO, Flotillin-2 KO and Flotillin-1/2 KO mice. **C)** Quantitative protein expression of Ncadherin (Ncad), Plakoglobin and Desmoglein-2 (DSG-2) relative to Ponceau in WT, Flotillin-1 KO, Flotillin-2 KO and Flotillin-1/2 KO mice. **D)** Relative mRNA expression of Ncad, Plakoglobin and DSG-2 and Flotillin-2 assessed by RT-qPCR in WT, Flotillin-1 KO, Flotillin-2 KO and Flotillin-1/2 KO mice. n indicates the number of mice per group. * p<0.05 and ** p<0.01 compared to WT, ## p<0.01 compared to Flotillin-1 KO and && p<0.01 compared to Flotillin-2 KO.

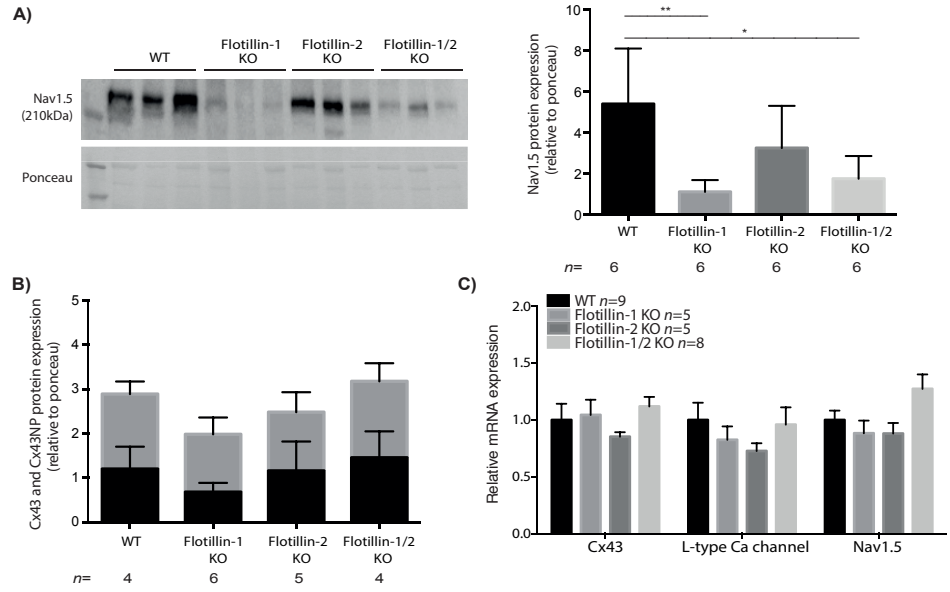

Figure 3. Effect of Flotillin KO on Cx43 and $Na_v1.5$. A) Representative Western Blot with respective Ponceau staining (left) and quantitative protein expression (right) of $Na_v1.5$ relative to Ponceau in WT, Flotillin-1 KO, Flotillin-2 KO and Flotillin-1/2 KO mice. **B)** Quantitative protein expression of Cx43 and its non-phosphorylated state Cx43NP relative to Ponceau in WT, Flotillin-1 KO, Flotillin-2 KO and Flotillin-1/2 KO mice. **C)** Relative mRNA expression of Cx43, L-type Calcium channel and $Na_v1.5$ assessed by RT-qPCR in WT, Flotillin-1 KO, Flotillin-2 KO and Flotillin-1/2 KO mice. n indicates the number of mice per group. * p<0.05 and ** p<0.01 compared to WT.

Beat period did not change between all conditions (Figure 4C). Spike amplitude, however, was significantly decreased in Flotillin-1 KD and Flotillin-2 KD cells compared to control cells (Figure 4D), and spike slope was significantly decreased in Flotillin-1 KD cells compared to control cells (Figure 4E). Conduction Velocity was unchanged after siRNA treatment (Figure 4F).

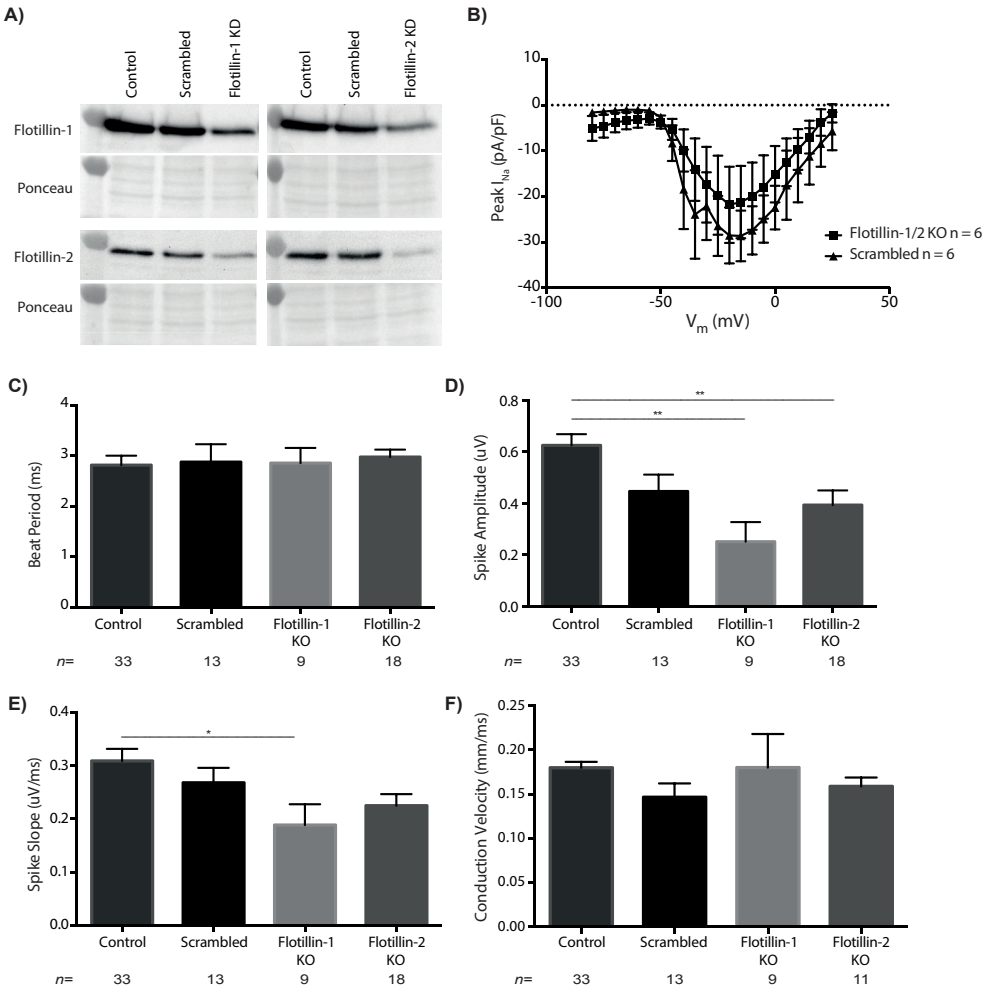

Figure 4. Electrical changes upon Flotillin knockdown in Neonatal Rat Cardiomyocytes. **A)** Representative Western Blot of Flotillin-1 and Flotillin-2 with respective Ponceau staining in control, scrambled, Flotillin-1 knockdown (KD) and Flotillin-2 KD neonatal rat cardiomyocytes (NRCMs). Electrical signal measured by a Multi-Electrode Array: **B)** Peak sodium current (pA/pF) in scrambled (triangles) and Flotillin-1/2 KD (squares) NRCMs. **C)** Beat period (ms) measured by MEAs in control, scrambled, Flotillin-1 KD and Flotillin-2 KD NRCMs. **D)** Spike amplitude (μV) measured by MEA in control, scrambled, Flotillin-1 KD and Flotillin-2 KD NRCMs. **E)** Spike slope (μV/ms) measured by MEAs in control, scrambled, Flotillin-1 KD and Flotillin-2 KD NRCMs. **F)** Conduction velocity (mm/ms) measured by MEA in control, scrambled, Flotillin-1 KD and Flotillin-2 KD NRCMs. n indicates the number of mice per group. * $p<0.05$ and ** $p<0.01$ compared to control NRCMs.

Discussion

Given their high evolutionary conservation, Flotillins are thought to have an important cellular function.[22] As mentioned earlier, Flotillins play, among others, a role in membrane trafficking, phagocytosis, cell-to-cell coupling, cell migration and adherens junction and desmosomal assembly, and are involved in various forms of cancer.[45]

Besides, our group showed previously that Flotillin-2 is present in the ID of humans and various animals.[5] In this study, we also demonstrated that Flotillin-1 is present in the cardiac ID (Figure 1). However, their biological role within cardiomyocytes and their potential involvement in cardiac remodeling has not yet been investigated. In our current study, we aimed at investigating the involvement of Flotillin-1 and Flotillin-2 in cardiac function and myocardial remodeling with special attention on their potential role in electrophysiological remodeling. To achieve that, we studied Flotillin KO mice and the effect of Flotillin KD in NRCMs.

Previously, it has been shown that Flotillin KO did not cause any phenotypic defects in mice, but Flotillin overexpression leads to disturbances of cell-cell adhesion molecules.[20] Also in the hearts that we studied, no overt structural aberrancies could be detected as hearts were not hypertrophied, nor contained elevated levels of fibrosis (Supplementary Figure 1). Although it has been shown that cadherin stabilization at the cell-cell junctions of myoblasts and breast cancer cells is Flotillin-dependent,[28] in our study, Flotillin KO did not seem to affect total Ncad protein and mRNA levels (Figure 2C and D), whereas co-immunoprecipitations of Ncad could only be confirmed with Flotillin-1 (Supplementary Figure 2). Possibly, not the total amount of Ncad in cardiomyocytes is altered after KO of Flotillins, but only the ratio between the distribution of the proteins between membranes and cytosol. To substantiate that, cell fractioning or super resolution microscopy experiments would be needed to answer this question.

Moreover, Flotillins have been reported to stabilize Desmogleins at the cell-to-cell junctions, and it has been suggested that loss of Flotillins could cause weakening of desmosomal junctions in keratinocytes due to the rapid turnover of Desmoglein-3 (DSG-3).[37] In the heart, instead of DSG-3, DSG-2 is expressed, which protein levels were unchanged after KO, although in mice its mRNA levels were significantly increased after Flotillin-1/2 KO, compared to WT. Since we did not investigate the localization of DSG-2 within the cardiomyocytes, the unchanged total amount DSG-2 after KO can not exclude that some of the DSG-2 Western Blot signal was derived from an increased amount of internalized DSG-2. Increased mRNA levels of DSG-2 might point into the direction of a rescue mechanism, where its expression is increased due to the destabilization of the desmosomes. *In vitro* experiments to test cell attachment could provide more knowledge on the role of Flotillins on the cardiac ID. On the other hand, previous studies have indicated that desmosomal dysfunction initiates cardiac remodeling and in particular dilated cardiomyopathy.[46-48] The fact that, at baseline, Flotillin-1, Flotillin-2 or double KO hearts did not show structural alterations suggests that indeed desmosomal integrity at the ID was maintained.

Furthermore, most other cardiac ID proteins seem to be unaffected by the KO (Figure 2C and D and Figure 3B and C), and/or binding to either Flotillin-1 or Flotillin-2 could not be confirmed due to a-specific binding of the target protein to the beads (Supplementary Figure 2). Even though Flotillins were reported to bind to Plakoglobin in epithelial cells and keratinocytes and in vitro,[36,37] neither Flotillin-1 (Supplementary Figure 2, middle panel), nor Flotillin-2 (Supplementary Figure 2, right panel) bound to Plakoglobin in our co-immunoprecipitations.

Interestingly, protein levels of the sodium channel $Na_V1.5$ were significantly reduced in Flotillin-1 and Flotillin-1/2 KO compared to WT mice (Figure 3A), although mRNA levels were unchanged, suggesting that Flotillin-1 could be involved in trafficking of $Na_V1.5$ to, or recycling from the membrane rather than in transcription regulation. This finding would be in line with results from Meister *et al.*, who showed that Flotillin-1 is involved cargo recognition for endosome trafficking.[49]

To investigate the effect of Flotillin reduction or absence on cardiac function, Flotillins were downregulated in cultured NRCMs as depicted in Figure 4A. Flotillin-1/2 KD resulted in a slight decrease of peak sodium current (Figure 4B), and Flotillin-2 KD in reduction in spike amplitude (Figure 4D) as compared to control cells. The latter was also seen in Flotillin-1 KD cells together with a reduction in the spike slope (Figure 4E, comparable to the dV/dt), compared to control cells. Although these differences were only significant compared to control cells and not to scrambled cells, it can be appreciated that e.g. the decrease in spike amplitude after Flotillin-1 KD can not only be explained by the effect of transfection. Intriguingly, lipid rafts, which happen to contain both Flotillins, but also e.g. $Na_V1.5$ and several potassium channels, are known to play a role in cell membrane excitability.[50] It has been hypothesized that $Na_V1.5$ in lipid rafts forms a reservoir for functional sodium channels and can be recruited when eeded.[51] To speculate, Flotillin KO or KD might therefore hamper the recruitment of $Na_V1.5$ to these functional sodium channels, or even lead to its degradation. This would be supported by the fact that we do not see changes in mRNA expression, but in protein levels and excitability of NRCMs. In case of the potassium channel protein $K_V2.1$, the rafts are shown to directly modulate its electrophysiological features, and interestingly, Flotillin-1 is reported to down-regulate the potassium current by binding $K_V2.1$ in the brain.[52-54] Further research on other ion channels, such as the potassium channel, but also the calcium channel, could therefore give more insight into the role of Flotillins in cardiac excitability.

Surprisingly, high levels of $Na_V1.5$ are found in cancer cells and the level of their expression and their activity is related to the aggressiveness of the cancer and the formation of metastases.[55] As explained in the introduction, Flotillin KO has been proven to reduce tumorigenesis and metastases, and in this study, we showed that it also causes decreased levels of $Na_V1.5$, which might suggest that $Na_V1.5$ levels might play a role in the Flotillin-induced effect on metastases. However, this speculation should be investigated in a different study.

Lastly, conduction velocity was not affected after Flotillin KD (Figure 4F), being in line with only slight changes in Cx43 mRNA and protein levels seen after KO in mice (Figure 3B and C). Although the relation between Cx43 and $Na_V1.5$ has been shown in several studies, especially

in combination with alterations in PKP2,[56-60] this does not seem to be of influence in the KO mice or the cultured NRCMs. The fact that PKP2 and Cx43 were unchanged in the KO mice suggests that the reduction of $Na_V1.5$ and the resulting electrical alterations are related to a different mechanism, possibly involving the lipid rafts.

Conclusion

Changes in expression and functionality of $Na_V1.5$ leading to disturbances of the electrical excitability of cardiomyocytes are observed in various cardiac diseases, such as long QT syndrome, Brugada syndrome and ACM.[61,62] In this study, we have shown that Flotillins might influence $Na_V1.5$ and the cardiac excitability. Therefore, the relation between Flotillins and $Na_V1.5$, but also other ion channels should be continuingly investigated. Finally, Flotillins could serve as potential proteins to check in mutation-negative patients, who suffer from cardiac diseases that are known to have a strong genetic basis.

References

1. Forbes MS, Sperelakis N. Intercalated discs of mammalian heart: a review of structure and function. Tissue Cell.1985;17(5):605-648.

2. Noorman M, van der Heyden MA, van Veen TA, et al. Cardiac cell-cell junctions in health and disease: Electrical versus mechanical coupling. J Mol Cell Cardiol.2009;47(1):23-31.

3. Elfgang C, Eckert R, Lichtenberg-Frate H, et al. Specific permeability and selective formation of gap junction channels in connexin-transfected HeLa cells. J Cell Biol.1995;129(3):805-817.

4. Vermij SH, Abriel H, van Veen TA. Refining the molecular organization of the cardiac intercalated disc. Cardiovasc Res.2017;10.1093/cvr/cvw259.

5. Soni S, Raaijmakers AJ, Raaijmakers LM, et al. A Proteomics Approach to Identify New Putative Cardiac Intercalated Disk Proteins. PLoS One.2016;11(5):e0152231.

6. Schulte T, Paschke KA, Laessing U, Lottspeich F, Stuermer CA. Reggie-1 and reggie-2, two cell surface proteins expressed by retinal ganglion cells during axon regeneration. Development.1997;124(2):577-587.

7. Bickel PE, Scherer PE, Schnitzer JE, Oh P, Lisanti MP, Lodish HF. Flotillin and epidermal surface antigen define a new family of caveolae-associated integral membrane proteins. J Biol Chem.1997;272(21):13793-13802.

8. Rivera-Milla E, Stuermer CA, Malaga-Trillo E. Ancient origin of reggie (flotillin), reggie-like, and other lipid-raft proteins: convergent evolution of the SPFH domain. Cell Mol Life Sci.2006;63(3):343-357.

9. Langhorst MF, Reuter A, Stuermer CA. Scaffolding microdomains and beyond: the function of reggie/flotillin proteins. Cell Mol Life Sci.2005;62(19-20):2228-2240.

10. Otto GP, Nichols BJ. The roles of flotillin microdomains--endocytosis and beyond. J Cell Sci.2011;124(Pt 23):3933-3940.

11. Solis GP, Hoegg M, Munderloh C, et al. Reggie/flotillin proteins are organized into stable tetramers in membrane microdomains. Biochem J.2007;403(2):313-322.

12. Santamaria A, Castellanos E, Gomez V, et al. PTOV1 enables the nuclear translocation and mitogenic activity of flotillin-1, a major protein of lipid rafts. Mol Cell Biol.2005;25(5):1900-1911.

13. Bauer M, Pelkmans L. A new paradigm for membrane-organizing and -shaping scaffolds. FEBS Lett.2006;580(23):5559-5564.

14. Liu J, Deyoung SM, Zhang M, Dold LH, Saltiel AR. The stomatin/prohibitin/flotillin/HflK/C domain of flotillin-1 contains distinct sequences that direct plasma membrane localization and protein interactions in 3T3-L1 adipocytes. J Biol Chem.2005;280(16):16125-16134.

15. Gkantiragas I, Brugger B, Stuven E, et al. Sphingomyelin-enriched microdomains at the Golgi complex. Mol Biol Cell.2001;12(6):1819-1833.

16. Neumann-Giesen C, Falkenbach B, Beicht P, et al. Membrane and raft association of reggie-1/flotillin-2: role of myristoylation, palmitoylation and oligomerization and induction of filopodia by overexpression. Biochem J.2004;378(Pt 2):509-518.

17. Frick M, Bright NA, Riento K, Bray A, Merrified C, Nichols BJ. Coassembly of flotillins induces formation of membrane microdomains, membrane curvature, and vesicle budding. Curr Biol.2007;17(13):1151-1156.

18. Babuke T, Ruonala M, Meister M, et al. Hetero-oligomerization of reggie-1/flotillin-2 and reggie-2/flotillin-1 is required for their endocytosis. Cell Signal.2009;21(8):1287-1297.

19. Neumann-Giesen C, Fernow I, Amaddii M, Tikkanen R. Role of EGF-induced tyrosine phosphorylation of reggie-1/flotillin-2 in cell spreading and signaling to the actin cytoskeleton. J Cell Sci.2007;120(Pt 3):395-406.

20. Hoehne M, de Couet HG, Stuermer CA, Fischbach KF. Loss- and gain-of-function analysis of the lipid raft proteins Reggie/Flotillin in Drosophila: they are posttranslationally regulated, and misexpression interferes with wing and eye development. Mol Cell Neurosci.2005;30(3):326-338.

21. Berger T, Ueda T, Arpaia E, et al. Flotillin-2 deficiency leads to reduced lung metastases in a mouse breast cancer model. Oncogene.2013;32(41):4989-4994.

22. Stuermer CA. The reggie/flotillin connection to growth. Trends Cell Biol.2010;20(1):6-13.

23. Stuermer CA, Lang DM, Kirsch F, Wiechers M, Deininger SO, Plattner H. Glycosylphosphatidyl inositol-anchored proteins and fyn kinase assemble in noncaveolar plasma membrane microdomains defined by reggie-1 and -2. Mol Biol Cell.2001;12(10):3031-3045.

24. Garin J, Diez R, Kieffer S, et al. The phagosome proteome: insight into phagosome functions. J Cell Biol.2001;152(1):165-180.

25. Hulsbusch N, Solis GP, Katanaev VL, Stuermer CA. Reggie-1/Flotillin-2 regulates integrin trafficking and focal adhesion turnover via Rab11a. Eur J Cell Biol.2015;94(11):531-545.

26. Munderloh C, Solis GP, Bodrikov V, et al. Reggies/flotillins regulate retinal axon regeneration in the zebrafish optic nerve and differentiation of hippocampal and N2a neurons. J Neurosci.2009;29(20):6607-6615.

27. Stuermer CA, Langhorst MF, Wiechers MF, et al. PrPc capping in T cells promotes its association with the lipid raft proteins reggie-1 and reggie-2 and leads to signal transduction. FASEB J.2004;18(14):1731-1733.

28. Guillaume E, Comunale F, Do Khoa N, Planchon D, Bodin S, Gauthier-Rouviere C. Flotillin microdomains stabilize cadherins at cell-cell junctions. J Cell Sci.2013;126(Pt 22):5293-5304.

29. Solis GP, Schrock Y, Hulsbusch N, Wiechers M, Plattner H, Stuermer CA. Reggies/flotillins regulate E-cadherin-mediated cell contact formation by affecting EGFR trafficking. Mol Biol Cell.2012;23(10):1812-1825.

30. Banning A, Ockenga W, Finger F, Siebrasse P, Tikkanen R. Transcriptional regulation of flotillins by the extracellularly regulated kinases and retinoid X receptor complexes. PLoS One.2012;7(9):e45514.

31. Banning A, Regenbrecht CR, Tikkanen R. Increased activity of mitogen activated protein kinase pathway in flotillin-2 knockout mouse model. Cell Signal.2014;26(2):198-207.

32. Liu J, Huang W, Ren C, et al. Flotillin-2 promotes metastasis of nasopharyngeal carcinoma by activating NF-kappaB and PI3K/Akt3 signaling pathways. Sci Rep.2015;5:11614.

33. Koh M, Yong HY, Kim ES, et al. A novel role for flotillin-1 in H-Ras-regulated breast cancer aggressiveness. Int J Cancer.2016;138(5):1232-1245.

34. Hazarika P, McCarty MF, Prieto VG, et al. Up-regulation of Flotillin-2 is associated with melanoma progression and modulates expression of the thrombin receptor protease activated receptor 1. Cancer Res.2004;64(20):7361-7369.

35. Guan Y, Song H, Zhang G, Ai X. Overexpression of flotillin-1 is involved in proliferation and recurrence of bladder transitional cell carcinoma. Oncol Rep.2014;32(2):748-754.

36. Kurrle N, Vollner F, Eming R, Hertl M, Banning A, Tikkanen R. Flotillins directly interact with gamma-catenin and regulate epithelial cell-cell adhesion. PLoS One.2013;8(12):e84393.

37. Vollner F, Ali J, Kurrle N, et al. Loss of flotillin expression results in weakened desmosomal adhesion and Pemphigus vulgaris-like localisation of desmoglein-3 in human keratinocytes. Sci Rep.2016;6:28820.

38. Yap AS, Gomez GA, Parton RG. Adherens Junctions Revisualized: Organizing Cadherins as Nanoassemblies. Dev Cell.2015;35(1):12-20.

39. Ludwig A, Otto GP, Riento K, Hams E, Fallon PG, Nichols BJ. Flotillin microdomains interact with the cortical cytoskeleton to control uropod formation and neutrophil recruitment. J Cell Biol.2010;191(4):771-781.

40. van Veen TA, van Rijen HV, Wiegerinck RF, et al. Remodeling of gap junctions in mouse hearts hypertrophied by forced retinoic acid signaling. J Mol Cell Cardiol.2002;34(10):1411-1423.

41. Fontes MS, Raaijmakers AJ, van Doorn T, et al. Changes in Cx43 and NaV1.5 expression precede the occurrence of substantial fibrosis in calcineurin-induced murine cardiac hypertrophy. PLoS One.2014;9(1):e87226.

42. Fontes MS, Kessler EL, van Stuijvenberg L, et al. CTGF knockout does not affect cardiac hypertrophy and fibrosis formation upon chronic pressure overload. J Mol Cell Cardiol.2015;88:82-90.

43. Jonsson MK, Vos MA, Mirams GR, et al. Application of human stem cell-derived cardiomyocytes in safety pharmacology requires caution beyond hERG. J Mol Cell Cardiol.2012;52(5):998-1008.

44. Ruijter JM, Ruiz Villalba A, Hellemans J, Untergasser A, van den Hoff MJ. Removal of between-run variation in a multi-plate qPCR experiment. Biomol Detect Quantif.2015;5:10-14.

45. Babuke T, Tikkanen R. Dissecting the molecular function of reggie/flotillin proteins. Eur J Cell Biol.2007;86(9):525-532.

46. Pluess M, Daeubler G, Dos Remedios CG, Ehler E. Adaptations of cytoarchitecture in human dilated cardiomyopathy. Biophys Rev.2015;7(1):25-32.

47. Kitamura H, Ohnishi Y, Yoshida A, et al. Heterogeneous loss of connexin43 protein in nonischemic dilated cardiomyopathy with ventricular tachycardia. J Cardiovasc Electrophysiol.2002;13(9):865-870.

48. Parvari R, Levitas A. The mutations associated with dilated cardiomyopathy. Biochem Res Int.2012;2012:639250.

49. Meister M, Banfer S, Gartner U, et al. Regulation of cargo transfer between ESCRT-0 and ESCRT-I complexes by flotillin-1 during endosomal sorting of ubiquitinated cargo. Oncogenesis.2017;6(6):e344.

50. Brisson L, Gillet L, Calaghan S, et al. Na(V)1.5 enhances breast cancer cell invasiveness by increasing NHE1-dependent H(+) efflux in caveolae. Oncogene.2011;30(17):2070-2076.

51. Maguy A, Hebert TE, Nattel S. Involvement of lipid rafts and caveolae in cardiac ion channel function. Cardiovasc Res.2006;69(4):798-807.

52. Pristera A, Okuse K. Building excitable membranes: lipid rafts and multiple controls on trafficking of electrogenic molecules. Neuroscientist.2012;18(1):70-81.

53. Martens JR, Navarro-Polanco R, Coppock EA, et al. Differential targeting of Shaker-like potassium channels to lipid rafts. J Biol Chem.2000;275(11):7443-7446.

54. Liu R, Yang G, Zhou MH, He Y, Mei YA, Ding Y. Flotillin-1 downregulates K(+) current by directly coupling with Kv2.1 subunit. Protein Cell.2016;7(6):455-460.

55. Besson P, Driffort V, Bon E, Gradek F, Chevalier S, Roger S. How do voltage-gated sodium channels enhance migration and invasiveness in cancer cells? Biochim Biophys Acta.2015;1848(10 Pt B):2493-2501.

56. Jansen JA, Noorman M, Musa H, et al. Reduced heterogeneous expression of Cx43 results in decreased Nav1.5 expression and reduced sodium current that accounts for arrhythmia vulnerability in conditional Cx43 knockout mice. Heart Rhythm.2012;9(4):600-607.

57. Cerrone M, Lin X, Zhang M, et al. Missense mutations in plakophilin-2 cause sodium current deficit and associate with a Brugada syndrome phenotype. Circulation.2014;129(10):1092-1103.

58. Sato PY, Musa H, Coombs W, et al. Loss of plakophilin-2 expression leads to decreased sodium current and slower conduction velocity in cultured cardiac myocytes. Circ Res.2009;105(6):523-526.

59. Sato PY, Coombs W, Lin X, et al. Interactions between ankyrin-G, Plakophilin-2, and Connexin43 at the cardiac intercalated disc. Circ Res.2011;109(2):193-201.

60. Cerrone M, Noorman M, Lin X, et al. Sodium current deficit and arrhythmogenesis in a murine model of plakophilin-2 haploinsufficiency. Cardiovasc Res.2012;95(4):460-468.

61. Shy D, Gillet L, Abriel H. Cardiac sodium channel NaV1.5 distribution in myocytes via interacting proteins: the multiple pool model. Biochim Biophys Acta.2013;1833(4):886-894.

62. Gillet L, Shy D, Abriel H. NaV1.5 and interacting proteins in human arrhythmogenic cardiomyopathy. Future Cardiol.2013;9(4):467-470.

Supplementary material

Protein	Gene	Assay ID
TBP	*Tbp*	Mm00446971_m1
B2m	*B2m*	Mm00437762_m1
GAPDH	*GAPDH*	Mm99999915_g1
Flotillin-1	*flotillin-1*	Mm00514948_m1
Flotillin-2	*flotillin-2*	Mm00514956_m1
Collagen 1α1	*Col1a1*	Mm00801666_g1
Collagen 1α2	*Col1a2*	Mm00483888_m1
Collagen 3α1	*Col3a1*	Mm01254476_m1
BNP	*Nppb*	Mm01255770_g1
Ncadherin	*Cdh2*	Mm01162497_m1
Plakoglobin	*jup*	Mm00550256_m1
Desmoglein-2	*Dsg*	Mm00514608_m1
Nav1.5	*scn5a*	Mm01342518_m1
Cx43	*GJA1*	Mm00439105_m1
L-type Ca channel	*Cacna1C*	Mm01188822_m1

Supplementary Table 1. Characteristics of qPCR primers used in this study. Protein, gene name and assay ID of all primers (all purchased from Applied Biosystems by Life Technologies Corp., Carlsbad, USA).

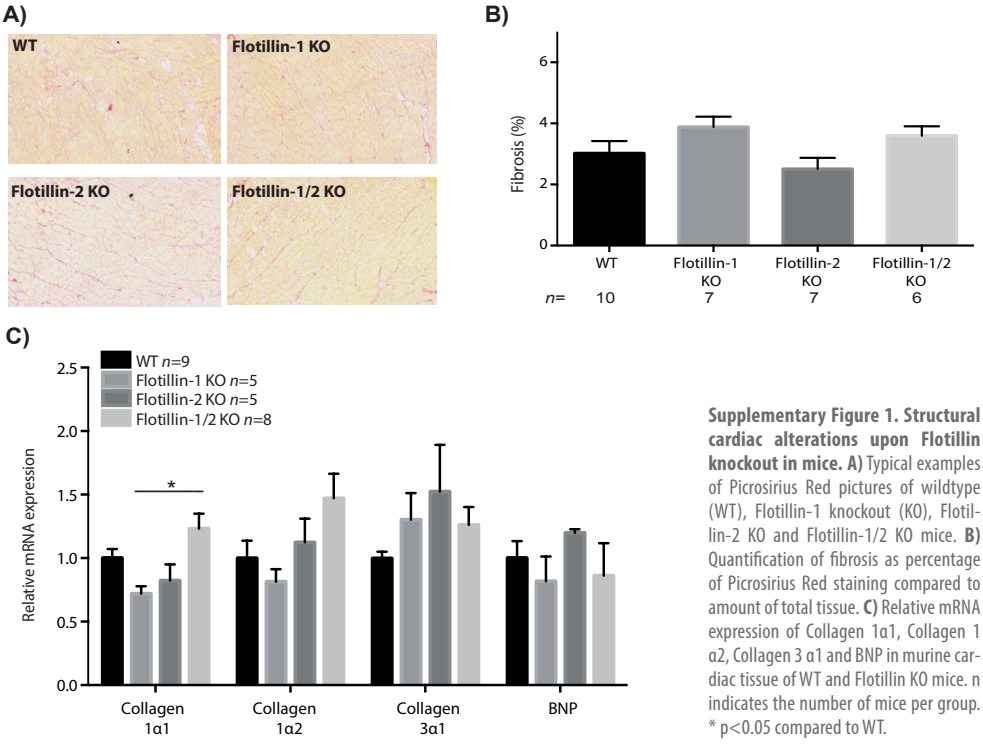

Supplementary Figure 1. Structural cardiac alterations upon Flotillin knockout in mice. A) Typical examples of Picrosirius Red pictures of wildtype (WT), Flotillin-1 knockout (KO), Flotillin-2 KO and Flotillin-1/2 KO mice. **B)** Quantification of fibrosis as percentage of Picrosirius Red staining compared to amount of total tissue. **C)** Relative mRNA expression of Collagen 1α1, Collagen 1 α2, Collagen 3 α1 and BNP in murine cardiac tissue of WT and Flotillin KO mice. n indicates the number of mice per group. * $p<0.05$ compared to WT.

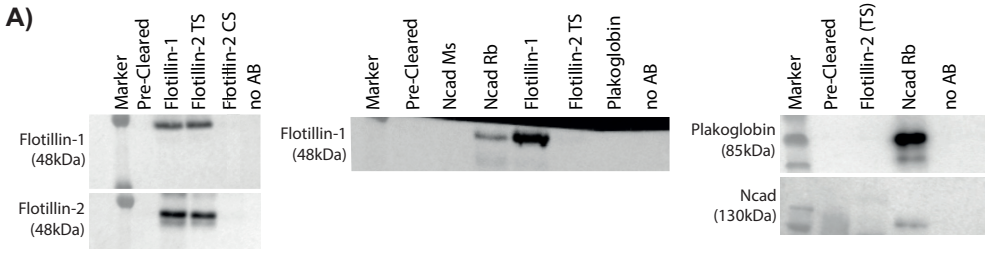

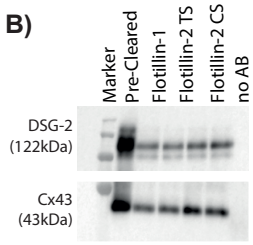

Supplementary Figure 2. Co-Immunoprecipitations of Flotillins and ID proteins. A) Representative Western Blots of Co-Immunoprecipitations for Flotillin-1, Flotillin-2, Plakoglobin and Ncadherin (Ncad) using Flotillin-1, Flotillin-2 Thermo Scientific (TS) and Flotillin-2 Cell Signaling (CS) antibodies (left panel), Ncad mouse (Ms), Ncad Rabbit (Rb), Flotillin-1, Flotillin-2 Thermo Scientific (TS) and Plakoglobin antibodies (middle panel), and Flotillin-2 Thermo Scientific (TS) and Ncad Rb antibodies (right panel) to fish. **B)** Representative Western Blots of Co-Immunoprecipitations for desmoglein-2 (DSG-2) and Connexin43 (Cx43) using Flotillin-1, Flotillin-2 Thermo Scientific (TS) and Flotillin-2 Cell Signaling (CS) antibodies, where binding of the protein to the beads leads to technical problems and hampers the analysis.

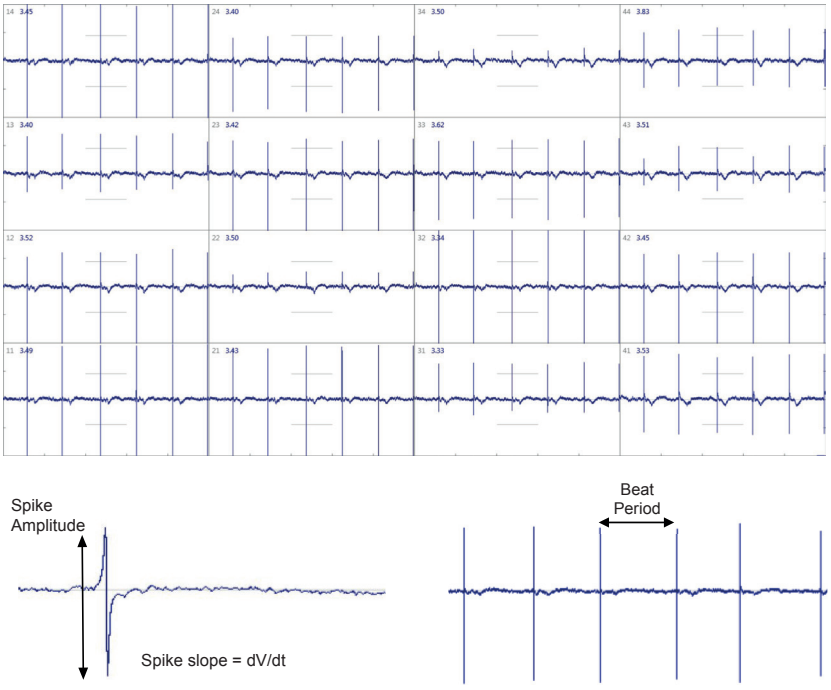

Supplementary Figure 3. MEA traces in Neonatal Rat Cardiomyocytes. Typical examples of the electrical signal obtained by 16 electrodes (left) and one electrode (right) of the Multi-electrode-array (MEA). Spike amplitude, spike slope and beat period are indicated.

PART 2

MYOCARDIAL REMODELING OF TISSUE ARCHITECTURE

“

The world is my country,
science is my religion.

Christiaan Huygens

Chapter

6

CTGF knockout does not affect cardiac hypertrophy and fibrosis formation upon chronic pressure overload

Magda S.C. Fontes[a,*], **Elise L. Kessler**[a,*], Leonie van Stuijvenberg[a], Maike A. Brans[a], Lucas L. Falke[b], Bart Kok[a], Andrew Leask[c], Harold V.M. van Rijen[a], Marc A. Vos[a], Roel Goldschmeding[b], Toon A.B. van Veen[a]
*These authors contributed equally to this study.

[a] *Department of Medical Physiology, Division of Heart & Lungs, University Medical Center Utrecht, Utrecht, The Netherlands*
[b] *Department of Pathology, University Medical Center Utrecht, Utrecht, The Netherlands*
[c] *Department of Dentistry, University of Western Ontario, Ontario, Canada*

J Mol Cell Cardiol 2015; 88:82-90

Abstract

Background: One of the main contributors to maladaptive cardiac remodeling is fibrosis. Connective tissue growth factor (CTGF), a matricellular protein that is secreted into the cardiac extracellular matrix by both cardiomyocytes and fibroblasts, is often associated with development of fibrosis. However, recent studies have questioned the role of CTGF as a pro-fibrotic factor. Therefore, we aimed to investigate the effect of CTGF on cardiac fibrosis, and on functional, structural, and electrophysiological parameters in a mouse model of CTGF knockout (KO) and chronic pressure overload.

Methods: A new mouse model of global conditional CTGF KO induced by tamoxifen-driven deletion of CTGF, was subjected to 16 weeks of chronic pressure overload via transverse aortic constriction (TAC, control was sham surgery).

Results: CTGF KO TAC mice presented with hypertrophic hearts, and echocardiography revealed a decrease in contractility on a similar level as control TAC mice. *Ex vivo* epicardial mapping showed a low incidence of pacing-induced ventricular arrhythmias (2/12 in control TAC *vs.* 0/10 in CTGF KO TAC, *n.s.*) and a tendency towards recovery of the longitudinal conduction velocity of CTGF KO TAC hearts. Picrosirius Red staining on these hearts unveiled increased fibrosis at a similar level as control TAC hearts. Furthermore, genes related to fibrogenesis were also similarly upregulated in both TAC groups. Histological analysis revealed an increase in fibronectin and vimentin protein expression, a significant reduction in Connexin-43 (Cx43) protein expression, and no difference in $Na_v1.5$ expression of CTGF KO ventricles as compared with sham treated animals.

Conclusion: Conditional CTGF inhibition failed to prevent TAC-induced cardiac fibrosis and hypertrophy. Additionally, no large differences were found in other parameters between CTGF KO and control TAC mice. With no profound effect of CTGF on fibrosis formation, other factors or pathways are likely responsible for fibrosis development.

Introduction

One of the main contributors to pathological cardiac remodeling is fibrosis.[1] Cardiac fibrosis refers to an accumulation of connective tissue in the extracellular matrix (ECM) that results from excessive deposition and/or decreased degradation of its components, including collagen.[2] Fibrosis can result in increased myocardial stiffness and impairment of electrical connections between cardiomyocytes, possibly leading to increased susceptibility to arrhythmias.[3] Additionally, the normal electrical impulse propagation can be disturbed by direct reduction of cell-to-cell coupling due to reduced or heterogeneously redistributed gap junction proteins, mainly Connexin-43 (Cx43), or by reduction in excitability of individual cardiomyocytes due to abnormal expression of the sodium channel $Na_v1.5$.[4,5]

Connective tissue growth factor (CTGF) is a matricellular protein that is involved in angiogenesis, tissue repair and a variety of types of fibrosis formation including cardiac fibrosis, through the regulation of several factors in ECM homeostasis.[6,7] Increased levels of CTGF have been found in patients with heart failure, ischemia and coronary artery disease.[8-10] Similar elevations were observed in injury-induced animal models of cardiac hypertrophy and fibrosis.[10-14] The implication of CTGF in fibrosis development/maintenance, but also the close relationship with the pro-fibrotic cytokine transforming growth factor beta-1 (TGF-β1), is well documented.[6,15] Some studies have also reported a decrease in fibrosis after inhibition of CTGF.[16] However, recent studies using transgenic mice overexpressing CTGF pointed towards a cardio-protective effect of CTGF, reporting similar amount of fibrosis after myocardial infarction or pressure overload compared to control mice.[17-19] Very recently, Accornero and colleagues showed that cardiac specific CTGF deletion in mice (or in combination with CTGF deletion from fibroblast) did not affect fibrosis, among other parameters, upon 2 or 8 weeks of pressure overload stimulation.[20] These contradicting findings show that the specific role of CTGF in the origin and progression of cardiac fibrosis is therefore not yet fully understood.

Research on CTGF could contribute to important insight into the underlying mechanisms of fibrosis and cardiac disease. In the heart, CTGF is secreted into the ECM by both fibroblasts and cardiomyocytes.[8] In order to target both cell types, we developed a new mouse model in which CTGF is conditionally knocked out (KO) in all cells of the body. The aim of our study was to investigate the effect of CTGF KO on fibrosis formation in the heart upon 16 weeks of chronic pressure overload, and consequently, the relation with remodeling of functional, structural, and electrophysiological parameters. For the latter ones, special attention has been paid at potential effects on conduction velocity, development of arrhythmias and modulation of the underlying molecular substrate.

Material & methods

GENERATION OF CONDITIONAL CTGF KNOCKOUT (KO) MICE

All experiments were conducted with consent of the Experimental Animal Ethics Committee of the University of Utrecht, The Netherlands. CTGF flox mice, in which a CTGF allele is flanked by loxP sites, were generated in the lab of Dr. Andrew Leask (University of Western Ontario, Canada).[21] To generate time-conditional CTGF full knockout mice, homozygous CTGF flox mice were crossed with mice ubiquitously expressing tamoxifen-inducible Cre recombinase (Cre-ERT2) under the control of the ROSA26 locus (ROSA26CreERT2; The Jackson Laboratory, Maine, USA). ROSA26CreERT2 and CTGF flox mice, both on C57Bl/6J genetic background, were crossbred for five generations and homozygous CTGFflox/floxROSA26-ERT/Cre mice were used in this study. Genotype of mice was confirmed by polymerase chain reaction (PCR) using the following primers: CTGF flox forward (5'-AAAGTCGCTCTGAGTTGTTAT-3') and reverse (5'-CCTGATCCTGGCAATTTCG-3'); ROSA26CreERT2 forward (5'-AATACCAATGCACTTGCCTGGATGG-3') and reverse (5'-GAAACAGCAATTACTACAACGGGAGTGG-3') and (5'-GGAGCGGGAGAAATGGATATG-3'). All animals were housed under standard conditions with controlled light, humidity and temperature, and with food and water *ad libitum*.

Tamoxifen (T5648; Sigma-Aldrich, St Louis, MO, USA) was dissolved at 10 mg/mL in corn oil (C8267; Sigma-Aldrich). To induce global CTGF gene ablation, adult CTGFflox/floxROSA26-ERT/Cre mice (13-14 weeks old) were injected intraperitoneally once a day with 0.1mL of tamoxifen for 4 consecutive days (designated hereafter as CTGF KO mice). Corresponding littermates were injected with only corn oil for 4 consecutive days (designated as control mice).

EXPERIMENTAL SET-UP

Two weeks after tamoxifen/vehicle injections, control and CTGF KO mice were subjected to transverse aortic constriction (TAC) or sham surgery as previously performed.[22] After surgery, all mice were followed for 16 weeks and the ones that completed the study were further analyzed: control sham (n=10), CTGF KO sham (n=9), control TAC (n=13), and CTGF KO TAC (n=10).

ELECTROCARDIOGRAPHY AND ECHOCARDIOGRAPHY

At 16 weeks after surgery, mice were anesthetized with isoflurane (2 % in O_2) and a 3-lead electrocardiogram (ECG) was recorded using PowerLab 4/30 and Dual Bio Amp (ADInstruments Ltd., UK). At least 100 complexes were averaged and analyzed off-line using LabChart 7 Pro (ADInstruments Ltd.). Subsequently, transthoracic echocardiography was performed to determine functional and structural parameters using Vevo 2100 System (VisualSonics Inc., Toronto, Canada) equipped with a 22-55MHz transducer (MS550D). Aortic peak velocity was measured by pulsed-wave Doppler with a 13-24MHz transducer (MS250) to confirm proper constriction (pressure gradient approximately 58 mmHg) in both TAC operated groups. Analysis off-line and calculations were performed using the Vevo 2100 software.

EPICARDIAL MAPPING OF LANGENDORFF PERFUSED MOUSE HEARTS

After transthoracic echocardiography, the chest was opened and the heart rapidly excised and perfused retrogradely on a Langendorff apparatus for epicardial mapping. The perfusion solution was carbogen-gassed at 37 °C and extracellular electrograms were recorded using a 19x13 multielectrode grid (0.3 mm spacing) placed on the epicardial surface of both the left and right ventricles of the heart as described previously.[23] Epicardial recordings were made during stimulation (2 times stimulation threshold) from the center of the grid at a basic cycle length (BCL) of 120ms. The effective refractory period (ERP) was determined for both ventricles. Local activation times of the recorded electrograms were determined off-line with custom made software based on Matlab (The MathWorks Inc., Natrick, USA) and used to calculate conduction velocity (CV), as previously described.[5] Susceptibility for arrhythmias was tested by programmed electrical stimulation using a standardized protocol as described before.[5]

IMMUNOHISTOCHEMISTRY

After Langendorff experiments, the hearts were snap frozen in liquid nitrogen. Subsequently, serial cryosections of the hearts were generated (10 µm thickness, in four-chamber view) for immunohistochemistry and histological analysis. Immunolabeling was performed as described previously,[24] using mouse monoclonal antibodies against vimentin (1:200, Sigma-Aldrich) and Cx43 (1:200, BD Transduction Laboratories, Breda, The Netherlands), and rabbit polyclonal antibodies against fibronectin (1:400, Sigma-Aldrich) and pan-cadherin (1:4000, Sigma-Aldrich). Secondary labeling was achieved by appropriate fluorescein isothiocyanate (FITC, 1:250) or Alexa Fluor 594 (1:100) conjugated anti-mouse or anti-rabbit whole IgG antibodies (Jackson ImmunoResearch Europe, Newmarket, United Kingdom).

Immunohistochemistry for CTGF detection was performed as described previously with slight modifications.[25] Briefly, heart cryosections of 10 µm thickness were fixed with 4 % paraformaldehyde (PFA) for 30 minutes, endogenous peroxidase activity was blocked, and heat-based antigen retrieval was performed in citrate buffer. Sections were then incubated overnight with goat polyclonal antibodies against CTGF (1:200, Santa Cruz Biotechnology, Heidelberg, Germany), followed by incubation of secondary labeling with horseradish peroxidase (HRP)-conjugated rabbit anti-goat IgG (1:100, Dako, Glostrup, Denmark) and goat anti-rabbit BrightVision-HRP (Immunologic BV, Duiven, The Netherlands). Sections were developed with NovaRED (Vector Laboratories, Burlingame, CA, USA), counterstained with hematoxylin and mounted with Pertex (Histolab Products AB, Gothenburg, Sweden).

After immunolabeling, sections were analyzed with an epifluorescence microscope (Nikon Eclipse 80i; Nikon Europe BV, Amstelveen, The Netherlands) and randomly chosen images were taken using NIS Elements BR 3.0 software. Quantification analysis was performed using ImageJ 1.35s software.[26]

HISTOLOGY

Frozen heart cryosections were fixed by 4 % PFA for 30 minutes, incubated with xylene and rehydrated in an ethanol series. Subsequently, sections were pre-incubated with 0.2 % phosphomolybdic acid (Sigma-Aldrich) and stained with 0.1 % Picrosirius red solution for 90 minutes. Afterwards, sections were incubated with 0.01M HCl for 2 minutes, dehydrated in a reverse ethanol series, incubated in xylene and sealed with Pertex (Histolab Products AB). For quantification analysis, sections were digitally scanned using Aperio ScanScope XT (Leica Microsystems BV, Son, The Netherlands) and pictures were taken using ImageScope software (Leica Microsystems BV). Pictures from 2-4 sections per heart were used to calculate the amount of fibrosis using ImageJ 1.35s software. The percentage of fibrosis was calculated as the fibrosis positive signal in the ventricles relative to the total ventricular surface area.

IMMUNOBLOTTING

Total cellular protein was isolated from ventricular tissue as described previously.[24] Protein samples were separated on 7 % or 10 % SDS-PAGE gel, electro-transferred on nitrocellulose membranes and blocked with 5 % milk powder. Equality of protein transfer was assessed by Ponceau S staining. Membranes were incubated with mouse monoclonal antibodies against Cx43 (1:250, BD Transduction Laboratories) and rabbit polyclonal antibodies against fibronectin (1:1000, Sigma-Aldrich), and $Na_V1.5$ (1:200, Sigma-Aldrich). Secondary labeling was performed with HRP-conjugated anti-mouse or anti-rabbit whole IgG antibodies (1:7000, Bio-Rad Laboratories, Hercules, CA, USA). Detection was performed using standard ECL procedure (GE Healthcare, Buckinghamshire, United Kingdom) with ChemiDoc XRS system (BioRad Laboratories). Quantification analysis was performed with ImageJ 1.35s software, where the protein of interest was corrected for correspondent Ponceau S staining.

REAL-TIME QUANTITATIVE PCR (RT-QPCR)

RT-qPCR on ventricular tissue was performed using TaqMan Gene Expression Assays (Applied Biosystems by Life Technologies Corp., Carlsbad, CA, USA) as described earlier.[14] Relative mRNA expression levels were determined for CTGF, CCN3, CCN5, brain natriuretic peptide (BNP), Collagen 1α1, Collagen 1α2, Collagen 3α1, TGF-β1, plasminogen activator inhibitor-1 (PAI-1), heat shock protein 47 (Hsp47), Cx43 and sodium channel $Na_V1.5$ (all from Applied Biosystems by Life Technologies Corp.). 60S acidic ribosomal protein P1 (RPLP1) (Applied Biosystems by Life Technologies Corp.) was used as internal control, since the levels did not differ between group samples (for specifics see Supplementary Table 1).

STATISTICAL ANALYSIS

Data are expressed as mean ± standard error of the mean (SEM). Statistical analyses were performed using two-way ANOVA followed by Tukey's multiple comparisons test. The survival data were analyzed using the log-rank test and arrhythmia inducibility analysed with Fisher exact test. All analyses were performed using GraphPad Prism 6.0 (GraphPad Software, La Jolla, CA, USA). A value of $p<0.05$ was considered statistically significant.

Results

In the present study, functional, structural, and electrical remodeling was investigated after chronic pressure overload in a new mouse model of global conditional CTGF knockout. The Kaplan-Meier survival curves in Figure 1A revealed a trend towards higher mortality after 16 weeks of TAC surgery in CTGF KO mice when compared with control mice (52 *vs*. 28 %, *n.s.*). The global conditional gene deletion of CTGF in both sham and TAC groups was confirmed in the ventricles with a reduction of 95-98 % on CTGF RNA and protein levels compared with respective controls ($p<0.05$, Figures 1B-C). CTGF knockout was also confirmed in the atria with a reduction in CTGF protein level of 98 % in sham and TAC groups compared with respective controls ($p<0.01$, Figure 1D). Additionally, in the control TAC group, CTGF was upregulated after surgery: 2.2-fold (mRNA) and 2.7-fold (protein) in the ventricles, and 1.6-fold (protein) in the atria ($p<0.01$, Figures 1B-D, respectively). In order to exclude potential redundancy of CTGF family members, RNA levels of CCN3 and CCN5 (also known as NOV and WISP-2, respectively) were analyzed (Supplementary Figures 1A-B). As shown in Supplementary Figure 1A, there are neither differences in CCN3 expression levels between sham and TAC nor between control and CTGF KO. In Supplementary Figure 1B, CCN5 was significantly upregulated after TAC, however, again there was not a statistical significance within the sham or TAC groups meaning no differential effect when CTGF was deleted.

MORPHOLOGICAL, ECHOCARDIOGRAPHIC AND ELECTROCARDIOGRAPHIC DATA

Sixteen weeks of pressure overload resulted in cardiac hypertrophy of CTGF KO mice to the same extent as the control mice, as evidenced by the increase of heart weight to body weight ratio and the increase of the hypertrophic marker BNP ($p<0.05$, Figures 2C-D). Moreover, no significant changes were found in lungs, liver or kidney weights (Table 1). Echocardiography revealed impaired cardiac contractility after TAC in control, as well as in CTGF KO mice (Figure 2A), with decreased fractional shortening compared to respective sham groups (22% in control TAC and 23 % in CTGF KO TAC *vs.* ±31 % in both sham groups, $p<0.05$, Figure 2B and Table 1). Furthermore, electrocardiographic parameters remained unchanged after TAC except for QRS and QTc intervals. These were significantly increased in control, but not in CTGF KO mice, where there was only a tendency of increased values (Table 2).

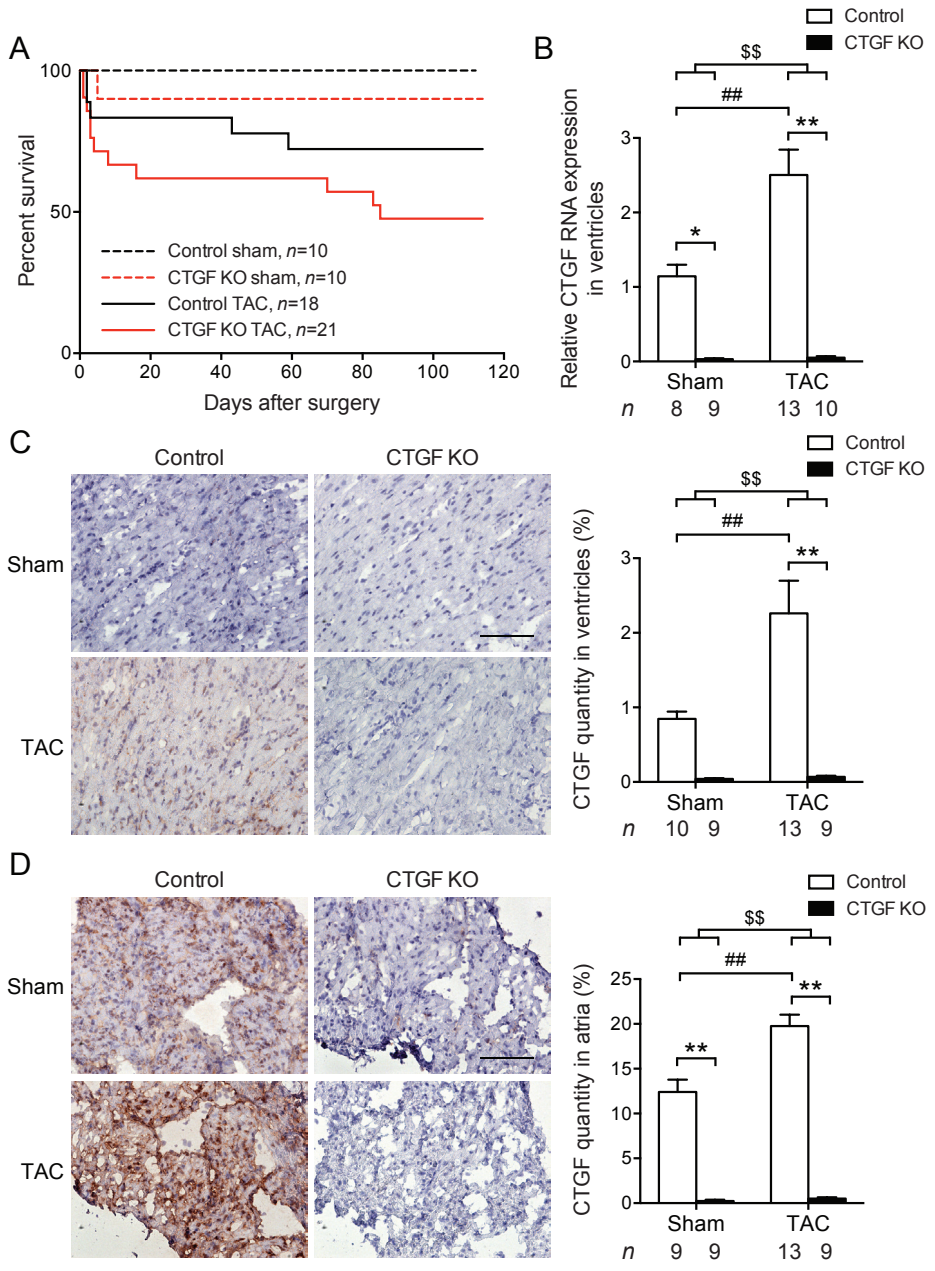

Figure 1. Characterization of CTGF conditional knockout mice after sham or TAC surgery. **A)** Kaplan-Meier survival curves of control and tamoxifen-induced conditional knockout of CTGF (CTGF KO) mice. **B)** CTGF RNA expression in the ventricles assessed by TaqMan RT-qPCR in control and CTGF KO mice. Representative images from control and CTGF KO ventricles **(C)** and atria **(D)** immunolabeled for CTGF (left), and respective quantification (right). Scale bar in C and D represent 100 µm. Black bars refer to CTGF KO mice and white bars to control mice; n indicates the number of mice per group. * $p<0.05$, ** $p<0.01$, ## $p<0.01$, §§ $p<0.01$.

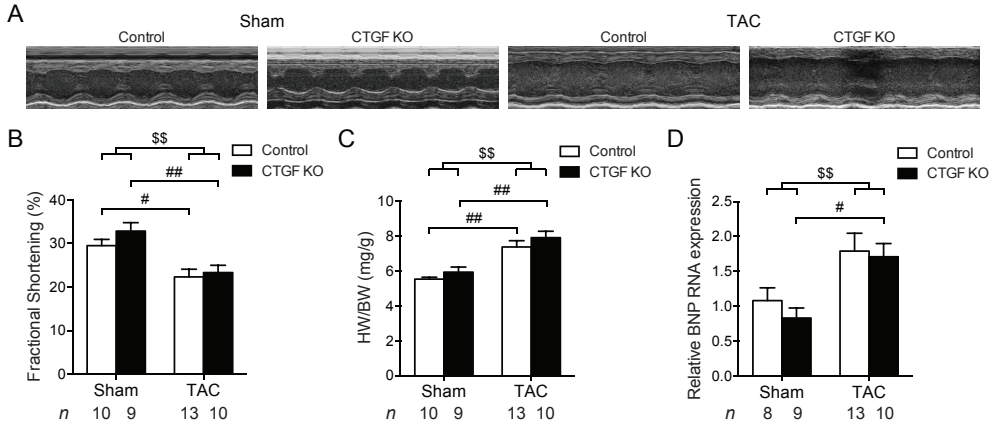

Figure 2. Tissue and echocardiographic parameters at 16 weeks of sham and TAC CTGF KO mice compared with controls. **A)** Typical examples of M-mode echocardiograms. **B** and **C)** Fractional shortening and heart weight to body weight ratio (HW/BW), respectively. **D)** BNP RNA expression in the ventricles assessed by TaqMan RT-qPCR in control and CTGF KO mice. Black bars refer to CTGF KO mice and white bars to control mice; n indicates the number of mice per group. # p<0.05, ## p<0.01, §§ p<0.01. BNP, brain natriuretic peptide.

Table 1. Tissue characteristics and echocardiographic measurements for Sham- and TAC-operated mice. Values are mean ± SEM. TAC, transverse aortic constriction; n, number of animals; HW/BW, heart weight to body weight ratio; LuW/BW, lungs weight to body weight ratio; LiW/BW, liver weight to body weight ratio; KW/BW, average kidneys weight to body weight ratio; LV, left ventricle; LVID,s and LVID,d, LV systolic and diastolic internal diameter, respectively; LV Vol,s and LV Vol,d, LV systolic and diastolic volume, respectively; SV, stroke volume; EF, ejection fraction; FS, fractional shortening; CO, cardiac output. * p<0.05 vs. control sham, ** p<0.01 vs. control sham, # p<0.05 vs. CTGF KO sham, ## p<0.01 vs. CTGF KO sham, § p<0.05 sham vs. TAC, §§ p<0.01 sham vs. TAC.

	Sham		TAC	
	Control	CTGF KO	Control	CTGF KO
n	10	9	13	10
Organ weights				
Body weight (g)	26.0 ± 1.2	27.4 ± 1.3	27.8 ± 1.5	25.7 ± 1.0
Heart weight (mg)§§	144.1 ± 7.6	161.3 ± 8.5	205.2 ± 15.3**#	201.7 ± 8.7**
HW/BW (mg/g)§§	5.5 ± 0.1	5.9 ± 0.3	7.4 ± 0.4**#	7.9 ± 0.4**##
LuW/BW (mg/g)	5.7 ± 0.2	5.7 ± 0.4	5.7 ± 0.3	6.2 ± 0.2
LiW/BW (mg/g)	3.8 ± 0.1	4.0 ± 0.1	3.6 ± 0.1	3.9 ± 0.1
KW/BW (mg/g)	5.3 ± 0.2	5.4 ± 0.1	5.2 ± 0.2	5.6 ± 0.2
Echocardiography				
LVID,s (mm)	2.8 ± 0.1	2.4 ± 0.2	3.2 ± 0.2	2.9 ± 0.2
LVID,d (mm)	4.0 ± 0.1	3.6 ± 0.2	4.1 ± 0.2	3.8 ± 0.2
LV Vol,s (µL)§	30.9 ± 4.0	22.5 ± 4.0	46.0 ± 8.2	35.0 ± 6.4
LV Vol,d (µL)	69.7 ± 5.8	56.9 ± 6.6	77.6 ± 10.2	63.8 ± 9.3
SV (µL)§	38.8 ± 2.3	34.4 ± 3.7	31.6 ± 2.7	28.7 ± 3.6
EF (%)§§	56.8 ± 2.2	61.7 ± 2.9	45.0 ± 3.2*##	47.1 ± 2.9##
FS (%)§§	29.5 ± 1.4	32.8 ± 2.0	22.3 ± 1.8*##	23.3 ± 1.7##
CO (mL/min)	16.1 ± 1.0	14.1 ± 2.1	14.5 ± 1.7	11.8 ± 1.9
LV mass (mg)§§	111.3 ± 9.8	110.7 ± 9.7	167.9 ± 15.2*#	162.4 ± 16.4

Table 2. Electrocardiographic and electrophysiological measurements for Sham- and TAC-operated mice. Values are mean ± SEM. TAC, transverse aortic constriction; n, number of animals/hearts; HR, heart rate; QTc, corrected QT interval using Bazett's formula; LV and RV, left and right ventricle, respectively; CVL and CVT, longitudinal and transversal conduction velocity, respectively; AR, anisotropic ratio; ERP, effective refractory period. * p<0.05 vs. control sham, ** p<0.01 vs. control sham, ## p<0.01 vs. CTGF KO sham, † p<0.05 vs. control TAC, §§ p<0.01 sham vs. TAC.

	Sham		TAC	
	Control	CTGF KO	Control	CTGF KO
n	10	9	13	10
Electrocardiography				
HR (beats/min)	455.8 ± 13.6	479.8 ± 30.1	461.4 ± 19.2	465.0 ± 28.7
RR interval (ms)	132.7 ± 4.0	130.4 ± 11.0	132.9 ± 5.7	134.5 ± 9.9
PR interval (ms)	38.0 ± 0.8	45.9 ± 6.4	41.9 ± 2.5	46.2 ± 4.3
P duration (ms)	9.7 ± 0.3	11.6 ± 0.9	10.9 ± 0.6	12.7 ± 1.2
QRS interval (ms)§§	10.1 ± 0.2	11.3 ± 0.6	12.2 ± 0.4**	12.5 ± 0.4**
QT duration (ms)§§	46.3 ± 1.3	52.2 ± 3.8	58.0 ± 3.0*	58.5 ± 2.9*
QTc duration (ms)§§	40.2 ± 1.1	45.7 ± 1.5	50.5 ± 2.4**	50.8 ± 1.8**
n	10	7/8	11/12	9/10
Electrophysiology				
LV CV_L (cm/s)	73.2 ± 1.9	74.1 ± 3.0	63.8 ± 3.6	72.0 ± 1.6
LV CV_T (cm/s)§§	53.4 ± 1.7	47.7 ± 2.5	44.0 ± 1.9**	42.0 ± 2.1**
RV CV_L (cm/s)§§	73.8 ± 2.5	77.1 ± 2.8	63.7 ± 2.0*##	71.2 ± 2.1
RV CV_T (cm/s)§§	58.4 ± 1.7	58.2 ± 3.1	49.1 ± 1.6	51.9 ± 3.9
LV AR (CV_L/CV_T)	1.38 ± 0.05	1.59 ± 0.13	1.46 ± 0.06	1.80 ± 0.09**†
RV AR (CV_L/CV_T)	1.27 ± 0.04	1.36 ± 0.11	1.31 ± 0.05	1.43 ± 0.10
LV ERP (ms)	65.0 ± 2.7	61.3 ± 5.8	74.0 ± 5.6	64.4 ± 4.7
RV ERP (ms)	51.0 ± 3.1	51.3 ± 4.0	51.8 ± 4.6	49.0 ± 4.1

ARRHYTHMIA INDUCTION AND CONDUCTION VELOCITY

Two out of twelve of the isolated Langendorff-perfused control hearts presented arrhythmias upon TAC, with sustained (>15 beats) polymorphic ventricular tachyarrhythmia (VT) as shown in figure 3A. Epicardial activation maps generated during VT revealed irregular activation patterns (Figure 3B). Additionally, one control TAC mouse showed 20 premature ventricular contractions (PVC) in 1 minute of electrocardiography recording (data not shown), although this mouse was not susceptible to arrhythmias in the Langendorff set-up. Arrhythmias were burst paced-induced in 17 % (2/12) of the control TAC hearts compared to 0 % of CTGF KO TAC hearts and both sham groups (*n.s.*, Figure 3C). The electrophysiological parameters obtained from epicardial activation maps of the left and right ventricles (LV and RV) are summarized in table 2 (bottom). The transversal conduction velocity (CVT) in the LV was significantly decreased by 18 % in control TAC and by 21 % in CTGF KO TAC hearts (44.0±1.9 and 42.0±2.1 respectively *vs.* 53.4±1.7 cm/s in control sham, $p<0.01$, Figure 3D and Table 2). Interestingly, the decrease in longitudinal CV seen in the RV of control TAC hearts was not found in the CTGF KO TAC hearts (Figure 3D and Table 2). This lead to an increase in the anisotropic ratio in the LV of CTGF KO TAC hearts compared to respective sham hearts (1.80±0.09 *vs.* 1.59±0.13 in CTGF KO sham, $p<0.05$, Table 2).

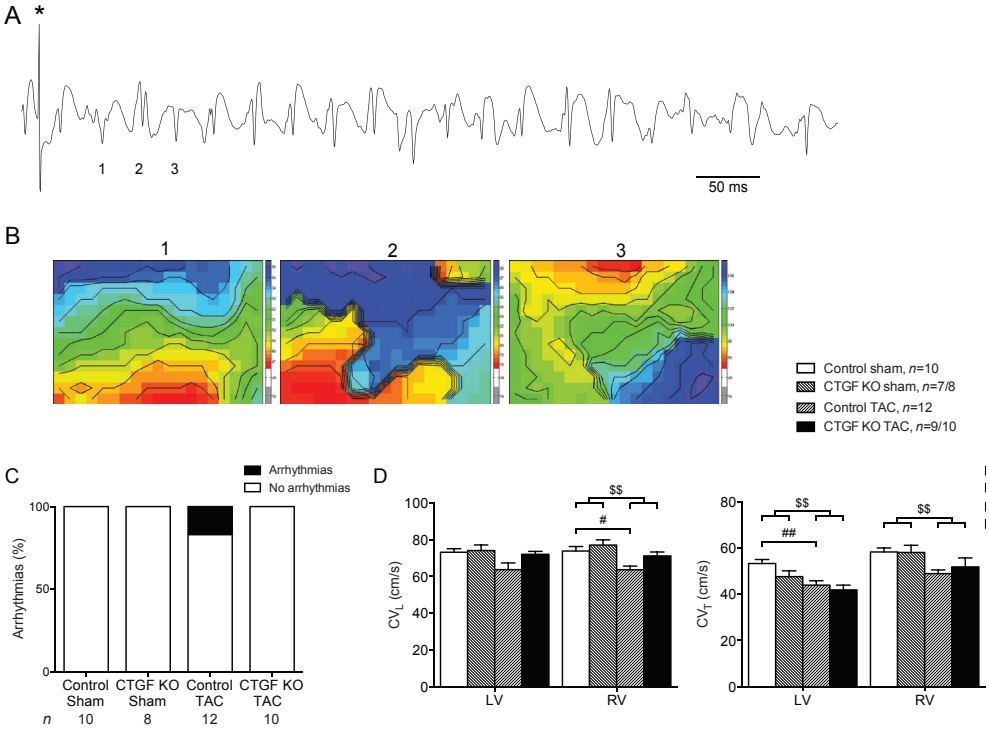

Figure 3. Arrhythmias and conduction velocity (CV) induced in perfused sham and TAC CTGF KO mouse hearts compared with controls. A) Representative epicardial electrogram of an induced polymorphic ventricular tachyarrhythmia (VT) in control TAC mice. Asterisk (*) indicates the last burst paced (cycle length of 36 ms) complex. **B)** Activation maps from 3 numbered VT complexes indicated in the epicardial electrogram in A. Black isochronal lines of activation are 1 ms apart. Red colour represent earliest activation time and blue colour the latest. **C)** Incidence of arrhythmias in control and CTGF KO mice. **D)** CV measured by epicardial mapping on the left ventricle (LV) and right ventricle (RV) in longitudinal (left) and transverse (right) directions. n indicates the number of mice per group. # p<0.05, ## p<0.01, §§ p<0.01.

FIBROSIS, CX43 AND $NA_V1.5$ EXPRESSION

Ventricular fibrosis as assessed by Picrosirius Red staining revealed a 1.6-fold increase of fibrosis in control hearts after pressure overload by TAC surgery compared with control sham ($p<0.01$, Figure 4B). Interestingly, the amount of fibrosis in the absence of CTGF was not different from control, showing a comparable increase after TAC (1.5-fold *vs.* CTGF KO sham, $p<0.05$, Figure 4B). Subsequently, the mRNA expression levels of several genes involved in connective tissue were analyzed (Figure 4C). Collagen (1α1, 1α2 and 3α1) RNA levels were increased after TAC surgery ($p<0.05$) although individual comparisons did not show significant differences (except collagen 1α2 between control sham and TAC). TGF-β1 RNA levels were similar between control and CTGF KO hearts, with an increase after TAC ($p<0.05$). PAI-1 and Hsp47 RNA levels, as gene targets of TGF-β1, did also not reveal any differences between control and CTGF KO hearts, although a significant increase was observed after TAC ($p<0.05$).

Levels of the extracellular matrix protein fibronectin and intermediate filament protein vimentin were also investigated. Fibronectin protein levels showed no statistical difference between the groups when assessed by immunoblotting (Supplementary Figures 2A-B), however, there was an increase in TAC groups when assessed by immunohistochemistry ($p<0.01$, Supplementary Figures 2C-D). Interestingly, vimentin immunolabeling was increased in TAC groups, with CTGF KO TAC hearts expressing significantly more vimentin than control TAC hearts ($p<0.01$, Supplementary Figures 2E-F).

Ventricular tissue was further investigated on other determinants involved in conduction characteristics. The expression level of the gap junction protein Cx43 was significantly reduced after TAC surgery in control hearts by 43 % when detected with immunoblotting and by 35 % with immunohistochemistry ($p<0.01$, Figures 5A-D). Similar reductions in Cx43 protein levels were observed on CTGF KO hearts. N-cadherin, a marker for intercalated disks was also analyzed with immunohistochemistry revealing unchanged levels between all groups (*n.s.*,

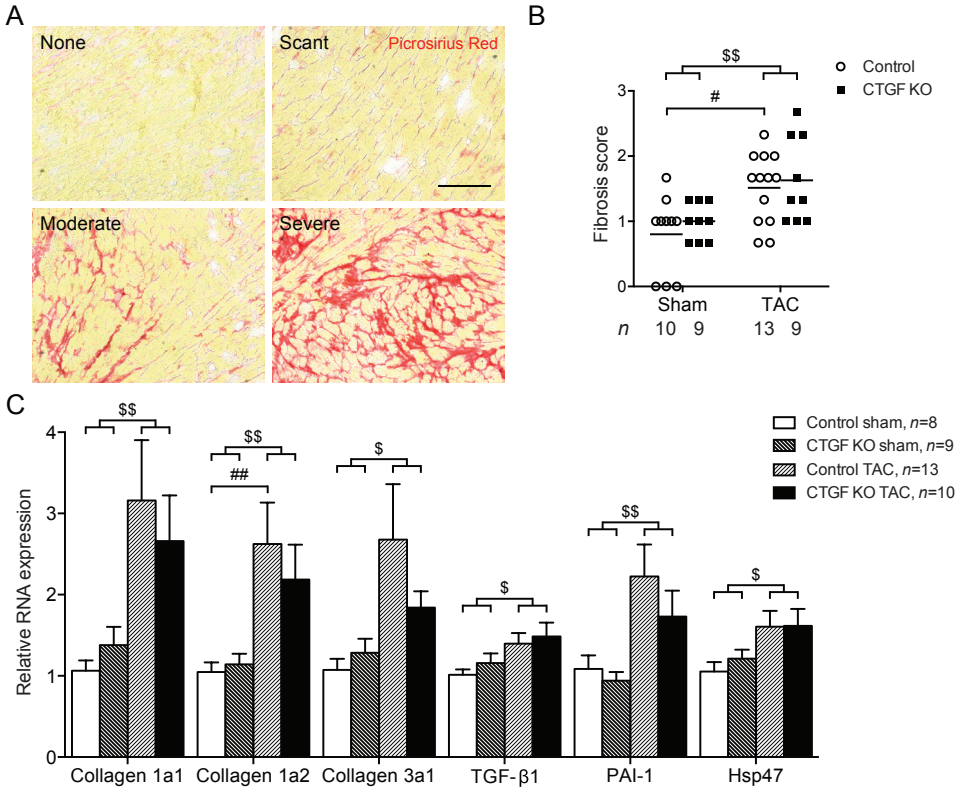

Figure 4. Fibrosis in isolated sham and TAC CTGF KO mouse ventricles compared with controls. **A)** Picrosirius Red representative images of the ventricles. Scale bar represents 100 µm. **B)** Quantification of Picrosirius Red staining. Black bars refer to CTGF KO mice and white bars to control mice. **C)** Collagen 1α1, Collagen 1α2, Collagen 3α1, TGF-β1, PAI-1 and Hsp47 RNA expression in the ventricles assessed by TaqMan RT-qPCR in control and CTGF KO mice. n indicates the number of mice per group. # p<0.05, ## p<0.01, § p<0.05, §§ p<0.01. TGF-β1, transforming growth factor beta-1; PAI-1, plasminogen activator inhibitor-1; Hsp47, heat shock protein 47.

Figure 5E). Additionally, there were no differences in Cx43 RNA levels after TAC or between control and CTGF KO hearts (*n.s.*, Figure 5F). Finally, the sodium channel $Na_V1.5$ was analyzed for protein and RNA levels, revealing no changes in $Na_V1.5$ expression between sham and TAC hearts or between control and hearts with CTGF KO (*n.s.*, Figures 5G-I).

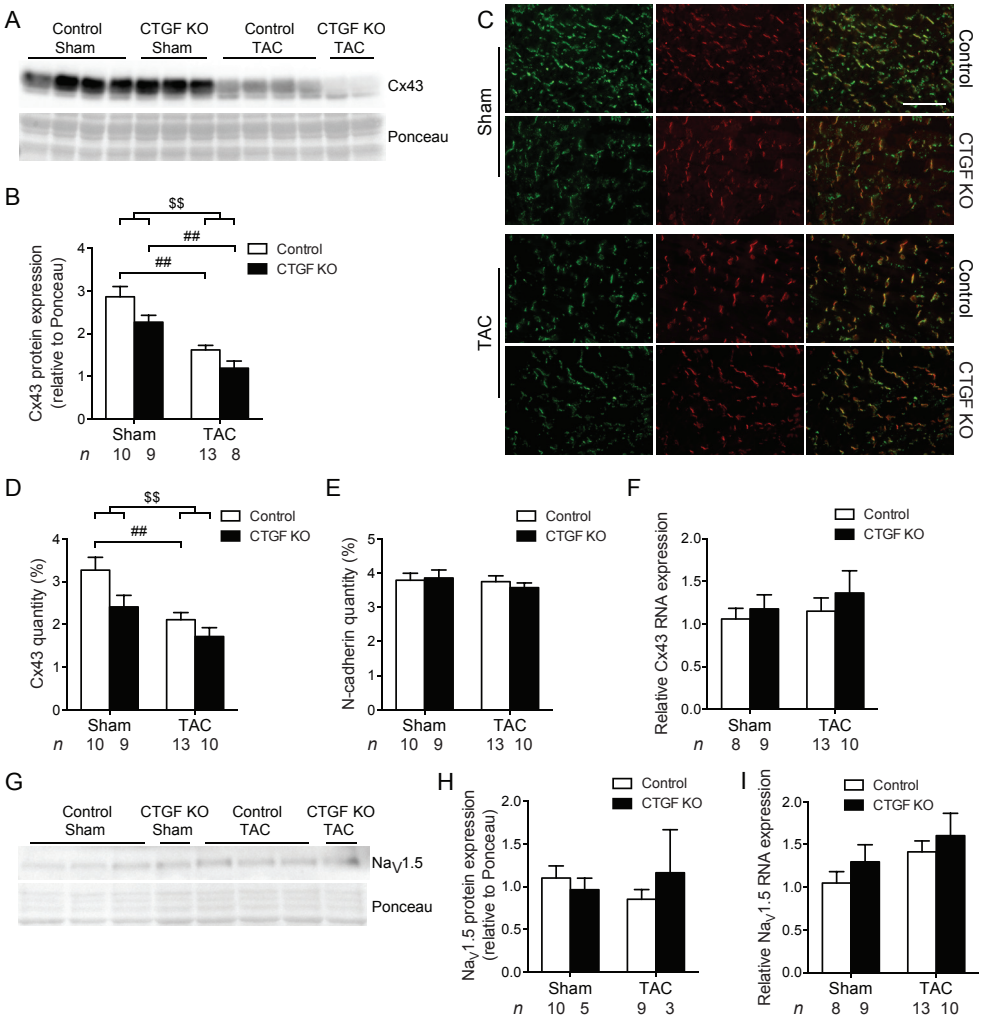

Figure 5. Connexin43 (Cx43) and $Na_V1.5$ expression in isolated sham and TAC CTGF KO mouse hearts compared with controls. A) Representative blot of Cx43 with respective ponceau staining below. **B)** Quantification of total Cx43 protein expression (Cx43/ponceau) exemplified in A. **C)** Representative images of Cx43 expression (green), N-cadherin expression (red) and merged images in control and CTGF KO mice. N-cadherin was used as a marker for intercalated discs. Scale bar represents 100 µm. **D)** Quantification of Cx43 immunolabeling exemplified in C. **E)** Quantification of N-cadherin immunolabeling exemplified in C. **F)** Cx43 RNA expression assessed by TaqMan RT-qPCR in control and CTGF KO mice. **G)** Representative blot of $Na_V1.5$ with respective ponceau staining below. **H)** Quantification of $Na_V1.5$ protein expression ($Na_V1.5$/ponceau) exemplified in G. **I)** $Na_V1.5$ RNA expression assessed by TaqMan RT-qPCR in control and CTGF KO mice. Black bars refer to CTGF KO mice and white bars to control mice; n indicates the number of mice per group. ## $p<0.01$, §§ $p<0.01$.

Discussion

In this study we investigated the role of CTGF on cardiac fibrosis and hypertrophy using CTGF-deficient mice by conditional KO in response to *in vivo* pathological stimuli of chronic pressure overload as induced by 16 weeks of TAC surgery. Additionally, the consequences of global CTGF deletion for functional, structural, and electrical remodeling in the mouse heart were also explored. The main finding of this study is that global conditional CTGF inhibition failed to prevent pressure overload induced: 1) increases in cardiac fibrosis and hypertrophy, 2) decreases in contractile function and in Cx43 protein expression. 3) In addition, there was a tendency towards prevention of CV slowing in CTGF KO TAC hearts.

One of the most suggested roles of CTGF (in different organs like lungs, kidneys and heart) is the involvement in formation and/or maintenance of fibrogenic processes.[6,27] Until recently, thorough *in vivo* functional analyses are scarce because of the lack of suitable animal models. Full CTGF KO mice die immediately after birth.[28] Therefore, we developed a new mouse model by global conditional KO of CTGF, in which we show that the expression levels of CTGF are extremely low in both sham and TAC hearts. Moreover, we observed an increased expression of CTGF in control hearts after 16 weeks of pressure overload stimulation. This finding mirrors data from other studies that identified high CTGF expression levels under different cardiovascular pathological conditions as seen in patients and in experimental animal models, including applied pressure overload.[8-14] These studies, including our control hearts, show that CTGF is upregulated in the fibrotic heart suggesting the connotation of CTGF as a pro-fibrotic factor. Besides that, CTGF can be regulated, among others, by the pro-fibrotic cytokine TGF-β1.[6,15] It would be anticipated that eliminating CTGF would reduce the amount of fibrosis in the heart, as was previously shown mainly in *in vitro* studies targeting CTGF.[16] Strikingly in our study, eliminating CTGF in cardiomyocytes, fibroblasts and all other cell types that potentially are able to release CTGF did not prevent formation of cardiac fibrosis after TAC. This observation was confirmed by different approaches. Besides using Picrosirius Red staining, we also demonstrate that levels of collagen genes, fibronectin, TGF-β1, PAI-1 and Hsp47 are not different in CTGF KO and control TAC hearts. This suggests that CTGF may not have a key role in the formation of cardiac fibrosis upon chronic pressure overload after all, although we can not completely exclude that the deletion of CTGF might have been compensated by other processes or factors.

Contradicting findings from recent *in vivo* studies have raised uncertainty about the implication of CTGF in fibrosis, but also in hypertrophy. Szabo and colleagues[29] inhibited CTGF by monoclonal antibodies and found different outcomes depending on the type of cardiac injury; upon TAC there was evidence of reduced hypertrophy and collagen gene expression, but no difference in collagen deposition, while with angiotensin II (Ang II) stimulation, another method to induce pressure overload, no effect on fibrotic or hypertrophic marker genes was detected. Studies using mice overexpressing CTGF specifically in cardiomyocytes have shown on one

hand an increase in fibrosis, but no effect on hypertrophy compared with controls upon pressure overload,[30] while another group that applied the same injury reported no effects on fibrosis deposition, but attenuated hypertrophy.[17] Using the same transgenic mouse model, but with applied myocardial infarction revealed a lower degree of hypertrophy with no aggravation on the amount of fibrosis,[18] while Ang II-induced injury demonstrated an involvement of CTGF in hypertrophy, but no change in fibrosis.[19] All these contradicting findings questions whether CTGF is essential for fibrosis formation or hypertrophy. In fact, in the present study we show that in addition to the lack of effect on fibrosis, CTGF KO did not alter the degree of hypertrophy after TAC, which was further strengthened by the unchanged levels of BNP in the ventricles and by echocardiography. Moreover, CTGF KO did not have an effect on contractility of the hearts after TAC, performing as poorly as control TAC mice. Again, independent studies using TAC mice with cardiac specific overexpression of CTGF showed different outcomes in terms of contractility.[17,30] In our study, we observed an increased mortality in CTGF KO TAC mice compared with control TAC mice, although not statistically significant. This fits with the finding of Gravning and colleagues,[18] who reported a reduction in mortality in their CTGF overexpressing myocardial infarction mouse model.

The gap junction protein Cx43, essential for cell-to-cell communication, is often reduced or abnormally localized in the diseased heart.[31] Here, we show that Cx43 protein expression was decreased in control hearts after TAC, though RNA levels remained unchanged. Similarly, Cx43 protein, but not RNA expression was downregulated in CTGF KO hearts. This suggests that CTGF is not involved in regulation of Cx43 expression. Nonetheless, it has been reported that recombinant CTGF added to cultured cardiomyocytes leads to acute upregulation of Cx43 and N-cadherin,[32] which is in a setting that is hard to compare to our 16 weeks of pressure overload.

The sodium channel $Na_V1.5$ is also very important for the normal propagation of the electrical impulse in the heart. Since there is no evidence that CTGF might influence or regulate $Na_V1.5$ expression, also in this study, no differences were found in $Na_V1.5$ protein and RNA expression after TAC in control or CTGF KO ventricles.

We previously showed that 16 weeks of pressure overload on *ex vivo* control hearts resulted in 18 %[5] or 44 %[22] of pacing-induced arrhythmias. Here we show a comparable percentage of arrhythmias (17 %) in our control TAC hearts. Although increased fibrosis and reduced Cx43 expression were still present in CTGF KO mice, surprisingly these hearts did not show any arrhythmias under electrical stimulation on the Langendorff perfusion system. To speculate, the absence of arrhythmias in CTGF KO TAC hearts could maybe be attributed to the fact that we observed a tendency towards recovery of the longitudinal CV, although transversal CV was still decreased like control TAC. The tendency to recovery in longitudinal CV cannot be directly related to Cx43 or $Na_V1.5$ as these proteins were not changed in CTGF KO TAC hearts when compared to control TAC. However, we cannot exclude a possible differential preservation of Cx43

at the intercalated disk, the actual site of intercellular conduction, since we did not separate our samples into junctional and non-junctional fractions. Neither we investigated potential changes in the phosphorylation status of Cx43, or in other post-translational modifications that could have affected the conduction velocity. In addition, increases in QRS and QTc of CTGF KO TAC hearts (significant when compared to control sham, but not when compared to CTGF KO sham hearts) and increase in LV anisotropic ratio points to an electrophysiological effect of CTGF, although this effect was rather small and probably not relevant for arrhythmia induction.

Our findings on the redundancy of CTGF on fibrosis, hypertrophy and cardiac function upon chronic pressure overload are supported by a very recent study that used different approaches to delete CTGF (or overexpress) and also subjected mice to pressure overload stimulation.[20] Although the overall conclusion of that study and ours strengthen each other, our data differ from that study since we followed mice chronically for 16 weeks instead of 2 or 8 weeks. Furthermore, effects on arrhythmogenesis and electrophysiological parameters were added and studied on the molecular level.

One limitation of this study that should be mentioned is that only mice surviving chronic pressure overload for 16 weeks were analysed, which might have influenced the obtained data considering that CTGF KO mice tended to die more (especially in the early phase upon TAC) than control mice. A second aspect to mention is that given the different modes of fibrosis formation upon chronic pressure overload and myocardial infarction, our data obtained in the present study should not be extrapolated directly to the remodeling phase after myocardial infarction.

Conclusion

Conditional CTGF inhibition failed to prevent TAC-induced cardiac fibrosis and hypertrophy. Additionally, other changes in response to TAC were comparable between CTGF KO and control TAC mice. With no profound effect of CTGF on fibrosis formation, other factors or pathways may be responsible for fibrosis development under these pathological conditions.

References

1. Swynghedauw B. Molecular mechanisms of myocardial remodeling. Physiol Rev.1999;79(1):215-262.
2. de Jong S, van Veen TA, de Bakker JM, Vos MA, van Rijen HV. Biomarkers of myocardial fibrosis. J. Cardiovasc. Pharmacol.2011;57(5):522-535.
3. Stein M, Boulaksil M, Jansen JA, et al. Reduction of fibrosis-related arrhythmias by chronic renin-angiotensin-aldosterone system inhibitors in an aged mouse model. Am J Physiol Heart Circ Physiol.2010;299(2):H310-321.
4. Jansen JA, Noorman M, Musa H, et al. Reduced heterogeneous expression of Cx43 results in decreased Nav1.5 expression and reduced sodium current that accounts for arrhythmia vulnerability in conditional Cx43 knockout mice. Heart Rhythm.2012;9(4):600-607.
5. Jansen JA, van Veen TA, de Jong S, et al. Reduced Cx43 expression triggers increased fibrosis due to enhanced fibroblast activity. Circ Arrhythm Electrophysiol.2012;5(2):380-390.
6. Daniels A, van Bilsen M, Goldschmeding R, van der Vusse GJ, van Nieuwenhoven FA. Connective tissue growth factor and cardiac fibrosis. Acta Physiol. (Oxf.).2009;195(3):321-338.
7. Shi-Wen X, Leask A, Abraham D. Regulation and function of connective tissue growth factor/CCN2 in tissue repair, scarring and fibrosis. Cytokine Growth Factor Rev.2008;19(2):133-144.
8. Chen MM, Lam A, Abraham JA, Schreiner GF, Joly AH. CTGF expression is induced by TGF-beta in cardiac fibroblasts and cardiac myocytes: a potential role in heart fibrosis. J Mol Cell Cardiol.2000;32(10):1805-1819.
9. Gabrielsen A, Lawler PR, Yongzhong W, et al. Gene expression signals involved in ischemic injury, extracellular matrix composition and fibrosis defined by global mRNA profiling of the human left ventricular myocardium. J Mol Cell Cardiol.2007;42(4):870-883.
10. Koitabashi N, Arai M, Kogure S, et al. Increased connective tissue growth factor relative to brain natriuretic peptide as a determinant of myocardial fibrosis. Hypertension.2007;49(5):1120-1127.
11. Ruperez M, Lorenzo O, Blanco-Colio LM, Esteban V, Egido J, Ruiz-Ortega M. Connective tissue growth factor is a mediator of angiotensin II-induced fibrosis. Circulation.2003;108(12):1499-1505.
12. Way KJ, Isshiki K, Suzuma K, et al. Expression of connective tissue growth factor is increased in injured myocardium associated with protein kinase C beta2 activation and diabetes. Diabetes.2002;51(9):2709-2718.
13. Ohnishi H, Oka T, Kusachi S, et al. Increased expression of connective tissue growth factor in the infarct zone of experimentally induced myocardial infarction in rats. J Mol Cell Cardiol.1998;30(11):2411-2422.

14. Fontes MS, Raaijmakers AJ, van Doorn T, et al. Changes in Cx43 and NaV1.5 expression precede the occurrence of substantial fibrosis in calcineurin-induced murine cardiac hypertrophy. PLoS One.2014;9(1):e87226.
15. Ruiz-Ortega M, Rodriguez-Vita J, Sanchez-Lopez E, Carvajal G, Egido J. TGF-beta signaling in vascular fibrosis. Cardiovasc. Res.2007;74(2):196-206.
16. Brigstock DR. Strategies for blocking the fibrogenic actions of connective tissue growth factor (CCN2): From pharmacological inhibition in vitro to targeted siRNA therapy in vivo. J Cell Commun Signal.2009;3(1):5-18.
17. Gravning J, Ahmed MS, von Lueder TG, Edvardsen T, Attramadal H. CCN2/CTGF attenuates myocardial hypertrophy and cardiac dysfunction upon chronic pressure-overload. Int J Cardiol.2013;168(3):2049-2056.
18. Gravning J, Orn S, Kaasboll OJ, et al. Myocardial connective tissue growth factor (CCN2/CTGF) attenuates left ventricular remodeling after myocardial infarction. PLoS One.2012;7(12):e52120.
19. Panek AN, Posch MG, Alenina N, et al. Connective tissue growth factor overexpression in cardiomyocytes promotes cardiac hypertrophy and protection against pressure overload. PLoS One.2009;4(8):e6743.
20. Accornero F, van Berlo JH, Correll RN, et al. Genetic analysis of CTGF as an effector of TGFbeta signaling and cardiac remodeling. Mol Cell Biol.2015;10.1128/MCB.00199-15.
21. Liu S, Shi-wen X, Abraham DJ, Leask A. CCN2 is required for bleomycin-induced skin fibrosis in mice. Arthritis Rheum.2011;63(1):239-246.
22. Boulaksil M, Winckels SK, Engelen MA, et al. Heterogeneous Connexin43 distribution in heart failure is associated with dispersed conduction and enhanced susceptibility to ventricular arrhythmias. Eur J Heart Fail.2010;12(9):913-921.
23. van Rijen HV, van Veen TA, van Kempen MJ, et al. Impaired conduction in the bundle branches of mouse hearts lacking the gap junction protein connexin40. Circulation.2001;103(11):1591-1598.
24. van Veen TA, van Rijen HV, Wiegerinck RF, et al. Remodeling of gap junctions in mouse hearts hypertrophied by forced retinoic acid signaling. J Mol Cell Cardiol.2002;34(10):1411-1423.
25. Falke LL, Dendooven A, Leeuwis JW, et al. Hemizygous deletion of CTGF/CCN2 does not suffice to prevent fibrosis of the severely injured kidney. Matrix Biol.2012;31(7-8):421-431.
26. Schneider CA, Rasband WS, Eliceiri KW. NIH Image to ImageJ: 25 years of image analysis. Nat Methods.2012;9(7):671-675.
27. Matsui Y, Sadoshima J. Rapid upregulation of CTGF in cardiac myocytes by hypertrophic stimuli: implication for cardiac fibrosis and hypertrophy. J Mol Cell Cardiol.2004;37(2):477-481.
28. Ivkovic S, Yoon BS, Popoff SN, et al. Connective tissue growth factor coordinates chondrogenesis and angiogenesis during skeletal development. Development.2003;130(12):2779-2791.

29. Szabo Z, Magga J, Alakoski T, et al. Connective tissue growth factor inhibition attenuates left ventricular remodeling and dysfunction in pressure overload-induced heart failure. Hypertension.2014;63(6):1235-1240.
30. Yoon PO, Lee MA, Cha H, et al. The opposing effects of CCN2 and CCN5 on the development of cardiac hypertrophy and fibrosis. J Mol Cell Cardiol.2010;49(2):294-303.
31. Fontes MS, van Veen TA, de Bakker JM, van Rijen HV. Functional consequences of abnormal Cx43 expression in the heart. Biochim Biophys Acta.2012;1818(8):2020-2029.
32. Adam O, Lavall D, Theobald K, et al. Rac1-induced connective tissue growth factor regulates connexin 43 and N-cadherin expression in atrial fibrillation. J Am Coll Cardiol.2010;55(5):469-480.

Supplementary material

Protein	Gene	Assay ID
RPLP-1	*Rplp1*	Mm02601846_g1
CTGF	*Ctgf*	Mm01192933_g1
BNP	*Nppb*	Mm01255770_g1
Collagen 1α1	*Col1a1*	Mm00801666_g1
Collagen 1α2	*Col1a2*	Mm00483888_m1
Collagen 3α1	*Col3a1*	Mm01254476_m1
TGF-β1	*TGF-β1*	Mm01178820_m1
PAI-1	*Serpine1*	Mm00435860_m1
Hsp47	*Serpinh1*	Mm00438058_g1
Cx43	*Gja1*	Mm00439105_m1
Nav1.5	*Scn5a*	Mm01342518_m1

Supplementary Table 1. References of the Applied Biosystems assays used in this study. Protein, gene name and assay ID of all primers (all purchased from Applied Biosystems by Life Technologies Corp., Carlsbad, USA).

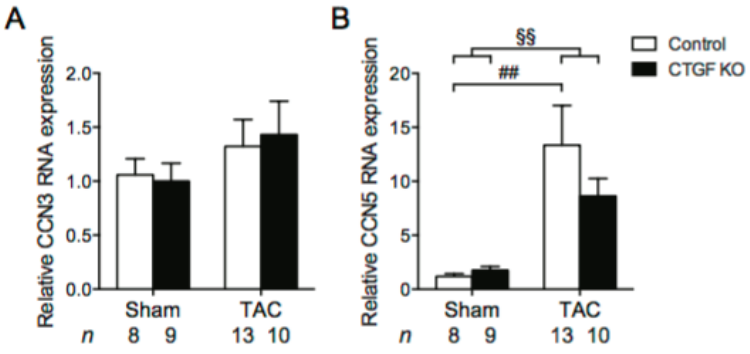

Supplementary Figure 1. CCN3 (A) and CCN5 (B) RNA expression levels (assessed by TaqMan RT-qPCR) in hearts isolated from sham and TAC CTGF KO mice (black bars) and controls (white bars). n indicates the number of mice per group. ## $p<0.01$, §§ $p<0.01$.

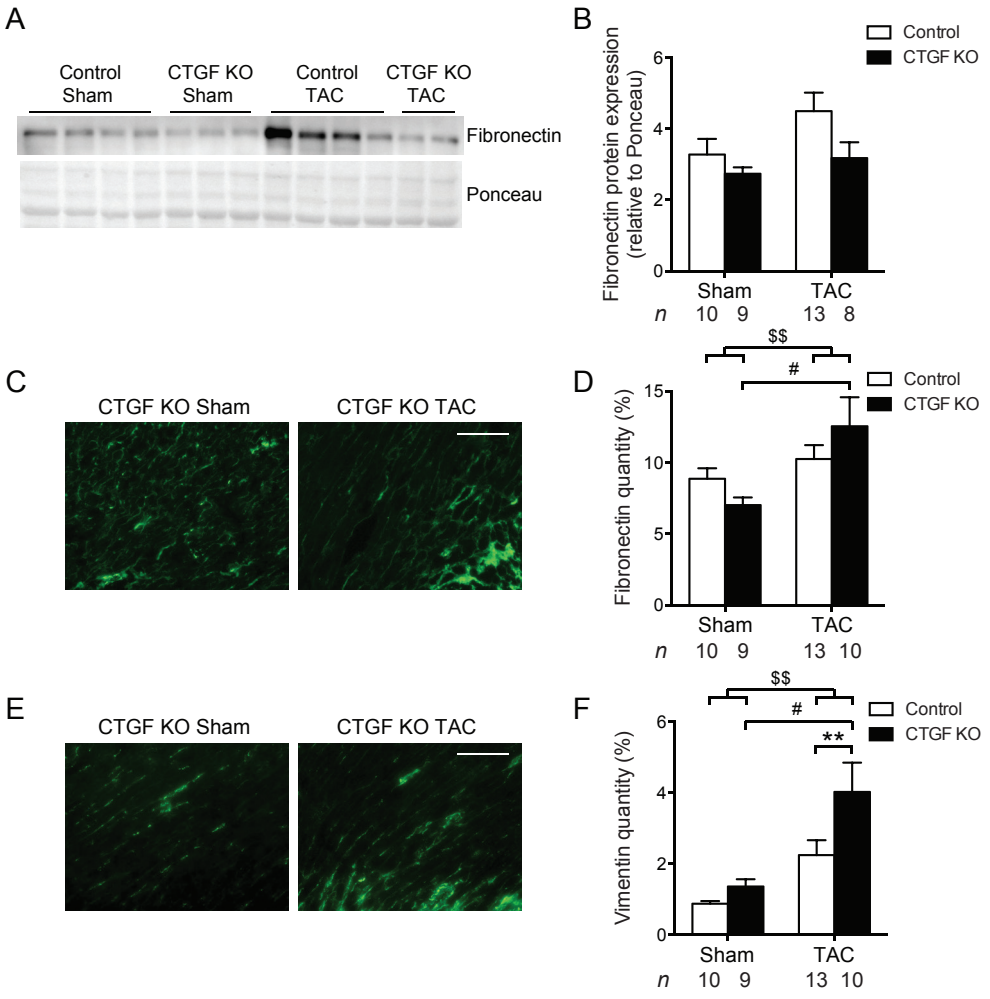

Supplementary Figure 2. Fibronectin and vimentin expression in isolated sham and TAC CTGF KO mouse ventricles compared with controls. A) Representative blot of fibronectin with respective ponceau staining below. **B)** Quantification of fibronectin protein expression (fibronectin/ponceau) exemplified in A. **C)** Representative images of fibronectin (green) expression in sham and TAC CTGF KO mice. Scale bar represents 100 µm. **D)** Quantification of fibronectin immunolabeling partly exemplified in C. **E)** Representative images of vimentin (green) expression in sham and TAC CTGF KO mice. Scale bar represents 100 µm. **F)** Quantification of vimentin immunolabeling partly exemplified in E. Black bars refer to CTGF KO mice and white bars to control mice; n indicates the number of mice per group. # $p<0.05$, §§ $p<0.01$, ** $p<0.01$.

“

Above all,
don’t fear difficult moments.
The best comes from them.

Rita Levi-Montalcini

Chapter

7

TLR2 knockout attenuates adverse cardiac remodeling in mice subjected to chronic pressure overload

Elise L. Kessler[a], Jiong-Wei Wang[b], Bart Kok[a], Maike A. Brans[a], Angelique Nederlof[a], Leonie van Stuijvenberg[a], Fatih Arslan[c,d], Carolyn S.P. Lam[e], Marc A. Vos[a], Dominique P.V. de Kleijn[b,c,f], Toon A.B. van Veen[a], Magda S.C. Fontes[a,g]

[a] *Department of Medical Physiology, Division of Heart & Lungs, University Medical Center Utrecht, Utrecht University, Utrecht, The Netherlands*
[b] *Department of Surgery, Yong Loo Lin School of Medicine, National University of Singapore, Cardiovascular Research Institute, National University Heart Centre, Singapore*
[c] *Department of Cardiology, Division of Heart & Lungs, University Medical Center Utrecht, Utrecht University, Utrecht, The Netherlands*
[d] *Laboratory Experimental Cardiology, Division of Heart & Lungs, University Medical Center Utrecht, Utrecht University, Utrecht, The Netherlands*
[e] *National Heart Centre Singapore and Duke-National University of Singapore, Singapore & UMC Groningen, the Netherlands*
[f] *Department of Vascular Surgery, University Medical Center Utrecht, Utrecht University, Utrecht, The Netherlands & Netherlands Heart Institute, Utrecht, the Netherlands*
[g] *Laboratory of Experimental Cardiology, Department of Cardiology, Heart Lung Center Leiden, The Netherland*

Manuscript submitted

Abstract

Background: The inflammatory Toll-like receptor (TLR) pathway is associated with maladaptive cardiac remodeling in ischemic injury, but involvement upon chronic pressure overload (PO) is not yet fully understood. In this study, we investigated the effect of TLR2 knockout (KO) on cardiac remodeling during chronic PO in mice subjected to transverse aortic constriction (TAC) surgery.

Methods: 35 male mice (age 10-12 weeks; wildtype (WT) or TLR2 KO) underwent sham or TAC surgery. Echocardiography and electrocardiography were recorded 2, 6 and 12 weeks after surgery. At 12 weeks, hearts were extracted for molecular and histological analysis.

Results: Interestingly, TAC in TLR2 KO mice (n=14) was associated with less hypertrophy, attenuated characteristics of contractility, and lower levels of inflammatory cytokines compared to WT TAC animals (n=11), which presented with reduced left ventricular ejection fraction (<35%), greatly enlarged hearts (heart weight/tibia length ratio 16.6±0.7 mg/mm), abnormal contraction characteristics, increased fibrosis and inflammation compared to Sham animals (n=10). Furthermore, in WT TAC animals high levels of TLR4 and TLR2 correlated with highest degree of hypertrophy and increased levels of the inflammatory cytokine interleukin 6 (IL-6).

Conclusion: These data show the association of adverse cardiac remodeling with high levels of TLR2 and TLR4, as well as attenuation of adverse remodeling in TLR2 KO TAC mice. This suggests that the TLR pathway may represent an important modifiable target in cardiac remodeling under chronic pressure overload.

Introduction

Hypertension is a major cardiovascular risk factor affecting a billion individuals worldwide and carrying one of the largest population attributable risks for heart failure (HF).[1] Pressure overload (PO) leads to cardiac remodeling associated with cardiac stiffness and arrhythmias, eventually culminating in HF.[2] In both clinical and animal studies, fibrosis is a major contributor to maladaptive remodeling.[3] Fibrosis is defined as the excessive secretion and/or impaired degradation of connective tissue, especially collagen, in the extracellular matrix.[3,4] During cardiac remodeling, activation of inflammatory pathways, such as the toll-like receptor (TLR) pathway, is a common observation.[5]

TLRs are crucial for initiation of the innate immune system by recognizing Damaged and Pathogen Associated Molecular Patterns (DAMPs and PAMPs, respectively).[6] The most abundant and best studied TLRs in the heart are TLR4 and TLR2, expressed in immune and cardiac non-immune cells (e.g. cardiomyocytes, fibroblasts and vascular endothelial cells).[7,8]

Upon ligand binding and activation of the TLR2 or TLR4 receptor, transcription factors like the nuclear factor kappa-light-chain-enhancer of activated B cells (NF-κB) are translocated to the nucleus. This induces expression of inflammatory cytokines and chemokines (e.g. interleukin-1beta (IL-1β), IL-6 and tumor necrosis factor-alpha (TNF-α)) leading to invasion of pro-inflammatory cells.[9] Chronic elevation of cytokines, such as IL-6 for example, has in turn been associated with various forms of cardiovascular diseases and HF, and seems to have a causal role in the development of coronary heart disease.[10,11] In congestive HF, plasma levels of IL-6 are used as an independent prognostic marker.[12] Furthermore, it has been shown that TLR4 stimulates adverse cardiac remodeling: up-regulation of TLR4 in rat cardiomyocytes worsens cardiac function and the phenotype of HF, and knockout (KO) of the TLR4 gene in mice results in less cardiac fibrosis and hypertrophy.[13-17]

The role of TLR2 in the heart is less clear, but it is associated with ischemia reperfusion injury, adverse remodeling after myocardial infarction (MI), contractile dysfunction, atherosclerosis and fibrosis.[18-20] However, results upon TLR2 KO during PO are contradicting: while attenuation of cardiac hypertrophy and fibrosis in TLR2 KO mice upon 2 weeks of PO or MI has been described, others reported that TLR2 deficient mice displayed increased fibrosis and hypertrophy upon 4 weeks of PO compared to wildtype (WT) mice.[19,21,22]

In our study, we aimed at determining the effect of TLR2 KO upon chronic PO (12 weeks of transverse aortic constriction (TAC) in mice) on the development of cardiac remodeling, including cardiac fibrosis and inflammation.

Material & methods

ANIMAL STUDY

Experiments were conducted conform the Guide for the Care and Use of Laboratory Animals published by the US National Institutes of Health (NIH Publication No. 85-23, revised 1985) with consent of the Experimental Animal Ethics Committee of the University Utrecht, The Netherlands. All mice were male to minimize hormonal influence and gender-dependent bias. TLR2 KO mice were commercially available (Jackson Laboratory, Bar Harbor, USA). Mice were housed under normal laboratory conditions (a 12 hour light/dark cycle with controlled humidity and temperature, and food and water *ad libitum*). After acclimatization, 10-12 weeks old mice underwent TAC or sham surgery under inhaled isoflurane anesthesia (2 % in O_2), as previously described.[23] Furthermore, all mice received subcutaneous injections of carprofen (5 mg/kg) as perioperative care. All mice were followed for 12 weeks, and surviving animals were further analyzed in the following 3 groups: TLR2 KO Sham (n=10), TLR2 KO TAC (n=14), and WT TAC (n=11). As described in literature, TLR2 KO Sham animals show heart weight/tibia length ratios (HW/TL), heart rate (HR), echocardiographic parameters, and collagen expression patterns that are comparable to WT Sham animals.[20,22] All experiments were performed in a blinded fashion.

GENOTYPING

To confirm global TLR2 KO, polymerase chain reaction (PCR) was performed on DNA isolated from liver biopsies using TLR2-specific oIMR3091 wildtype (5'-ACGAGCAAGATCAACAGGAGA-3'), oIMR3041 common/heterozygous (5'-CTTCCTGAATTTGTCCAGTA-3') and oIMR3043 mutant (5'-GGGCCAGCTCATTCCTCC CAC-3') oligonucleotides. PCR amplification was repeated 35 times with Taq DNA polymerase (GE Healthcare, Buckinghamshire, UK) under the following conditions: denaturation for 30 seconds at 94 °C, annealing for 30 seconds at 65 °C and elongation for 30 seconds at 72 °C. PCR products (wildtype 499bp and mutant 334bp) were visualized by agarose gel electrophoresis.

ELECTROCARDIOGRAPHY AND ECHOCARDIOGRAPHY

Two, 6 and 12 weeks after surgery, mice were anesthetized with 2 % isoflurane in O_2 and a 3-lead electrocardiogram (ECG) was recorded using PowerLab 4/30 and Dual Bio Amp (AD Instruments Ltd., Oxford, UK). A minimum of 150 complexes were averaged and analyzed with LabChart 7 Pro (AD Instruments Ltd.). At the same time-points as ECG, also transthoracic echocardiography was performed with the Vevo 2100 System (VisualSonic Inc., Toronto, Canada) using a 22-55MHz transducer (MS550D). To confirm appropriate constriction in all TAC operated animals, aortic peak velocity was measured by pulsed-wave Doppler with a 13–24 MHz transducer (MS250). Analysis was performed with the Vevo 2100 software (VisualSonic Inc.).

HISTOLOGY AND IMMUNOHISTOCHEMISTRY

Twelve weeks after surgery, mice were sacrificed by aortic transection, and hearts were weighted and snap-frozen in liquid nitrogen. Serial four-chamber view cryosections of 10 µm were generated.

To detect cardiac fibrosis, cryosections were stained with 0.1 % Picrosirius Red solution, scanned and analyzed as previously described.[24] The amount of fibrosis was calculated as the positive red signal in the ventricles relative to the total ventricular surface area.

To assess cell size, immunolabeling was performed using a mouse monoclonal antibody against dystrophin (1:1500, Sigma-Aldrich, Saint Louis, USA) as described previously.[25] Secondary labeling was achieved by fluorescein isothiocyanate (FITC) anti-mouse whole IgG antibody (1:250, Jackson ImmunoResearch Europe, Newmarket, UK). Sections were analyzed with an epifluorescence microscope (Nikon Eclipse 80i; Nikon Europe BV, Amstelveen, The Netherlands) and randomly chosen images were taken using the NIS Elements BR 3.0 software (Nikon Instruments Europe B.V., Amsterdam, The Netherlands). Quantification analysis was performed using the ImageJ 1.48v software (National Institutes of Health, USA). Cell size was defined as cross sectional cardiomyocyte area, and cells with a Feret ratio>1.25 were excluded.

REAL-TIME QUANTITATIVE PCR (RT-QPCR)

For RT-qPCR on ventricular tissue, TaqMan Gene Expression Assays (all from Applied Biosystems by Life Technologies Corp., Carlsbad, USA) were used as described earlier.[26] As an internal control, the geometric mean of Succinate Dehydrogenase Complex Flavoprotein Subunit A (SDHA), Ribosomal Protein Lateral Stalk Subunit P1 (RPLP-1) and TATA-binding protein (TBP) mRNA was used. Relative mRNA expression levels were determined for brain natriuretic peptide (BNP), Collagen 1α1 (Col1α1), Collagen 1α2 (Col1α2), Collagen 3α1 (Col3α1), transforming growth factor beta 1 (TGF-β1), plasminogen activator inhibitor-1 (PAI-1), heat shock protein 47 (HSP47), matrix metalloproteinase 9 (MMP-9), metallopeptidase inhibitor 1 (TIMP-1), IL-6, IL-1β, NF-κB, TNF-α and TLR4. Assay ID's are listed in Supplementary Table 1.

STATISTICS

Data are expressed as mean ± standard error of the mean (SEM). Statistical analyses were performed using appropriate parametric or non-parametric tests (one-way ANOVA followed by Tukey's multiple comparisons test or Kruskal-Wallis followed by Dunn's multiple comparison test, respectively). The survival data were analyzed using the log-rank test. All analyses were performed with GraphPad Prism 6.0 (GraphPad Software Inc., La Jolla, USA) or SPSS (IBM SPSS Statistics for Windows 20.0, Armonk, USA). A value of $p<0.05$ was considered statistically significant.

Results

VALIDATION OF THE ANIMAL MODEL

Global TLR2 KO in all KO animals was confirmed by PCR (data not shown). Pressure gradients at 2, 6 and 12 weeks after surgery confirm the effectiveness of the TAC surgery in both TAC groups (at 12 weeks: 61.6±3.6 mmHg in TLR2 KO TAC and 61.7±4.4 mmHg in WT TAC *vs.* 3.5±0.3 mmHg in TLR2 KO Sham, Table 2; individual pressure data are depicted in Supplementary Figure 1). TAC groups showed significantly increased mortality, but no significant differences were seen between TAC operated WT and TLR2 KO mice (100 % survival of TLR2 KO Sham *vs.* 64 % in TLR2 KO TAC and 49 % in WT TAC animals).

HYPERTROPHY AND MORPHOLOGY

Pressure overload, due to 12 weeks of TAC, resulted in cardiac hypertrophy as assessed by several techniques. HW/TL was significantly increased in WT TAC (16.6±0.7 mg/mm) compared to TLR2 KO TAC (13.2±0.8 mg/mm) and for both groups when compared to TLR2 KO Sham (10.0±0.3 mg/mm, Figure 1A and Table 1). Cell size was significantly increased in WT TAC mice compared to TLR2 KO TAC and TLR2 KO Sham (376±23 μm^2 in WT TAC *vs.* 309±17 μm^2 in TLR2 KO TAC and 274±15 μm^2 in TLR2 KO Sham, Figure 1B). LV mass after 12 weeks of TAC was increased in WT and TLR2 KO TAC animals compared to TLR2 KO Sham (Figure 1C and Table 2). mRNA levels of the hypertrophic marker BNP were significantly increased in WT TAC when compared to TLR2 KO TAC, but also in both TAC groups when compared to TLR2 KO Sham (Figure 1D).
Liver and lung weights were not altered. Kidneys showed reduced weights after TAC in both groups, although this reduction was significantly more pronounced in TLR2 KO TAC (Table 1).

Table 1. Tissue characteristics of TLR2 KO Sham, TLR2 KO TAC and WT TAC mice 12 weeks after surgery. Values are mean ± SEM. TAC, transverse aortic constriction; KO, knockout; WT, wild type; n, number of animals; HW/TL, heart weight to tibia length ratio; LuW/TL, lungs weight to tibia length ratio; LiW/TL, liver weight to tibia length ratio; KW/TL, average kidneys weight to tibia length ratio. * p<0.05 and ** p<0.01 compared to TLR2 KO Sham; # p<0.05 and ## p<0.01 compared to TLR2 KO TAC.

	Sham	TAC	
	TLR2 KO	TLR2 KO	WT
n	10	14	11
Body weight (g)	35.5±0.8	33.9±0.6	33.0±0.5*
Heart weight (mg)	184.2±5.6	242.5±15.9	304.6±13.0**
Tibia Length (mm)	18.4±0.1	18.4±0.0	18.3±0.1
HW/TL (mg/mm)	10.0±0.3	13.2±0.8*	16.6±0.7**##
LuW/TL (mg/mm)	9.7±0.2	11.8±1.4	13.7±2.0
LiW/TL (mg/mm)	83.5±2.5	73.6±2.6	80.7±3.6
KW/TL (mg/mm)	10.6±0.3	8.9±0.2**	9.7±0.3*#

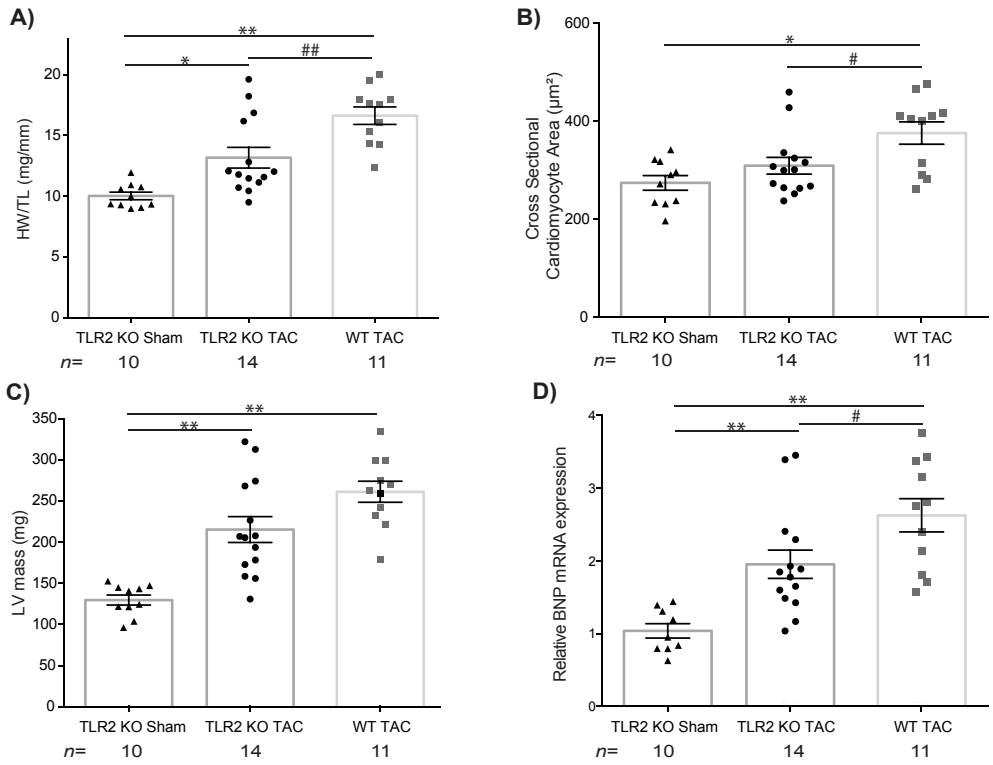

Figure 1. Hypertrophic parameters in TLR2 KO and WT mice 12 weeks after Sham or TAC surgery. **A)** Heart weight to tibia length ratio (HW/TL, mg/mm) of TLR2 KO Sham, TLR2 KO TAC and WT TAC mice 12 weeks after surgery. **B)** Cross sectional cardiomyocyte area (μm^2) assessed by fluorescent dystrophin labeling; exclusion criterion was a Feret ratio >1.25 (max/min diameter). **C)** Left ventricular mass (LV mass, mg) measured by echocardiography after 12 weeks of TAC or Sham surgery. **D)** Ventricular mRNA expression of brain natriuretic peptide (BNP) assessed by TaqMan RT-qPCR. n indicates the number of mice per group. * $p<0.05$ and ** $p<0.01$ compared to TLR2 KO Sham; # $p<0.05$ and ## $p<0.01$ compared to TLR2 KO TAC.

CARDIAC FUNCTION AND CONTRACTILITY

At 2, 6 and 12 weeks after surgery, ECG and echocardiography were performed. ECG after 12 weeks showed significantly prolonged QRS intervals in WT TAC compared to TLR2 KO TAC and TLR2 KO Sham (12.7±0.4 ms in WT TAC *vs.*11.4±0.3 ms in TLR2 KO TAC and 10.6±0.3 ms in TLR2 KO Sham, Table 2). QTc intervals were significantly increased in the WT TAC group when compared to TLR2 KO TAC and TLR2 KO Sham (57.0±2.3 ms in WT TAC *vs.* 51.1±1.9 ms in TLR2 KO TAC and 42.2±0.6 ms in TLR2 KO Sham). Echocardiographic data after 12 weeks of surgery indicates reduced contractility and cardiac function in WT TAC animals, with a significantly decreased ejection fraction (EF), fractional shortening (FS) and cardiac output (CO), when compared to TLR2 KO Sham animals (Table 2). Only stroke volume (SV) was significantly decreased in TLR2 KO TAC compared to TLR2 KO Sham. Nearly all other echocardiographic data measured in WT TAC mice differed significantly from the Sham group, while this appeared to be far less pronounced comparing the TLR2 KO TAC with the Sham animals (Table 2).

Table 2. Echocardiographic and electrocardiographic measurements of TLR2 KO Sham, TLR2 KO TAC and WT TAC mice 12 weeks after surgery. Values are mean ± SEM. LV, left ventricle; LVAW,s and LVAW,d, end-systolic and end-diastolic LV anterior wall thickness, respectively; LVPW,s and LVPW,d, end-systolic and end-diastolic LV posterior wall thickness, respectively; LVID,s and LVID,d, LV internal diameter end-systole and end-diastole, respectively; LV Vol,s and LV Vol,d, end-systolic and end-diastolic LV volume, respectively; EF, ejection fraction; FS, fractional shortening; SV, stroke volume; CO, cardiac output. * $p<0.05$ and ** $p<0.01$ compared to TLR2 KO Sham; # $p<0.05$ and ## $p<0.01$ compared to TLR2 KO TAC.

	Sham	TAC	
	TLR2 KO	TLR2 KO	WT
n	10	14	11
Echocardiography			
Pressure gradient (mmHg)	3.5±0.3	61.6±3.6**	61.7±4.4**
LVAWs (mm)	1.3±0.1	1.5±0.0	1.4±0.1
LVAWd (mm)	0.9±0.1	1.1±0.0**	1.2±0.1**
LVPWs (mm)	1.1±0.1	1.3±0.1	1.3±0.1
LVPWd (mm)	0.8±0.0	1.1±0.1**	1.1±0.1**
LVID,s (mm)	2.8±0.2	3.6±0.2*	4.2±0.2**
LVID,d (mm)	4.1±0.1	4.4±0.1	4.8±0.2**
LV Vol,s (µL)	31.4±4.0	56.5±8.7	81.7±9.2**
LV Vol,d (µL)	72.6±3.3	88.3±7.4	108.1±8.4**
LV mass (mg)	129.6±6.1	215.2±15.7**	261.1±12.8**
EF (%)	58.0±4.0	39.7±4.1	26.1±3.1**
FS (%)	30.8±2.7	19.6±2.2	12.2±1.5**
SV (µL)	41.2±1.7	31.7±2.1*	26.4±2.3**
CO (mL/min)	19.0±1.2	16.2±1.1	13.3±1.1**
Electrocardiography			
Heart Rate (bpm)	427.8±18.4	479.8±14.9	480.2±15.5
RR (ms)	142.4±5.7	126.6±3.9*	126.3±4.2
PR (ms)	42.7±0.8	42.8±1.4	42.8±1.5
P (ms)	9.8±0.2	10.3±0.3	11.2±0.5
QRS (ms)	10.6±0.3	11.4±0.3	12.7±0.4**#
QTc (ms)	42.2±0.6	51.1±1.9	57.0±2.3**##

FIBROSIS

The amount of cardiac fibrosis 12 weeks after surgery was assessed by a Picrosirius Red staining, as shown in figure 2A. Both TLR2 KO and WT TAC groups showed a significantly increased amount of fibrosis compared to TLR2 KO Sham (2.7±0.4 % for TLR2 KO TAC and 2.0±0.3 % for WT TAC *vs.* 0.8±0.1 % in TLR2 KO Sham, Figure 2B), but this increase did not differ between both TAC groups. Moreover, relative mRNA expression levels of fibrosis-related genes were determined by RT-qPCR as depicted in figure 2C. Interestingly, cardiac Col1α2 and Col3α1 mRNA levels as well as TGF-β1 and its gene target HSP47 were significantly increased in WT TAC when compared to the TLR2 KO TAC group. Not surprisingly, these genes, with addition of Col1α2 and PAI-1 (another gene target of TGF-β1), were also significantly elevated in WT TAC *vs.* TLR2 KO Sham. Col1α2, Col3α1 and PAI-1 were also increased in TLR2 KO TAC compared to TLR2 KO Sham. Although MMP-9 levels did not differ between groups, its inhibitor TIMP-1 was significantly increased in WT TAC and TLR2 KO TAC compared to TLR2 KO Sham.

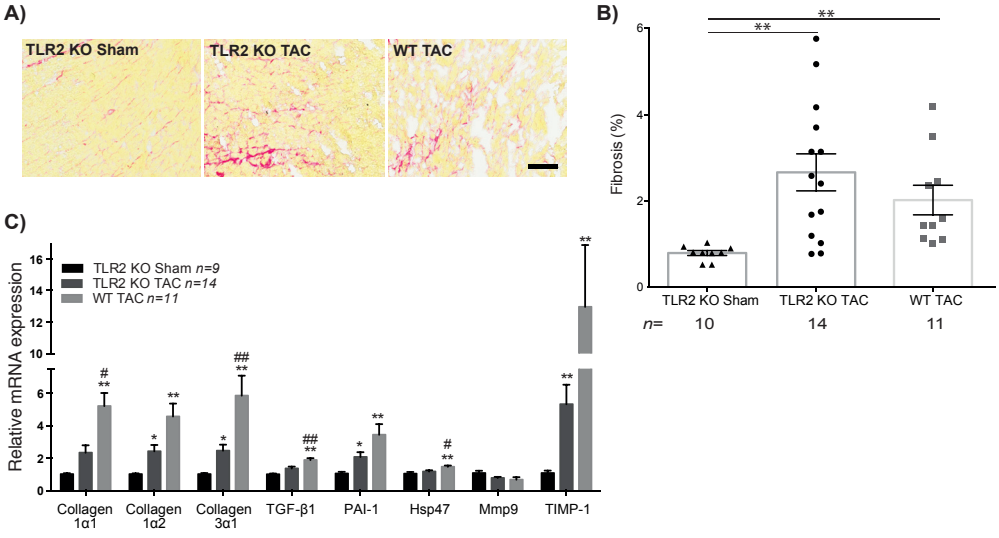

Figure 2. Fibrosis and fibrosis-related parameters 12 weeks after Sham or TAC surgery. **A)** Representative pictures of ventricular Picrosirius Red staining on TLR2 KO Sham, TLR2 KO TAC and WT TAC mice. Percentages are positive red signal in the ventricles relative to the total ventricular surface area. Scale bar indicates 100μm. **B)** Quantification of Picrosirius Red staining as a percentage of whole tissue. **C)** Ventricular mRNA expression of Collagen 1α1, Collagen 1α2, Collagen 3α1, transforming growth factor beta 1 (TGF-β1), plasminogen activator inhibitor-1 (PAI-1), heat shock protein 47 (HSP47), matrix metalloproteinase 9 (MMP-9) and metallopeptidase inhibitor 1 (TIMP-1) assessed by TaqMan RT-qPCR in TLR2 KO Sham, TLR2 KO TAC and WT TAC groups. n indicates the number of mice per group. * $p<0.05$ and ** $p<0.01$ compared to TLR2 KO Sham; # $p<0.05$ and ## $p<0.01$ compared to TLR2 KO TAC.

INFLAMMATION

To investigate the consequences of TLR2 KO on inflammation, the downstream pathway of TLR2 and its possible binding partner TLR4 were examined. Cardiac mRNA levels of the cytokines IL-6 and IL-1β were significantly increased in the WT TAC group (7.6±2.0 for IL-6 and 8.2±5.5 for IL-1β) compared to TLR2 KO TAC (2.2±0.4 for IL-6 and 1.2±0.1 for IL-1β) and TLR2 KO Sham (1.4±0.6 for IL-6 and 1.1±0.2 for IL-1β, Figure 3A). Transcription factor NF-κB and cytokine TNF-α were not statistically different in all groups, but mRNA levels of TLR4 were significantly increased in WT TAC compared to TLR2 KO TAC animals (2.1±0.1 *vs.* 1.6±0.1, respectively) and in both TAC groups compared to TLR2 KO Sham (1.0±0.1, Figure 3A).

Having established lower TLR4 and IL-6 mRNA levels in the TLR2 KO TAC compared to the WT TAC, we investigated whether in the WT TAC group, high levels of both TLR2 and TLR4 mRNA were associated with increased HW/TL (Figure 3B) and increased levels of the cytokine IL-6 (Figure 3C). Indeed, these data reveal a tendency that high levels of HW/TL and IL-6 are seen in animals with the higher levels of TLR2 and TLR4.

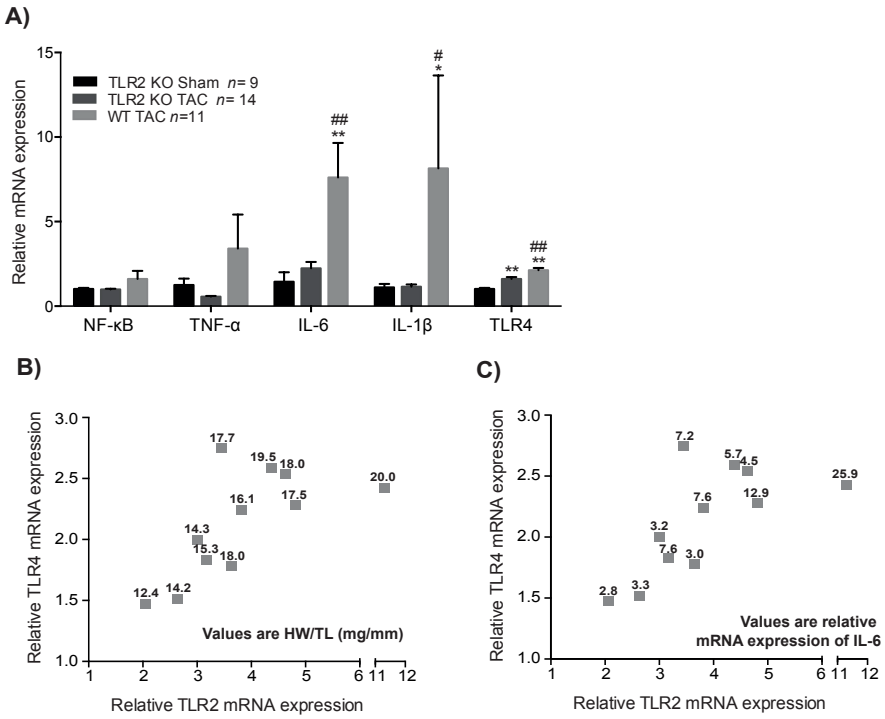

Figure 3. Inflammatory parameters 12 weeks after Sham or TAC surgery. **A)** Ventricular mRNA expression of nuclear factor kappa-light-chain-enhancer of activated B cells (NF-κB), tumor necrosis factor-alpha (TNF-α), interleukin-6 (IL-6), IL-1β and TLR4 assessed by TaqMan RT-qPCR in TLR2 KO Sham, TLR2 KO TAC and WT TAC groups. n indicates number of mice per group. **B)** Correlation between mRNA expressions of TLR2 and TLR4 of WT TAC animals 12 weeks after surgery. Values indicate individual HW/TL (mg/mm) per mouse. **C)** Correlation between mRNA expressions of TLR2 and TLR4 of WT TAC animals 12 weeks after surgery. Values indicate individual levels of the relative mRNA levels of the cytokine IL-6 per mouse. * $p<0.05$ and ** $p<0.01$ compared to TLR2 KO Sham; # $p<0.05$ and ## $p<0.01$ compared to TLR2 KO TAC.

TWO DISTINCT TLR2 KO TAC GROUPS IN ADVERSE REMODELING AFTER CHRONIC PO

Surprisingly but interesting, during the analysis of all the individual mouse data, we developed the strong impression that the animals within the TLR2 KO TAC group displayed a tendency to separate into two distinct phenotypes. The far majority (10/14 mice) within this group showed a significant attenuated adverse remodeling when compared to the WT TAC group, as illustrated by the data discussed thus far. A minority (4/14 mice), however, showed adverse cardiac remodeling comparable to that in the WT TAC group. For almost all of the parameters analyzed, the 4 versus 10 individual mice in this group behaved in a similar fashion. To assure that the observed differences in phenotype were not based on unrecognized differences in the followed experimental procedure, we verified all potential factors that could have been of importance. Doing that, we assured that there could not have been any influence of genotype, age, gender (all mice were male) and changes over time in pressure gradient (Supplementary Figure 1). Furthermore, the 4 mice that likely differed from the other 10 were no littermates, were not housed in the same cage and did not receive surgery on the same day. In Supplementary Figures 1 to 3, we indicated the 4 aberrant animals of the TLR2 TAC group in red circles and the other 10 in black circles. Here, a clear difference existed in hypertrophic markers (Supplementary Figures 2A and 2B), and following that, a presentation of reduced contraction characteristics (Supplementary Figures 2C, 3A and 3B), markers of fibrosis (Supplementary Figure 2D) and activation of inflammatory pathways (Supplementary Figures 3C and 3D). Correlation between EF and HW/TL shows a clear separation in this group (Supplementary Figure 3A) that developed over time, as can be seen in a correlation between EF and LVmass at 2, 6 and 12 weeks after surgery (Supplementary Figure 3B). Interestingly, correlations between TLR4 and HW/TL (Supplementary Figure 3C) and EF (Supplementary Figure 3D), and the level of IL-6 (Supplementary Figure 3E) point at a potential importance for the expression level of TLR4, since separation is clearly visible in these correlations.

Discussion

Inflammatory pathways, such as the TLR pathway, have been associated with adverse cardiac remodeling and HF. The main TLRs in the heart are TLR4 and TLR2. TLR4 is indicated to be involved in fibrosis, adverse remodeling and hypertrophy,[14-16] though less is known about the role of TLR2. Therefore, we investigated the effect of TLR2 KO in mice upon chronic PO (12 weeks of TAC). Even though TLR2 KO TAC animals showed signs of hypertrophy and fibrosis, levels of hypertrophic marker BNP, cell size and HW/TL were significantly reduced when compared to WT TAC animals. Furthermore, these mice presented with normal cardiac function (electrocardiographic and echocardiographic measurements) and inflammatory parameters comparable to TLR2 KO Sham animals. All TLR2 KO Sham animals were viable suggesting that TLR2 KO alone does not cause problems in cardiac development and function, or sudden cardiac death. Mortality after TAC was increased, as previously described in literature,[24,27] and comparable between WT TAC and TLR2 KO TAC groups. In WT TAC animals, increased cardiac hypertrophy, abnormal contraction characteristics as well as increased levels of inflammation and fibrosis demonstrated adverse cardiac remodeling.

We therefore concluded that TLR2 KO upon TAC preserves EF and other parameters of cardiac function and attenuates adverse cardiac remodeling. This has also been seen upon ischemic injury for example, where TLR2 KO improved contractile performance and cardiac function.[18] In our study, however, the interplay of mRNA levels of TLR2, TLR4 and IL-6 seemed to be able to predict the outcome of cardiac remodeling in WT TAC animals, where high mRNA levels of both TLRs were associated with high levels of IL-6 and HW/TL (Figures 3B and 3C).

To speculate, these findings could potentially explain the discrepancies seen in previous studies on TLR2. Wang et al. for instance showed decreased fibrosis after TLR2 KO compared to WT animals. Although they did not report TLR4 levels, downstream targets of both TLR2 and TLR4 (e.g. IL-1β, IL-6 and TNF-α) were decreased suggesting that both pathways were inhibited.[20] Bualeong *et al.*, however, reported that TLR2 KO could not attenuate development of hypertrophy upon TAC and, in line with our findings, their KO mice had significantly increased levels of TLR4.[22] As mentioned before, high TLR4 levels are associated with cardiac hypertrophy and fibrosis, and up-regulation in cardiomyocytes worsens the cardiac phenotype.[14] Moreover, TLR4 is increased in the myocardium of patients with advanced HF, and in patients undergoing bypass surgery that present with reduced EF compared to patients with preserved EF.[13,28] Although few studies investigated the effect of TLRs upon chronic pressure overload, both TLR2 and TLR4 were reported to be increased in the circulation after acute MI and chronic HF.[29,30]

How, and if, the two TLRs interact in the heart still is unresolved. Both TLR2 and TLR4 can activate the same downstream targets, such as NF-κB, and KO of this target protects against ventricular dilatation and fibrosis after MI and preserves LV function in mice.[31] Moreover, cardiac specific inhibition of NF-κB protects against ischemia reperfusion injury by increasing calcium re-uptake into the sarcoplasmic reticulum, suggesting indeed a role for both receptors in maladaptive remodeling.[32]

In general, TLRs can form homo- and heterodimers, enhancing or inhibiting receptor signaling. TLR4s are known to form homodimers with each other, and TLR2 and TLR4 are suggested to form heterodimers in the brain, but not yet reported in the heart.[6,33] In addition, the endogenous ligand Fibronectin Extra Domain A has been shown to activate both TLR2 and TLR4 and is expressed in the heart after MI, where it is involved in adverse remodeling and fibrosis.[34] Interaction between TLR2 and TLR4 has also been suggested after LPS and High Mobility Group Box-1 stimulation, although double TLR2 – TLR4 KO experiments were not performed.[35,36] The amount of redundancy and expression of endogenous ligands, but also heterodimerization and interaction between TLR and TLR4 could therefore influence the outcome of cardiac remodeling, but needs more investigation.

Furthermore, levels of IL-6 are increased in mice with high levels of TLR2 and TLR4 in the WT TAC group (Figure 3C), but also more increased in WT TAC animals compared to KO animals (Supplementary Figure 3E). The latter might have been influenced by the obvious absence of TLR2. Since chronic elevated levels of IL-6 are associated with heart failure and cardiovascular mortality, this probably partially explains the deterioration of mice in the WT TAC group, but also the four badly performing mice in the TLR2 KO TAC group.[10,37] Finally, in murine and rat models, deletion of IL-6 prevented LV hypertrophy, dysfunction and fibrosis upon hypertension and decreased levels of fibrosis upon diabetic cardiomyopathy, pointing at a more profound role for the interaction between the TLRs and IL-6.[38-41] This suggests that activation of TLR2 solely does not induce HF, but rather the interplay of TLR2 with TLR4, which might mediate cardiac remodeling in PO and represent potential modifiable targets.

Study limitations

The data presented in this study suggest a maladaptive role for high levels of TLR2 and TLR4, and tentatively as a consequence also for IL-6 in cardiac remodeling upon chronic PO. As explained, in this study we did not include a TLR2 KO Sham group since literature data have already excluded differences in cardiac performance between this group and WT Sham animals.[24,42] The strong tendency of separated phenotypes within the TLR2 TAC group that we displayed in the supplemental figures 1-3 revealed multiple significant differences, though the difference in size of the (sub) groups (4 *vs.* 10) is a point of attention.
To acquire more insight regarding the role of TLR2, and its conjunction with TLR4, in affecting pro-inflammatory pathways that drive adverse cardiac remodeling, more in depth in vitro and interventional studies need to be performed that, however, go beyond the scope of this study.

Conclusion

Upon chronic PO, TLR2 KO protects against cardiac hypertrophy and preserves EF in the vast majority of mice. TLR2 and TLR4 mRNA levels are associated with the cardiac remodeling response upon PO. This suggests that the TLR pathway may represent an important modifiable target in cardiac remodeling under chronic pressure overload.

References

1. Writing Group M, Mozaffarian D, Benjamin EJ, et al. Heart Disease and Stroke Statistics-2016 Update: A Report From the American Heart Association. Circulation.2016;133(4):e38-360.

2. Ponikowski P, Voors AA, Anker SD, et al. 2016 ESC Guidelines for the diagnosis and treatment of acute and chronic heart failure: The Task Force for the diagnosis and treatment of acute and chronic heart failure of the European Society of Cardiology (ESC) Developed with the special contribution of the Heart Failure Association (HFA) of the ESC. Eur Heart J.2016;37(27):2129-2200.

3. Swynghedauw B. Molecular mechanisms of myocardial remodeling. Physiol Rev.1999;79(1):215-262.

4. Krenning G, Zeisberg EM, Kalluri R. The origin of fibroblasts and mechanism of cardiac fibrosis. J Cell Physiol.2010;225(3):631-637.

5. Dick SA, Epelman S. Chronic Heart Failure and Inflammation: What Do We Really Know? Circ Res.2016;119(1):159-176.

6. Botos I, Segal DM, Davies DR. The structural biology of Toll-like receptors. Structure.2011;19(4):447-459.

7. Mann DL. The emerging role of innate immunity in the heart and vascular system: for whom the cell tolls. Circ Res.2011;108(9):1133-1145.

8. Flo TH, Halaas O, Torp S, et al. Differential expression of Toll-like receptor 2 in human cells. J Leukoc Biol.2001;69(3):474-481.

9. Takeda K, Akira S. Toll-like receptors in innate immunity. Int Immunol.2005;17(1):1-14.

10. Danesh J, Kaptoge S, Mann AG, et al. Long-term interleukin-6 levels and subsequent risk of coronary heart disease: two new prospective studies and a systematic review. PLoS Med.2008;5(4):e78.

11. Interleukin-6 Receptor Mendelian Randomisation Analysis C, Swerdlow DI, Holmes MV, et al. The interleukin-6 receptor as a target for prevention of coronary heart disease: a mendelian randomisation analysis. Lancet.2012;379(9822):1214-1224.

12. Wollert KC, Drexler H. The role of interleukin-6 in the failing heart. Heart Fail Rev.2001;6(2):95-103.

13. Avlas O, Bragg A, Fuks A, et al. TLR4 Expression Is Associated with Left Ventricular Dysfunction in Patients Undergoing Coronary Artery Bypass Surgery. PLoS One.2015;10(6):e0120175.

14. Liu L, Wang Y, Cao ZY, et al. Up-regulated TLR4 in cardiomyocytes exacerbates heart failure after long-term myocardial infarction. J Cell Mol Med.2015;19(12):2728-2740.

15. Ehrentraut H, Weber C, Ehrentraut S, et al. The toll-like receptor 4-antagonist eritoran reduces murine cardiac hypertrophy. Eur J Heart Fail.2011;13(6):602-610.

16. Dong RQ, Wang ZF, Zhao C, et al. Toll-like receptor 4 knockout protects against isoproterenol-induced cardiac fibrosis: the role of autophagy. J Cardiovasc Pharmacol Ther.2015;20(1):84-92.

17. Timmers L, Sluijter JP, van Keulen JK, et al. Toll-like receptor 4 mediates maladaptive left ventricular remodeling and impairs cardiac function after myocardial infarction. Circ Res.2008;102(2):257-264.

18. Arslan F, Smeets MB, O'Neill LA, et al. Myocardial ischemia/reperfusion injury is mediated by leukocytic toll-like receptor-2 and reduced by systemic administration of a novel anti-toll-like receptor-2 antibody. Circulation.2010;121(1):80-90.

19. Shishido T, Nozaki N, Yamaguchi S, et al. Toll-like receptor-2 modulates ventricular remodeling after myocardial infarction. Circulation.2003;108(23):2905-2910.

20. Wang L, Li YL, Zhang CC, et al. Inhibition of Toll-like receptor 2 reduces cardiac fibrosis by attenuating macrophage-mediated inflammation. Cardiovasc Res.2014;101(3):383-392.

21. Higashikuni Y, Tanaka K, Kato M, et al. Toll-like receptor-2 mediates adaptive cardiac hypertrophy in response to pressure overload through interleukin-1beta upregulation via nuclear factor kappaB activation. J Am Heart Assoc.2013;2(6):e000267.

22. Bualeong T, Kebir S, Hof D, et al. Tlr2 deficiency does not limit the development of left ventricular hypertrophy in a model of transverse aortic constriction induced pressure overload. J Negat Results Biomed.2016;15:9.

23. Boulaksil M, Winckels SK, Engelen MA, et al. Heterogeneous Connexin43 distribution in heart failure is associated with dispersed conduction and enhanced susceptibility to ventricular arrhythmias. Eur J Heart Fail.2010;12(9):913-921.

24. Fontes MS, Kessler EL, van Stuijvenberg L, et al. CTGF knockout does not affect cardiac hypertrophy and fibrosis formation upon chronic pressure overload. J Mol Cell Cardiol.2015;88:82-90.

25. van Veen TA, van Rijen HV, Wiegerinck RF, et al. Remodeling of gap junctions in mouse hearts hypertrophied by forced retinoic acid signaling. J Mol Cell Cardiol.2002;34(10):1411-1423.

26. Fontes MS, Raaijmakers AJ, van Doorn T, et al. Changes in Cx43 and NaV1.5 expression precede the occurrence of substantial fibrosis in calcineurin-induced murine cardiac hypertrophy. PLoS One.2014;9(1):e87226.

27. Mohammed SF, Storlie JR, Oehler EA, et al. Variable phenotype in murine transverse aortic constriction. Cardiovasc Pathol.2012;21(3):188-198.

28. Birks EJ, Felkin LE, Banner NR, Khaghani A, Barton PJ, Yacoub MH. Increased toll-like receptor 4 in the myocardium of patients requiring left ventricular assist devices. J Heart Lung Transplant.2004;23(2):228-235.

29. Methe H, Kim JO, Kofler S, Weis M, Nabauer M, Koglin J. Expansion of circulating Toll-like receptor 4-positive monocytes in patients with acute coronary syndrome. Circulation.2005;111(20):2654-2661.

30. Foldes G, von Haehling S, Okonko DO, Jankowska EA, Poole-Wilson PA, Anker SD. Fluvastatin reduces increased blood monocyte Toll-like receptor 4 expression in whole blood from patients with chronic heart failure. Int J Cardiol.2008;124(1):80-85.

31. Frantz S, Hu K, Bayer B, et al. Absence of NF-kappaB subunit p50 improves heart failure after myocardial infarction. FASEB J.2006;20(11):1918-1920.

32. Zhang XQ, Tang R, Li L, et al. Cardiomyocyte-specific p65 NF-kappaB deletion protects the injured heart by preservation of calcium handling. Am J Physiol Heart Circ Physiol.2013;305(7):H1089-1097.

33. Wang YC, Zhou Y, Fang H, et al. Toll-like receptor 2/4 heterodimer mediates inflammatory injury in intracerebral hemorrhage. Ann Neurol.2014;75(6):876-889.

34. Schoneveld AH, Hoefer I, Sluijter JP, Laman JD, de Kleijn DP, Pasterkamp G. Atherosclerotic lesion development and Toll like receptor 2 and 4 responsiveness. Atherosclerosis.2008;197(1):95-104.

35. Good DW, George T, Watts BA, 3rd. Toll-like receptor 2 is required for LPS-induced Toll-like receptor 4 signaling and inhibition of ion transport in renal thick ascending limb. J Biol Chem.2012;287(24):20208-20220.

36. van Zoelen MA, Yang H, Florquin S, et al. Role of toll-like receptors 2 and 4, and the receptor for advanced glycation end products in high-mobility group box 1-induced inflammation in vivo. Shock.2009;31(3):280-284.

37. Su D, Li Z, Li X, et al. Association between serum interleukin-6 concentration and mortality in patients with coronary artery disease. Mediators Inflamm.2013;2013:726178.

38. Melendez GC, McLarty JL, Levick SP, Du Y, Janicki JS, Brower GL. Interleukin 6 mediates myocardial fibrosis, concentric hypertrophy, and diastolic dysfunction in rats. Hypertension.2010;56(2):225-231.

39. Zhao L, Cheng G, Jin R, et al. Deletion of Interleukin-6 Attenuates Pressure Overload-Induced Left Ventricular Hypertrophy and Dysfunction. Circ Res.2016;118(12):1918-1929.

40. Zhang Y, Wang JH, Zhang YY, et al. Deletion of interleukin-6 alleviated interstitial fibrosis in streptozotocin-induced diabetic cardiomyopathy of mice through affecting TGFbeta1 and miR-29 pathways. Sci Rep.2016;6:23010.

41. Fuchs M, Hilfiker A, Kaminski K, et al. Role of interleukin-6 for LV remodeling and survival after experimental myocardial infarction. FASEB J.2003;17(14):2118-2120.

42. Rockman HA, Ross RS, Harris AN, et al. Segregation of atrial-specific and inducible expression of an atrial natriuretic factor transgene in an in vivo murine model of cardiac hypertrophy. Proc Natl Acad Sci U S A.1991;88(18):8277-8281.

Supplementary material

Supplementary Table 1. Characteristics of qPCR primers used in this study. Protein, gene name and assay ID of all primers (all purchased from Applied Biosystems by Life Technologies Corp., Carlsbad, USA).

Protein	Gene	Assay ID
SDHA	*Sdha*	Mm01352366_m1
RPLP-1	*Rplp1*	Mm02601846_g1
TBP	*Tbp*	Mm00446971_m1
BNP	*Nppb*	Mm01255770_g1
Collagen 1α1	*Col1a1*	Mm00801666_g1
Collagen 1α2	*Col1a2*	Mm00483888_m1
Collagen 3α1	*Col3a1*	Mm01254476_m1
TGF-β1	*TGF-β1*	Mm01178820_m1
PAI-1	*Serpine1*	Mm00435860_m1
HSP47	*Serpinh1*	Mm00438058_g1
IL-6	*Il6*	Mm00446190_m1
IL1-β	*Il1b*	Mm00434228_m1
NF-κB	*NF-κB*	Mm00477798_m1
TNF-α	*Tnf*	Mm00443258_m1
TIMP-1	*Timp1*	Mm00441818_m1
MMP-9	*Mmp9*	Mm00442991_m1
TLR4	*Tlr4*	Mm00445273_m1
TLR2	*Tlr2*	Mm00442346_m1

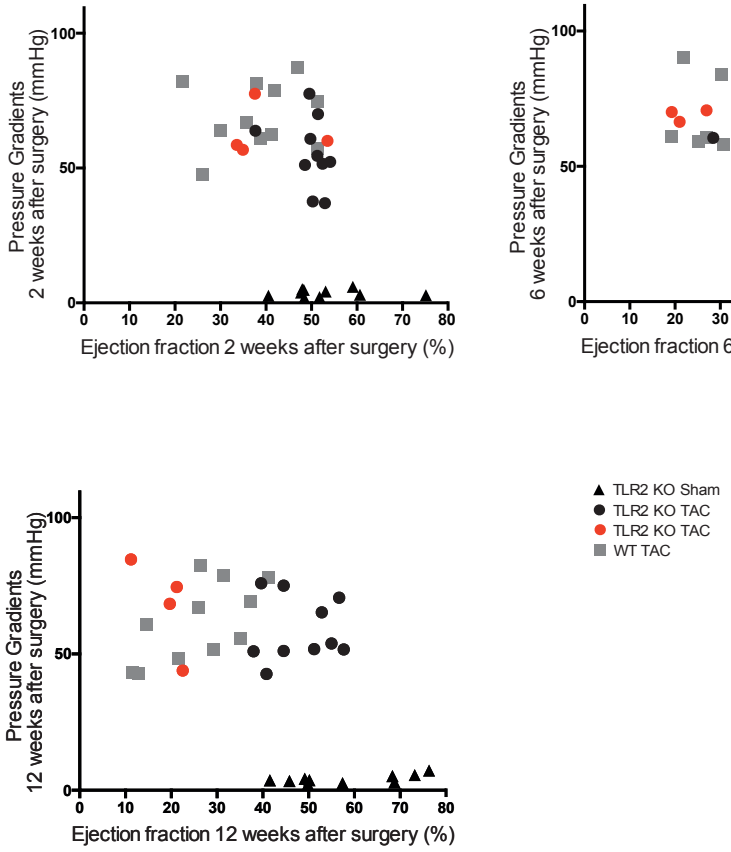

Supplementary Figure 1. Validation of the pressure overload model. Correlation between ejection fraction (%) and pressure gradients over time at 2 weeks (upper left panel), 6 weeks (upper right panel) and 12 weeks (lower left panel) after surgery. Black triangles depict mice of the TLR2 KO Sham group, black and red circles mice from the TLR2 KO TAC group, and grey squares mice from the WT TAC group. Red circles indicate mice with highest HW/TL and lowest EF.

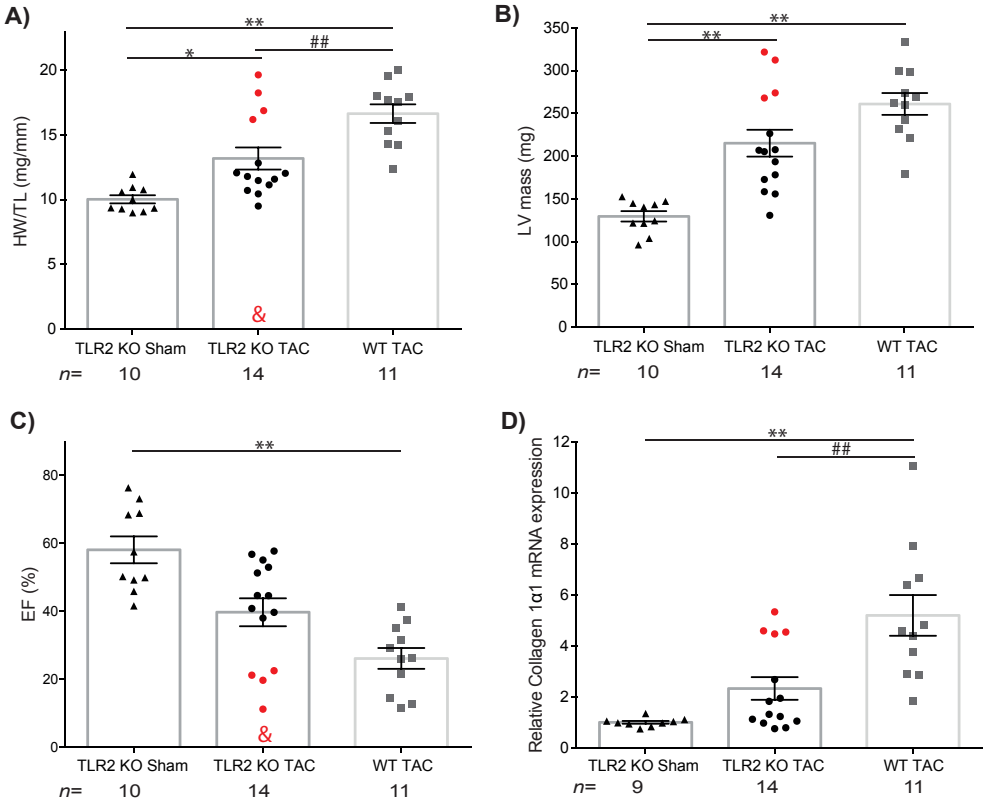

Supplementary Figure 2. Separation of TLR2 KO mice 12 weeks after TAC surgery. **A)** Heart weight to tibia length ratio (HW/TL, mg/mm) of TLR2 KO Sham, TLR2 KO TAC and WT TAC mice 12 weeks after surgery. Black triangles depict mice of the TLR2 KO Sham group, black and red circles mice from the TLR2 KO TAC group, and grey squares mice from the WT TAC group. Red circles indicate mice with highest HW/TL and lowest EF. **B)** Left ventricular mass (LV mass, mg) measured by echocardiography after 12 weeks of TAC or Sham surgery. **C)** Ejection fraction (EF, %) measured by echocardiography after 12 weeks of TAC or Sham surgery. **D)** Ventricular mRNA expression of Collagen 1α1 assessed by TaqMan RT-qPCR. n indicates the number of mice per group. * $p<0.05$ and ** $p<0.01$ compared to TLR2 KO Sham; # $p<0.05$ and ## $p<0.01$ compared to TLR2 KO TAC; & $p<0.05$ in mice with highest HW/TL and lowest EF (red dots) of the TLR2 KO TAC group compared to the rest of the TLR2 KO TAC animals (black dots).

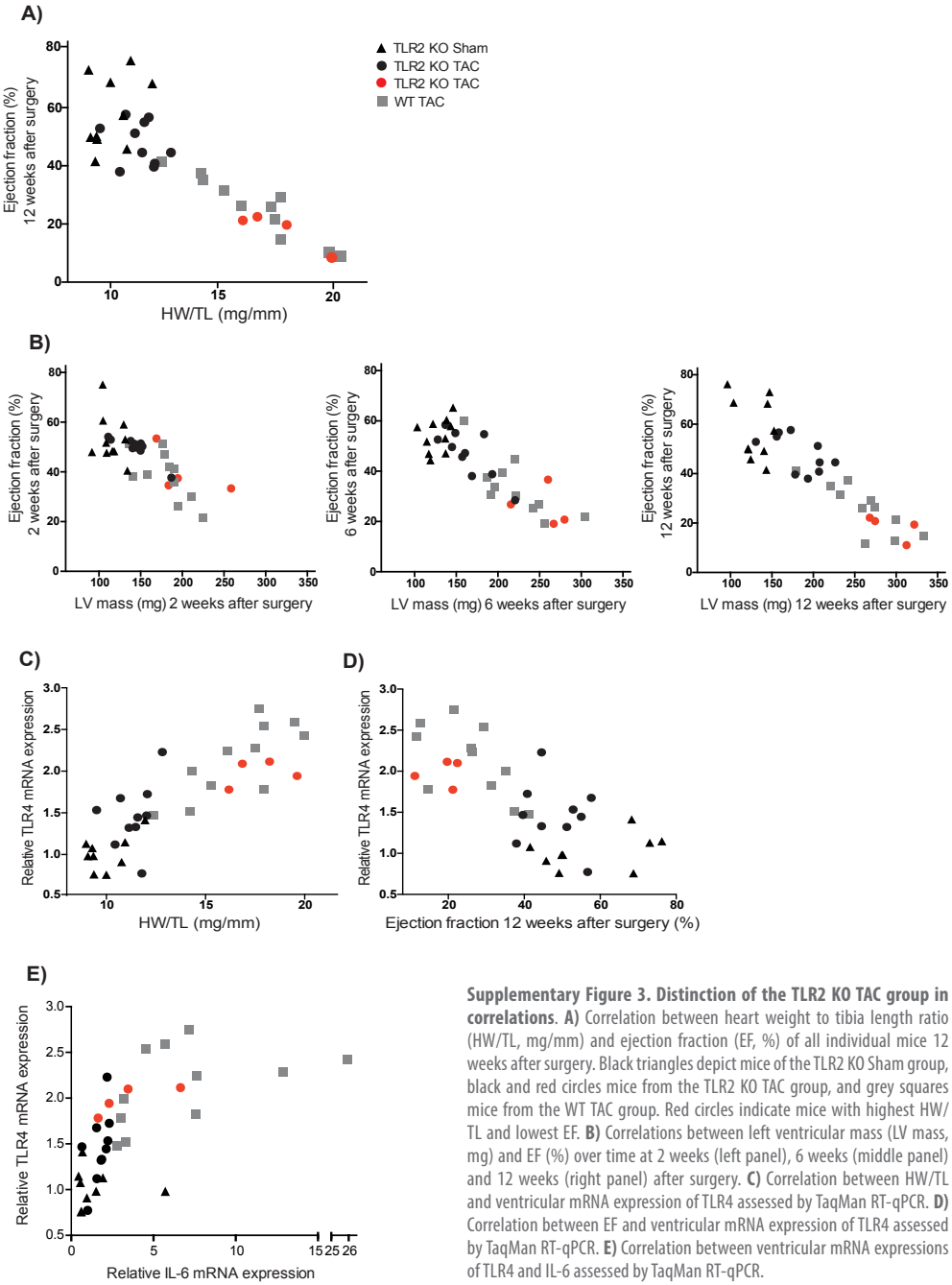

Supplementary Figure 3. Distinction of the TLR2 KO TAC group in correlations. A) Correlation between heart weight to tibia length ratio (HW/TL, mg/mm) and ejection fraction (EF, %) of all individual mice 12 weeks after surgery. Black triangles depict mice of the TLR2 KO Sham group, black and red circles mice from the TLR2 KO TAC group, and grey squares mice from the WT TAC group. Red circles indicate mice with highest HW/TL and lowest EF. **B)** Correlations between left ventricular mass (LV mass, mg) and EF (%) over time at 2 weeks (left panel), 6 weeks (middle panel) and 12 weeks (right panel) after surgery. **C)** Correlation between HW/TL and ventricular mRNA expression of TLR4 assessed by TaqMan RT-qPCR. **D)** Correlation between EF and ventricular mRNA expression of TLR4 assessed by TaqMan RT-qPCR. **E)** Correlation between ventricular mRNA expressions of TLR4 and IL-6 assessed by TaqMan RT-qPCR.

“

Everyone you will ever meet
knows something you don’t.

Bill Nye

Addendum to chapter

7

Leukocytic toll-like receptor 2 deficiency preserves cardiac function and reduces fibrosis in sustained pressure overload

Jiong-Wei Wang[a,b], Magda S.C. Fontes[c,d], Xiaoyuan Wang[a,b], Suet Yen Chong[a,b], **Elise L. Kessler**[c], Ya-Nan Zhang[a,b], Judith J. de Haan[e], Fatih Arslan[e], Saskia C.A. de Jager[e,f], Leo Timmers[e], Toon A.B. van Veen[c], Carolyn S.P. Lam[g,h], Dominique P.V. de Kleijn[a,b,e,i,j]

[a] *Department of Surgery, YLL School of Medicine, National University of Singapore, Singapore*
[b] *Cardiovascular Research Institute (CVRI), National University Heart Centre Singapore (NUHCS) and National University Health System (NUHS), Singapore, Singapore*
[c] *Department of Medical Physiology, Division of Heart & Lungs, University Medical Center Utrecht, Utrecht, The Netherlands*
[d] *Laboratory of Experimental Cardiology, Department of Cardiology, Heart Lung Center Leiden, Leiden University Medical Center, Leiden, The Netherlands*
[e] *Department of Cardiology, University Medical Center Utrecht, Utrecht, The Netherlands*
[f] *Laboratory of Translational Immunology, University Medical Center Utrecht, Utrecht, The Netherlands*
[g] *National Heart Centre Singapore, Duke-NUS Graduate Medical School, Singapore, Singapore*
[h] *Cardiology, University Medical Center, Groningen, the Netherlands.*
[i] *Department of Vascular Surgery, University Medical Center Utrecht, Utrecht, the Netherlands*
[j] *Netherlands Heart Institute, Utrecht, the Netherlands*

Scientific Reports 2017; 7: 9193

Abstract

Background: An involvement of Toll-like receptor 2 (TLR2) has been established in cardiac dysfunction after acute myocardial infarction; however, its role in chronic pressure overload is unclear. We sought to evaluate the role of TLR2 in cardiac hypertrophy, fibrosis and dysfunction in sustained pressure overload.

Methods: We induced pressure overload via transverse aortic constriction (TAC) in $TLR2^{-/-}$ and wild type (WT) mice, and followed temporal changes over 8 weeks.

Results: Despite similar increases in heart weight, left ventricular (LV) ejection fraction (EF) and diastolic function (mitral E/A ratio) were preserved in $TLR2^{-/-}$ mice but impaired in WT mice following TAC. TAC produced less LV fibrosis in $TLR2^{-/-}$ mice associated with lower mRNA levels of collagen genes (Col1α1 and Col3α1) and lower protein level of TGF-β1, compared to WT mice. Following TAC, the influx of macrophages and CD3 T cells into LV was similar between $TLR2^{-/-}$ and WT mice, whereas levels of cyto/chemokines were lower in the heart and plasma in $TLR2^{-/-}$ mice. $TLR2^{-/-}$ bone marrow-derived cells protected against LVEF decline and fibrosis following TAC.

Conclusion: Our findings show that leukocytic TLR2 deficiency protects against LV dysfunction and fibrosis probably via a reduction in inflammatory signaling in sustained pressure overload.

Introduction

Hypertension carries one of the highest population attributable risk factors for heart failure in the general population.[1] The development of left ventricular (LV) hypertrophy, diastolic dysfunction or reduction in ejection fraction signifies the presence of early Stage B heart failure in chronically hypertensive patients, and heralds progression to symptomatic Stage C heart failure.[2] Understanding the mechanisms underlying LV hypertrophy and dysfunction in sustained pressure overload is therefore critically important for the prevention of heart failure.
Inflammation is recognized as a key mechanism for heart failure progression. Circulating inflammatory markers, such as interleukin-6 (IL-6) and tumor necrosis factor alpha (TNF-α) are elevated in patients with heart failure.[3] These markers are, among others, regulated by Toll-like receptors[4] - transmembrane receptors that recognize 'pathogen-associated molecular patterns' of exogenous microorganisms and 'danger-associated molecular patterns' of endogenous danger signals.[5,6] We previously showed that Toll-like receptor 2 (TLR2) on leukocytes determined infarct size after ischemia/reperfusion injury and subsequent adverse LV remodeling.[7,8] The role of TLR2 in LV hypertrophy and dysfunction without myocardial ischemia, however, is less clear. Renal ischemia-induced LV hypertrophy was reduced in TLR2$^{-/-}$ mice at 15 days after reperfusion, with a reduced systemic proinflammatory response.[9] In doxorubicin-induced cardiomyopathy without hypertrophy, TLR2 inhibition reduced LV ejection fraction (LVEF) decline and fibrosis at 8 weeks.[10] In contrast, angiotensin-induced LV hypertrophy was similar between TLR2$^{-/-}$ and WT at 7 days, but TLR2 deficiency in bone marrow-derived cells reduced fibrosis and inflammation.[11] Data in transverse aortic constriction (TAC) models are conflicting: TLR2 deficiency exacerbated cardiac dysfunction in spite of reduced hypertrophy and fibrosis at 14 and 28 days in one study;[12] while in another study, TLR2 deficiency increased LV hypertrophy at the same time points.[13]

In this study, we induced sustained pressure overload using TAC for a much longer period of 8 weeks in TLR2$^{-/-}$ and WT mice. We determined the temporal changes to identify the role of TLR2 in the development of LV hypertrophy, systolic/diastolic dysfunction, fibrosis and inflammation over time. We showed that TLR2 deficiency resulted in preservation of LV systolic/diastolic function and less LV fibrosis related to lower collagen formation and less cytokine/chemokine production in the TLR2$^{-/-}$ heart. These changes were mediated by leukocytic TLR2, and not cardiac TLR2, in response to sustained pressure overload.

Material & methods

ANIMALS AND ETHICS APPROVAL

C57BL/6J (wild type, WT) and TLR2$^{-/-}$ mice (Stock No: 004650) were purchased from Jackson Laboratory and were maintained under a 12/12-hour light-dark cycle (lights on at 7 AM, lights off at 7 PM) at the Comparative Medicine Animal Vivarium at National University of Singapore. The mice received standard diet and water *ad libitum*. Genotyping was routinely performed with the TLR2 specific primers as recommended by the Jackson Laboratory (Supplementary Figure S4):[14,15] WT forward 5'-ACGA GCAAGATCAACAGGAGA-3'; mutant forward 5'-GGGCC AGCTCATTCCTCCCAC-3'; common reverse (for both genotypes) 5'-CTTCCTGAATTTGTCCAGTA-CA-3'. Male WT or TLR2$^{-/-}$ mice (10-12 weeks old; 20-25 g) were used for all experiments. Animal numbers used for each experiment were indicated in the table and figure legends. All the procedures involving animal handling were performed with prior approval and in accordance with the protocols and guidelines of the Institutional Animal Care and Use Committee (IACUC), National University of Singapore.

GENERATION OF PRESSURE OVERLOAD IN MICE

Mice were anesthetized with a mixture of 0.5 mg/kg medetomidine (Pfizer Animal Health, Exton, PA, USA), 5.0 mg/kg Dormicum (Sciencelab.com, Inc., Texas, USA) and 0.05 mg/kg Fentanyl (Pfizer Pharmaceuticals Group, New York, USA) via intra-peritoneal injection, intubated and ventilated with a rodent ventilator (Harvard Apparatus). Transverse aortic constriction (TAC) was performed as previously described.[16] Briefly, the transverse aortic arch was exposed by a median sternotomy and bonded against a blunt 27-gauge needle with a 7-0 suture followed by prompt removal of the needle. Sham operated mice underwent the same procedure without aortic binding. The mice were recovered from anesthesia by subcutaneous injection of 2.5 mg/kg Atipamezole (Pfizer Animal Health, Exton, PA, USA) and 0.5 mg/kg Flumazenil (Sagent Pharmaceuticals, Illinois, USA) followed by 0.1 mg/kg Temgesic (Hospira Inc., Illinois, USA) for analgesia. Sustained pressure overload was induced with less than 10 % mortality in both WT and TLR2$^{-/-}$ mice during 8 weeks follow up. Mice with ratio of right to left carotid artery flow between 6-8 at both week 3 and week 8 post-TAC were included for this study.

BONE MARROW TRANSPLANTATION

Chimeric mice were generated as previously described[8] to study the contribution of TLR2 expression on circulating cells and parenchymal cells to pressure overload-induced heart failure. Bone marrow (BM) cells were collected from WT and TLR2$^{-/-}$ mice by flushing humeri, femurs and tibiae with RPMI-1640 medium. Recipient mice received 5x106 BM cells after receiving a single dose of 7Gy radiation from a Biobeam 8000 (137Cs source) irradiator (Gamma-Service Medical GmbH, Leipzig, Germany). Mice were allowed to recover for 6 weeks to ensure stable engraftment of the donor BM cells. Hereafter, chimerization was confirmed by flow cyto-

metry analysis of TLR2 expression on peripheral blood cells (rat-anti-mouse TLR2 monoclonal antibody conjugated with FITC, eBioscience Inc., San Diego, CA, USA) with CyAn ADP Analyzer (Beckman Coulter, Indianapolis, IN, USA). Recipient WT mice with TLR2$^{-/-}$ BM were referred to as WT/TLR2$^{-/-}$ BM mice, and recipient TLR2$^{-/-}$ mice with WT BM were called TLR2$^{-/-}$/WT BM mice.

QUANTITATIVE REAL-TIME-PCR ANALYSIS

Left ventricles were minced and grinded in liquid nitrogen. Total mRNA was extracted from mouse heart tissue with RNeasy Mini Kit (Qiagen, Hilden, Germany) following manufacturer's instruction. cDNA was synthesized with 250 ng total mRNA using QuantiTect-Reverse-Transcription Kit (Qiagen). qPCR was performed in triplicate with iTaq Universal SYBR Green Supermix (Bio-Rad, Hercules, CA, USA) and measured in CFX96 Touch™ Real-Time PCR Detection System (Bio-Rad). GAPDH was used as an internal control. The primers used for qRT-PCR included: GAPDH, 5'-GTGGAGTCATACTGGAACATGTAG-3' (forward) and 5'-AATGGTGAAGGTCGGTGTG-3' (reverse); Col1a1, 5'-TCAAGGTCTACTGCAACATGG-3' (forward) and 5'-AATCCATCGGTCATGCTCTCT-3' (reverse); Col3a1, 5'-GATGCCATTAGAGCCACGTT-3' (forward) and 5'-AAGAGTGGTGACAGAGGAGAA-3' (reverse); ANP, 5'-AGGTGGTCTAGCAGGTTCT-3' (forward) and 5'-CTTCCTCGTCTTGGCCTTT-3' (reverse); BNP, 5'-CTTTTCTCTTATCAGCTCCAGCA-3' (forward) and 5'-CTGCTTTTCCTTTATCTGTCACC-3' (reverse).

QUANTITATIVE MEASUREMENT OF CYTOKINES AND CHEMOKINES

Concentrations of cytokines and chemokines in heart tissue and plasma were measured with the Bio-Plex Pro Mouse Cytokine 23-Plex immunoassay and the Pro TGF-β 3-Plex Immunoassay (Bio-Rad) on a Bio-Plex 200 multiplex suspension array system (Bio-Rad) according to the manufacturer's protocol. Snap-frozen left ventricles were minced and proteins were isolated with Bio-Plex™ Cell Lysis Kit (Bio-Rad). 1.5 mg of protein per sample was loaded and concentrations of analytes were expressed as pg/mg protein. Undiluted plasma samples were used for multiplex assay and concentrations of analytes were expressed as pg/mL.

MMP-2 AND MMP-9 ACTIVITY ASSAYS

Total protein was extracted from mouse heart tissue with Tris-HCl buffer (50 mM, Ph 7-8) containing 0.1 % Tween 20. The tissue was homogenized in the buffer followed by centrifugation at 10,000 g for 15 min. Supernatant was collected and used for analyzing MMP-2 and MMP-9 activity with respective kits (QuickZyme Biosciences, Leiden, The Netherlands). 3 mg of protein per sample was loaded and concentrations of active MMPs were expressed as pg/mg protein.

IMMUNOHISTOCHEMISTRY

Isolated mouse left ventricles were fixed with 4 % formalin and embedded in paraffin. Tissue sections (5 µm) were stained for CD3 (T cells; rabbit anti-human CD3, clone F7.2.38, Dako, Glostrup, Denmark) and MAC-3 (macrophages; rat anti-mouse MAC-3, clone M3/84, BD Biosciences, Heidelberg, Germany). Sections were incubated with the primary antibodies at 4 °C overnight followed by incubation with goat anti-rat (Life technologies, Singapore) or goat anti-rabbit

(Abcam, Cambridge, UK) secondary antibodies conjugated to horseradish peroxidase (HRP) at room temperature for 1 hour. The NovaRED Peroxidase (HRP) Substrate kit was used to visualize the staining according to the manufacturer's instruction (Vector Laboratories, Burlingame, Ca, USA). All sections were counterstained with haematoxylin to visualize cell nuclei. Staining was imaged under a Nikon Eclipse Ti inverted microscope (Nikon Instruments Inc., Tokyo, Japan) and analyzed by NIS-Element AR Analysis software 4.5 version (Nikon Instruments Inc.). T cells and macrophages were quantitated in the whole ventricle area by automatic detection and the results were presented as percentage of total heart cells. Interstitial fibrosis was quantified by Picrosirius Red staining of collagen and expressed as percentage of total tissue area. Three whole ventricle sections were used to quantify inflammatory cells or fibrosis for each mouse heart.

CARDIAC FUNCTION ASSESSMENT

Cardiac function was assessed with a high frequency ultrasound system Vevo® 2100 (Visualsonics, Toronto, Canada) and analyzed with Vevo® 2100 software, version 1.7.0. Echocardiography was performed on mice under general anesthesia (1-1.5% isoflurane, Baxter, Singapore) at indicated time points. Body temperature was monitored with a rectal probe and maintained at 36-37 °C. Volumes and functional parameters were measured and analyzed by a blinded researcher.

STATISTICAL ANALYSIS

Comparisons between groups in time were performed using a General Linear model (GLM) for multivariate analysis or GLM for repeated measurements with LSD post hoc testing. Mann Whitney U test was used to determine differences between groups at individual timepoints. Related-Samples Wilcoxon Signed Rank test was used to determine difference between time points. Values were reported as mean±SEM. p-value≤0.05 was considered statistically significant. Data were analyzed with SPSS software (IBM® SPSS® Statistics version 22.0).

DATA AVAILABILITY

All data generated or analysed during this study are included in this published article and its Supplementary Information files.

Results

TLR2 DEFICIENCY PRESERVED CARDIAC FUNCTION IN HYPERTENSIVE LV HYPERTROPHY

Sustained pressure overload was induced by TAC with less than 10 % mortality in both WT and TLR2$^{-/-}$ mice during 8 weeks follow up. LV weights increased similarly following TAC in WT and TLR2$^{-/-}$ mice (Figure 1A) with all mice having a right/left carotid velocity ratio between 6 and 8. Also, mRNA levels of atrial natriuretic peptide (ANP) and brain natriuretic peptide (BNP), two hypertrophic markers, were increased similarly in both WT and TLR2$^{-/-}$ mice (Supplementary Figure S1). Lung weight did not differ between WT and TLR2$^{-/-}$ mice (Figure 1B). For cardiac function, LVEF was significantly lower in WT mice compared to TLR2$^{-/-}$ mice during 8 weeks follow-up after TAC (Figure 1C, $p<0.0001$). Furthermore, E/A ratio was reduced in WT mice 7 days after TAC ($p<0.001$ compared to baseline, Figure 1D), but not in TLR2$^{-/-}$ mice, and was lower in the WT group compared to the TLR2$^{-/-}$ group during 8 weeks follow-up after TAC ($p<0.0001$). No significant change in LVEF or E/A ratio was observed in the sham-operated animals (Figure 1C and D).

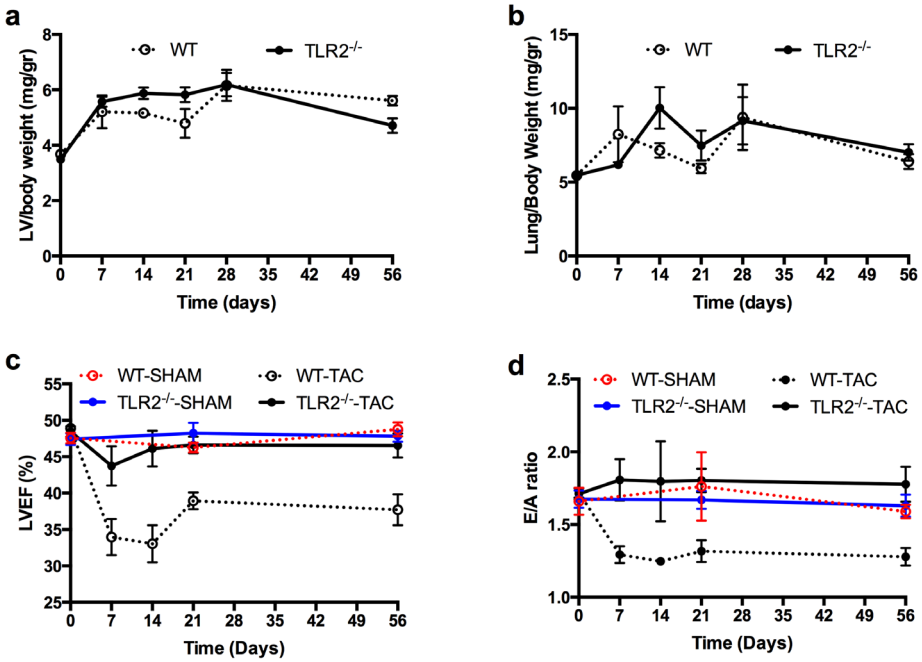

Figure 1. Left ventricle weight, lung weight and cardiac function after sustained pressure overload. **A,B)** Mouse LV and lungs were extracted before TAC (baseline, n=10-12 per genotype), or 7 days (n=6-7 per genotype), 14 days (n=8-10 per genotype), 21 days (n=6 per genotype), 28 days (n=6-9 per genotype) and 56 days (n=21-26 per genotype) after TAC from WT and TLR2$^{-/-}$ mice. Wet LV weight and lung weight were corrected for body weight. No significant differences in LV or lung weight between WT and TLR2$^{-/-}$ mice were detected. **C,D)** LVEF as an indicator for cardiac systolic function and E/A ratio as an indicator for cardiac diastolic function were determined with echocardiography at indicated timepoints after TAC. n=14 for WT-SHAM, n=12 for TLR2$^{-/-}$-SHAM, n=26 for WT-TAC and n=22 for TLR2$^{-/-}$-TAC. GLM model analysis was performed, p<0.0001 between WT-TAC and TLR2$^{-/-}$-TAC.

TLR2 DEFICIENCY REDUCED INTERSTITIAL FIBROSIS IN THE HEART

Myocardial fibrosis is an important hallmark of maladaptive hypertrophy induced by pressure overload[17] and is associated with myocardial stiffness and development of heart failure in hypertensive rats.[18] Having established that TLR2 deficiency protects against reduction of EF and E/A ratio following TAC, we investigated if interstitial fibrosis was lower in TLR2$^{-/-}$ TAC hearts in accordance with a better cardiac function. As shown in figure 2A, severe interstitial fibrosis was observed in WT hearts after 8 weeks' TAC, but not in TLR2$^{-/-}$ TAC hearts or sham hearts. Compared to baseline, cardiac fibrosis increased 7 days after TAC in both WT (p<0.01) and TLR2$^{-/-}$ (p<0.05) mice. Comparing the WT-TAC with the TLR2$^{-/-}$-TAC group during 8 weeks follow-up (Figure 2B) showed that the TLR2$^{-/-}$ TAC group had less interstitial fibrosis (p<0.001). Cardiac fibrosis was significantly lower in TLR2$^{-/-}$ mice compared to WT mice at 4 weeks (p=0.002) and 8 weeks (p=0.000). To investigate if the reduced fibrosis in TLR2$^{-/-}$ mice was due to reduced collagen production or increased collagen breakdown, mRNA levels of the most abundant cardiac Col1α1 and Col3α1 were determined as well as activity of the most abundant Matrix Metalloproteases (MMPs) -2 and MMP-9. Messenger RNA levels of Col1α1 and Col3α1 were significantly lower in TLR2$^{-/-}$ hearts compared to WT hearts after TAC (Figure 3A and B, p<0.05). MMP-2 and -9 activity levels, however, did not differ between TLR2$^{-/-}$ and WT mice after TAC (Figure 3C, Supplementary Figure S2).

Transforming growth factor beta (TGF-β) is an important modulator of cardiac fibrosis with all three TGF-β isoforms (TGF-β1, TGF-β2 and TGF-β3) expressed in mammalian hearts.[19] Measurement of protein levels of TGF-β1, TGF-β2 and TGF-β3 in the heart after TAC showed that TGF-β1 levels in the heart were higher in WT mice compared to TLR2$^{-/-}$ mice at 2 weeks (p=0.006) and at 3 weeks (p=0.041) after TAC (Figure 3D). Levels of TGF-β2 and TGF-β3 (Supplementary Figure S2) were not different between WT and TLR2$^{-/-}$ mice after TAC. These higher TGF-β1 levels at 2 and 3 weeks in WT hearts preceded the increase in interstitial fibrosis in WT hearts at 4 and 8 weeks after TAC (Figure 2B).

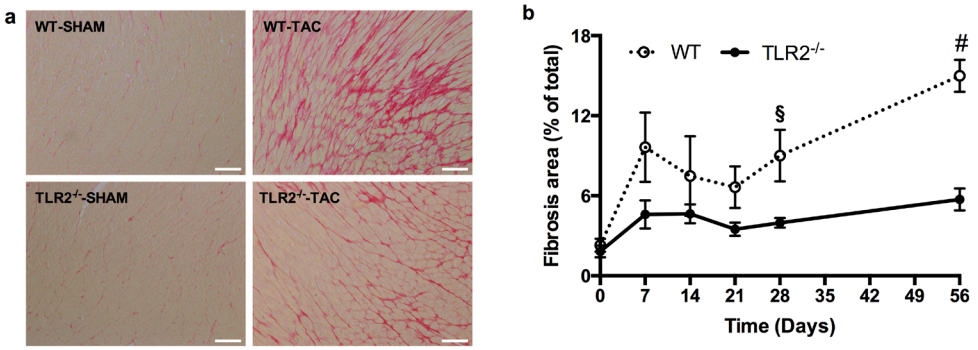

Figure 2. Interstitial fibrosis in the heart. **A)** Representative images of heart sections stained with Picrosirius Red to show collagen deposition. Scale bars=100 µm. **B)** Quantification of Picrosirius Red stained area (fibrosis area) as % of the whole LV area at indicated timepoints after TAC. The numbers of mouse hearts extracted at each timepoint for each genotype of mice were the same as described in Figure 1. §p<0.01, #p<0.001.

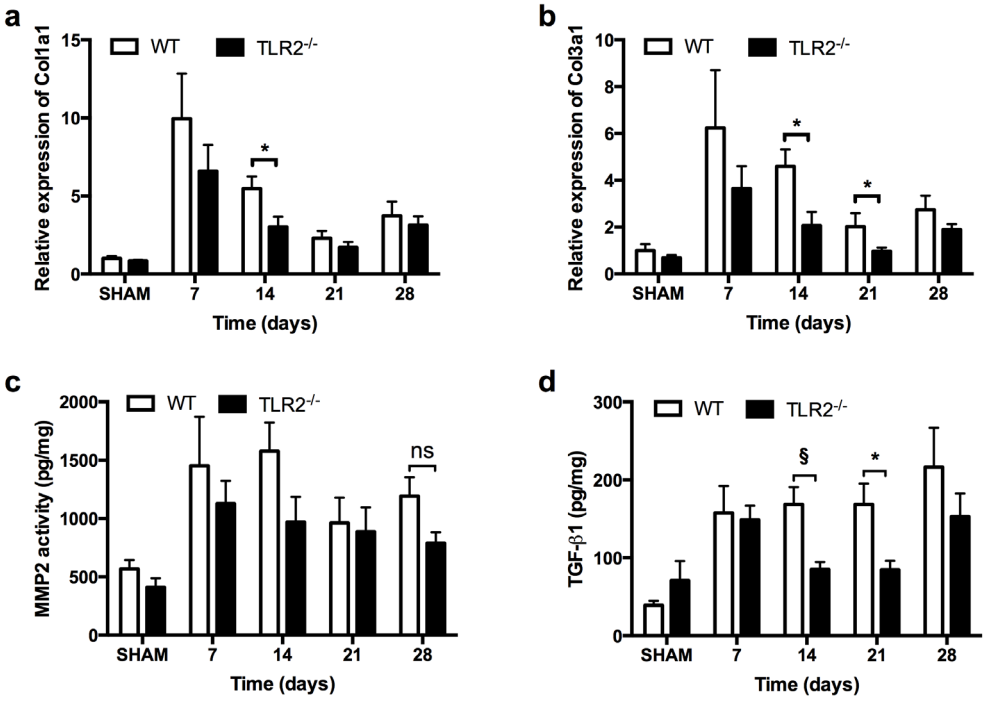

Figure 3. Collagen synthesis and breakdown in the heart. **A,B)** Relative expression of Col1α1 and Col3α1 in the heart were quantified by qRT-PCR and normalized to WT-SHAM. GAPDH was used as an internal control. **C)** Activity of MMP2 in heart tissue was determined at indicated timepoints. **D)** Protein level of TGF-β1 in heart tissue was determined by multiplex assay at indicated timepoints. Bars represent mean±SEM. Mouse hearts were extracted at indicated timepoints, n=6-8 mice per genotype per timepoint. Mann Whitney U test was performed to determine the difference between groups at individual timepoints; *p<0.05, §p<0.01, ns indicating not significant.

TLR2 DEFICIENCY REDUCED LV INFLAMMATORY CYTOKINE/CHEMOKINE LEVELS, BUT NOT INFLAMMATORY CELL INFLUX, FOLLOWING TAC

TAC induced the recruitment of inflammatory cells such as T cells and macrophages in the heart (Figure 4).[20,21] Immunohistochemistry showed that a large number of CD3 positive T cells (Figure 4A and B) and MAC3 positive macrophages (Figure 4C and D) were recruited to the hearts in both WT and TLR2$^{-/-}$ mice after TAC compared to the respective sham-operated animals. However, no differences in the increase of T cells or macrophages were observed between WT and TLR2$^{-/-}$ mouse groups (Figure 4B and D). To confirm these data, we also isolated cells from heart tissue at 1 week and 3 weeks after TAC for flow cytometric analysis (FACS). FACS showed that similar amount of inflammatory cells were recruited to the hearts of WT and TLR2$^{-/-}$ mice in response to pressure overload (Supplementary Figure S3).

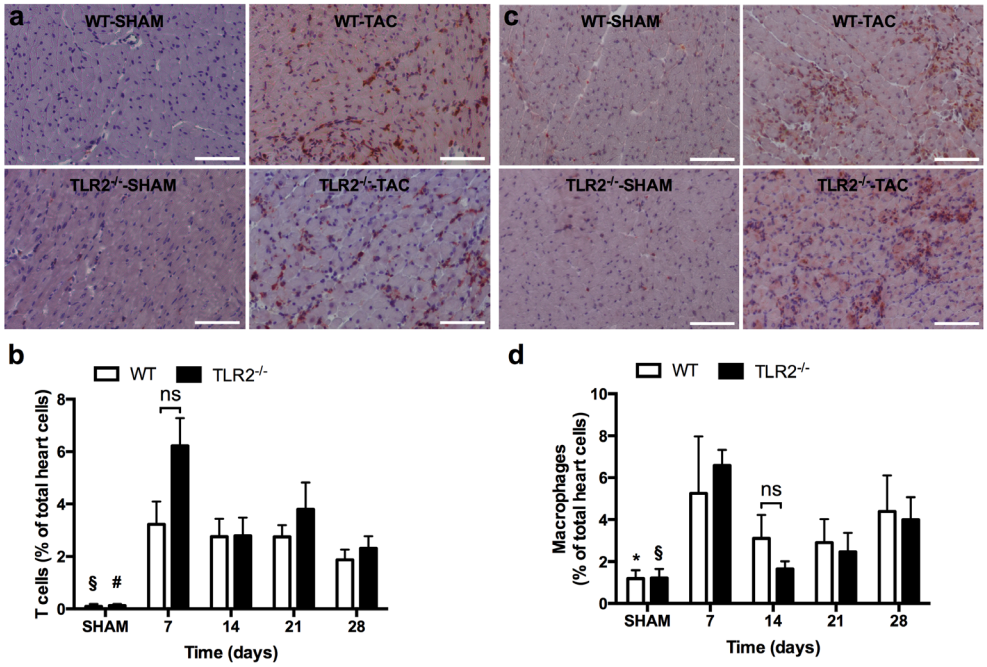

Figure 4. Influx of T cells and macrophages to the heart in response to pressure overload. LV sections were stained and quantified for CD3 positive T cells **(A,B)** and MAC3 positive macrophages **(C,D)** by immunohistochemistry. Representative sections stained for T cells (A; in brown) and macrophages (C; in brown) and the cell nuclei were counterstained in blue. Scale bars=100 µm. **(B,D)** Quantification of T cells and macrophages at indicated timepoints after TAC. Bars represent mean±SEM. Mouse hearts were extracted at indicated timepoints, n= 6-10 mice per genotype per timepoint. Mann Whitney U test was performed to determine the difference between groups; *p<0.05, §p<0.01 and #p<0.001 indicate the differences between SHAM and 7 days after TAC for WT and TLR2$^{-/-}$ mice, respectively; ns indicates not significant.

Cytokine/chemokine levels were determined in heart tissue and plasma (Table 1). Lower levels of IL-1α, IL-2, IFN-γ, MCP-1 and MIP-1α protein were found in TLR2$^{-/-}$ hearts after TAC but were not detectable in the plasma. Lower levels of plasma TNFα, IL-6, KC, Rantes, IL12p40, IL12p70, IL3, and G-CSF were found in TLR2$^{-/-}$ mice compared to WT mice after TAC. The level of anti-inflammatory factor MIP-1β was higher in TLR2$^{-/-}$ hearts.[22]

TLR2 DEFICIENCY ON BONE MARROW-DERIVED CELLS MEDIATED THE CARDIAC PROTECTIVE EFFECTS FOLLOWING TAC

Bone-marrow (BM) transplantation was performed to determine if preservation of cardiac function was dependent on TLR2 on BM-derived cells. Four groups of chimaeric mice were created: recipient WT mice with TLR2$^{-/-}$ BM (WT/TLR2$^{-/-}$ BM mice), recipient WT mice with WT BM (WT/WT BM mice), recipient TLR2$^{-/-}$ mice with TLR2$^{-/-}$ BM (TLR2$^{-/-}$/TLR2$^{-/-}$ BM mice) and recipient TLR2$^{-/-}$ mice with WT BM (TLR2$^{-/-}$/WT BM mice). BM chimaerization was confirmed by flow cytometry 6 weeks after transplantation (<5 % TLR2$^{+/+}$ leukocytes in WT/TLR2$^{-/-}$ BM mice). As shown in figure 5A, LVEF was different among the four groups of BM chimaeric mice (p<0.0001). *Post hoc* ana-

Table 1. Level of cytokines and chemokines in the heart and plasma after TAC. Mouse hearts and plasma were obtained at indicated timepoints for measurement of protein levels with multiplex assays. *p<0.05, §p<0.01, #p<0.001, non-parametric test compared to WT mice at respective timepoints. n= 6-8 per timepoint per genotype of mice. MCP-1, monocyte chemoattractant protein-1; IL-1α, interleukin 1 alpha; IL-2, interleukin 2; IL-3, interleukin 3; IL-6, interleukin 6; IFN-Y, interferon gamma; MIP-1α, macrophage inflammatory protein 1 alpha; MIP-1β, macrophage inflammatory protein 1 beta; IL-12p40, interleukin-12 p40; IL-12p70, interleukin-12 p70; G-CSF, granulocyte-colony stimulating factor; KC, keratinocyte chemoattractant; RANTES, Regulated on Activation, Normal T Cell Expressed and Secreted, also known as chemokine (C-C motif) ligand 5 (CCL5); TNF-α, tumor necrosis factor-alpha.

	WT					TLR2-/-				
Cytokines and chemokines in the heart (pg/mg)										
Protein	**Baseline**	**Day 7**	**Day 14**	**Day 21**	**Day 28**	**Baseline**	**Day 7**	**Day 14**	**Day 21**	**Day 28**
MCP-1	27±7	183±127	37±2	39±4	41±7	20±4	56±7	29±5	25±2§	26±2*
IL-1α	18±5	22±3	25±1	36±1	36±7	24±2	17±3	20±4	18±3*	27±6
IL-2	37±14	32±4	39±3	64±8	42±8	27±4	32±8	22±5*	26±6§	16±4*
IFN-Y	54±17	26±7	51±3	70±13	78±33	54±17	23±5	45±13	28±5*	33±7
MIP-1α	5±1	50±38	9±1	8±2	10±2	3±1	11±2	14±10	4±0	5±0*
MIP-1β	5±1	18±10	6±1	6±1	5±0	6±1	18±3	13±5	13±3*	15±3§
Cytokines and chemokines in the plasma (pg/mL)										
Protein	**Baseline**	**Day 7**	**Day 14**	**Day 21**	**Day 28**	**Baseline**	**Day 7**	**Day 14**	**Day 21**	**Day 28**
IL-3	29±2	29±2	30±5	36±1	27±2	28±4	23±3	16±2	24±3§	21±3
IL-12p40	97±7	124±11	122±12	110±10	100±15	113±10	87±6*	79±11*	99±8	98±7
IL-12p70	204±20	195±38	195±38	246±13	188±17	189±27	149±20	101±15*	153±19§	135±20
G-CSF	45±4	46±4	42±4	59±7	38±2	41±9	30±3*	22±3*	31±3#	39±7
KC	27±3	41±10	33±4	38±3	27±3	25±5	34±5	18±4*	26±1§	34±6
MIP-1β	38±3	38±4	34±5	37±3	30±3	39±3	42±4	33±4	41±6	29±4
RANTES	6±1	7±0	7±1	7±0	6±1	5±1	4±0*	3±1*	4±0§	5±0
TNF-α	427±24	395±21	393±52	451±27	333±25	394±29	422±53	291±36*	457±67	267±46
IL-6	19±10	11±1	8±1	12±1	8±1	14±3	9±1	7±1	8±1*	8±1

lysis showed that LVEF in WT/WT BM mice and TLR2$^{-/-}$/WT BM mice was lower than that in WT/TLR2$^{-/-}$ BM mice and TLR2$^{-/-}$/TLR2$^{-/-}$ BM mice (p=0.002). LVEF in WT/TLR2$^{-/-}$ BM mice was higher than that in TLR2$^{-/-}$/WT BM mice at all the timepoints after TAC (p<0.05). No differences in LVEF were found between WT/WT BM mice and TLR2$^{-/-}$/WT BM mice, neither between WT/TLR2$^{-/-}$ BM mice and TLR2$^{-/-}$/TLR2$^{-/-}$ BM mice. In contrast to LVEF, no significant difference was detected in E/A ratio among the four types of BM chimaeric mice (p=0.246, Figure 5B). To investigate if radiation differentially affected E/A ratio in TLR2$^{-/-}$ and WT mice, E/A ratio at baseline (before TAC) in TLR2$^{-/-}$ mice that were not radiated was compared to that in radiated TLR2$^{-/-}$ mice received

TLR2$^{-/-}$ BM (TLR2$^{-/-}$/TLR2$^{-/-}$ BM mice) 6 weeks after BM transplantation. This was also done for WT mice. The results revealed no difference in E/A ratio in TLR2$^{-/-}$ mice (1.71±0.04 for TLR2$^{-/-}$ mice before radiation *versus* 1.61±0.09 for TLR2$^{-/-}$/TLR2$^{-/-}$ BM mice, p=0.476). The E/A ratio in WT mice, however, did differ before and after radiation (1.71±0.03 for WT mice before radiation *versus* 1.52±0.04 for WT/WT BM mice, p=0.006).

To examine whether cardiac fibrosis was attributed to TLR2 on the BM-derived leukocytes, collagen deposition in LV tissue from BM chimaeric mice was analyzed with Picrosirius Red staining. As shown in figure 5C, interstitial fibrosis at 8 weeks after TAC was different among the four types of BM chimaeric mice (p=0.003). Among the groups, fibrosis was lower in WT/TLR2$^{-/-}$ BM mice compared to TLR2$^{-/-}$/WT BM mice (p=0.001) and WT/WT BM mice (p=0.021), but similar compared to TLR2$^{-/-}$/ TLR2$^{-/-}$ mice (p=0.841). LV hypertrophy at 8 weeks after TAC, as determined by LV wet weight corrected for body weight, did not differ among the 4 types of BM chimaeric mice (Figure 5D, p=0.895).

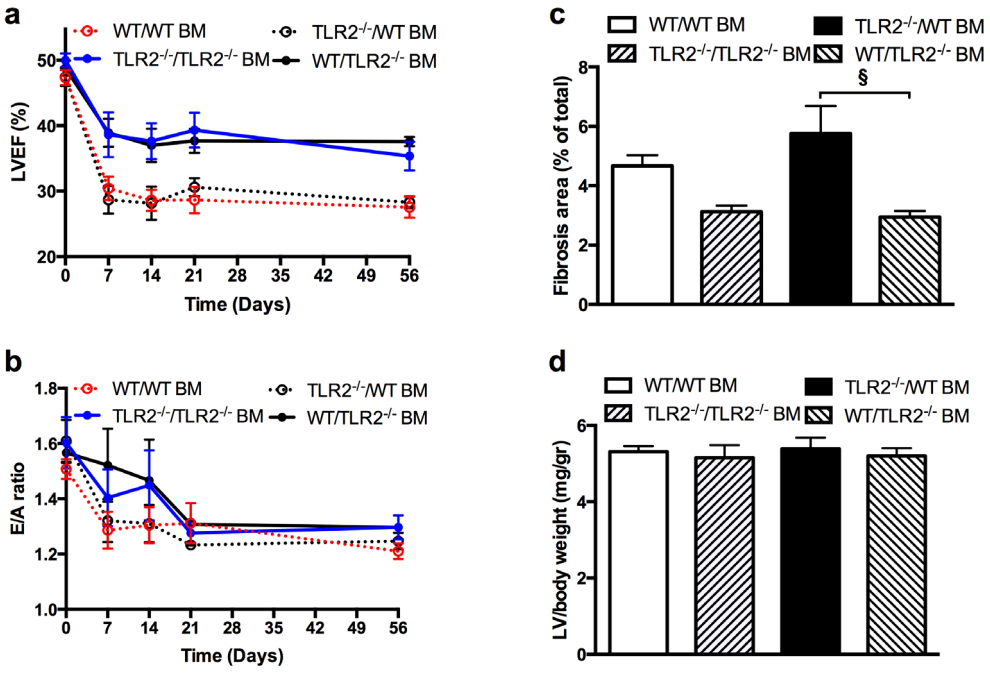

Figure 5. Cardiac function, fibrosis and hypertrophy after TAC in bone marrow chimaeric mice. **A)** LVEF measured by echocardiography at 0 day (baseline), 7 days, 14 days, 21 days, and 56 days after TAC in 4 types of BM chimaeric mice consisting of WT mice with TLR2$^{-/-}$ BM (WT/TLR2$^{-/-}$ BM), TLR2$^{-/-}$ mice with WT BM (TLR2$^{-/-}$/WT BM), WT with WT BM (WT/WT BM) and TLR2 with TLR2 BM (TLR2$^{-/-}$/TLR2$^{-/-}$ BM) showing a large difference between the 4 types of BM transplantation (p<0.001). **B)** E/A ratio measured by echocardiography at 0 day, 7 days, 14 days, 21 days, and 56 days after TAC in the 4 types of BM chimaeric mice. **C)** Fibrotic area as % of LV area at 8 weeks after TAC using Picrosirius Red staining in the 4 types of BM chimaeric mice. Fibrotic area was different between the 4 types of BM transplantation analyzed with Kruskal-Wallis test (p=0.001). Difference in fibrotic area between WT/TLR2$^{-/-}$ BM and TLR2$^{-/-}$/WT BM was determined with Mann-Whitney U test; §p<0.01. D) Hypertrophy as measured by wet LV weight corrected for body weight in mg/g at 8 weeks after TAC in the 4 types of BM chimaeric mice. n= 6-10 per type of BM chimaeric mice.

Discussion

The role of TLR2 in cardiac remodeling and dysfunction following ischemic cardiac injuries has been established;[7,8,23,24] however, its role in the setting of sustained pressure overload remains unclear. We now provide a longitudinal study up to 8 weeks after TAC focusing on the temporal changes in cardiac function, hypertrophy, fibrosis and inflammation. Our data demonstrate that TLR2 deficiency preserves both cardiac systolic and diastolic function via reduction of fibrosis and inflammation but not hypertrophy induced by pressure overload. The effects of TLR2 on pressure overload induced cardiac dysfunction are attributed to TLR2 on the BM-derived leukocytes.

Cardiac hypertrophy is a major (mal-)adaptive response to pressure overload as well as an important risk factor for heart failure in hypertension.[25] The role of TLR2 in cardiac hypertrophy is however conflicting in the literature. Higashikuni *et al.* showed a lower heart weight in TLR2$^{-/-}$ mice measured at 14 days and 28 days after TAC.[12] In contrast, another study found a higher heart weight in TLR2$^{-/-}$ mice compared to WT at 14 and 28 days, but no difference was detected in left ventricle weight between WT and TLR2$^{-/-}$ mice.[13] We found in this study that hypertrophy, as evidenced by the increase in LV weight and mRNA levels of two hypertrophic markers ANP and BNP, occurred in both WT and TLR2$^{-/-}$ mice to a similar extent from week 1 up to week 8 in response to sustained pressure overload (Figure 1A and Supplementary Figure S1), showing that TLR2 is not involved in hypertrophy. The discrepancies among the three studies may be explained by a few reasons. Higashikuni *et al.*[12] used a milder 25 gauge needle that is in line with no difference in heart weight between TLR2$^{-/-}$ and sham at 28 days. We and Bualeong *et al.*[13] achieved more severe aortic constriction using a 27 gauge needle, and both studies did not find a difference in left ventricular weight suggesting that the role of TLR2 probably depends on the severity of pressure overload. Furthermore, both studies found that lung weight after TAC did not differ between TLR2$^{-/-}$ and WT mice. Besides clear differences in procedure, the role of the mouse origin is unclear[13] and in all these studies mice are on a C57Bl/6 background.

Severe pressure overload leads to cardiac dysfunction as indicated by decreased LVEF.[16,26-28] In line with this, we observed a quick and strong reduction of LVEF at 7 days following severe TAC with 27 gauge needle in WT mice (p=0.003) (Figure 1C). LVEF was higher in TLR2$^{-/-}$ mice compared to WT mice from 1 week up to 8 weeks after TAC. This is in contrast with Higashikuni *et al.*,[12] who found that LVEF in TLR2$^{-/-}$ was lower than WT at 14 and 28 days after TAC. In this earlier study, however, LVEF in WT mice at 14 days after TAC was not different from sham, in contrast to a decrease in LVEF at the same time point after TAC in C56Bl/6 mice described in other studies.[16,26-28] Once again, this discrepancy may be due to differences in the severity of the imposed pressure overload using the 25 gauge versus 27 gauge needles.

Left ventricular diastolic dysfunction occurs in hypertensive heart disease in both human and animals.[18,29] The mitral E/A ratio, a parameter of LV diastolic function, has not previously been measured in TLR2$^{-/-}$ mice. We showed for the first time that after TAC, mitral E/A ratio was preserved in association with reduced LV fibrosis in TLR2$^{-/-}$ hearts. Together with higher fibrosis in WT hearts, Col1α1 and Col3α1 mRNA levels as well as TGFβ1 protein levels involved in collagen synthesis were higher in WT hearts, while MMP levels did not differ. TGFβ1 protein levels were higher in WT just before fibrosis increased. Collectively, these findings suggest that reduced LV fibrosis in TLR2 deficient hearts following TAC was related to decreased collagen synthesis rather than increased collagen breakdown. This is in agreement with the lower mRNA levels of Col3α1 and TGFβ1 in TLR2$^{-/-}$ hearts after TAC described in an earlier study.[12] Lower interstitial fibrosis in TLR2$^{-/-}$ hearts has also been described in doxorubicin-induced cardiomyopathy[10] and in response to angiotensin perfusion.[11]

In the pressure-overloaded heart, interstitial fibrosis causes cardiac dysfunction and inflammation is believed one of the main stimulators of fibrosis.[17] In line with this, we observed a large number of T cells and macrophages recruited to the heart after TAC as previously reported[20,21] as well as an elevation of cytokines/chemokines in both plasma and heart tissue in response to pressure overload, preceding cardiac fibrosis (Figures 2, 4 and Table 1). In contrast to a reduced influx of inflammatory cells after myocardial ischemia reperfusion injury,[8] TLR2 deficiency did not reduce inflammatory cell influx into the pressure-overloaded heart compared to WT mice. TLR2 deficiency, however, reduced cytokines/chemokines levels in both plasma and heart tissue after TAC. This suggests that cardiac inflammation in pressure overload is regulated by TLR2 via production of cyto/chemokines rather than recruitment of inflammatory cells to the heart. As a result, the reduced production of cytokines/chemokines in TLR2$^{-/-}$ mice may subsequently lead to less activation of profibrotic pathways in myofibroblasts and therefore decelerate fibrosis.

Our BM transplantation experiments showed that it was TLR2 deficiency on BM-derived cells rather than the parenchymal cells (such as cardiomyocytes and endothelial cells) responsible for the preservation of LVEF and reduction of fibrosis in TLR2$^{-/-}$ mice subjected to sustained pressure overload. This is in agreement with a previous study showing that after ischemia/reperfusion the infarct size was determined by TLR2 on BM-derived cells.[8] Adverse remodeling after myocardial infarction has also been shown to be dependent on bone marrow TLR430 or NFkB-p50.31 In contrast to our findings, Higashikuni *et al.*[12] concluded that lack of TLR2 on the parenchymal heart cells, but not the BM-derived cells was involved in regulation of cardiac function. Reasons for this discrepancy are unclear, but may involve differences in methodology or mouse strain.

Finally, our BM transplantation experiments revealed the surprising finding that TLR2 deficiency might protect hearts from radiation-induced diastolic dysfunction. Radiation is known to induce fibrosis and diastolic dysfunction in the heart.[32] We therefore hypothesized that TLR2$^{-/-}$ mice may have reduced radiation-induced fibrosis and thereby preserved diastolic dysfunction. Indeed we found that following radiation alone without TAC, WT mice had lower E/A ratio whereas TLR2$^{-/-}$ mice had preserved E/A ratio. This differential response to radiation in TLR2$^{-/-}$ versus WT mice will confound the interpretation of E/A ratios following BM transplantation and TAC. Still, the implication of this unexpected finding for the role of TLR2 in radiation-induced injury deserves further study.

In summary, our data show that TLR2 on BM-derived leukocytes is involved in the response of the heart to sustained pressure overload. TLR2 deficiency does not affect hypertrophy but reduces fibrosis and protects from cardiac systolic and diastolic dysfunction. Targeting leukocytic TLR2 may provide a novel therapeutic target to prevent cardiac dysfunction and heart failure due to chronic hypertension.

References

1. Kannel WB, Castelli WP, McNamara PM, McKee PA, Feinleib M. Role of blood pressure in the development of congestive heart failure. The Framingham study. N Engl J Med.1972;287(16):781-787.

2. Yancy CW, Jessup M, Bozkurt B, et al. 2013 ACCF/AHA guideline for the management of heart failure: a report of the American College of Cardiology Foundation/American Heart Association Task Force on Practice Guidelines. J Am Coll Cardiol.2013;62(16):e147-239.

3. Ter Maaten JM, Damman K, Verhaar MC, et al. Connecting heart failure with preserved ejection fraction and renal dysfunction: the role of endothelial dysfunction and inflammation. Eur J Heart Fail.2016;18(6):588-598.

4. Brikos C, O'Neill LA. Signalling of toll-like receptors. Handb Exp Pharmacol.2008;10.1007/978-3-540-72167-3_2(183):21-50.

5. Frantz S, Monaco C, Arslan F. Danger signals in cardiovascular disease. Mediators Inflamm.2014;2014:395278.

6. Matzinger P. The danger model: a renewed sense of self. Science.2002;296(5566):301-305.

7. Arslan F, Houtgraaf JH, Keogh B, et al. Treatment with OPN-305, a humanized anti-Toll-Like receptor-2 antibody, reduces myocardial ischemia/reperfusion injury in pigs. Circ Cardiovasc Interv.2012;5(2):279-287.

8. Arslan F, Smeets MB, O'Neill LA, et al. Myocardial ischemia/reperfusion injury is mediated by leukocytic toll-like receptor-2 and reduced by systemic administration of a novel anti-toll-like receptor-2 antibody. Circulation.2010;121(1):80-90.

9. Trentin-Sonoda M, da Silva RC, Kmit FV, et al. Knockout of Toll-Like Receptors 2 and 4 Prevents Renal Ischemia-Reperfusion-Induced Cardiac Hypertrophy in Mice. PLoS One.2015;10(10):e0139350.

10. Ma Y, Zhang X, Bao H, et al. Toll-like receptor (TLR) 2 and TLR4 differentially regulate doxorubicin induced cardiomyopathy in mice. PLoS One.2012;7(7):e40763.

11. Wang L, Li YL, Zhang CC, et al. Inhibition of Toll-like receptor 2 reduces cardiac fibrosis by attenuating macrophage-mediated inflammation. Cardiovasc Res.2014;101(3):383-392.

12. Higashikuni Y, Tanaka K, Kato M, et al. Toll-like receptor-2 mediates adaptive cardiac hypertrophy in response to pressure overload through interleukin-1beta upregulation via nuclear factor kappaB activation. J Am Heart Assoc.2013;2(6):e000267.

13. Bualeong T, Kebir S, Hof D, et al. Tlr2 deficiency does not limit the development of left ventricular hypertrophy in a model of transverse aortic constriction induced pressure overload. J Negat Results Biomed.2016;15:9.

14. Okun E, Griffioen KJ, Son TG, et al. TLR2 activation inhibits embryonic neural progenitor cell proliferation. J Neurochem.2010;114(2):462-474.

15. Wooten RM, Ma Y, Yoder RA, et al. Toll-like receptor 2 is required for innate, but not acquired, host defense to Borrelia burgdorferi. J Immunol.2002;168(1):348-355.

16. Hu Z, Wang JW, Yu D, et al. Aberrant Splicing Promotes Proteasomal Degradation of L-type CaV1.2 Calcium Channels by Competitive Binding for CaVbeta Subunits in Cardiac Hypertrophy. Sci Rep.2016;6:35247.

17. Creemers EE, Pinto YM. Molecular mechanisms that control interstitial fibrosis in the pressure-overloaded heart. Cardiovasc Res.2011;89(2):265-272.

18. Conrad CH, Brooks WW, Hayes JA, Sen S, Robinson KG, Bing OH. Myocardial fibrosis and stiffness with hypertrophy and heart failure in the spontaneously hypertensive rat. Circulation.1995;91(1):161-170.

19. Li JM, Brooks G. Differential protein expression and subcellular distribution of TGFbeta1, beta2 and beta3 in cardiomyocytes during pressure overload-induced hypertrophy. J Mol Cell Cardiol.1997;29(8):2213-2224.

20. Nevers T, Salvador AM, Grodecki-Pena A, et al. Left Ventricular T-Cell Recruitment Contributes to the Pathogenesis of Heart Failure. Circ Heart Fail.2015;8(4):776-787.

21. Laroumanie F, Douin-Echinard V, Pozzo J, et al. CD4+ T cells promote the transition from hypertrophy to heart failure during chronic pressure overload. Circulation.2014;129(21):2111-2124.

22. Fahey TJ, 3rd, Tracey KJ, Tekamp-Olson P, et al. Macrophage inflammatory protein 1 modulates macrophage function. J Immunol.1992;148(9):2764-2769.

23. Shishido T, Nozaki N, Yamaguchi S, et al. Toll-like receptor-2 modulates ventricular remodeling after myocardial infarction. Circulation.2003;108(23):2905-2910.

24. Selejan S, Poss J, Walter F, et al. Ischaemia-induced up-regulation of Toll-like receptor 2 in circulating monocytes in cardiogenic shock. Eur Heart J.2012;33(9):1085-1094.

25. Frey N, Olson EN. Cardiac hypertrophy: the good, the bad, and the ugly. Annu Rev Physiol.2003;65:45-79.

26. Mohammed SF, Storlie JR, Oehler EA, et al. Variable phenotype in murine transverse aortic constriction. Cardiovasc Pathol.2012;21(3):188-198.

27. Shirakabe A, Zhai P, Ikeda Y, et al. Drp1-Dependent Mitochondrial Autophagy Plays a Protective Role Against Pressure Overload-Induced Mitochondrial Dysfunction and Heart Failure. Circulation.2016;133(13):1249-1263.

28. Gao C, Ren S, Lee JH, et al. RBFox1-mediated RNA splicing regulates cardiac hypertrophy and heart failure. J Clin Invest.2016;126(1):195-206.

29. Weber KT. Are myocardial fibrosis and diastolic dysfunction reversible in hypertensive heart disease? Congest Heart Fail.2005;11(6):322-324; quiz 325.

30. Timmers L, Sluijter JP, van Keulen JK, et al. Toll-like receptor 4 mediates maladaptive left ventricular remodeling and impairs cardiac function after myocardial infarction. Circ Res.2008;102(2):257-264.

31. Timmers L, van Keulen JK, Hoefer IE, et al. Targeted deletion of nuclear factor kappaB p50 enhances cardiac remodeling and dysfunction following myocardial infarction. Circ Res.2009;104(5):699-706.

32. Darby SC, Cutter DJ, Boerma M, et al. Radiation-related heart disease: current knowledge and future prospects. Int J Radiat Oncol Biol Phys.2010;76(3):656-665.

Supplementary material

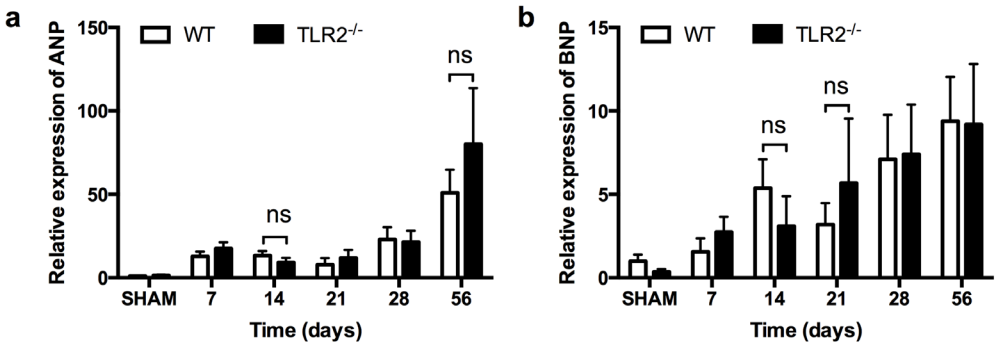

Supplementary Figure S1. Expression of cardiac hypertrophic markers. mRNA levels of atrial natriuretic peptide (ANP) and brain natriuretic peptide (BNP) in the heart were determined at indicated timepoints after transverse aortic constriction (TAC). Relative expression of ANP (**A)** and BNP **(B)** was quantified by qRT-PCR and normalized to wild type (WT) SHAM animals. GAPDH was used as an internal control. Bars represent mean±SEM. n= 5-8 mice per group per timepoint. Mann Whitney U test was performed to determine the difference between groups at individual timepoints; ns, not significant.

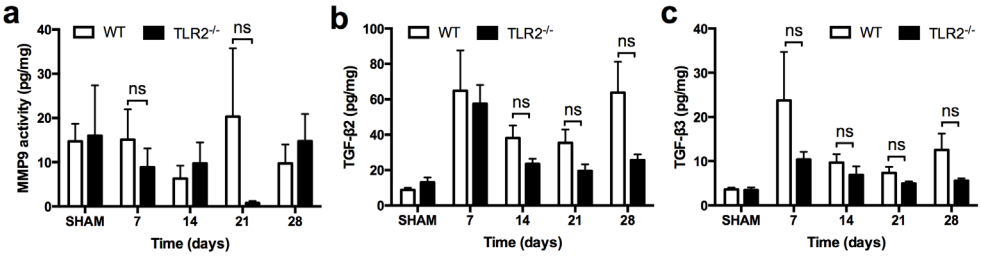

Supplementary Figure S2. MMP9 activity and TGF-β2 protein levels in heart tissue. **A)** Activity of MMP9 was determined in mouse hearts extracted from sham-operated mice (SHAM) or mice subjected to TAC at 7 days, 14 days, 21 days and 28 days. **B-C)** Protein levels of TGF-β2 in heart tissue were determined by multiplex assay at indicated timepoints. Bars represent mean±SEM. n= 6-8 mice per genotype per timepoint. Mann Whitney U test was performed to determine the difference between groups at individual timepoints; ns, not significant.

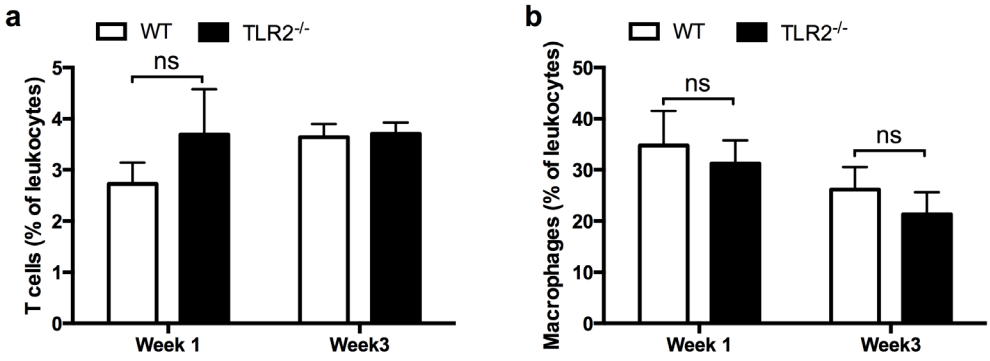

Supplementary Figure S3. Recruitment of inflammatory cells to the heart after sustained pressure overload. Extracted left ventricles were minced into small pieces (around 1 mm^2) and digested at 37°C for 20 min under gentle agitation in Dulbecco's Phosphate Buffered Saline conatining 1000 U/ml DNase I (Sigma-Aldrich), 2.6 U/ml Liberase TL (Roche Diagnostics) and 10 mM HEPES. The dissociated cells were filtered with a 40 µm cell strainer (BD Biosciences). For flow cytometry, cells were resuspended and stained with PE-CF594 rat anti-mouse CD45 (BD Biosciences) for leukocytes, Alexa Fluor® 700 rat anti-mouse CD4 (eBiosciences) for T cells, PE-Cyanine7 rat anti-mouse F4/80 (eBiosciences) for macrophages. Bars represent mean±SEM. n= 4 per group for mice sacrificed at 1 week after TAC; n=5 for WT and n=4 for $TLR2^{-/-}$ mice sacrificed at 3 weeks after TAC; ns, not significant, two-way ANOVA with Bonferroni post hoc test.

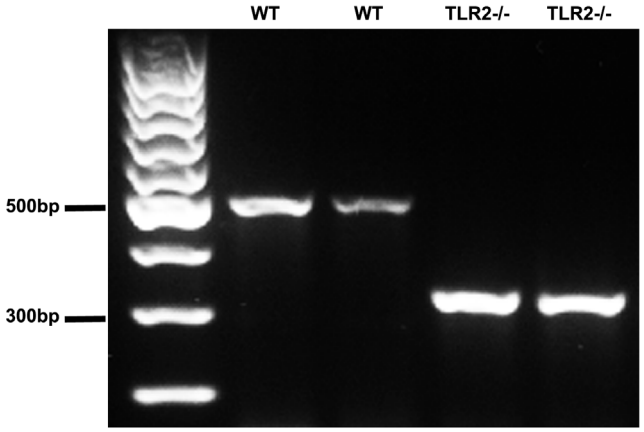

Supplementary Figure S4. Mouse genotyping. Mouse genomic DNA was extracted from the mouse ear biopsy. PCR was performed using DreamTaq Green PCR Master Mix (Thermo Fisher Scientific) according to the manufacture's instruction with a PCR thermal cycler (T100 Thermal Cycler, Bio-Rad). The yielded PCR products (wild type 499bp and mutant 334bp) were separated by 2% agarose gel electrophoresis (120V for 1 hour) and visualized with ChemiDoc Gel Imaging System (Bio-Rad). GeneRuler 100bp DNA Ladder (Thermo Fisher Scientific) was used as a molecular size reference. WT, wild type mice; $TLR2^{-/-}$, TLR2 deficient mice.

“

The good thing about science
is that it’s true,
whether or not you believe in it.

Neil Degrasse Tyson

Chapter

8

General discussion and future perspectives

General discussion

Heart Failure (HF) is a major health burden worldwide and is caused by pathophysiological myocardial remodeling, such as electrical, structural and contractile remodeling.[1] Even though all types are initiated to keep up with the increased cardiac work load, they eventually lead to impairment of impulse propagation and pump function.

In this thesis, we investigated these aspects of myocardial remodeling upon human cardiomyopathies, and experimentally mimicked in mouse models of induced pressure overload (PO).

PATHOPHYSIOLOGICAL MYOCARDIAL REMODELING

Starting with **chapter 1**, the preface of this thesis, we defined myocardial remodeling as a combination of structural, electrical and contractile remodeling and explained its major impact during pathophysiology. However, one should keep in mind that the different forms are sometimes mixed-up in literature. Structural remodeling can also lead to electrical remodeling, and contractile remodeling partially consists of electrical and structural components, as described in this chapter. In **chapter 2**, a review article, we described the most prominent alterations of the myocardium in various cardiomyopathies. This includes changes of the intercalated disc (ID), which structure and function are explained in the following chapters of **part 1** of this thesis (Chapter 3, 4 and 5); and in e.g. tissue architecture, such as hypertrophy, fiber disarray, cell size and fibrosis (described in **part 2** of this thesis (Chapter 6 and 7)). Myocardial tissue remodeling in general mostly appears in a heterogeneous manner, creating by definition inhomogeneous electrical and mechanical coupling, which predisposes to reentry arrhythmias and aggravates deterioration into the HF phenotype.

PART 1 – REMODELING OF THE INTERCALATED DISC

Following the introducing chapters, **part 1** of this thesis focuses in detail on alterations of the ID. The ID is the region connecting the longitudinal ends of two adjacent cardiomyocytes, housing, as far as we know today, junctions like desmosomes, adherens junctions and gap junctions, but also ion channels, such as the sodium channel $Na_V1.5$.[2] Desmosomes and adherens junctions are responsible for the mechanical coupling between the cells, where desmosomes link to the intermediate filaments within the cells and adherens junctions connect actin filaments of two cardiomyocytes. Desmosomes are mainly built-up by Desmoglein-2 (DSG-2), Desmocollin-2 (DSC-2), Plakophilin-2 (PKP2), Desmoplakin (DSP), β-catenin and Plakoglobin (also called γ-catenin), whereas adherens junctions mainly contain N-cadherin (Ncad) but also again Plakoglobin. Electrical connection between the cells is guaranteed by gap junctions, which in the ventricles are predominantly composed of Connexin-43 (Cx43). These junctions enable electrical coupling between cardiomyocytes and allow small molecules to pass from one cytosol to the other.[3] Ion channels, such as the sodium channel $Na_V1.5$ enable excitation of the cardiomyocytes.[2] To complicate this organization, which for long has been

regarded to be separated into different domains, new techniques, such as for instance mass spectrometry, proteomics and super resolution microscopy, newly defined the ID.[4] In 2010, dos Remedios and colleagues stated that there are about 200 proteins known to reside in the mammalian ID.[5] However, mass spectrometry and proteomics studies conducted by several research groups over the last few years demonstrated the presence of more and more proteins in the ID, of which exact location and function were unknown so far.[4,5] Therefore, the amount of identified ID proteins has dramatically increased since 2010 and so has the knowledge on their relation to HF. Besides that, modern microscopy techniques demonstrated that proteins of the different junctions or even junctions themselves can interact with each other to form large and complicated macro-molecular complexes.[2,6]
The junctions, which account for the electrical and mechanical coupling of the myocardium, are often affected during different cardiomyopathies, as has been extensively described in **chapter 1 and 2**. Furthermore, identifying new ID proteins and focusing on their functional interactions and role during HF, is likely to be very useful regarding future therapy.

In this thesis, we investigated in particular the effect of Arrhythmogenic Cardiomyopathy (ACM, **chapter 3**) and pediatric Dilated Cardiomyopathy (DCM, **chapter 4**) on ID remodeling. Moreover, the potential role of one of the recently identified proteins of the ID was studied in **chapter 5**, again in ACM and DCM, but also in genetically interfered mouse models.

THE ID IN ARRHYTMOGENIC CARDIOMYOPATHY

In **chapter 3** we investigated the molecular alterations in the ID of patients with ACM, which is a mostly heritable non-ischemic heart disease. ACM patients often present with electrical problems even before any structural disturbances can be observed, which makes it a very complex and difficult disease to study. Molecularly, disturbances of Cx43 and $Na_V1.5$ are often reported together with high amounts of fibro-fatty replacement of the myocardium.[7,8] ACM most often is caused by mutations in genes encoding for several desmosomal proteins, such as PKP2, Plakoglobin, DSC-2, DSP or DSG-2, or even in non-desmosomal genes, such as the transmembrane protein 43 (TMEM-43), phospholamban (PLN), desmin and transforming growth factor beta-3 (TGF-β3).[9-19] However, only in about 60 % of all patients, a genetic mutation responsible for the disease has been identified, which highlights the need for additional research, in order to uncover mutations in different proteins not associated with ACM thus far. Interestingly, although PKP2 is the most abundant mutation amongst ACM patients, PKP2 heterozygous mice show only a very mild phenotype in absence of any environmental stressors.[20] However, induced PKP2 haploinsufficiency in mice results in a sodium current deficit and arrhythmogenesis, which could be triggered via flecainide.[21] Recently it has been discovered that tamoxifen induced PKP2 knockout (KO) in mice leads to a reduction in expression of e.g. the Ryanodine receptor 2 (Ryr2), Ankyrin-B (Ank2) and the L-type calcium channel (Cacna1c), causing disturbances in calcium handling prior to the onset of overt structural myocardial remodeling.[22] This could at least partially explain the phenomenon seen in many ACM patients, who indeed often present with arrhythmias in a structurally normal heart during the concealed phase of the disease.

Like it is seen in the general population, most of our patients (**chapter 3**) were carrying a mutation in the desmosomal protein PKP2. However, ACM is seen as a disease of the whole ID, since mutations in desmosomal proteins for instance lead to disturbances of the entire ID and therefore structural and especially electrical problems as described above.[23,24] It has already been shown in cultured cardiomyocytes that loss of PKP2 leads to a decrease in sodium current and a slower conduction velocity, and that this can also affect the expression of the gap junction protein Cx43.[25,26] Furthermore, this relation between gap junctions, the desmosomes and sodium channels could be confirmed, since induced heterogeneous expression of Cx43 in mice resulted in downregulation of sodium current and an increased propensity to develop arrhythmias.[27] It was also reported in zebrafish that a genetic defect in Plakoglobin could induce a 70% - 80% reduction in sodium current density.[28] To specify the value of the findings derived from experimental animal models, we examined myocardial specimens obtained from ACM patients, focusing on potential aberrancies in several ID proteins, and also assessed the amount of fibrosis. In most of the patients signals for Cx43, the desmosomal and adherens junction protein Plakoglobin and the sodium channel $Na_V1.5$ were reduced when compared to control tissue. This, for the first time, confirmed the initial findings observed in animal models to be comparable to the human situation. Especially the alterations seen in localization of Plakoglobin are intriguing, since this protein was shown to translocate to the nucleus by Asimaki *et al.*[29] In 14-20 patients, alterations in localization of Plakoglobin were reported and this was always accompanied by a reduction in Cx43, $Na_V1.5$, or both. Given their role in signal transduction and regulation of gene expression, ID proteins like Plakoglobin could act as modifiable targets for disease treatment in the future. In ACM mice for instance, normalization of Plakoglobin levels increased survival of all animals and restored their cardiac function.[30] Furthermore, drugs acting on ID proteins were shown to be very efficient against ACM in zebrafish.[28] This latter study revealed promising results for future therapy since disease-causing targets could be identified and *in vitro* studies showed prevention and even regression of the disease when the intervention with a glycogen synthesis kinase (GSK-3β) inhibitor (SB21) was applied in the early phases of cardiac remodeling. SB21 is an activator of the canonical Wnt signaling, including β-catenin and Plakoglobin (also called γ-catenin) at the ID as described in the **addendum of this discussion**. Even though treatment with SB21 in theory is a very promising drug for ACM patients, its involvement in the Wnt signaling and therefore in cancer development can't be overlooked and care should be taken, when aiming to treat patients with SB21.

THE ID AND DILATED CARDIOMYOPATHY

ACM is not the only disease caused by mutations in ID proteins. Mutations in desmosomal genes, such as DSP-1, DSG-2, PKP2 and β-catenin can also lead to DCM.[31-34] DCM is the most common cardiomyopathy in adults and children and is associated with muscle dysfunction and/or volume overload, identified by cardiac chamber dilatation and reduced systolic function as has been described in **chapter 2 and 4**. It is often characterized by severe structural remodeling, including deposition of fibrosis, cell lengthening and the mentioned cardiac dilatation.[35,36] Immunohistological disturbances of ID proteins upon adult DCM have been repor-

ted manifold, such as of Ncad, Plakoglobin, β-catenin, and the gap junction protein Cx43.[37-41] However, embryonic and pediatric DCM has not been studied thoroughly which is mainly caused by the fact that the absolute amount of affected children is low and availability of specimen to study is scarce. Nevertheless, such studies could give insights into the DCM disease progression, because of the re-activation of embryonic gene patterning during DCM and HF.[42] Therefore, in **chapter 4** we investigated the early spatio-temporal constitution of the ID in pediatric DCM patients compared to pediatric control material and adult DCM patients and controls. Again, we fluorescently stained myocardial specimens and assessed fibrosis. Although the normal constitution of the ID during development is not yet very clear, and not all proteins are located at the ID or even laterally during birth,[43] we aimed at investigating the differences between normal pediatric development and pathophysiology during pediatric DCM. Potential effects on Cx43 and $Na_V1.5$ were difficult to determine, since neither of these proteins did reach their final destination in the age-matched control specimens, when mirrored to the specimens we studied. Interestingly, although increased levels were reported in adult DCM patients,[41] in our pediatric patients with DCM signals for Plakoglobin were not disturbed, but all patients showed a disturbed translocation of DSG-2, even when underlying mutations in DSG-2 were absent. This has never been reported before in adult patients, but suggests that translocation of DSG-2 to the ID is delayed or disturbed in the early life-stages of DCM patients. Reduction and heterogeneous distribution of DSG-2 could weaken the myocardium by mechanical uncoupling of cardiomyocytes, facilitating the DCM phenotype. Furthermore, the resulting loss of mechanical strength could enable fibrosis formation. Just like in ACM patients, the amount of fibrosis was severely increased in our pediatric patients, which can in turn affect both the mechanical and electrical set-up of the heart, as has been discussed in **part 2** of this thesis.

NEWLY IDENTIFIED MEMBERS OF THE ID

Why alterations in certain ID proteins lead to DCM or ACM is not fully understood and may be, at least partially, due to disturbances in so far unknown players of cardiac remodeling. As described in the first part of this chapter, our knowledge on the composition of the ID is not yet complete, and more and more proteins are identified in the ID that could play a role in myocardial remodeling. In the last chapter of the first part of this thesis, **chapter 5**, we hence investigated the role of Flotillin-1 and Flotillin-2, which are proteins newly discovered in the ID.[4] Both homologous proteins are present in most mammalian cell types and enriched in the ID. They consist of two termini, responsible for membrane attachment and oligomerization. In detail, the N-terminus of both Flotillins contains a prohibitin homology domain (PHB) that leads to association with the plasma membrane and can directly interact with F-actin, but apparently not with tubulin or vimentin.[44] The stomatin/prohibitin/flotillin/HflK/C (SPFH) domain directs the Flotillins to non-caveolar lipid rafts, which are regulating parts of the cell membrane with high molecular signaling and transportation. However, neither of the two Flotillins contains a transmembrane domain and are therefore only attached to the membranes.[45,46]

The C-terminus is responsible for (hetero-) oligomerization, which can direct Flotillins from the cell membrane to the cytosol.[47]

Although the Flotillins are known to play a role in a plethora of different cellular and pathophysiological processes, almost nothing has been reported about their role in the heart.[45] A previous study from our group already showed that Flotilin-2 is present in the cardiac ID, and protein levels were altered in patients with DCM and ACM.[4] In **chapter 5**, we demonstrated that also Flotillin-1 is present in the cardiac ID. Besides, using eQTL data, a correlation between Flotillin-1, and to a lesser extend Flotillin-2, and the QRS of the electrocardiogram could be established. Therefore, we investigated the effect of Flotillin knockout (KO) and knockdown (KD) on ID proteins and conduction/excitation in mice and neonatal rat cardiomyocytes (NRCMs), respectively. KO of Flotillin-1 or both Flotillins in mice leads to a reduction in $Na_V1.5$, and in NRCMs, KD of both Flotillins showed a tendency towards decreased peak sodium current. Furthermore, Flotillin-1 KD resulted in a decreased spike amplitude (measurement for amount of ion channels) and spike slope (interpreted as the dV/dt) during multi electrode array (MEA) experiments. Notably, KO did not show an effect on hypertrophy or fibrosis, suggesting a role of especially Flotillin-1 on electrical conduction and excitability. It has also been described previously that Flotillins bind to e.g. Ncad, Plakoglobin and DSG-2,[48,49] which could partially be confirmed in our study, but Flotillin KO did not result in changes of the mentioned proteins. Since expression of ID proteins was not altered, we hypothesize that Flotillin plays a role in trafficking of $Na_V1.5$.
It is intriguing that Flotillins and $Na_V1.5$ are both present in lipid rafts, which are parts of the membrane very active in transportation and signaling.[50] In addition, other ion channels are also known to reside in lipid rafts. The interaction between Flotillins and $Na_V1.5$ does not seem to be mediated by PKP2 or Cx43, and further research into rafts would be of great interest to investigate a possible direct interaction.

In summary, the research described in **part 1** shows that proteins of the ID work together and disturbances of one of them can affect others and therefore the mechanical and electrical balance of the heart. Overlap and differences in ID disturbances between for instance ACM and DCM, like they have been shown in **chapter 3** and **chapter 4** of this thesis, underline the thin boarder between various heart diseases. Moreover, high amounts of structural disturbances have been seen in both ACM and DCM patients, but were not prominent in mice subjected to Flotillin KO as described in **chapter 5**, suggesting that Flotillin itself alters the electrical components of the heart, playing a role in electrical rather than structural myocardial remodeling.
ID alterations only make up one fraction of myocardial remodeling. As has been shown in **chapter 3** and **chapter 4**, patients with ACM and DCM present with high amounts of fibrosis. Of course, mechanical dysfunction of cardiomyocytes might induce apoptosis, which contributes to fibrosis formation, but also reduced gap junction coupling has been reported to enhance fibrosis formation. Besides, sodium channel as well as desmosomal dysfunction have been associated with altered calcium homeostasis in cardiomyocytes.[22,51] In turn, activated calcium-sensitive signal transduction pathways can stimulate transcription of fibrosis-associated genes.[52] Therefore, in the second part of this thesis, we focus more on pathophysiological remodeling of the tissue architecture and investigated two other and related entities, namely fibrosis and inflammation.

PART 2 – STRUCTURAL REMODELING OF TISSUE ARCHITECTURE

Part 2 of this thesis focuses on structural remodeling of tissue architecture upon PO, induced by transverse aortic constriction (TAC) in mice. In both clinical and animal studies, PO leads to myocardial remodeling associated with cardiac stiffness and arrhythmias, which can eventually culminate in HF.[1] Fibrosis, which is defined as the excessive secretion and/or impaired degradation of connective tissue, especially collagen in the extracellular matrix, is a major contributor to maladaptive remodeling.[36,53] Notably, structural remodeling can also facilitate electrical problems by redirecting the electrical conduction throughout the heart.[54] Furthermore, during myocardial remodeling, activation of inflammatory pathways, such as the toll-like receptor (TLR) pathway, is a common observation.[55] Therefore, we focused on fibrosis by studying the connective tissue growth factor (CTGF, **chapter 6**) and on inflammation by studying the Toll-like receptor 2 (TLR2, **chapter 7 and its addendum**).

STRUCTURAL REMODELING: FIBROSIS

In detail, **chapter 6** presents a study performed in CTGF KO mice subjected to chronic PO induced by TAC (for 16 weeks). CTGF is a matricellular protein commonly reported to be increased upon various diseases and thought to be causative for cardiac fibrosis.[56-58] Furthermore, CTGF is increased in all sorts of animal models of cardiac hypertrophy and fibrosis.[52,58-61] Therefore, we hypothesized that CTGF KO in mice would reduce fibrosis formation and preserve their cardiac function upon PO. In contrast to what was expected, we were not able to depress cardiac fibrosis or hypertrophy, challenging the causative association of CTGF with fibrosis. Interestingly, the pro-fibrotic role of CTGF had been questioned previously by Gravning *et al.*, who overexpressed CTGF in the murine hearts in combination with either myocardial infarction (MI) or aortic banding. Upon MI, in their study, this lead to a reduced mortality, less cardiac hypertrophy and decreased left ventricular dilatation, and in both models it did not lead to increase of the expected cardiac fibrosis.[62,63] Although we used a global KO, at the same time as we reported our findings, also another group that used heart-specific alterations supported our findings. They showed that after heart-specific KO or overexpression, cardiac function and fibrosis were unaltered in aging or murine hearts subjected to TAC.[64] Following KO, fractional shortening was not increased compared to controls and also hypertrophy was not reduced. Moreover, KO in cardiomyocytes and fibroblasts did not lead to a decrease of fibrosis after TAC compared to controls.[64] Very recently, another group found that cardiac-restricted overexpression of CTGF even lead to less collagen and TGF-β after angiotensin II perfusion and concluded that CTGF could actually protect against cardiac remodeling.[65]

Nevertheless, it can not be neglected that still many publications can be found, where CTGF is observed to be increased in fibrotic tissue or even reported to be responsible for fibrosis formation. This is not only in cardiac research, but also in all fibrosis-related research fields, where CTGF is still seen as an attractive therapeutic target. Fibroblasts-specific CTGF KO or treatment with CTGF antibody in mice for instance was shown to reduce collagen formation and vascular injury in systemic sclerosis.[66]

Intriguingly, CTGF has been shown to induce cellular senescence in various cell types. Cellular senescence is a stress response to cellular injury, such as DNA damage, mitochondrial dysfunction, but also oncogenic activation, inflammation and aging.[67,68] It is thought to be irreversible, causes an arrest of cellular proliferation and growth, and hampers the apoptotic abilities of many cell types (human fibroblasts for instance, but not endothelial cells) under various circumstances.[69,70] Furthermore, gene expression is altered in senescent cells, which often seems to be unrelated to the growth arrest, but more to e.g. extracellular matrix remodeling and promotion of inflammation and cardiomyocyte hypertrophy.[67,71,72] This suggest an important role for senescent cells in structural remodeling. In fibroblasts after skin damage and *in vitro* for instance, CTGF induced senescence and these cells were able to express an anti-fibrotic phenotype, including upregulation of matrix metalloproteinases (MMPs) and downregulation of collagens.[73]
Differences in the fibrotic and inflammatory response upon CTGF overexpression or KO might actually result from the cells' ability to undergo cell senescence, rather than a direct effect caused by CTGF.

STRUCTURAL REMODELING: INFLAMMATION

In **chapter 7 and its addendum**, we once more used a TAC model to induce PO, but this time in TLR2 KO mice and for 12 weeks. We chose to decrease the time of TAC, because of a dramatic drop-out of animals between 12 and 16 weeks of TAC. TLR2 is a receptor on immune and cardiac non-immune cells (e.g. cardiomyocytes, fibroblasts and vascular endothelial cells), initiating the innate immune system by recognition of Damaged and Pathogen Associated Molecular Patterns (DAMPs and PAMPs, respectively).[74-76] TLR2 together with TLR4 are the most abundant TLRs in the heart and it has been shown that both can stimulate adverse myocardial remodeling after MI.[77,78] However, the role of TLR2 upon chronic PO is less well studied than TLR4, and first results of TLR2 KO were contradicting with either decreased or increased amounts of cardiac fibrosis after 2 and 4 weeks of PO, respectively.[79,80] To investigate the effect of TLR2 KO on chronic PO, we performed two independent studies. We first subjected TLR2 KO mice to 12 weeks of TAC to induce chronic PO in **chapter 7**. In the **addendum to chapter 7**, we used 8 weeks of TAC and additionally preformed bone marrow transplantation experiments.
In **chapter 7**, KO of TLR2 upon TAC lead to reduced hypertrophy, attenuated depression of contractility and lower levels of inflammatory cytokines compared to WT TAC animals. In addition, in the **addendum to chapter 7**, we found decreased amounts of fibrosis and preserved ejection fraction (EF) in the TLR2 KO TAC group compared to WT TAC after 8 weeks of TAC. In both studies, levels of certain cytokines and chemokines were analyzed in the KO compared to WT animals. Besides, after 12 weeks of TAC in the WT TAC group high levels of TLR4 and TLR2 correlated with the highest degree of hypertrophy and increased levels of the inflammatory cytokine interleukin 6 (IL-6). These studies together show that TLR2 KO protects against adverse cardiac remodeling following chronic pressure overload of 8 and 12 weeks. Moreover, it suggests an interplay of TLR2, TLR4 and IL-6 during PO. In line with this, very recently, Bagchi *et al.* reported that TLR2 rather than TLR4 is responsible for adverse myocardial remodeling

upon global ischemia-reperfusion injury in rats and in interleukin 1- (IL-10) KO mice.[81] Interestingly, after 8 weeks of TAC, transplantation with TLR2 KO bone marrow-derived cells protected against a reduction in EF and attenuated fibrosis formation, highlighting that immune cells derived from the bone marrow might worsen the course of HF. This suggests that the TLR pathway, including the bone marrow derived cells, may represent an important target in myocardial remodeling upon chronic PO.

For a translation into a clinical setting, blocking of TLR receptors might give more complications than one of its downstream targets, such as IL-6, which was shown to be increased in WT TAC mice in **chapter 7**. However, care should be taken when interfering with IL-6, since contradicting results have been obtained so far. IL-6 deficient mice for instance, show on the one hand increased acute toxin-induced liver fibrosis,[82] but on the other hand attenuated liver fibrosis when treated with tertachloride.[83] Moreover, it has been shown that IL-6 is responsible for pathological hypertrophy and fibrosis in cardiac allograft rejection,[84] and in a meta-analysis of 40 studies in humans, IL-6 blockage was shown to be a promising target for coronary heart disease. Whether this is also the case in PO has to be investigated, but interestingly, knockdown of IL-6 in rats hampered cold-induced hypertension.[85]

Future perspectives

Research on the cause, process and treatment/reversal of myocardial remodeling is of high importance to delay or favorable halt HF. Of course, aspects of myocardial remodeling are manifold and the consequences are staggering. As a result, often only parts of the whole remodeling process can be studied at once.

In **part 1**, we showed that knowledge on ID proteins and their interaction with e.g. the extracellular matrix or intracellular components can shed a light on various diseases and pathophysiological processes. In the future, ID proteins could act as modifiable targets for disease treatment, as described above in **chapter 3** for ACM. However, in order to ensure proper treatment (e.g. with SB21), molecular alterations have to be understood completely (e.g. concerning the Wnt pathway), underlining the importance of molecular and histological research on that matter. This of course also accounts for other diseases, such as DCM. Therefore, specimens of pediatric DCM patients were used in **chapter 4** to study earliest onset of the disease and its molecular consequences. In the future, more children could be included in this cohort and e.g. a DSG-2 KO animal model could be used to investigate DCM, even though DSG-2 KO animals seem to develop a more ACM-like phenotype than DCM.[86]

That the constitution of the ID is far from unraveled is shown in **chapter 5** about Flotillins. These proteins might play a role in $Na_v1.5$ trafficking and further research should be conducted to investigate its role in cell attachment and to uncover its molecular binding partners.

In **part 2** of this thesis, we subjected genetically modified mice to TAC surgeries and investigated the role of CTGF in cardiac fibrosis and of TLR2 in cardiac inflammation. In **chapter 6**, CTGF brought some interesting results, questioning the whole paradigm of its role in fibrosis formation. **Chapter 7 and its addendum**, on the other hand, underlined the important aspect of inflammation in HF upon PO. Although of course the human situation itself is still the best model to study a disease, mouse models are a good starting point to investigate the role of certain proteins by KO. However, one should keep in mind that they do not totally mimic the human situation, but only approach it to a certain extent. It is of utmost importance that in the coming years more human specimens will be collected and made available to the research community for the study of genetic, molecular and histological patterning of cardiac remodeling at the basis of the disease. Subsequently, to gain more mechanistic insight, the most suitable experimental models can be applied. Beyond the mouse models that we applied, research questions should preferably also be tested, and obtained data be validated in different platforms, which could be larger animals, human induced pluripotent stem cells and bioinformatics.

Conclusion

Myocardial remodeling is initiated to support the heart in difficult times, but eventually exacerbates the damage leading to pump failure. In this thesis, we have shown that remodeling of the ID can lead to ACM and DCM and certain alterations are specific for one of them (e.g. reduction of Plakoglobin) and others overlap in both (changes in Desmoglein-2, fibrosis). Moreover, we showed that so far unidentified proteins in the ID, such as Flotillins, might play an important role in electrical excitability of the heart, and thereby highlight the importance of elucidating the complete composition of the ID in detail. Furthermore, we have shown that CTGF, which is a protein long thought to be pro-fibrotic, does probably not cause fibrosis itself, but is rather a mediator of the fibrotic pathway. Lastly, we demonstrated in two studies that the inflammatory receptor TLR2 might pose a modifiable target for chronic PO, since KO attenuates adverse myocardial remodeling upon TAC in mice. In this thesis, we therefore successfully investigated several aspects of myocardial remodeling, broadening the knowledge on underlying molecular mechanisms of HF.

References

1. Ponikowski P, Voors AA, Anker SD, et al. 2016 ESC Guidelines for the diagnosis and treatment of acute and chronic heart failure: The Task Force for the diagnosis and treatment of acute and chronic heart failure of the European Society of Cardiology (ESC)Developed with the special contribution of the Heart Failure Association (HFA) of the ESC. Eur Heart J.2016;37(27):2129-2200.
2. Vermij SH, Abriel H, van Veen TA. Refining the molecular organization of the cardiac intercalated disc. Cardiovasc Res.2017;10.1093/cvr/cvw259.
3. Elfgang C, Eckert R, Lichtenberg-Frate H, et al. Specific permeability and selective formation of gap junction channels in connexin-transfected HeLa cells. J Cell Biol.1995;129(3):805-817.
4. Soni S, Raaijmakers AJ, Raaijmakers LM, et al. A Proteomics Approach to Identify New Putative Cardiac Intercalated Disk Proteins. PLoS One.2016;11(5):e0152231.
5. Estigoy CB, Ponten F, Odeberg J, et al. Intercalated discs: multiple proteins perform multiple functions in non-failing and failing human hearts. Biophys Rev.2009;1(1):43.
6. Pinali C, Bennett HJ, Davenport JB, et al. Three-dimensional structure of the intercalated disc reveals plicate domain and gap junction remodeling in heart failure. Biophys J.2015;108(3):498-507.
7. Corrado D, Link MS, Calkins H. Arrhythmogenic Right Ventricular Cardiomyopathy. N Engl J Med.2017;376(1):61-72.
8. Saffitz JE. Arrhythmogenic cardiomyopathy and abnormalities of cell-to-cell coupling. Heart Rhythm.2009;6(8 Suppl):S62-65.
9. van der Zwaag PA, van Rijsingen IA, Asimaki A, et al. Phospholamban R14del mutation in patients diagnosed with dilated cardiomyopathy or arrhythmogenic right ventricular cardiomyopathy: evidence supporting the concept of arrhythmogenic cardiomyopathy. Eur J Heart Fail.2012;14(11):1199-1207.
10. Otten E, Asimaki A, Maass A, et al. Desmin mutations as a cause of right ventricular heart failure affect the intercalated disks. Heart Rhythm.2010;7(8):1058-1064.
11. Merner ND, Hodgkinson KA, Haywood AF, et al. Arrhythmogenic right ventricular cardiomyopathy type 5 is a fully penetrant, lethal arrhythmic disorder caused by a missense mutation in the TMEM43 gene. Am J Hum Genet.2008;82(4):809-821.
12. Gerull B, Heuser A, Wichter T, et al. Mutations in the desmosomal protein plakophilin-2 are common in arrhythmogenic right ventricular cardiomyopathy. Nat Genet.2004;36(11):1162-1164.
13. Pilichou K, Nava A, Basso C, et al. Mutations in desmoglein-2 gene are associated with arrhythmogenic right ventricular cardiomyopathy. Circulation.2006;113(9):1171-1179.

14. Syrris P, Ward D, Evans A, et al. Arrhythmogenic right ventricular dysplasia/cardiomyopathy associated with mutations in the desmosomal gene desmocollin-2. Am J Hum Genet.2006;79(5):978-984.
15. Asimaki A, Syrris P, Wichter T, Matthias P, Saffitz JE, McKenna WJ. A novel dominant mutation in plakoglobin causes arrhythmogenic right ventricular cardiomyopathy. Am J Hum Genet.2007;81(5):964-973.
16. Groeneweg JA, van der Zwaag PA, Olde Nordkamp LR, et al. Arrhythmogenic right ventricular dysplasia/cardiomyopathy according to revised 2010 task force criteria with inclusion of non-desmosomal phospholamban mutation carriers. Am J Cardiol.2013;112(8):1197-1206.
17. Heuser A, Plovie ER, Ellinor PT, et al. Mutant desmocollin-2 causes arrhythmogenic right ventricular cardiomyopathy. Am J Hum Genet.2006;79(6):1081-1088.
18. Rampazzo A, Nava A, Malacrida S, et al. Mutation in human desmoplakin domain binding to plakoglobin causes a dominant form of arrhythmogenic right ventricular cardiomyopathy. Am J Hum Genet.2002;71(5):1200-1206.
19. Beffagna G, Occhi G, Nava A, et al. Regulatory mutations in transforming growth factor-beta3 gene cause arrhythmogenic right ventricular cardiomyopathy type 1. Cardiovasc Res.2005;65(2):366-373.
20. Grossmann KS, Grund C, Huelsken J, et al. Requirement of plakophilin 2 for heart morphogenesis and cardiac junction formation. J Cell Biol.2004;167(1):149-160.
21. Cerrone M, Noorman M, Lin X, et al. Sodium current deficit and arrhythmogenesis in a murine model of plakophilin-2 haploinsufficiency. Cardiovasc Res.2012;95(4):460-468.
22. Cerrone M, Montnach J, Lin X, et al. Plakophilin-2 is required for transcription of genes that control calcium cycling and cardiac rhythm. Nat Commun.2017;8(1):106.
23. Akdis D, Brunckhorst C, Duru F, Saguner AM. Arrhythmogenic Cardiomyopathy: Electrical and Structural Phenotypes. Arrhythm Electrophysiol Rev.2016;5(2):90-101.
24. Corrado D, Link MS, Calkins H. Arrhythmogenic Right Ventricular Cardiomyopathy. N Engl J Med.2017;376(15):1489-1490.
25. Sato PY, Coombs W, Lin X, et al. Interactions between ankyrin-G, Plakophilin-2, and Connexin43 at the cardiac intercalated disc. Circ Res.2011;109(2):193-201.
26. Sato PY, Musa H, Coombs W, et al. Loss of plakophilin-2 expression leads to decreased sodium current and slower conduction velocity in cultured cardiac myocytes. Circ Res.2009;105(6):523-526.
27. Jansen JA, Noorman M, Musa H, et al. Reduced heterogeneous expression of Cx43 results in decreased Nav1.5 expression and reduced sodium current that accounts for arrhythmia vulnerability in conditional Cx43 knockout mice. Heart Rhythm.2012;9(4):600-607.
28. Asimaki A, Kapoor S, Plovie E, et al. Identification of a new modulator of the intercalated disc in a zebrafish model of arrhythmogenic cardiomyopathy. Sci Transl Med.2014;6(240):240ra274.

29. Asimaki A, Tandri H, Huang H, et al. A new diagnostic test for arrhythmogenic right ventricular cardiomyopathy. N Engl J Med.2009;360(11):1075-1084.
30. Zhang Z, Stroud MJ, Zhang J, et al. Normalization of Naxos plakoglobin levels restores cardiac function in mice. J Clin Invest.2015;125(4):1708-1712.
31. Norgett EE, Hatsell SJ, Carvajal-Huerta L, et al. Recessive mutation in desmoplakin disrupts desmoplakin-intermediate filament interactions and causes dilated cardiomyopathy, woolly hair and keratoderma. Hum Mol Genet.2000;9(18):2761-2766.
32. Posch MG, Posch MJ, Geier C, et al. A missense variant in desmoglein-2 predisposes to dilated cardiomyopathy. Mol Genet Metab.2008;95(1-2):74-80.
33. Hirschy A, Croquelois A, Perriard E, et al. Stabilised beta-catenin in postnatal ventricular myocardium leads to dilated cardiomyopathy and premature death. Basic Res Cardiol.2010;105(5):597-608.
34. Ramond F, Janin A, Di Filippo S, et al. Homozygous PKP2 deletion associated with neonatal left ventricle noncompaction. Clin Genet.2017;91(1):126-130.
35. Nakayama Y, Shimizu G, Hirota Y, et al. Functional and histopathologic correlation in patients with dilated cardiomyopathy: an integrated evaluation by multivariate analysis. J Am Coll Cardiol.1987;10(1):186-192.
36. Swynghedauw B. Molecular mechanisms of myocardial remodeling. Physiol Rev.1999;79(1):215-262.
37. Parvari R, Levitas A. The mutations associated with dilated cardiomyopathy. Biochem Res Int.2012;2012:639250.
38. Kitamura H, Ohnishi Y, Yoshida A, et al. Heterogeneous loss of connexin43 protein in nonischemic dilated cardiomyopathy with ventricular tachycardia. J Cardiovasc Electrophysiol.2002;13(9):865-870.
39. Kostin S, Rieger M, Dammer S, et al. Gap junction remodeling and altered connexin43 expression in the failing human heart. Mol Cell Biochem.2003;242(1-2):135-144.
40. Ehler E, Horowits R, Zuppinger C, et al. Alterations at the intercalated disk associated with the absence of muscle LIM protein. J Cell Biol.2001;153(4):763-772.
41. Pluess M, Daeubler G, Dos Remedios CG, Ehler E. Adaptations of cytoarchitecture in human dilated cardiomyopathy. Biophys Rev.2015;7(1):25-32.
42. Dirkx E, da Costa Martins PA, De Windt LJ. Regulation of fetal gene expression in heart failure. Biochim Biophys Acta.2013;1832(12):2414-2424.
43. Vreeker A, van Stuijvenberg L, Hund TJ, Mohler PJ, Nikkels PG, van Veen TA. Assembly of the cardiac intercalated disk during pre- and postnatal development of the human heart. PLoS One.2014;9(4):e94722.
44. Langhorst MF, Solis GP, Hannbeck S, Plattner H, Stuermer CA. Linking membrane microdomains to the cytoskeleton: regulation of the lateral mobility of reggie-1/flotillin-2 by interaction with actin. FEBS Lett.2007;581(24):4697-4703.
45. Bodin S, Planchon D, Rios Morris E, Comunale F, Gauthier-Rouviere C. Flotillins in intercellular adhesion - from cellular physiology to human diseases. J Cell Sci.2014;127(Pt 24):5139-5147.

46. Rivera-Milla E, Stuermer CA, Malaga-Trillo E. Ancient origin of reggie (flotillin), reggie-like, and other lipid-raft proteins: convergent evolution of the SPFH domain. Cell Mol Life Sci.2006;63(3):343-357.
47. Solis GP, Hoegg M, Munderloh C, et al. Reggie/flotillin proteins are organized into stable tetramers in membrane microdomains. Biochem J.2007;403(2):313-322.
48. Vollner F, Ali J, Kurrle N, et al. Loss of flotillin expression results in weakened desmosomal adhesion and Pemphigus vulgaris-like localisation of desmoglein-3 in human keratinocytes. Sci Rep.2016;6:28820.
49. Kurrle N, Vollner F, Eming R, Hertl M, Banning A, Tikkanen R. Flotillins directly interact with gamma-catenin and regulate epithelial cell-cell adhesion. PLoS One.2013;8(12):e84393.
50. Brisson L, Gillet L, Calaghan S, et al. Na(V)1.5 enhances breast cancer cell invasiveness by increasing NHE1-dependent H(+) efflux in caveolae. Oncogene.2011;30(17):2070-2076.
51. Jansen JA, van Veen TA, de Jong S, et al. Reduced Cx43 expression triggers increased fibrosis due to enhanced fibroblast activity. Circ Arrhythm Electrophysiol.2012;5(2):380-390.
52. Fontes MS, Raaijmakers AJ, van Doorn T, et al. Changes in Cx43 and NaV1.5 expression precede the occurrence of substantial fibrosis in calcineurin-induced murine cardiac hypertrophy. PLoS One.2014;9(1):e87226.
53. Krenning G, Zeisberg EM, Kalluri R. The origin of fibroblasts and mechanism of cardiac fibrosis. J Cell Physiol.2010;225(3):631-637.
54. de Jong S, van Veen TA, van Rijen HV, de Bakker JM. Fibrosis and cardiac arrhythmias. J Cardiovasc Pharmacol.2011;57(6):630-638.
55. Dick SA, Epelman S. Chronic Heart Failure and Inflammation: What Do We Really Know? Circ Res.2016;119(1):159-176.
56. Chen MM, Lam A, Abraham JA, Schreiner GF, Joly AH. CTGF expression is induced by TGF-beta in cardiac fibroblasts and cardiac myocytes: a potential role in heart fibrosis. J Mol Cell Cardiol.2000;32(10):1805-1819.
57. Gabrielsen A, Lawler PR, Yongzhong W, et al. Gene expression signals involved in ischemic injury, extracellular matrix composition and fibrosis defined by global mRNA profiling of the human left ventricular myocardium. J Mol Cell Cardiol.2007;42(4):870-883.
58. Koitabashi N, Arai M, Kogure S, et al. Increased connective tissue growth factor relative to brain natriuretic peptide as a determinant of myocardial fibrosis. Hypertension.2007;49(5):1120-1127.
59. Ruperez M, Lorenzo O, Blanco-Colio LM, Esteban V, Egido J, Ruiz-Ortega M. Connective tissue growth factor is a mediator of angiotensin II-induced fibrosis. Circulation.2003;108(12):1499-1505.
60. Way KJ, Isshiki K, Suzuma K, et al. Expression of connective tissue growth factor is increased in injured myocardium associated with protein kinase C beta2 activation and diabetes. Diabetes.2002;51(9):2709-2718.
61. Ohnishi H, Oka T, Kusachi S, et al. Increased expression of connective tissue growth factor in the infarct zone of experimentally induced myocardial infarction in rats. J Mol Cell Cardiol.1998;30(11):2411-2422.

62. Gravning J, Orn S, Kaasboll OJ, et al. Myocardial connective tissue growth factor (CCN2/CTGF) attenuates left ventricular remodeling after myocardial infarction. PLoS One.2012;7(12):e52120.
63. Gravning J, Ahmed MS, von Lueder TG, Edvardsen T, Attramadal H. CCN2/CTGF attenuates myocardial hypertrophy and cardiac dysfunction upon chronic pressure-overload. Int J Cardiol.2013;168(3):2049-2056.
64. Accornero F, van Berlo JH, Correll RN, et al. Genetic Analysis of Connective Tissue Growth Factor as an Effector of Transforming Growth Factor beta Signaling and Cardiac Remodeling. Mol Cell Biol.2015;35(12):2154-2164.
65. Zhang Y, Yan H, Guang GC, Deng ZR. Overexpressed connective tissue growth factor in cardiomyocytes attenuates left ventricular remodeling induced by angiotensin II perfusion. Clin Exp Hypertens.2017;39(2):168-174.
66. Makino K, Makino T, Stawski L, Lipson KE, Leask A, Trojanowska M. Anti-connective tissue growth factor (CTGF/CCN2) monoclonal antibody attenuates skin fibrosis in mice models of systemic sclerosis. Arthritis Res Ther.2017;19(1):134.
67. Campisi J. Aging, cellular senescence, and cancer. Annu Rev Physiol.2013;75:685-705.
68. Wiley CD, Velarde MC, Lecot P, et al. Mitochondrial Dysfunction Induces Senescence with a Distinct Secretory Phenotype. Cell Metab.2016;23(2):303-314.
69. Hampel B, Malisan F, Niederegger H, Testi R, Jansen-Durr P. Differential regulation of apoptotic cell death in senescent human cells. Exp Gerontol.2004;39(11-12):1713-1721.
70. Chen QM, Liu J, Merrett JB. Apoptosis or senescence-like growth arrest: influence of cell-cycle position, p53, p21 and bax in H2O2 response of normal human fibroblasts. Biochem J.2000;347(Pt 2):543-551.
71. Baker DJ, Childs BG, Durik M, et al. Naturally occurring p16(Ink4a)-positive cells shorten healthy lifespan. Nature.2016;530(7589):184-189.
72. Sun R, Zhu B, Xiong K, et al. Senescence as a novel mechanism involved in beta-adrenergic receptor mediated cardiac hypertrophy. PLoS One.2017;12(8):e0182668.
73. Jun JI, Lau LF. CCN2 induces cellular senescence in fibroblasts. J Cell Commun Signal.2017;11(1):15-23.
74. Mann DL. The emerging role of innate immunity in the heart and vascular system: for whom the cell tolls. Circ Res.2011;108(9):1133-1145.
75. Botos I, Segal DM, Davies DR. The structural biology of Toll-like receptors. Structure.2011;19(4):447-459.
76. Flo TH, Halaas O, Torp S, et al. Differential expression of Toll-like receptor 2 in human cells. J Leukoc Biol.2001;69(3):474-481.
77. Liu L, Wang Y, Cao ZY, et al. Up-regulated TLR4 in cardiomyocytes exacerbates heart failure after long-term myocardial infarction. J Cell Mol Med.2015;19(12):2728-2740.
78. Timmers L, Sluijter JP, van Keulen JK, et al. Toll-like receptor 4 mediates maladaptive left ventricular remodeling and impairs cardiac function after myocardial infarction. Circ Res.2008;102(2):257-264.

79. Higashikuni Y, Tanaka K, Kato M, et al. Toll-like receptor-2 mediates adaptive cardiac hypertrophy in response to pressure overload through interleukin-1beta upregulation via nuclear factor kappaB activation. J Am Heart Assoc.2013;2(6):e000267.
80. Bualeong T, Kebir S, Hof D, et al. Tlr2 deficiency does not limit the development of left ventricular hypertrophy in a model of transverse aortic constriction induced pressure overload. J Negat Results Biomed.2016;15:9.
81. Bagchi AK, Akolkar G, Mandal S, Ayyappan P, Yang X, Singal PK. Toll-like receptor 2 dominance over Toll-like receptor 4 in stressful conditions for its detrimental role in the heart. Am J Physiol Heart Circ Physiol.2017;312(6):H1238-H1247.
82. Kovalovich K, DeAngelis RA, Li W, Furth EE, Ciliberto G, Taub R. Increased toxin-induced liver injury and fibrosis in interleukin-6-deficient mice. Hepatology.2000;31(1):149-159.
83. Natsume M, Tsuji H, Harada A, et al. Attenuated liver fibrosis and depressed serum albumin levels in carbon tetrachloride-treated IL-6-deficient mice. J Leukoc Biol.1999;66(4):601-608.
84. Diaz JA, Booth AJ, Lu G, Wood SC, Pinsky DJ, Bishop DK. Critical role for IL-6 in hypertrophy and fibrosis in chronic cardiac allograft rejection. Am J Transplant.2009;9(8):1773-1783.
85. Crosswhite P, Sun Z. Ribonucleic acid interference knockdown of interleukin 6 attenuates cold-induced hypertension. Hypertension.2010;55(6):1484-1491.
86. Rizzo S, Lodder EM, Verkerk AO, et al. Intercalated disc abnormalities, reduced Na(+) current density, and conduction slowing in desmoglein-2 mutant mice prior to cardiomyopathic changes. Cardiovasc Res.2012;95(4):409-418.

“

The important thing is
never to stop questioning.

Albert Einstein

Addendum to chapter

8

A fishing trip to cure Arrhythmogenic Cardiomyopathy?

Elise L. Kessler[a]; Toon A.B. van Veen[a]

[a] *Department of Medical Physiology, Division of Heart&Lungs, University Medical Center Utrecht, The Netherlands7*

Annals of Translational Medicine 2015, 3: 90

Abstract

The paper entitled "Identification of a New Modulator of the Intercalated Disc in a Zebrafish Model of Arrhythmogenic Cardiomyopathy", as published in 2014 in Science Translational Medicine, examined the effects of the newly discovered drug SB216763 (SB21) on Arrhythmogenic Cardiomyopathy (ACM). In this paper, the authors focused on mechanisms underlying ACM and the accompanying molecular and cellular alterations. Most importantly they showed that SB21 was able to rescue and partly reverse the ACM phenotype in three different experimental models: 1) a zebrafish model of Naxos disease induced by the overexpression of the 2057del2 mutation in Plakoglobin. 2) neonatal rat cardiomyocytes overexpressing the same mutation in Plakoglobin. 3) cardiomyocytes derived from induced pluripotent stem cells expressing two different forms of mutations in Plakophilin-2. This editorial will focus on the potency and possible restrictions concerning SB21 treatment as a potential intervention for ACM and the usefulness of the applied zebrafish models in general.

Editorial

Arrhythmogenic Cardiomyopathy (ACM; also known as arrhythmogenic right ventricular cardiomyopathy/dysplasia, ARVC/D) is a progressive and primarily heritable heart disease that is caused by mutations in mainly desmosomal genes. Of those genes, mutations are most commonly found in the gene encoding Plakophilin-2.[1]

ACM is characterized by degenerative fibro-fatty replacement of cardiomyocytes, alterations of gap junctions and ion channels (especially Cx43 and $Na_V1.5$),[2,3] and redistribution of Plakoglobin from the junctions to the nucleus.[4] In the last decade a vast amount of knowledge has been acquired about the etiology of this relatively rare disease and the difficult mode of diagnosis has been improved through a refined definition of the Task Force Criteria.[5] Despite of that, the mechanisms that trigger the manifestation and progression of the disease with in particular the arrhythmogenic aspect are only at the onset of understanding. In the article of Asimaki and co-workers, the authors used three different experimental models that were able to recapitulate aspects of the disease as seen in patients, and by this, they accomplished to gain important insights into the underlying mechanisms.

The different models that were studied revealed several aspects of the disease as seen in patients. The zebrafish over expressing the Plakoglobin 2057del2 mutation (causing Naxos disease) showed cardiomegaly, peripheral edema and a reduced cardiac output. This was accompanied with electrical remodeling (reduction of I_{Na}, I_{k1} and depolarization of the resting membrane potential) and 55 % mortality when maturity was reached. Other molecular hallmarks of ACM, being a reduction of Cx43, $Na_V1.5$, and Plakoglobin at the membrane, were shown in the two *in vitro* models of cultured cardiomyocytes expressing clinically relevant mutated desmosomal proteins (Plakoglobin and Plakophilin-2). Most notable in this study, through application of a library of 4200 small molecules to the mutated zebrafish, the authors discovered a pharmacological tool that could prevent and even reverse the ACM phenotype with normalization of all the detrimental aspects listed above.

In the filed of experimental cardiac research, more and more zebrafish models are used due to various advantages in comparison to other animal models. Mammalian and zebrafish hearts, for instance, share well-conserved cardiac structures such as atria, ventricles, valves and even a cardiac conduction system.[6] Although zebrafish hearts are very tiny, it is possible to record ECGs that show a morphology, which is surprisingly similar to human ECG's. The first ECG's can already be taken at about 5 days post fertilization, where P and R waves can be seen that mirror atrial and ventricular depolarization respectively.[7] Full ECG's are possible after 35 days post fertilization.[8] Additionally, the zebrafish's heart rate is much closer to the human heart rate than that of a mouse, thereby making it a suitable model to study e.g. QT syndrome and arrhythmias.[9,10] Furthermore, various action potential parameters are highly similar between humans and zebrafish. In both species, the upstroke during depolarization is dominated by sodium currents, the plateau phase by L-type calcium channels, and the repolarization by the rapidly activa-

ting delayed rectifier potassium currents (I_{Kr}). The latter plays a prominent role in drug induced arrhythmias and is, for example, not present in mice.[11]

Besides these benefits, zebrafish models are popular to perform large library screenings, as also applied in the currently discussed study, and proof of principle experiments. The fish are inexpensive, have a high fertility (female fish can produce approximately 200 eggs a week) and show many advantages like small size, short generation time (most organs including a contracting heart tube is developed within 24 hours post fertilization), transparency during development, genetic tractability and the ability to survive without a functional cardiovascular system during development.[6,12] Of course there are still some disadvantages compared to mammalian models like the mouse, one of them being the poor availability of antibodies that specifically recognize the proteins in fish.[12]

The drug that was selected through the screen in zebrafish, SB216763 (SB21), is an inhibitor of the glycogen synthesis kinase GSK-3β and therefore an activator of the canonical Wnt pathway. Canonical Wnt pathways play an important role in various cellular processes, such as axis duplication, cell transformation, cardiac development and differentiation, cell-cell adhesion and hypertrophy.[13] All canonical Wnt pathways include β-catenin as a downstream substrate. Beyond the central role of GSK-3β, also the involvement of SAP97 is an intriguing finding since localization of this protein was not only found to be disturbed in ACM patients, but it is also associated with anchoring of $Na_v1.5$ and I_{k1} channels in the intercalated disc. The data in this study suggest that during development of the disease mislocalization (maybe due to trafficking defects) of these proteins is downstream of GSK-3β and that, similar as in patients, increased stretch of the cardiomyocytes/myocardium triggers a change in molecular signaling. Prevention of mislocalization or restoration of these proteins in the intercalated disc as mediated by SB21 therapy might have serious anti-arrhythmic consequences.

SB21 administration holds significant promise as therapy for ACM, a disease without an appropriate treatment yet. However, care should be taken when for instance children at risk to develop the disease (mutation carriers) are treated, because of the important role of canonical Wnt pathways in development and its various targets in the heart and other organs. Other aspects that demand attention besides the off target effects, include of course the systemic consequences of chronic treatment (given the ubiquitous role of GSK-3β) and to answer the question whether reversibility of the diseased myocardium still holds promise if the myocardium already shows aspects of fibro-fatty replacement, a common observation during progression of the disease in ACM patients.

Finally, although the zebrafish model will certainly not completely replace experimental mammalian models like the mouse in the future, the study by Asimaki *at al.* shows that the model already offers considerable advantages, leading in combination with appropriately chosen additional model systems, to the discovery of a potential therapy for ACM.

References

1. van Tintelen JP, Entius MM, Bhuiyan ZA, et al. Plakophilin-2 mutations are the major determinant of familial arrhythmogenic right ventricular dysplasia/cardiomyopathy. Circulation.2006;113(13):1650-1658.
2. Saffitz JE. Arrhythmogenic cardiomyopathy and abnormalities of cell-to-cell coupling. Heart Rhythm.2009;6(8 Suppl):S62-65.
3. Noorman M, Hakim S, Kessler E, et al. Remodeling of the cardiac sodium channel, connexin43, and plakoglobin at the intercalated disk in patients with arrhythmogenic cardiomyopathy. Heart Rhythm.2013;10(3):412-419.
4. Asimaki A, Tandri H, Huang H, et al. A new diagnostic test for arrhythmogenic right ventricular cardiomyopathy. N Engl J Med.2009;360(11):1075-1084.
5. Marcus FI, McKenna WJ, Sherrill D, et al. Diagnosis of arrhythmogenic right ventricular cardiomyopathy/dysplasia: proposed modification of the task force criteria. Circulation.2010;121(13):1533-1541.
6. Tu S, Chi NC. Zebrafish models in cardiac development and congenital heart birth defects. Differentiation.2012;84(1):4-16.
7. Forouhar AS, Hove JR, Calvert C, Flores J, Jadvar H, Gharib M. Electrocardiographic characterization of embryonic zebrafish. Conf Proc IEEE Eng Med Biol Soc.2004;5:3615-3617.
8. Milan DJ, Jones IL, Ellinor PT, MacRae CA. In vivo recording of adult zebrafish electrocardiogram and assessment of drug-induced QT prolongation. Am J Physiol Heart Circ Physiol.2006;291(1):H269-273.
9. Wehrens XH, Doevendans PA, Ophuis TJ, Wellens HJ. A comparison of electrocardiographic changes during reperfusion of acute myocardial infarction by thrombolysis or percutaneous transluminal coronary angioplasty. Am Heart J.2000;139(3):430-436.
10. Leong IU, Skinner JR, Shelling AN, Love DR. Zebrafish as a model for long QT syndrome: the evidence and the means of manipulating zebrafish gene expression. Acta Physiol (Oxf).2010;199(3):257-276.
11. Nemtsas P, Wettwer E, Christ T, Weidinger G, Ravens U. Adult zebrafish heart as a model for human heart? An electrophysiological study. J Mol Cell Cardiol.2010;48(1):161-171.
12. Poon KL, Brand T. The zebrafish model system in cardiovascular research: A tiny fish with mighty prospects. Glob Cardiol Sci Pract.2013;2013(1):9-28.
13. van de Schans VA, Smits JF, Blankesteijn WM. The Wnt/frizzled pathway in cardiovascular development and disease: friend or foe? Eur J Pharmacol.2008;585(2-3):338-345.

APPENDIX

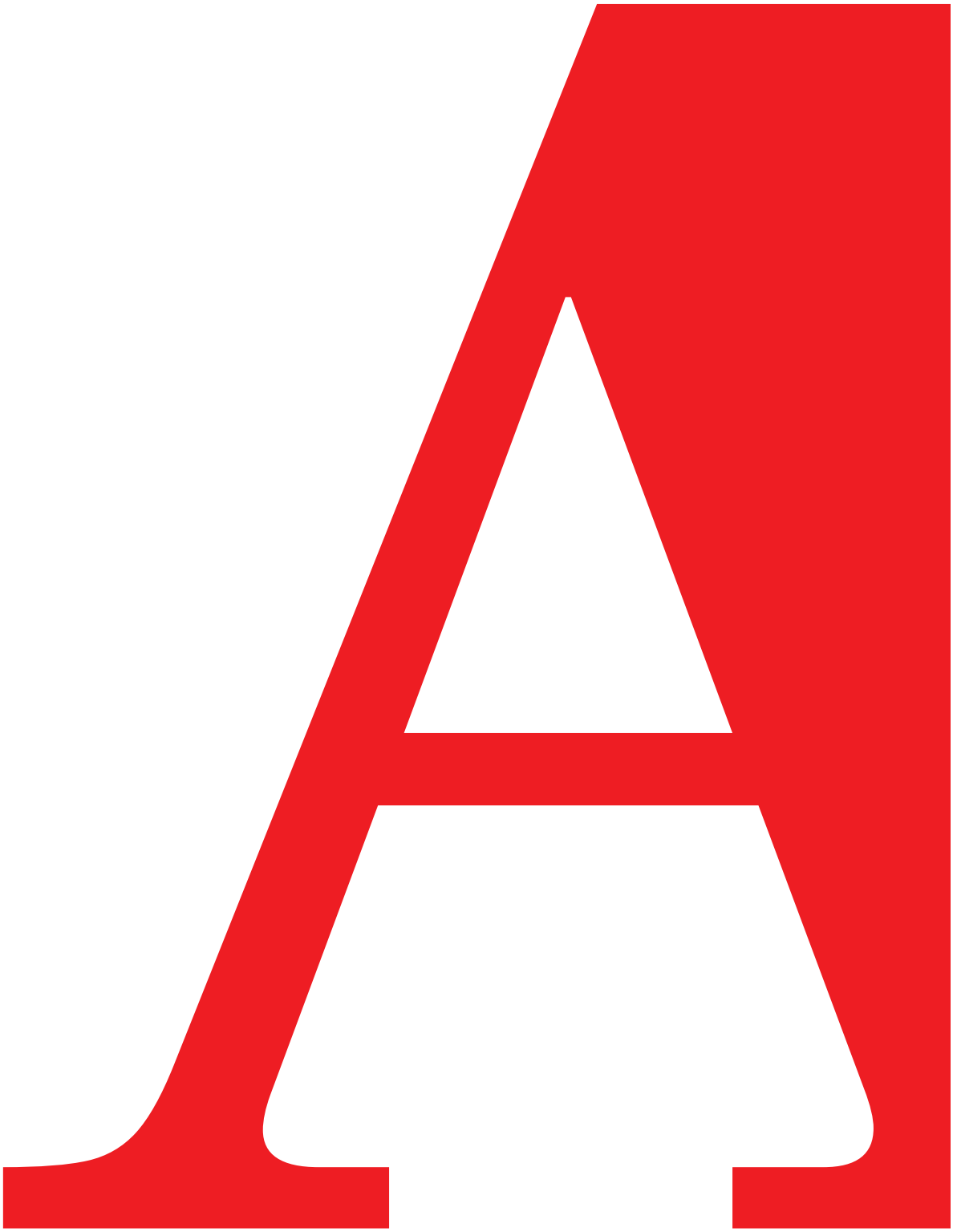

“

It always seems impossible
until it is done.

Nelson Mandela

English summary

Myocardial remodeling

The life-long purpose of our heart is to pump blood containing oxygen and nutrients to all cells of our body. In order to fulfill this destiny, every individual cell of the cardiac muscle (=myocardium) has to contract coordinately to guarantee sufficient blood outflow. To achieve this, an electrical impulse is generated and has to travel uninterruptedly throughout the heart, which results in temporarily elevated intracellular calcium levels that in turn lead to cell contraction. Cardiac damage due to disease, pressure overload or aging can disturb this cooperative work, which might lead to injury, rhythm disorders, pump failure and eventually heart failure (HF).

HF is a major health concern and one of the main causes of death in the western society. It is accompanied by myocardial remodeling, which is an initial natural rescue process of the heart in an attempt to adapt to the altered circumstances. However, when the multi-factorial remodeling is massive and appears in a heterogeneous manner, it unfortunately aggravates the cardiac damage. At multidisciplinary levels, research focuses on identifying modifiable targets for potential biomedical interventions.

Myocardial remodeling consists of electrical, structural and contractile remodeling. Electrical remodeling alters the excitability of the cardiac cells and the propagation of the electrical impulse, which can lead to rhythm disorders. Structural remodeling includes apoptosis, hypertrophy, inflammation and fibrosis formation, which impair cardiac pump function. Contractile remodeling includes alterations in calcium handling and myofilaments and thereby crosses the bridge between electrical and structural remodeling. All types of remodeling can exist independently, but are also able to affect each other.

FIBROSIS AND INFLAMMATION

Important players in structural remodeling discussed in this thesis are fibrosis and inflammation. Fibrosis is defined by an excessive amount of extracellular matrix formation, as a consequence of a disturbed equilibrium between deposition and degradation of mainly collagens. Inflammation within the heart, but also circulating chemokines and cytokines can trigger programmed cell death (apoptosis), hypertrophy, and also lead to fibrosis formation. These structural changes are initiated to reduce wall stress of the heart and to increase cardiac strength, but lead to stiffness of the heart, eventually causing pump problems. Furthermore, an increased amount of the extracellular matrix can in turn disturb the propagation of the electrical impulse, which might lead to heart rhythm disorders.

THE INTERCALATED DISC

One structure, which plays an important role during myocardial remodeling, is the intercalated disc (ID). The ID is the region between the longitudinal ends of adjacent cardiomyocytes, connecting these cells both mechanically and electrically by various junctional protein com-

plexes and ion channels. The main junctions in the ID are adherens junctions, desmosomes and gap junctions, where the first two are responsible for mechanical and the latter for electrical connection. Adherens junctions mainly contain the proteins N-cadherin (Ncad) and Plakoglobin (also called γ-catenin), and desmosomes are mainly built-up by Desmoglein-2 (DSG-2), Desmocollin-2 (DSC-2), Plakophilin-2 (PKP2), Desmoplakin (DSP), β-catenin and also Plakoglobin. Gap junctions in the ventricles are predominantly composed of Connexin 43 (Cx43). Moreover, ion channels, such as the sodium channel $Na_v1.5$, ensure the excitability of the cells and therefore facilitate rapid propagation of the electrical impulse throughout the myocardium.
The amount of identified proteins in the ID has dramatically increased over the last years. Modern techniques have shown that proteins, which were thought to be part of different junctions, can interact with each other to form complicated macro-molecular complexes, actually connecting individual mechanical and electrical junctions. Mutations in, or mislocalization of ID proteins can cause various cardiomyopathies, since alterations in individual proteins can affect the constitution of the complexes and their functioning, which are also often affected during cardiac diseases. Therefore, research on the composition and function of the ID could give more insight into genetic and non-genetic cardiomyopathies and is likely to be very useful regarding future therapy.

Aim

In this thesis, we focused on myocardial remodeling of predominantly the ID and tissue architecture during various cardiomyopathies such as Dilated Cardiomyopathy (DCM), Hypertrophic Cardiomyopathy (HCM), Ischemic Cardiomyopathy (ICM), and Arrhythmogenic Cardiomyopathy (ACM); and upon pressure overload in mice, where we studied the effect of fibrosis and inflammation.

This thesis

This thesis starts with a preface and a review on myocardial remodeling. The preface in **chapter 1** gives a definition of myocardial remodeling and introduces the ID. Furthermore, we describe the research questions and the thesis outline. In the literature study in **chapter 2**, we provide an overview of the different myocardial remodeling processes observed during various cardiomyopathies (DCM, HCM, ICM and ACM), and introduce heterogenic remodeling as an important risk factor for cardiac failure. Subsequently, this thesis is divided into two parts: **Part 1**: Myocardial remodeling of the ID, including chapter 3, chapter 4 and chapter 5; and **Part 2**: Myocardial remodeling of tissue architecture upon pressure overload, including chapter 6 and chapter 7.

Chapter 3 is a study on the role of myocardial tissue remodeling in ACM, which is a genetic cardiomyopathy, mainly caused by mutations in genes encoding for ID proteins (such as PKP2, Plakoglobin, DSC-2, DSP or DSG-2, or even in non-desmosomal genes, such as the transmembrane protein 43 (TMEM-43), phospholamban (PLN), desmin and transforming growth factor beta-3 (TGF-β3)). The disease is characterized by replacement of the myocardium by fat and fibrosis, and heterogeneous downregulation of proteins of the ID is a common observation in animal models mimicking the disease. In this chapter, we studied the composition of the IDs of right-ventricular septum biopsies and post-mortem specimens from ACM patients (mostly having mutations in PKP2). Here, we demonstrate for the first time in human material that Plakoglobin signals in the hearts of ACM patients are often reduced, together with Cx43 and $Na_V1.5$. In a later editorial, which is the **addendum to chapter 8**, we also describe advantages and disadvantages of a proposed treatment for ACM (with a drug named SB21) interfering with the ID proteins and the Wnt signaling pathway.
Mutations in ID proteins can also lead to other cardiomyopathies, such as DCM. Therefore, in **chapter 4** we investigate the differences in ID composition and fibrosis between pediatric DCM patients and pediatric control material. Moreover, we compare these results to adult DCM patients and controls. Surprisingly translocation of DSG-2 to the ID was disturbed in all pediatric patients, even when no underlying mutations in DSG-2 were found. Although this has never been reported before in adult patients, it suggests that translocation of DSG-2 to the ID is delayed or disturbed in the early life-stages of DCM patients. Furthermore, just like seen in ACM patients, the amount of fibrosis was severely increased in the pediatric patients, possibly affecting mechanical and electrical interplay of the heart.
ID protein mutations can account for the majority of ACM patients and are common in DCM patients. However, often underlying mutations of DCM or ACM patients have not been identified, which could be, at least partially, explained by disturbances in so far unknown players of myocardial remodeling. Therefore, we investigated the role of Flotillin-1 and Flotillin-2, which are membrane-associated proteins lately discovered in the ID in **chapter 5**. In mice and neonatal rat cardiomyocytes lacking these proteins, we found that the sodium channel $Na_V1.5$ was reduced and in the cardiomyocytes, electrical excitability was impeded. For the future, it would be uttermost interesting to investigate the interplay of Flotillins and $Na_V1.5$ at the lipid raft region of the membranes, which might be of importance for cardiac impulse propagation.

In **part 2** of this thesis, we induced pressure overload by transverse aortic constriction (TAC) in genetically modified mice to investigate myocardial remodeling. In detail, in **chapter 6**, we used mice lacking the gene for the connective tissue growth factor (CTGF knockout (KO) mice) and applied TAC for 16 weeks to induce myocardial remodeling. Since CTGF was reported to enhance fibrosis formation, we expected KO mice to show reduced fibrosis formation and a better cardiac function. However, our mice did not show decreased cardiac fibrosis or hypertrophy. Interestingly, since then, various groups made similar observations, challenging the causative association of CTGF with fibrosis.

In **chapter 7** and the **addendum to chapter 7**, we again used genetically modified mice (KO of the toll-like receptor 2 (TLR2)) and induced TAC for 12 and 8 weeks, respectively. TLR2 is involved in innate immunity and was reported to induce inflammation upon myocardial infarction causing adverse cardiac remodeling. KO in TLR2 TAC mice in both studies reduced the amount of hypertrophy and improved cardiac contractility compared to wildtype TAC mice. Furthermore, the amounts of cytokines and chemokines were reduced in KO mice and correlations were found between TLR2, TLR4 and the cytokine interleukin-6 (IL-6) in wildtype TAC mice. Interestingly, transplantation with TLR2 KO bone marrow-derived cells prior to 8 weeks of TAC, protected against a reduction in cardiac function and attenuated fibrosis formation. These studies highlight that TLR2, TLR4 and IL-6 could be therapeutic targets in the future and immune cells derived from the bone marrow might worsen the course of HF.
Finally, in **chapter 8**, all chapters are discussed in the light of current research and future perspectives are formulated.

Conclusion

Even though myocardial remodeling is a natural process induced to rescue the failing heart, it eventually leads to cardiac damage, pump failure and possibly to HF. In this thesis, we have shown that remodeling of the ID can lead to cardiomyopathies, such as ACM and DCM, and that so far unidentified proteins in the ID (such as Flotillins) might play a newly uncovered role in electrical excitability of the heart. Furthermore, we have shown that CTGF is probably not a causative factor for fibrosis itself, but rather a mediator of the fibrotic pathway. Lastly, we demonstrated in two studies that TLR2 might pose a modifiable target for chronic pressure overload, since KO attenuates adverse myocardial remodeling upon TAC in mice.
In this thesis, we have therefore successfully investigated several aspects of myocardial remodeling, such as the involvement of alterations in the ID, fibrosis formation and the role of certain inflammatory receptors. With that, we gained more knowledge on the underlying molecular mechanisms of HF.

“

Als ik zou willen dat je het begreep,
had ik het wel beter uitgelegd.

Johan Cruijff

Samenvatting in het Nederlands

Myocardial remodeling

Het levenslange doel van ons hart is om alle cellen van ons lichaam te voorzien met bloed dat zuurstof en voedingsstoffen bevat. Hiervoor moet elke individuele cel van de hartspier (= myocard) gecoördineerd samentrekken om voldoende bloedcirculatie te waarborgen. Dit wordt bereikt door een elektrische impuls die in het hart wordt gegenereerd en vervolgens ononderbroken door het hart moet reizen. Deze impuls leidt tot tijdelijk verhoogde intracellulaire calciumniveaus, die op hun beurt tot celcontractie leiden. Schade aan het hart door ziekte, drukoverbelasting of veroudering kan dit coöperatieve werk verstoren, wat kan leiden tot letsel, ritmestoornissen, pompfalen en uiteindelijk hartfalen (HF).
HF is een groot gezondheidsprobleem en een van de meest voorkomende doodsoorzaken in de westerse samenleving. Het wordt veroorzaakt door myocardiale remodellering, wat een natuurlijk redding proces is van het hart in een poging om zich aan te passen aan de veranderde omstandigheden. Wanneer de remodellering echter te massaal is en heterogeen optreedt in het hart, verergert het helaas hartschade. Op multidisciplinaire niveaus richt het onderzoek zich op het aantonen van modificeerbare targets voor potentiële biomedische interventies.
Myocardiale remodellering bestaat uit elektrische, structurele en contractiele remodellering. Elektrische remodellering van het hart verandert de prikkelbaarheid van de individuele hartspiercellen en de voortgeleiding van de elektrische impuls, wat kan leiden tot ritmestoornissen. Structurele remodellering omvat apoptose (= geprogrammeerde celdood), hypertrofie (= vergroting van de hartspiercellen), ontsteking en fibrose (=vorming van littekenweefsel), waardoor de pompfunctie van het hart wordt aangetast. Contractiele remodellering is gedefinieerd als veranderingen in calciumstromen in de cellen en opbouw van de contractiele elementen van de cel (= myofilamenten) en verbindt hierdoor elektrische en structurele remodellering. Alle vormen van remodellering kunnen onafhankelijk bestaan, maar kunnen elkaar ook beïnvloeden.

FIBROSE EN ONTSTEKING

Belangrijke spelers in structurele remodellering die in dit proefschrift worden besproken zijn fibrose en ontsteking. Fibrose is gedefinieerd als een overmatige hoeveelheid extracellulaire matrix, als gevolg van een verstoord evenwicht tussen aanmaak en afbraak van voornamelijk collagenen. Ontsteking binnen het hart, maar ook circulerende ontstekingsbevorderende eiwitten, zoals chemokinen en cytokinen, kunnen apoptose en hypertrofie veroorzaken en bovendien leiden tot fibrose vorming. Deze structurele veranderingen worden geïnduceerd om de wandspanning van het hart te verminderen en de kracht te verhogen, maar leiden uiteindelijk tot stijfheid van het hart, waardoor pompproblemen kunnen ontstaan. Bovendien kan een overmatige hoeveelheid extracellulaire matrix op zijn beurt de voortgeleiding van de elektrische impuls verstoren, wat kan leiden tot hartritmestoornissen.

DE INTERCALAIRSCHIJF

Eén structuur die een belangrijke rol speelt tijdens myocardiale remodellering, is de intercalairschijf (ID). De ID is het gebied aan de longitudinale uiteinden van aangrenzende cardiomyocy-

ten, die deze cellen zowel mechanisch als elektrisch verbinden door verschillende eiwitstructuren (= junctions) en ionenkanalen. De belangrijkste junctions in de ID zijn adherens junctions, desmosomen en gap junctions, waarbij de eerste twee verantwoordelijk zijn voor mechanische en de laatste voor elektrische koppeling van de cellen. Adherens junctions bevatten voornamelijk de eiwitten N-cadherin (Ncad) en Plakoglobin (ook wel y-catenin genoemd), en desmosomen worden voornamelijk opgebouwd door Desmoglein-2 (DSG-2), Desmocollin-2 (DSC-2), Plakophilin-2 (PKP2), Desmoplakin (DSP), β catenin en Plakoglobin. Gap junctions in de ventrikels bestaan voornamelijk uit Connexine-43 (Cx43). Bovendien maken ionkanalen, zoals het natriumkanaal $Na_v1.5$, de prikkelbaarheid van de cellen mogelijk en faciliteren daarom de snelle voortgeleiding van de elektrische impuls door het hele myocard.
De hoeveelheid eiwitten, die in de ID zijn geïdentificeerd, is de afgelopen jaren drastisch toegenomen. Moderne technieken hebben aangetoond dat eiwitten die deel uitmaken van verschillende junctions een interactie aan kunnen gaan met elkaar om ingewikkelde complexen te vormen die de individuele mechanische en elektrische junctions kunnen verbinden. Mutaties in, of mislokalisatie van ID eiwitten kunnen verschillende ziekten van de hartspier (= soorten cardiomyopathie) veroorzaken, aangezien afwijkingen in individuele eiwitten de samenstelling van de junctions en complexen en hun werking kunnen beïnvloeden. Onderzoek naar de samenstelling en functie van de ID kan daarom meer inzicht geven in genetische en niet-genetische soorten van cardiomyopathie en zal waarschijnlijk zeer nuttig zijn voor toekomstige therapie.

Doel

In dit proefschrift richten we ons op myocardiale remodellering van vooral de ID en de weefselarchitectuur tijdens verschillende soorten cardiomyopathie zoals gedilateerde cardiomyopathie (DCM), hypertrofe cardiomyopathie (HCM), ischemische cardiomyopathie (ICM) en aritmogene cardiomyopathie (ACM). Daarnaast bestuderen we het effect van drukoverbelasting van het hart op fibrose en ontsteking in diverse genetisch gemanipuleerde muismodellen.

Dit proefschrift

Dit proefschrift begint met een voorwoord en een literatuurstudie over myocardiale remodellering. Het voorwoord in **hoofdstuk 1** geeft een definitie van myocardiale remodellering en introduceert de ID. Daarnaast beschrijven we de onderzoeksvragen en schetsen we de opbouw van het proefschrift. In de literatuurstudie in **hoofdstuk 2** geven we een overzicht van de verschillende myocardiale remodelleringsprocessen die tijdens verschillende soorten cardiomyo-

pathie (DCM, HCM, ICM en ACM) optreden en introduceren we heterogene remodellering als een belangrijke risicofactor voor HF. De navolgende hoofdstukken van dit proefschrift zijn in twee delen verdeeld. Hoofdstukken 3, 4 en 5 vormen **deel 1** en betreffen myocardiale remodellering van de ID; hoofdstukken 6 en 7 vormen **deel 2** en betreffen myocardiale remodellering van de weefselarchitectuur bij drukoverbelasting.

Hoofdstuk 3 is een studie over de rol van myocardiale remodellering in ACM. ACM is een genetische cardiomyopathie, welke voornamelijk wordt veroorzaakt door mutaties in genen die voor ID-eiwitten coderen (zoals PKP2, Plakoglobin, DSC 2, DSP of DSG-2), maar ook in niet-desmosomale genen, zoals het transmembraanproteïn 43 (TMEM-43), phospholamban (PLN), desmin en de transformerende groeifactor beta-3 (TGF-β3). De ziekte wordt gekenmerkt door vervanging van het myocard door vet en fibrotisch weefsel; en vermindering van eiwitten in de ID wordt waargenomen in diermodellen die de ziekte nabootsen. In dit hoofdstuk bestuderen we de samenstelling van de ID in rechts-ventriculaire septum biopten en post-mortem weefsel van ACM-patiënten (meestal met mutaties in PKP2). Hier demonstreren we voor het eerst in menselijk materiaal dat Plakoglobin samen met Cx43 en $Na_V1.5$ in de harten van ACM-patiënten vaak verminderd is. In een latere literatuurstudie, het **addendum van hoofdstuk 8**, beschrijven we ook voor- en nadelen van een voorgestelde therapie voor ACM (met een geneesmiddel genaamd SB21), welke ID-eiwitten en de Wnt signalering beïnvloedt.

Mutaties in ID-eiwitten kunnen ook leiden tot andere soorten cardiomyopathie, zoals DCM. Daarom onderzoeken we in **hoofdstuk 4** de verschillen in ID samenstelling en fibrose tussen zeer jonge (= pediatrische) DCM-patiënten en leeftijd gepaard controle materiaal. Bovendien vergelijken we deze resultaten met volwassen DCM patiënten en controle materiaal. Zeer verrassend bleek dat de verplaatsing van DSG-2 naar de ID in alle pediatrische patiënten was verstoord, ook al werden er geen onderliggende mutaties in DSG-2 gevonden. Hoewel dit nog nooit eerder bij volwassen patiënten is gemeld, suggereert het dat de verplaatsing van DSG-2 naar de ID is vertraagd of verstoord in de vroege levensstadia van deze DCM-patiënten. Bovendien was de hoeveelheid fibrose, net als bij ACM-patiënten, aanzienlijk verhoogd bij de pediatrische patiënten, waardoor de mechanische en elektrische wisselwerking van het hart mogelijk is beïnvloed.

In de meerderheid van de ACM-patiënten zijn mutaties in ID-eiwitten aangetoond en deze mutaties zijn ook gebruikelijk in DCM-patiënten. Echter, vaak zijn de onderliggende mutaties van DCM- of ACM-patiënten nog niet geïdentificeerd. Dit kan gedeeltelijk worden verklaard door veranderingen in tot nu toe onbekende spelers van myocardiale remodellering. Daarom hebben we in **hoofdstuk 5** de rol van de membraangeassocieerde eiwitten Flotillin-1 en Flotillin-2 onderzocht, die recentelijk in de ID zijn ontdekt. Bij muizen en in cardiomyocyten van net geboren ratten bij wie deze eiwitten ontbreken, vonden we dat het natriumkanaal $Na_V1.5$ verminderd aanwezig was, en dat in de cardiomyocyten de elektrische prikkelbaarheid werd belemmerd. Voor de toekomst zou het interessant zijn om de interactie van Flotillins en $Na_V1.5$ in specifieke delen van de membranen (zogenaamde lipid-rafts) te onderzoeken die van belang kunnen zijn voor impuls voortgeleiding in het hart.

In **deel 2** van dit proefschrift hebben wij drukoverbelasting door transversale aorta constrictie (TAC) in genetisch gemodificeerde muizen geïnduceerd om myocardiale remodellering te on-

derzoeken. In het bijzonder in **hoofdstuk 6** hebben we muizen gebruikt die de bindweefselgroeifactor CTGF missen door een zogenaamde knockout (KO) van dit gen. Vervolgens hebben we daarna gedurende 16 weken de drukoverbelasting opgelegd om myocardiale remodellering te veroorzaken. Aangezien CTGF als een pro-fibrotische factor werd beschouwd, verwachtten we dat KO-muizen minder fibrosevorming en een betere hartfunctie zouden tonen. Onze muizen lieten echter geen vermindering zien in fibrose of hypertrofie. Sindsdien hebben verschillende onderzoeksgroepen vergelijkbare observaties gedaan, waardoor de sturende bijdrage van CTGF aan fibrose vorming in twijfel kan worden getrokken.
In **hoofdstuk 7 en het addendum van hoofdstuk 7** gebruikten we opnieuw genetisch gemodificeerde muizen (KO van de Toll-like receptor 2 (TLR2)) en induceerden we wederom TAC gedurende 12 en 8 weken. TLR2 is betrokken bij de aangeboren immuniteit en veroorzaakt bijvoorbeeld ontsteking na een hartinfarct, waardoor myocardiale remodellering kan worden veroorzaakt. In vergelijking met controle (= wildtype) TAC-muizen bleek in beide studies na TLR2 KO in TAC muizen de hoeveelheid hypertrofie verminderd en de contractiliteit van het hart verbeterd. Bovendien waren in KO-muizen cytokinen en chemokinen verlaagd en werden er in wildtype TAC-muizen verbanden gevonden tussen TLR2, TLR4 en de cytokine interleukine-6 (IL-6). Interessant is dat transplantatie van beenmerg afgeleide cellen uit TLR2 KO muizen voorafgaand aan 8 weken TAC beschermt tegen een verslechtering van de hartfunctie en de fibrose vorming reduceert. Uit deze studies blijkt dat TLR2, TLR4 en IL-6 in de toekomst therapeutische targets kunnen gaan vormen en dat immuuncellen die afkomstig zijn van het beenmerg het verloop van HF kunnen verergeren.

Ten slotte worden in **hoofdstuk 8** alle hoofdstukken met de blik op huidig onderzoek besproken en worden toekomstperspectieven geformuleerd.

Conclusie

Hoewel myocardiale remodellering een natuurlijk proces is dat wordt geïnduceerd om het falende hart te redden, leidt het uiteindelijk tot hartschade, pompfalen en mogelijk tot HF. In dit proefschrift hebben we aangetoond dat remodellering van de ID kan leiden tot verschillende soorten cardiomyopathie, zoals ACM en DCM, en dat tot nu toe niet geïdentificeerde eiwitten in de ID (zoals Flotillins) een nieuwe rol kunnen spelen in elektrische prikkelbaarheid van het hart. Verder hebben we aangetoond dat CTGF zelf waarschijnlijk geen oorzaak is voor fibrose, maar eerder een tussenschakel van de fibrotische signaaloverdracht. Tenslotte hebben we in twee studies aangetoond dat TLR2 een modificeerbaar target voor chronische drukoverbelasting kan zijn, aangezien KO van TLR2 myocardiale remodellering na TAC in muizen afzwakt.
In dit proefschrift hebben we daarom verschillende aspecten van myocardiale remodellering succesvol onderzocht, zoals de betrokkenheid van veranderingen in de ID, fibrosevorming en de rol van bepaalde ontstekingsreceptoren. Daarmee hebben we meer kennis gekregen over de onderliggende moleculaire mechanismen van HF.

“

Wenn wir wüssten, was wir tun,
würde man es nicht Forschung nennen.

Albert Einstein

Zusammenfassung in deutscher Sprache

Myocardial remodeling

Die lebenslange Aufgabe unseres Herzens ist es, Blut mit Sauerstoff und Nährstoffen zu allen Zellen unseres Körpers zu pumpen. Um diese Aufgabe zu erfüllen, muss jede einzelne Zelle des Herzmuskels (= Myokard) koordiniert kontrahieren, damit ein ausreichender Blutstrom aus dem Herz gewährleistet werden kann. Um dies zu gewährleisten, wird ein elektrischer Impuls im Herzen erzeugt, der sich dann ununterbrochen durch das ganze Organ fortbewegen muss. Dieser Impuls führt zu einem vorübergehend erhöhten intrazellulären Kalziumspiegel, der seinerseits zur Zellkontraktion führt. Herzschäden durch Krankheit, Drucküberlastung oder Alterung können diese kooperative Arbeit stören, was zu Verletzungen, Rhythmusstörungen, Pumpversagen und schließlich Herzinsuffizienz (HI) führen kann.
HI ist eines der größten Gesundheitsprobleme und eine der Haupt-Todesursachen in der westlichen Gesellschaft. Es wird durch den Umbau des Herzmuskelgewebes (= myokardiale Remodellierung) verursacht, der anfänglich ein natürlicher Rettungsprozess des Herzens ist, um sich an die veränderten Umstände anzupassen. Wenn jedoch die Remodellierung massiv wird und uneinheinheitlich (= heterogen) erscheint, verschlimmert sie den Herzschaden. Auf multidisziplinärer Ebene konzentriert sich die Forschung auf die Identifizierung von veränderbaren Faktoren für mögliche biomedizinische Interventionen.
Die myokardiale Remodellierung besteht aus elektrischer, struktureller und kontraktiler Remodellierung. Elektrische Remodellierung ändert die Erregbarkeit der Herzzellen und den Verlauf des elektrischen Impulses, was zu Rhythmusstörungen führen kann. Strukturelle Remodellierung umfasst Apoptose (= programmierter Zelltod), Hypertrophie (= Vergrößerung der Herzzellen), Entzündungen und Fibrose (= Bildung von Narbengewebe), welche die Herzpumpfunktion beeinträchtigen können. Kontraktile Remodellierung umfasst Veränderungen in der Kalzium-Handhabung und den kontraktilen Elementen des Herzmuskels (= Myofilamenten) und verbindet elektrische und strukturelle Remodellierung. Alle Arten der Remodellierung können unabhängig voneinander entstehen, sich aber auch gegenseitig beeinflussen.

FIBROSE UND ENTZÜNDUNG

Wichtige Bestandteile der strukturellen Remodellierung, die in dieser Dissertation behandelt werden, sind Fibrose und Entzündung. Fibrose wird als ein Überfluss an Bindegewebe definiert, die als Folge eines gestörten Gleichgewichts zwischen Ablagerung und Abbau von hauptsächlich Kollagenen entsteht. Entzündungen im Herzen sowie zirkulierende entzündungsfördernde Proteine, wie Chemokine und Zytokine, können Apoptose und Hypertrophie auslösen und auch zur Fibrosebildung führen. Diese strukturellen Veränderungen werden eingeleitet, um die Belastung auf die Wände des Herzens zu reduzieren und damit die Kraft des Herzens zu erhöhen. Jedoch führen sie auch zur Versteifung des Herzmuskels, was schließlich zu Pumpproblemen führt. Darüber hinaus kann eine erhöhte Menge an Bindegewebe wiederum die Ausbreitung des elektrischen Impulses stören, was zu Herzrhythmusstörungen führen kann.

DIE INTERCALATED DISC

Eine Struktur, die bei der myokardialen Remodellierung eine wichtige Rolle spielt, ist die intercalated disc (ID). Die ID ist die Region zwischen den Längsenden benachbarter Herzzellen (= Kardiomyozyten), die diese Zellen sowohl mechanisch als auch elektrisch durch verschiedene verbindende Proteinstrukturen (= junctions) und Ionenkanäle in Kontakt bringt. Die Hauptverbindungen in der ID sind Adherens Junctions, Desmosomen und Gap Junctions, wobei die ersten beiden für den mechanischen und letztere für den elektrischen Anschluss verantwortlich sind. Adherens Junctions enthalten hauptsächlich die Proteine N-Cadherin (Ncad) und Plakoglobin (auch γ-Catenin genannt) und Desmosomen werden hauptsächlich von Desmoglein-2 (DSG-2), Desmocollin-2 (DSC-2), Plakophilin- 2 (PKP2), Desmoplakin (DSP), β-Catenin und auch Plakoglobin aufgebaut. Gap Junctions in den Ventrikeln des Herzens bestehen überwiegend aus Connexin 43 (Cx43). Darüber hinaus sorgen Ionenkanäle, wie der Natriumkanal $Na_V1.5$, für die Erregbarkeit der Zellen und erleichtern so eine schnelle Ausbreitung des elektrischen Impulses im gesamten Myokard.

Die Anzahl der identifizierten Proteine in der ID hat in den letzten Jahren enorm zugenommen. Moderne Techniken haben gezeigt, dass Proteine, von denen man glaubte, sie seien Teil von verschiedenen Junctions, miteinander interagieren können, um komplizierte Komplexe zu bilden, die wiederum einzelne mechanische und elektrische Junctions verbinden. Mutationen oder Fehllokalisationen von ID Proteinen können verschiedene Kardiomyopathien verursachen, da Veränderungen in einzelnen Proteinen die Konstitution der Junctions und Komplexe und deren Funktionsweise beeinflussen können. Daher kann unsere Forschung einen besseren Einblick in die Zusammensetzung und Funktion der ID in genetischen und nicht-genetischen Kardiomyopathien geben und ist darum von großer Bedeutung für zukünftige Therapien.

Ziel

In dieser Dissertation konzentrieren wir uns überwiegend auf die myokardiale Remodellierung der ID und der Gewebearchitektur bei verschiedenen Kardiomyopathien, wie z.B. Dilatative Kardiomyopathie (Dilated Cardiomyopathy (DCM)), Hypertrofe Kardiomyopathie (Hypertrophic Cardiomyopathy (HCM)), Ischämische Kardiomyopathie (Ischemic Cardiomyopathy (ICM)) und Arrhythmogene Kardiomyopathie (Arrhythmogenic Cardiomyopathy (ACM)). Außerdem erforschen wir den Effekt von Drucküberlastung bei Mäuseherzens bezüglich der Entstehung und Entwicklung von Fibrose und Entzündung.

Diese Dissertation

Diese Dissertation beginnt mit einem Vorwort und einer Literaturstudie über myokardiale Remodellierung. Das Vorwort in **Kapitel 1** gibt eine Definition von myokardialer Remodellierung und führt die ID ein. Darüber hinaus beschreiben wir die Forschungsfragen und den Aufbau dieser Dissertation. In der Literaturstudie in **Kapitel 2** geben wir einen Überblick über die verschiedenen myokardialen Remodellierungs-Prozesse, die bei verschiedenen Kardiomyopathien (DCM, HCM, ICM und ACM) beobachtet wurden und führen heterogene Remodellierung als wichtigen Risikofaktor für HI ein. Die darauffolgenden Kapitel dieser Arbeit sind in zwei Teile aufgeteilt: Kapitel 3, Kapitel 4 und Kapitel 5 formen **Teil 1** und behandeln die myokardiale Umgestaltung der ID. Kapitel 6 und Kapitel 7 formen **Teil 2** und behandeln die myokardiale Remodellierung der Gewebearchitektur bei Drucküberlastung.

Kapitel 3 ist eine Studie über die Rolle der myokardialen Remodellierung in ACM. ACM ist eine genetische Kardiomyopathie, die hauptsächlich durch Mutationen in Genen verursacht wird, die für ID-Proteine kodieren (wie PKP2, Plakoglobin, DSC-2, DSP oder DSG-2, oder sogar in nicht-Desmosomale Gene wie dem Transmembranprotein 43 (TMEM-43), Phospholamban (PLN), Desmin und transformierendem Wachstumsfaktor beta-3 (TGF-β3)). Die Krankheit ist gekennzeichnet durch die Verdrängung des Myokards durch Fett und Fibrose. Außerdem ist auch eine heterogene Verminderung von ID Proteinen sichtbar in Tiermodellen, mit denen die Krankheit nachgeahmt wird. In diesem Kapitel wird die Zusammensetzung der IDs in Biopten des rechtsventrikulären Septums und von post-mortem Gewebeproben von ACM Patienten (meist mit Mutationen in PKP2) untersucht. Wir zeigen hier zum ersten Mal an menschlichem Material, dass Plakoglobin-Signale zusammen mit Cx43 und $Na_V1.5$ in den Herzen der ACM-Patienten oft abgenommen haben. In einem späteren Artikel, der das **Addendum zu Kapitel 8** ist, beschreiben wir auch Vor- und Nachteile einer vorgeschlagenen Behandlung für ACM (mit einem Medikament namens SB21), welche die ID-Proteine und den Wnt-Signalisierungsweg beeinflusst.

Mutationen in ID-Proteinen können auch zu anderen Kardiomyopathien wie DCM führen. Daher untersuchen wir in **Kapitel 4** die Unterschiede in der ID-Zusammensetzung und der Fibrose zwischen Material von sehr jungen (= pädiatrischen) DCM- und Kontrollpatienten. Darüber hinaus vergleichen wir diese Ergebnisse mit erwachsenen DCM- und Kontrollpatienten. Überraschenderweise ist die Migration von DSG-2 zur ID bei allen pädiatrischen Patienten gestört, auch wenn keine zugrunde liegenden Mutationen in DSG-2 gefunden wurden. Obwohl dies bisher bei erwachsenen Patienten noch nicht dokumentiert wurde, deutet es darauf hin, dass die Translokation von DSG-2 zur ID in den frühen Lebensstadien von DCM-Patienten verzögert oder gestört wird. Darüber hinaus ist, genau wie bei ACM-Patienten, Fibrose bei den pädiatrischen Patienten stark erhöht, wodurch möglicherweise das mechanische und elektrische Zusammenspiel des Herzens beeinträchtigt wurde.

Bei einem Großteil der ACM- und DCM-Patienten sind Mutationen in ID-Proteinen üblich und ein regelmäßiger Fund, aber häufig kann die zugrunde liegende Mutation auch nicht identifiziert werden. Dies könnte zumindest teilweise durch eventuelle Mutationen oder Störungen in bisher unbekannten Spielern der myokardialen Remodellierung erklärt werden. Daher haben wir in **Kapitel 5** die Rolle der Membran-assoziierten Proteinen Flotillin-1 und Flotillin-2 untersucht, die kürzlich in der ID entdeckt wurden. Bei Mäusen und in Kardiomyozyten von kurz zuvor geborenen Ratten, denen diese Proteine fehlen, entdeckten wir, dass der Natriumkanal $Na_V1.5$ reduziert war und die elektrische Erregbarkeit in den Kardiomyozyten behindert wurde. Für die Zukunft wäre es äußerst interessant, das Zusammenspiel der Flotillins mit $Na_V1.5$ in speziellen Regionen der Membranen (den sogenannten lipid-rafts) zu untersuchen, die für die Impulsausbreitung im Herzen von Bedeutung sein könnten.
In Teil 2 dieser Dissertation verursachen wir eine Drucküberlastung im Herzen von genetisch veränderten Mäusen durch transversale Verengung der Aorta (transvers aortic constriction, TAC), um die myokardiale Remodellierung zu erforschen. Genau genommen verwenden wir in **Kapitel 6** Mäuse, bei denen wir das Gen für den Bindegewebswachstumsfaktor CTGF gelöscht haben (Knockout (KO) Mäuse). Die TAC bleibt für 16 Wochen bestehen, um myokardiale Remodellierung hervorzurufen. Da regelmäßig berichtet wurde, dass CTGF die Fibrosebildung steigert, erwarten wir in den KO-Mäusen eine verminderte Fibrosebildung und eine bessere Herzfunktion. Allerdings zeigen unsere Mäuse keine verminderte Fibrose oder Hypertrophie im Herzen. Interessanterweise haben seither verschiedene Gruppen ähnliche Beobachtungen gemacht und somit die anfängliche Assoziation von CTGF mit Fibrose in Frage gestellt.
In **Kapitel 7 und dem Addendum zu Kapitel** 7 verwendeten wir wiederrum genetisch veränderte Mäuse (KO des Toll-like Rezeptors 2 (TLR2)) und verursachen TAC für 12 bzw. 8 Wochen. TLR2 ist an der angeborenen Immunität beteiligt und kann Entzündungen nach einem Myokardinfarkt hervorrufen, was für myokardiale Remodellierung des Herzens sorgt. KO in TLR2 TAC-Mäusen in beiden Studien reduziert Hypertrophie und verbessert die Kontraktilität des Herzens im Vergleich zu Kontroll-TAC-Mäusen. Darüber hinaus ist die Mengen an Zytokinen und Chemokinen in KO-Mäusen reduziert. Auch wurden Korrelationen zwischen TLR2, TLR4 und dem Cytokin Interleukin-6 (IL-6) in Wildtyp-TAC-Mäusen gefunden. Interessanterweise schützt die Transplantation mit Zellen aus dem Knochenmark von TLR2-KO-Tieren nach 8 Wochen TAC gegen eine Verringerung der Herzfunktion und schwächt Fibrosebildung ab. Diese Studien zeigen, dass TLR2, TLR4 und IL-6 in der Zukunft therapeutische „Targets" darstellen könnten und, dass Immunzellen aus dem Knochenmark den Verlauf der HI verschlechtern können.

Schließlich werden in **Kapitel 8** alle Kapitel in Anbetracht der aktuellen Forschung diskutiert und zukünftige Perspektiven formuliert.

Schlussfolgerung

Obwohl die myokardiale Remodellierung ein natürlicher Prozess ist, der dazu dient, das scheiternde Herz zu retten, führt es schließlich zu Herzschäden, Pumpausfall und möglicherweise zu HI. In dieser Dissertation haben wir gezeigt, dass eine Umgestaltung der ID zu Kardiomyopathien wie ACM und DCM führen kann und, dass bisher nicht identifizierte Proteine in der ID (wie Flotillins) eine neuartige Rolle bei der elektrischen Erregbarkeit des Herzens spielen könnten. Darüber hinaus haben wir gezeigt, dass CTGF wahrscheinlich kein ursächlicher Faktor für die Fibrose selbst ist, sondern nur einen Teil der Fibrosebildung ausmacht. Schließlich haben wir in zwei Studien gezeigt, dass TLR2 ein veränderbarer „Target" für eine chronische Drucküberlastung darstellen könnte, da KO die myokardiale Remodellierung, die auf eine TAC folgt, bei Mäusen abschwächt.
In dieser Dissertation haben wir deshalb erfolgreich einige Aspekte der myokardialen Remodellierung untersucht, wie Veränderungen in der ID, die Fibrosebildung und die Rolle bestimmter Entzündungs-Rezeptoren. Damit haben wir mehr Wissen über die zugrundeliegenden molekularen Mechanismen von HI gewonnen.

“

At times the world may seem an unfriendly and sinister place, but believe that there is much more good in it than bad. All you have to do is look hard enough, and what might seem to be a series of unfortunate events may in fact be the first steps of a journey.

Lemony Snicket

Acknowledgements

Hey Hey everyone :-)
Er zijn zo veel mensen die ik graag wil bedanken voor de totstandkoming van mijn proefschrift. De volgorde is dan soms ook compleet arbitrair en geeft vooral geen prioriteit weer. Bovendien verontschuldig ik me nu alvast als ik je vergeten ben. Dus alvast aan iedereen bedankt! Schonmal Danke an alle! Thanks to everyone!
Ik wil natuurlijk wel beginnen met mijn begeleiders: **Marc**, ik weet nog hoe ik als student bij jou op de kamer zat en jij mijn carrière in de vorm van een piramide op een vel papier getekend hebt. Op dat moment dacht ik dat ik alles kon worden wat ik wilde. Door de jaren heen hebben we vaak over mijn carrière gepraat en ook al waren wij het soms niet helemaal eens, je hebt mij altijd gepusht en getriggerd. Dat is één van de redenen dat ik nog steeds het gevoel heb dat ik inderdaad alles kan worden als ik er maar hard genoeg voor werk, dankje! En ik beloof je dat ik snel weer een keer met een paar biertjes je kamer binnen gelopen kom! **Toon**, je hebt mij bij de hand genomen toen ik nog een student was en je hebt me steeds meer los gelaten tijdens mijn carrière. Je hebt me de juiste kant opgeduwd toen ik het nodig had en mij mijn eigen beslissingen laten nemen toen ik er klaar voor was. Door jou voel ik me een volwaardig deel van de wetenschap en heb ik een kritische (nou ja veel mensen zullen nu zeggen dat ik altijd al kritisch was) blik gekregen op de wetenschap. Je was er niet alleen op professioneel vlak, maar ook met persoonlijke raad. Dankje voor je begrip en je ondersteuning!
Dank aan mijn **beoordelingscommissie** voor het kritisch lezen en beoordelen van mijn proefschrift. En bijzondere dank aan **Roel** voor het accepteren van het voorzitterschap.
Mijn **paranimfen**, super bedankt voor jullie hulp! Ik zou jullie beide niet meer willen missen in mijn leven, dus op naar jullie promoties! **Birgit**, toen jij op onze afdeling kwam, kon ik je moeilijk inschatten. Maar al snel heb ik gemerkt dat jij een van de meest loyale, eerlijke, behulpzame en hilarische mensen bent die ik ken. Ik ben blij dat je toen (tijdens de sushi, wie had het verwacht…) zei dat je mijn paranimf wilde worden. En natuurlijk **Merle**, vanaf ons tutorgroepje bij Biologie hebben we samen bijna alle vakken gedaan en vonden mensen ons een 'angstaanjagend-duo'…hahaha. Maar, wij zijn gewoon top samen (en vooral sinds dat onze Erwins het ook nog zo goed met elkaar kunnen vinden).
Und hier zwischendurch natürlich **Anna**, ja du machst das! Ohne dich wäre dieses Buch ja überhaupt nu ein großer Haufen zusammenhangloser Papiere. Danke für deine Mühen und deine Geduld mit mir und meinem Buch (und meinen Panikattacken) und, dass du mir jetzt schon seit dem Gymnasium eine Top-Freundin bist. Und danke auch an **Michi** für deine Freundschaft und euren genialen Fotoshoot: Ich sehe mich immer noch auf eurem Boden liegen...wann gehen wir mal wieder Laser-gamen?
En dan natuurlijk ook dank aan alle collega's van de **Medische Fysiologie**: **Tonny**, ik ken weinig mensen die zo vol liefde en interesse voor andere mensen zitten als jij. Je bent een top hulp met alle werk gerelateerde vragen en problemen, maar nog veel beter met persoonlijke dingen. Dankje! Je was er vanaf het begin voor me en ik heb zo veel leuke momenten met jou gedeeld. Je voelt altijd aan hoe het met me gaat en hebt mij op moeilijke momenten een schouder aangeboden. Bovendien geef jij de beste knuffels! **Leonie**, wat ik hier ook zeg, het is niet genoeg!

Dankje! Ik vind het fantastisch dat ik mijn allereerste Western Blot met jou gedaan heb en we de laatste Western Blots voor mijn boekje ook weer samen gedaan hebben. Ik hoop dat we nog even samen aan een bench kunnen zitten en over van alles en nog wat kunnen babbelen (en oh ja, dankje voor het vast houden van de pasta, he!). **Alex**, a special hey hey to you! Early in the morning, we were often the only ones and we shared our frustrations, but also had a lot of fun and good conversations. I realized that no matter what we do, we always end-up sitting in front of each other. Thanks for your help with stupid PRISM and Illustrator and for the good times in our room. **Marcel,** bedankt voor de bloemen! Je bent een top collega. Je weet bijna alles wat op de afdeling gebeurt en ik waardeer je professionele instelling, die altijd gepaard gaat met een gezonde portie zwarte humeur en sarcasme. Geweldig! **Lotte**, je hebt me veel geleerd over de zebravissen en we hebben hard gewerkt. Succes met je boekje en ik kom graag weer eens langs om te helpen. **Joanne**, mijn super student. Dankje voor al je hulp tijdens je stage en leuk dat je bij ons je PhD doet! **Jet**, je was meestal het eerste gezicht in de ochtend dat ik zag op het lab, dat blijft wel hangen, he?!? Dankje voor je vrolijkheid in de ochtend. **David**, je bent een ontzettend vrolijk mens en ik denk dat je ook een ontzettend goede arts bent. Vooral heel veel plezier met je patiënten, jullie zullen zeker lol hebben! **Yuan**, okay officially you are not my colleague anymore, but I will still mention you here. Together in our room, we had unexpectedly good conversations about anything and everything. Good luck back in China. **Sanne** de Jong, bij jouw vak heb ik mijn eerste echte college gegeven en ik voelde me enorm gesteund door jou. Bovendien zaten wij niet zonder reden beide in het winnende team bij de labstapdag :-)! **Marti**, je zet je altijd in voor de studenten en probeert je eigen cursus continu te verbeteren. Dat is erg leuk om te zien. Dankje voor je tips en tricks rondom het lab. **Maria**, dankje dat ik mijn Electives in Hong Kong mocht doen en dat jij in mij geloofde. Ik wens je heel veel plezier met al je vrije tijd nu! **Teun**, dankje voor je hulp met Patchen en met alle vragen die wij op de afdeling over onze computers hebben. **Marien**, ook al hebben wij nooit veel samen gewerkt, het was toch altijd wel gezellig samen op het lab en we hebben erg goede gesprekken kunnen voeren. Thanks! **Helen** en **Chantal**, bedankt voor de girl-power tijdens onze wekelijkse werkbesprekingen en succes met jullie boekjes. **Maike**, dankje voor al je hulp en vooral geduld met de muizen. Bedankt voor de gezelligheid: **Muge**, **Agnieszka**, **Doreth**, **Valerie** en de gezellige **studenten**. Maar ook erg bedankt aan alle ex-collega's van de Medische Fysiologie. En dan moet ik beginnen met **Harold**. Dankzij jouw college over ACM (wat toen nog ARVC/D was) werd ik enthousiast over hartonderzoek en wilde ik graag bij jullie stage lopen. Dankje dat je dit mogelijk gemaakt hebt. Hierop moet dan natuurlijk dank aan **Maartje** volgen. Mijn eerste stage heb ik bij jou gedaan en ook was je er even niet (omdat je naar Amerika ging) ik voelde me goed begeleid en je hebt er zeker voor gezorgd dat ik wilde blijven. **Hanneke**, je bent niet alleen een oud collega, maar ook een super vriendin. Laten we snel weer samen op vakantie gaan en het glas heffen op onze boekjes (als we dan niet de volgende dag moeten gaan werken, hé Toon?!?!). **Mathilde**, thanks girl for all your help! Good luck with your PhD and Postdoc. **Vincent**, bedankt voor alle diepgaande discussies over filosofie, wetenschap, politiek en religie, maar vooral ook over alle domme grappen en nutteloze hilarische avonden samen met een borrel of met een min of meer goede film (nouja wij vonden het dan meestal wel erg goed,

maar als je het Erwin vraagt, ligt het niveau van onze films/series wat lager denk ik :-)). **Magda**, thanks for all your help and patience. I had a great time at Oliviers Tuesday and in Milan. And it was hilarious to be you for one day and eat a lot of cookies. En natuurlijk mijn studenten in de afgelopen jaren: **Joanne**, **Mimount**, **Angelique** en **Joëlle**. Ik volg graag jullie carrières en vind het altijd leuk om jullie weer eens te zien. Ik ben trots dat jullie allemaal jullie eigen weg gevonden hebben/aan het zoeken zijn en wens jullie veel succes met alles! **Bart**, mijn bench-buurman! Man wat hadden wij toch lol dansend en zingend op het lab. Dankje voor al je hulp en we moeten snel weer een Indiaas gaan eten! **Martin**, ook was het niet zo vaak, maar bedankt voor je hulp met patchen. **Sanne** Korte, het voorbereiden van vakken was altijd erg leuk en snel weer gaan lunchen enzo! **Rianne**, dankje dat je mijn sparringpartner was voor mijn BKO! En natuurlijk ook dank aan **Albert**, **Sofieke**, **Iris**, **Bastiaan**, **Rosanne**, **Malin**, **Tessa**, **Siddarth**, **Nele, John** en **Ivar** voor alle momenten van hulp, adviezen en ondersteuning.
Collega's, maar dan niet van de Medische Fysiologie: Thanks to everyone from **CVON Predict** for good cooperation and nice meetings. Dankje ook aan de mensen van **Write your Future**, ontzettend leuk om met jullie samen te werken. Op naar een mooi eindresultaat! **Barend,** heel erg bedankt voor je de sparrings-middag voor de crazy idea. **Peter Nikkels**, bedankt voor je hulp met de pediatrische DCM studie. Het was erg leerzaam om met jou achter de microscoop te zitten. **Roel Goldschmeding**, bedankt voor de hulp tijdens mijn Master en PhD. Afspraken met jou zijn altijd erg leuk en ik leer er elke keer een hoop van. Ik hoop dat we in de toekomst nog vaker op jouw kamer over verschillende wetenschappelijke onderwerpen gaan sparren. **Hester den Ruijter**, bedankt voor al je hulp met de grants! Ik hoop dat het ons snel lukt om een project op te starten :-) **Gideon**, dankje voor je hulp met de HELPFul database! **Tim Leiner**, bedankt voor je hulp met de grant en HELPFul patiënten. Ben al zo benieuwd naar je data. **Antje Banning** und **Ritva Tikkanen**, vielen vielen Dank für alle Herzen und Daten. Ich arbeite hart am Fertigstellen des Flotillin-Artikels. **Jiong-Wei Wang** thanks for the good work together on the TLR2 study and the help with my book. **Dominique de Kleijn** dankje voor de leuke discussies tijdens de koffie en je hulp. **Anne** en **Fiona** van de Toxicologie bedankt voor de super hulp met de MEA. **Mario Delmar** thanks for traveling all the way for my defense and your input. **Anneline te Riele**, erg dankje voor de gezelligheid als we samen college geven en naar congressen te gaan (en dan tussendoor even te shoppen :-)). Ook bedankt aan **Peter-Paul** en **Aisha** en iedereen van de experimentele Cardiologie, en **Charlotte**, **Evelyne**, **Monika**, **Marta** en **Sandra** from the Hubrecht Institute. A lot of thanks to Hong Kong, too. **Reinhard Renneberg**, danke, dass ich in deinem Labor an der HKUST ein Praktikum machen durfte. Geniess deinen Ruhestand und schick mir mal wieder ein paar Cartoons! **Jan**, man man Jan. Ich bin ja mal so gespannt, was du in ein paar Jahren so treibst. Irgendwie denke ich, dass ich dich dann in einem Mega-Auto und einer Mega-Mansion vor finde. Vergiss mich dann nicht, gell?!? **Vivien**, it is so nice that we see each other occasionally. Let's keep in touch, it is always a lot of fun! And also **Godfrey** and **Mimi**, thanks for the great time! Also many thanks to **Jeffrey Saffitz** and **Andre Kleber**, for making my time in Boston unforgattable and especially for the good discussions and food. **Angeliki** and **Valentin** (oh mi gode!), my duck-family, I really enjoyed being in the lab with you two and all the amazing stories we shared! And of course thanks **Ann Yee** for being

such a wonderful landlady and host; I miss the Somersetroad!
En natuurlijk dank aan een heleboel vrienden en familie! En dan begin ik met een vriendschap die op het lab begonnen is: thanks Medical Physiology chicks **Hanneke**, **Joyce** en **Carmen**! Super leuk dat we elkaar nog zo regelmatig zien en elke keer zo veel lol hebben. Ik ben altijd super benieuwd wat nu weer de nieuwste avonturen zijn en als we elkaar zien heb ik altijd keelpijn en buikpijn van het lachen! **Adriaan** Raaijmakers, ja jou moet ik hier zeker ook noemen (niet alleen je zus-lief). Thanks voor veel gezellige avonden met pizza en Game of Thrones! We moeten bijna een andere serie zoeken! Bio-chicks: **Dieuwertje**, **Danielle** en **Milou**. Ahhhh we hebben al zo veel samen beleefd (niet alleen in Nederland) en we verhuizen om en om steeds naar andere steden, waardoor we altijd 'on the move' blijven, maar elkaar toch elke keer weer opzoeken. Houden zo! Thanks voor jullie vriendschap! En dan hier natuurlijk ook nog een keer thanks **Didi** (Dieuwertje en Diana) voor alle gezellige DDEE-spelletjes- en BBQ avonden! Hier ook nog een keer, maar nu samen **Merle** en **Erwin**, leuk dat we zo leuke dubbeldates hebben! Op naar de volgende keer sushi :-) Thanks ook aan de Boston-girls: **Marion**, **Pauline** en **Annebel**. #Waarisjelampje #Smores #SeaKajaking #Shootingrange #RedSocks #NewYork #JumpingPauly #Brooklinebarcrash #Paulyzoekthaardignity #bigbelly #gsnp #Whiskeys, jullie zijn amazing! Snel weer een reünie plannen en dit keer met escalatie! En natuurlijk aan **Casper** voor een super leuke tijd in Boston. Special thanks to the unicorns! **Annebel**, wat zou ik zonder jou doen? Je luistert naar mij als ik zorgen heb en geeft me altijd goede tips (ook vindt Erwin dat soms niet :-)). Je bent een geweldige vriendin en ik zie ons ooit allemaal in Amersfoort naast elkaar wonen en dan kunnen we eindelijk elke dag bij elkaar op de koffie (of nou, doe mij maar Mango-Kokos thee)! **Danny**, bedankt voor alle gezelligheid en loyaliteit! Ik weet dat wij altijd op jou kunnen rekenen! Snel weer samen er op uit! **Melle**, **Katharina** und **Chrissi**, auch sehen wir einander nicht mehr so viel, Danke dafür, dass es wenn wir uns sehen, immer so anfühlt, als wäre das letzte Mal Gestern gewesen! En natuurlijk mag ik Lake Diving niet vergeten, en vooral de duik-EC en **Ron** en **Luc**, **Arthur** (met **Annemieke**) en **Judith**. En natuurlijk niet te vergeten **Rob**, we willen echt nog proberen om langs te komen in Kopenhagen (en anders wordt het wel weer een ander mooi land...nu eerst even weer Nederland! :-P). Thanks voor vele goede gesprekken en avonden lol. En natuurlijk ook dank aan **Bastiaan en Cindy**, **Wilfred en Annabelle**, **Sandra en Henk**, **Maarten en Michelle, Eva en Merlin** en **Kelly**, omdat met jullie mijn vriendenkring nog groter en leuker is geworden.
Und natürlich ganz besonders viel Dank an die Menschen, die mich schon mein ganzen Leben lang begleiten! Meine liebe **Familie Kessler**, ihr ward immer für mich da! **Anna**, **Tante Wally** (und auch noch **Alter Gette**), ihr ward wie meine eigenen Großeltern. Danke für eure Liebe und einfach das beste Essen der Welt. **Näne**, 5 Euro für jede 1 im Zeugnis war denk ich der beste Ansporn, den ich je hatte (und glücklicherweise für mich ein besserer Deal, als für dich). Danke, dass du an mich geglaubt hast! Ich vermisse dich! **Oma** Enzkofen, scheinbar sehe ich dir ziemlich ähnlich (zumindest wenn ich böse gucke…) hoffentlich bin ich dir auch in vielen anderen Dingen ähnlich! **Gette Hans und Angelika** mit **Julian** und **Steffen**, danke, dass ihr so fest an mich glaubt. **Tante Regina und Roland**, ich freue mich immer unglaublich über Mails mit Nachrichten aus dem Süden! **Uli**, **Fredy** en **Joris**, dit moet wel in Duits/

Nederlands. Of het nu een HIM Konzert, der Weihnachtsmarkt, ein Die Drei ??? Konzert oder poffertjes eten in Utrecht of bij het strand is, jullie zijn een geweldig trio. We komen altijd erg graag bij jullie en jullie zijn natuurlijk ook altijd welkom hier! Bedankt voor de steun! Auch vielen Dank an **Otto** mit **Giesela**, **Florian**, **Christoph** mit **Evi, Anna-Lena, Luisa** und **Lukas** ihr macht Enzkofen und Familienfeiern immer zu richtigen Festen! **Egon** und **Wally** mit **Tim, Jan** und **Maik**, ich freue mich jedes Mal, wenn ich euch sehe. Lassen wir das weiterhin regelmäßig (2 mal im Jahr ist ja auch regelmäßig) tun. **Martin**, ich warte nur noch auf den Moment bis du nach Thailand auswanderst, aber dann kommen wir auf jeden Fall vorbei!
Heel veel dank gaat ook aan **Lili**. Je bent meer dan een tante voor mij. Door jou en **André** heb ik me al vanaf het begin van mijn Nederland-avontuur thuis gevoeld. Bedankt daarvoor. Ik heb het gevoel dat ik altijd welkom ben bij jullie en het voelt dan ook als thuis komen als ik bij jullie door de deur stap. **Vincent**, we kunnen over alles praten (want je vindt altijd alles interessant) en wat leuk dat je de biomedische wereld wilt gaan verkennen, dus op naar de Nobelprijs! **Ingeborg**, ook al doen wij niet meer zo vaak spelletjes, ik zie je nog steeds als een van de meest waardige opponenten! Je bent een ontzettend slimme meid en je zal je eigen weg gaan vinden, dat weet ik zeker. Ik ben trots op jullie twee!
Ook kan ik jullie niet meer persoonlijk bedanken: **Oma**, bedankt dat je mij altijd verwend en zo goed voor mij gezorgd hebt. **Opa**, ach wat had ik zonder jou moeten doen. Je was mijn held. In die tijd dat ik bij jou heb gewoond, heb ik zo veel over jou en je leven te weten gekregen en hebben we ontzettend veel goede gesprekken gehad. Ik ben blij dat ik je in de laatste jaren van je leven mocht begeleiden.
Niet alleen aan mijn eerste familie heb ik veel te danken, maar ook aan **Geertje** en **Cor**, jullie hebben mij vanaf de eerste dag het gevoel gegeven dat ik bij de familie hoor en ik kan altijd op jullie rekenen. **Ingrid**, meid ik heb in jou een super leuke schoonzus gevonden en hoop op nog heel veel bezoekjes aan de Efteling samen (of iets anders **Jeffrey** :-)). Bedankt ook aan **Niels**, **Johanneke, Charlotte** en **Juliette**, succes in jullie geweldige stek en laten we snel weer eens BBQ'en ofzo. **Bé**, **Elly** en **Boukje** bedankt; **Arthur** danke! Wat heb ik toch een leuke schoonfamilie erbij gekregen. En **Baike** mag ik natuurlijk niet vergeten!
So jetzt sind wir bei den Menschen angelangt, die mich am längsten kennen/denken, dass die mich am besten kennen ;-) und mich vor allem schon am längsten aushalten! **Frederike und Lennard**: What if I'm far from home? Oh, brother, I will hear you call. What if I lose it all? Oh sister, I will help you out! Oh, if the sky comes falling down; for you, there's nothing in this world I wouldn't do. Jedes Mal, wenn ich dieses Lied höre, denke ich an euch. Und ich meine jedes Wort! **Frederike**, schon sehr früh hast du mir beigebracht, wie toll Lernen ist. Danke, dass du mich und meine Neugier immer unterstützt hast und mir so eine tolle große Schwester bist! Und danke, dass du und **Victor** mich als eure Trauzeugin haben wollen, das bedeutet mir sehr viel! **Lennard**, bei uns können die Fetzen fliegen oder wir sind unzertrennlich. Danke, dass ich auf dich zählen kann, wenn ich dich brauche! Auch wenn du deinen Weg doch nicht in der Wissenschaft gehst, bin ich davon überzeugt, dass du immer deinen eigenen Weg finden wirst (und Knarre und Handschellen stehen dir auch ziemlich gut!). **Mama & Papa**, danke für alles. Danke, dass ihr immer an mich geglaubt habt und mir beigebracht habt, dass ich alles

werden kann, was ich will. Danke, dass ihr mich und meinen Dickkopf ausgehalten habt und mich immer unterstützt habt. Danke für eure Wärme und Liebe! **Mama**, danke dass du mir meine positive Einstellung zum Leben beigebracht hast und die Überzeugung, dass alles seinen Sinn hat und man am Besten die schönen Seiten am Leben sehen soll. **Papa**, danke, dass du deinem Muck immer die richtige Portion Autorität und Freiheit gegeben hast. Danke für deine Fröhlichkeit, deine Offenheit und dein Enthusiasmus, mit dem du durchs Leben gehst.
Last, but for sure not least: **Erwin**, DANKJE! Je bent mijn schat, mijn partner in crime, mijn feestbeest, mijn travel companion, mijn couch potato, mijn aapje en gewoon alles wat ik me kan voorstellen. Je bent mijn anker als ik het moeilijk heb, je maakt mij vrolijk als niemand anders het kan. Je staat achter mij en je bent er altijd voor me. Jij kan mij aan! My world crumbles, when you are not here! Oh nee wacht: I wear goggles, when you are not here :-)

“

The first draft
of anything is shit.

Ernest Hemingway

List of publications

Full manuscripts

Elise L. Kessler, Jiong-Wei Wang, Bart Kok, Maike A. Brans, Angelique Nederlof, Leonie van Stuijvenberg, Fatih Arslan, Carolyn S.P. Lam, Marc A. Vos, Dominique P.V. de Kleijn, Toon A.B. van Veen, Magda S.C. Fontes. TLR2 Knockout attenuates adverse cardiac remodeling in mice subjected to chronic pressure overload. *Submitted*

Jiong-Wei Wang, Magda S.C. Fontes, Xiaoyuan Wang, Suet Yen Chong, **Elise L. Kessler**, Ya-Nan Zhang, Judith J. de Haan, Fatih Arslan, Saskia C.A. de Jager, Leo Timmers, Toon A.B. van Veen, Carolyn S.P. Lam, Dominique P.V. de Kleijn. Leukocytic Toll-Like receptor 2 deficiency preserves cardiac function and reduces fibrosis in sustained pressure overload. *Scientific Reports* 2017; 7: 9193.

Elise L. Kessler, Peter G.J. Nikkels, Toon A.B. van Veen.
Disturbed Desmoglein-2 in the intercalated disc of pediatric patients with Dilated Cardiomyopathy. *Human Pathology* 2017; 67: 101-108.

Magda Fontes*, **Elise L. Kessler***, Leonie van Stuijvenberg, Maike A. Brans, Lucas L. Falke, Bart Kok, Andrew Leask, Harold V.M. van Rijen, Marc A. Vos, Roel Goldschmeding, Toon A.B. van Veen. CTGF knockout does not affect cardiac hypertrophy and fibrosis formation upon chronic pressure overload. *Journal of Molecular and Cellular Cardiology* 2015; 88: 82-90.

Elise L. Kessler and Toon A.B. van Veen. A fishing trip to cure arrhythmogenic cardiomyopathy? *Annals of Translational Medicine* 2015; 3(7): 90.

Elise L. Kessler, Mohammed Boulaksil, Harold V.M. van Rijen, Marc A. Vos, Toon A.B. van Veen. Passive ventricular remodeling in cardiac disease: Focus on heterogeneity. *Frontiers in Physiology* 2014; 5: 482.

Maartje Noorman*, Sara Hakim*, **Elise L. Kessler***, Judith Groeneweg, Moniek G.P.J. Cox, Angeliki Asimaki, Harold V.M. van Rijen, Leonie van Stuijvenberg, Halina Chkourko, Marcel A.G. van der Heyden, Marc A. Vosa, Nicolaas de Jonge, Jasper J. van der Smagt, Dennis Dooijes, Aryan Vink, Roel A. de Weger, Andras Varro, Jacques M.T. de Bakker, Jeffrey E. Saffitz, Thomas J. Hund, Peter J. Mohler, Mario Delmar, Richard N.W. Hauer, Toon A.B. van Veen. Remodeling of the cardiac sodium channel, Connexin43, and Plakoglobin at the intercalated disc in patients with Arrhythmogenic Cardiomyopathy. *Heart Rhythm* 2013; 10(3): 412-9.

* Authors contributed equally

Abstracts

Elise L. Kessler, Peter G.J. Nikkels, Toon A.B. van Veen. Disturbed Desmoglein-2 in the intercalated disc of pediatric patients with Dilated Cardiomyopathy. *European Heart Journal* 2017; 38: 1345.

Shan-Shan Zhang, Dagmar A. Kuhn, **Elise L. Kessler**, Angeliki Asimaki, Valentin Sottas, Dimitri Vanhecke, Barbara Rothen-Rutishauser, Jeffrey E. Saffitz, Robin M. Shaw, Andre G. Kleber. Arrhythmogenic Cardiomyopathy mutations cause disassembly of the Cx43 forward trafficking machinery, which can be rescued by GSK-3β inhibition. *Circulation* 2014; 130: A15042.

Der Mensch muß bei dem
Glauben verharren, daß das
Unbegreifliche begreiflich sei:
er würde sonst nicht forschen.

Johann Wolfgang von Goethe

Curriculum vitae

Elise Laura Kessler

Elise Laura Kessler was born on September 6th, 1988 in Karlsruhe, Germany. In 2008 she graduated from secondary school (Markgrafen Gymnasium) and completed her training as a medical assistant to work for almost one year for the Johanniter Unfallhilfe.
In 2009, she moved to the Netherlands to start the Bachelors program Biology at the Utrecht University, where she was a selected member of the Bachelor-Honours-program. Here, Elise became interested in the cardiovascular system and performed an extended Bachelor internship at the department of Medical Physiology, University Medical Center Utrecht (UMCU) under supervision of Dr. Van Veen about the involvement of the intercalated disc in Arrhythmogenic Cardiomyopathy. After her graduation in 2012, she started the Masters program Biology of Disease at the Graduate School of Life Sciences of the Utrecht University. During this Master, she was a selected member of the Master-Honours-program of Life Sciences and performed three internships: The first internship was at the Chemistry and Biotechnology department of the Hong Kong University of Science and Technology, where she did research on cardiac troponin biomarkers under supervision of Professor Dr. Renneberg. The second internship was at the department of Medical Physiology, UMCU under supervision of Dr. Van Veen, where she investigated the role of CTGF in pathophysiological development of cardiac fibrosis. Her third internship was at the Pathology department of the Beth Israel Medical Center (Harvard Medical School), Boston, USA. Under supervision of Professor Dr. Saffitz, she studied the molecular mechanisms of (Arrhythmogenic) Cardiomyopathy. In 2014 she obtained her Masters degree *cum laude*.
Right after her Masters, she started her PhD at the department of Medical Physiology, UMCU under supervision of Professor Dr. Vos and Dr. Van Veen. During this period, she received her university teaching certificate (Basis Kwalificatie Onderwijs (BKO)). The results obtained during her PhD track are described in this thesis entitled 'Myocardial remodeling during pathophysiology: Relevance for cardiac dysfunction', which she will defend on the 25th of January 2018.
Currently, Elise is working as a post-doctoral researcher at the department of Medical Physiology, UMCU.